Applications of Polyvinylamine in Removal of Heavy Metals from Wastewater by Polymer-Enhanced Ultrafiltration and Adsorption

by

Yifeng Huang

A thesis

presented to the University of Waterloo

in fulfillment of the

thesis requirement for the degree of

Doctor of Philosophy

in

Chemical Engineering

Waterloo, Ontario, Canada, 2016

AUTHOR's DECLARATION

I hereby declare that I am the sole author of this thesis. This is a true copy of the thesis, including any required final revisions, as accepted by my examiners.

I understand that my thesis may be made electronically available to the public.

Abstract

In this study, water-soluble polyvinylamine (PVAm) was used as chelating agent for heavy metal removal from wastewater by polymer-enhanced ultrafiltration (PEUF). The effects of parameters involved in the ultrafiltration (UF) process, the interaction properties of PVAm and heavy metals, as well as the batch operation of PEUF process were investigated. In addition, the synthesis of thiol functionalized PVAm and its applicability for Hg(II) adsorptive removal were studied.

The removal of eight toxic heavy metals (e.g., Co(II), Cu(II), Ni(II), Pb(II), Fe(III), Cd(II), Zn(II), and Mn(II)) from water by a PVAm-enhanced ultrafiltration was investigated. By forming stable PVAm-metal complexes in the aqueous solution, the heavy metals can be separated from water using UF membrane. The removal rate for Pb(II), Cu(II), and Fe(III) can achieve as high as 99%, 97%, and 98% by PVAm-enhanced ultrafiltration, respectively. The sulfate divalent anion was found to be able to cause the precipitation of the soluble PVAm-metal complexes. The mechanism of the precipitation formation and its effect on the performance of PEUF were investigated.

Further, this technique was used for Hg(II) removal from wastewater. A mercury removal as high as 99% was obtained. Over the feed mercury concentration range tested (0 - 50 ppm), the PVAm dosage used did not affect the mercury rejection considerably, while water flux was reduced significantly at a higher dosage of PVAm. A flux vs pressure relationship typical of UF of macromolecular solutes was observed, and the limiting flux appeared to follow the gel layer formation model. The fouled membrane surface was cleaned periodically with dilute hydrochloric acid to recover the membrane permeability. Mercury removal with the

PEUF was also tested with a simulated chlor-alkali wastewater that contained mercury and other chemicals (i.e., sodium chloride and sulphate), and the accompanying compounds in the feed solution was shown to influence the performance of PEUF for mercury removal.

A mathematical model for batch operation of PEUF process for mercury removal was developed. Its applicability was testified using three different water-soluble polymers (i.e., PVAm, polyethyleneimine (PEI), and poly(acrylic acid) (PAA)) by comparing with the experimental data. The performance of the three polymers for mercury removal by PEUF process decreased as the order PVAm > PEI > PAA at the same polymer concentration and operating conditions. The membrane fouling was found to have profound influences on the modelling of batch operation of PEUF process. For a given recovery task, the mercury concentration in the feed, the mercury recovery rate, the batch operating time and the membrane area needed to achieve the desired recovery can be predicted if the concentration dependence of the perm-selectivity of the process (i.e., when the UF membrane and the water-soluble polymer are selected) is known.

To enhance the removal efficiency and the selectivity towards Hg(II), the PVAm was chemically functionalized by thiol groups. The synthesized PVAm derivative (denoted as PVAm-SH) was found to be insoluble in water and showed good adsorption capability for Hg(II) in aqueous solution. The adsorption isotherms and kinetics were investigated. Thermodynamic estimation showed that the Hg(II) sorption onto PVAm-SH is endothermic.

Acknowledgements

PhD research is a long and hard journey in one's life. I cannot finish the thesis without the supports and assistants by many people during this period. I would like to take out this opportunity to carry out my appreciation and gratitude to all of them.

At the very beginning, I would like to express my sincere thanks to my supervisor, Professor Xianshe Feng for providing me such a great opportunity to study in University of Waterloo. He led me into the field of membrane technology, inspired me and arouse my passion and desire in scientific research. His vision and knowledge guided me throughout the course of my PhD research. His support and encouragement helped me overcome the difficulties I met in my research as well as my ordinary life. His tolerance and patience allowed me to correct my mistakes in the research and improved my research skills. He is more like a father to me. With his love, advice and encouragement, I will become a better scientist in the future.

I would like to thank all my PhD examination committee members, Professor Christine Moresoli, Professor Neil McManus, Professor Zhongchao Tan and Professor Hongde Zhou, for their comments and suggestions on my research and thesis.

I am thankful to Professor Lu Shao in Harbin Institute of Technology, who was my supervisor for my Master degree. He helped me a lot for my PhD application and recommended me to University of Waterloo. He shared his experience in scientific research and gave me valuable advices for my PhD work.

My thanks also go to the current and previous group members in our lab. They never hesitated to express their supports, suggestions and friendliness during my PhD study. Dr.

Dihua Wu and Dr. Yijie Hu helped me for my experimental design and set-up at the beginning, and gave me many useful suggestions related to my research. Min Guan, also my dearest friend in Canada, gave tons of help and support to me and my family. I would like to thank Dr. Gil J. Francisco, Dr. Haoli Zhou, Dr. Ying Zhang, Dr. Prodip Kundu, Dr. Muhammad Farooq Usman, Dr. Yongqiang Yang, Dr. Yong Zhou, Dr. Xiaodong Wang, Dr. Zhongde Wang, Shuixiu Lai, Boya Zhang, Xincheng Xu, Kai Wu, Kevin Bailey, Melanie Snow, Aoran Gao, Bo Qiu, Jingjing Zhang and Jingjing Sun. I would like to express my thanks to Dr. Minghui Liu and Yong Ding for FTIR test, Ralph Dickhout for ICP-OES test, Bert Habicher for membrane cell fixing, Dr. Wei Zhang and Shaofan Sun for surface tension analysis, and Dr. Chang Guo for his help and suggestion in the synthesis experiment.

I wish to extend my thanks to all the friends who helped and influenced me in the past four years. My friend Likun Hu helped me settled down when I came to Canada in 2011. Wei Yi, one of my roommates, whose positive attitude to life encourage me a lot. I would also like to take this chance to express my special thanks to those all who helped me for my wedding ceremony in September 2015.

Last, but not the least, I would like to appreciate my family, especially my parents, my parents-in-law and my wife, for their understanding, comfort, support, encouragement and love to help me complete this object. This thesis is dedicated to them.

Table of Contents

List of Figures

List of Tables

List of Symbols

A	Efficient membrane area, m^2
A'	Pre-exponential factor in Arrhenius equation
C	Instantaneous mercury concentration in the kinetic adsorption, ppm
C_0	Initial mercury concentration in the kinetic adsorption, ppm
C_f, C_p	Metal concentration in the feed and permeate respectively, ppm
C_b	Solute concentration in the bulk feed, wt%
C_g	Gel concentration, wt%
C_e	Concentration of Hg(II) in aqueous media at the adsorption equilibrium, ppm
E_a	Activation energy of adsorption
ΔG_{SL}	Free energy of interaction when a solid is immersed in a liquid, mJ/m^2
ΔG_{SWM}	Interfacial free energy of adhesion between two solid materials at contact when immersed in water, mJ/m^2
ΔG_{SWS}	Interfacial free energy of cohesion, mJ/m^2
$\Delta G°$	Gibbs free energy change
$\Delta H°$	Enthalpy change
J	Permeation flux, L/(h·m^2), kg/(h·m^2)
J_v	Volumetric permeation flux, L/(h·m^2)
J_a	Average flux decline caused by membrane fouling
K	Kozeny-Carman coefficient
K_s, K_i, K_c, K_t	Empirical fouling coefficients in standard pore blocking, intermediate pore blocking, cake layer formation, and total pore blocking models respectively

K_L, K_F	Langmuir and Freundlich constant respectively
K_a	Adsorption equilibrium constant
k	Mass transfer coefficient
k_1, k_2	Rate constant in pseudo-first and pseudo-second order adsorptions
L_p	Solvent permeability coefficient
L	Mass ratio of PVAm to mercury(II) in the feed
l_m	Membrane thickness, m
m	Mass of permeate sample collected, g
M	Mass of the PVAm-SH used in the kinetic adsorption, g
M_a, M_b, M_c	Instantaneous concentrations of mercury in the retentate, permeate, and cumulated product respectively, ppm
n	Heterogeneity factor in the Freundlich model
ΔP	Transmembrane pressure difference, Pa
P_a, P_b, P_c	Instantaneous concentrations of PVAm in the retentate, permeate, and cumulated product respectively, wt%
Q	Adsorption capacity, mg/g, mmol/g
r_1, r_2	Retention rate of mercury and PVAm respectively
r_p	pore radius
R_m, R_p	Rejections of metal and PVAm respectively
R_e	Removal efficiency of mercury in adsorption
R	Gas constant
S	Pore internal surface area, m^2
ΔS°	Entropy change

t	time, h
T	temperature, ℃
V	Volume of the aqueous solution in the kinetic adsorption, L
V_f, V_p	Volume of retentate and cumulated product respectively, L

Greek letters

β_e	Activity coefficient of adsorbate at the adsorption equilibrium
γ	Total surface tension, mJ/m^2
γ^{LW}, γ^{AB}	Apolar and polar part of the total surface tension respectively, mJ/m^2
γ^+, γ^-	Electron-accepticity and electron-donicity parameter of polar part of surface tension respectively, mJ/m^2
ε	Membrane porosity
η	Viscosity of the solvent
θ	Contact angle, °
π	Solute osmotic pressure
σ	Reflection coefficient
τ	Tortuosity of the pores

List of Abbreviations

Polymers and chemicals

CA	cellulose acetate
PAA	poly(acrylic acid)
PAEI	poly(N-acetyl ethyleneimine)
PAN	polyacrylonitrile
PC	polycarbonate
PE	polyethylene
PEI	polyethyleneimine
PES	polyethersulfone
γ-PGA	poly(γ-glutamic acid)
PHEI	poly(N-hydroxyethyl ethyleneimine)
PMA	poly(methacrylic acid)
PNS	poly(glycidylmethacrylate)
PS	polysulfone
PSS	poly(sodium 4-styrenesulfonate)
PVA	poly(vinyl alcohol)
PVAm	polyvinylamine
PVAm-SH	polyvinylamine derivative with thiol group
PVDF	polyvinylidene fluoride
DCC	Dicyclohexylcarbodiimide
EDTA	Ethylenediaminetetraacetic acid

NHS   N-hydroxysuccinimide

NTA   Nitrilotriacetic acid

Membrane technology

ED   electrodialysis

MEUF   micellar-enhanced ultrafiltration

MF   microfiltration

MWCO   molecular weight cut-off

NF   nanofiltration

PEUF   polymer-enhanced ultrafiltration

RO   reverse osmosis

UF   ultrafiltration

Characterizations

FT-IR   Fourier transform infrared spectroscopy

ICP-OES   inductively coupled plasma optical emission spectrometry

UV-vis   ultraviolet-visible spectrophotometry

SEM   scanning electron microscopy

Chapter 1

Introduction

1.1 Background

Heavy metals, in anionic or cationic forms, and some semi-metalloid ions (e.g., arsenic and boron) are the dominant contaminants in water recycle resulting from manufacturing and mining. They represent a serious water pollution problem, threatening the environment and human health [Batley and Florence, 1976; Dabrowski *et al.*, 2004]. Some soluble heavy metals (e.g., cobalt, chromium, copper, mercury, manganese, nickel, and lead) can cause serious damage to the central nervous system (lead, mercury), kidneys (copper, lead, mercury), skin, teeth (nickel, chromium), liver or lungs (nickel, mercury, lead, copper) [Fu and Wang, 2011; Monier and Abdel-Latif, 2013]. Too much intake of some of the metals at high levels may even result in death. Unlike organic contaminants, heavy metal ions cannot be bio-degraded in nature, which makes the remediation a technical challenge [Ozay *et al.*, 2009; Bessboussea *et al.*, 2012]. The current environmental regulations on heavy metals are increasingly stringent, whereas the global need for most heavy metals continues to increase as a result of the rapid development of modern industry. Thus there is an urgent need to develop efficient and effective techniques for processing wastewater containing soluble heavy metals.

Membrane separation processes such as reverse osmosis (RO), electrodialysis (ED), and nanofiltration (NF) have been used in removing heavy metal ions from aqueous solutions [Ba

et al., 2009; Urgun-Demirtas *et al.*, 2012]. They have already grown from a simple laboratory tool to a mature industrial process. However, these processes are capital- and/or energy-intensive because of the high operating pressures or high power consumptions needed [De and Mondal, 2013].

Recently, a new separation technique based on polymer-ennhanced ultrafiltration (PEUF) technique has been proposed and investigated [Spivakove *et al.*, 1985; Li *et al.*, 2008; Zerze *et al.*, 2013]. It is essentially an ultrafiltration process but the solute rejection is enhanced by a polymer that will capture or bind the heavy metals. The mechanism associated with PEUF is that the heavy metals in the aqueous phase can be attached to water-soluble polymers to form macromolecular metal-coordinated compounds, whose size is much larger than the molecular weight cut-off (MWCO) of the UF membranes used [Geckeler *et al.*, 1980; Juang *et al.*, 2003], and such macromolecules will be retained by the membrane, thereby separating the heavy metals from water.

Compared to other commonly used separation methods (e.g., adsorption, ion-exchange, chemical precipitation and flocculation), PEUF has several advantages over them: 1) the separation in PEUF occurs in a homogeneous phase, whereas the other methods listed above are based on two-phase partitions which may have potential problems associated with interphase mass transfer or heterogeneous reaction. In other cases where homogeneous aqueous solutions are preferred, additional treatment procedures (e.g., desorption and back extraction) are often needed, and this increases the processing cost and complicates the process design [Rivas *et al.*, 2003]; 2) PEUF seems to be more effective for treating low metal concentrations to meet the discharge limits than others; 3) PEUF affords selective separation of target species from multicomponent solutions with possible recovery.

The water-soluble polymers, which are the key component in PEUF, should meet three general requirements for use as chelating agents: high content of chelating sites or complex formation groups (e.g., amino, imino, carboxyl and sulfonic acid groups), sufficient solubility in aqueous solutions, and a molecular weight greater than the MWCO of the UF membranes used [Geckeler *et al.*, 1980]. There has been a considerable deal of work on the application of such polymers for heavy metal removal since Geckeler and Bayer [1985] proposed this concept called liquid-phase polymer-based retention in the 1980s. Almost all of the papers they and other researchers published to date focused on the synthesis of new water-soluble polymers, the interactions between the polymers and different heavy metals, and the capacity of heavy metals that can be bonded by the polymers.

Although a great number of water-soluble polymers have been used as chelating agents in PEUF, so far only a few show great potential for the industrial-scale processes, including PEI [Spivakove *et al.*, 1985; Molinari *et al.*, 2007; Cojocaru *et al.*, 2009; Labanda *et al.*, 2011; Almutairi F. M. *et al.*, 2012; Camarillo *et al.*, 2012], PAA [Cañizares *et al.*, 2008; Rivas and Palencia, 2011], poly(sodium 4-styrenesulfonate) (PSS) [Korus, 2012]. For practical applications, the chelating agents must have high binding capacity, fast kinetics, and good selectivity toward heavy metals. They also need to be commercially available, easy to prepare and economical feasible.

Nowadays, polyvinylamine, a relatively new amine polymer that was not commercially available until recently, has attracted a lot of interests due to its unique properties. Although PVAm is one of the simplest water-soluble amine-containing polymers, it received little attention before the 1990s due to technical difficulty for its prepatration [Jones *et al.*, 1944; Hong and Pelton, 2002], and many efforts were made subsequently to synthesize and produce

3

PVAm. Like poly(vinyl alcohol), PVAm can only be produced indirectly because it cannot be produced from conventional polymerization with monomers. Several monomers containing amino groups such as N-vinylacetamide, N-vinylsuccinimide, N-vinylphthalimide and N-vinylformamide have been studied for synthesis of PVAm [Bolto, 1995]. Eventually, successful polymerization of poly(N-vinylformamide) and subsequent hydrolysis led to a commercial route of PVAm synthesis [Hong and Pelton, 2002]. Then the applicability of PVAm for various applications [Hu *et al.*, 2012; Qiao *et al.*, 2013] began to be evaluated due to its increased availability. There is a large number of primary amino groups on the PVAm chains (up to 95%), which provide sufficient chelating sites for complexing heavy metal ions [Teyssie *et al.*, 1965], making it an ideal polymeric chelating agent in the PEUF process.

In addition, the high chemical reactivity of PVAm also offers possibility of chemical modifications by which various functional groups (S and P containing groups) may be incorporated into PVAm chains. The modified PVAm derivatives with a strong affinity towards some specific metal ions may enhance their removal efficiency in PEUF [Bayer *et al.*, 1980]. However, the addition of new functional groups onto PVAm chains may change its solubility in aqueous solutions [Saad *et al.*, 2013]. In this case, the insoluble PVAm derivatives with specific functional groups may then be used as an adsorbent for several heavy metals. No published work about PVAm as a polymer chelating agent in PEUF has been found to date. The present work, which will deal with heavy metal removal by PEUF and adsorption using PVAm and its derivatives, will not only expand the scope of application of PVAm in heavy metal treatment but also complement the theory of PEUF process for heavy metal capture.

1.2 Research objectives

The objectives of this research were to study the application of water-soluble PVAm in removing heavy metals from wastewater. The thesis work consisted of the following:

1. To investigate the feasibility of using PVAm as a polymer chelating agent for the removal of heavy metals from aqueous solutions through ultrafiltration process;

2. To study the effects of operating conditions on the separation performance of PEUF, and to develop a mathematical model for batch operation of PEUF;

3. To chemically modify the PVAm by grafting thiol functional groups for use as an adsorbent for mercury(II) capture from wastewater.

1.3 Scope of the thesis

This thesis consists of seven chapters. The scope of each chapter is listed as follows:

Chapter 1 presents the research background and the objectives of the study. A literature review on the UF membrane process, the fundamentals and applications of PEUF technique, and the polymer-metal interactions are presented in Chapter 2. A brief introduction of flocculation and adsorption is also included in this chapter.

Chapter 3 investigates the feasibility of using water-soluble PVAm as chelating agents to remove heavy metals from water by PEUF technique. Compounds of eight heavy metals, including Pb(II), Cu(II), Fe(III), Co(II), Ni(II), Zn(II), Mn(II) and Cd(II) were tested as the representative heavy metals in water, interactions between PVAm and the heavy metals in aqueous solutions were found to have a profound influence on the metal removal efficiency. In addition, the counter anions presented in the solutions also affected the state of the polymer-

metal complexes. Certain PVAm-metal complexes were shown to aggregate and precipitate out of the solutions if the sulfate concentration were high enough.

Chapter 4 deals with Hg(II) removal from wastewater using PEUF, and the effects of the operating parameters in the UF process on Hg(II) removal were studied. The concentration polarization and membrane fouling resulted from the PVAm used in the PEUF process were investigated and discussed. To study the applicability of this technique for possible industrial applications, the PVAm-enhanced UF was used to treat a simulated chlor-alkali wastewater that contained mercury and other chemicals, relevant to the chlor-alkali process.

The study in Chapter 4 showed that the PEUF technique was efficient to recover mercury from wastewater. Therefore, batch operation of PEUF process was studied in Chapter 5, including a mathematical modeling of the process. Three water-soluble polymers (i.e., PVAm, PEI and PAA) were used as chelating agents for mercury. The applicability of the model equations developed for batch operation was validated with experimental data. In addition, the significance of membrane fouling in PEUF was shown to depend on the water-soluble polymer used, and membrane fouling should be taken into account for the model to properly predict the metal removal efficiency unless the membrane fouling by the polymer was insignificant.

To further broaden the application of PVAm and enhance the mercury removal rate, thiol functionalization of PVAm was conducted in Chapter 6. By forming a stable amide bond, the thiol functional groups were successfully grafted onto PVAm chains to produce a new PVAm derivative: PVAm-SH. It was found that the synthesized PVAm-SH was insoluble in water and showed a high adsorption capacity towards Hg(II) in aqueous solutions. The adsorption isotherms and kinetics were studied. The effects of solution pH and presence of other salts on

the sorption properties were investigated as well. In addition, desorption study was also included in this chapter to look into regeneration of the spent adsorbent for reuse in the process.

The general conclusions drawn from this work and the major contributions to original research are summarized in Chapter 7. Several recommendations for future work are also provided. Figure 1.1 shows an overview of this thesis structure.
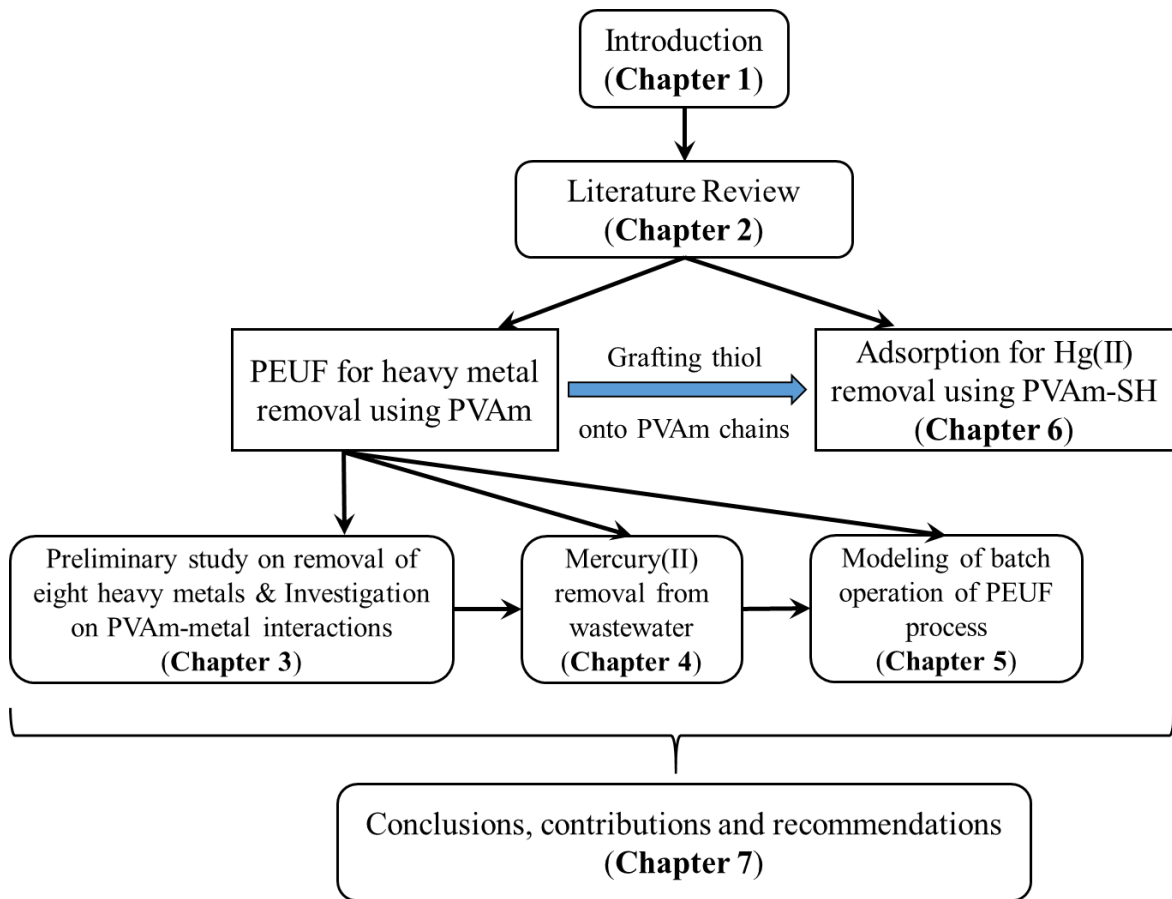
Figure 1.1 Thesis structure and the relationships between each chapter

Chapter 2

Literature Review

Polymer-enhanced ultrafiltration is a relatively new "hybrid" process that combines metal coordination on a polymer with membrane filtration. It was first called liquid-phase polymer-based retention by Spivakov et al. [1985] who published their pioneering work in Nature in 1985. Many efforts have been made to synthesize water-soluble polymers for effective interactions with different heavy metals since the 1980s. Nowadays, much attention is paid to the membrane process when applying this technique for the removal of heavy metals, and the process is more commonly called polymer-enhanced ultrafiltration or polymer-assisted ultrafiltration [Tuncay *et al.*, 1994; Juang and Chiou, 2000; Molinari *et al.*, 2007]. This process has become a new branch of ultrafiltration. Besides the heavy metal ions, PEUF process is also considered to have potential uses in removing some organic matter, if suitable interacting polymers are available.

This chapter will provide the background information about the fundamentals of polymer-enhanced ultrafiltration, as well as the ultrafiltration membranes commonly used. The nature of polymer-metal interactions will also be reviewed here. In addition, some other techniques for heavy metal separation are briefly introduced as well to have a better understanding of the advantages and characteristics of PEUF.

2.1 Ultrafiltration membrane technology

Ultrafiltration technology is a pressure-driven membrane process for liquid separations. There is little fundamental difference between UF and such other conventional membrane processes in water treatment as microfiltration (MF), nanofiltration (NF), and reverse osmosis (RO), except for the sizes of the pores on the membrane and the substances to be rejected. The membrane separation is primarily based on size exclusion. Normally, UF is able to retain molecules with sizes in the order of 100 nm. Figure 2.1 shows the size range of solutes that can be separated using UF and other membrane processes [Fane *et al.*, 2011].
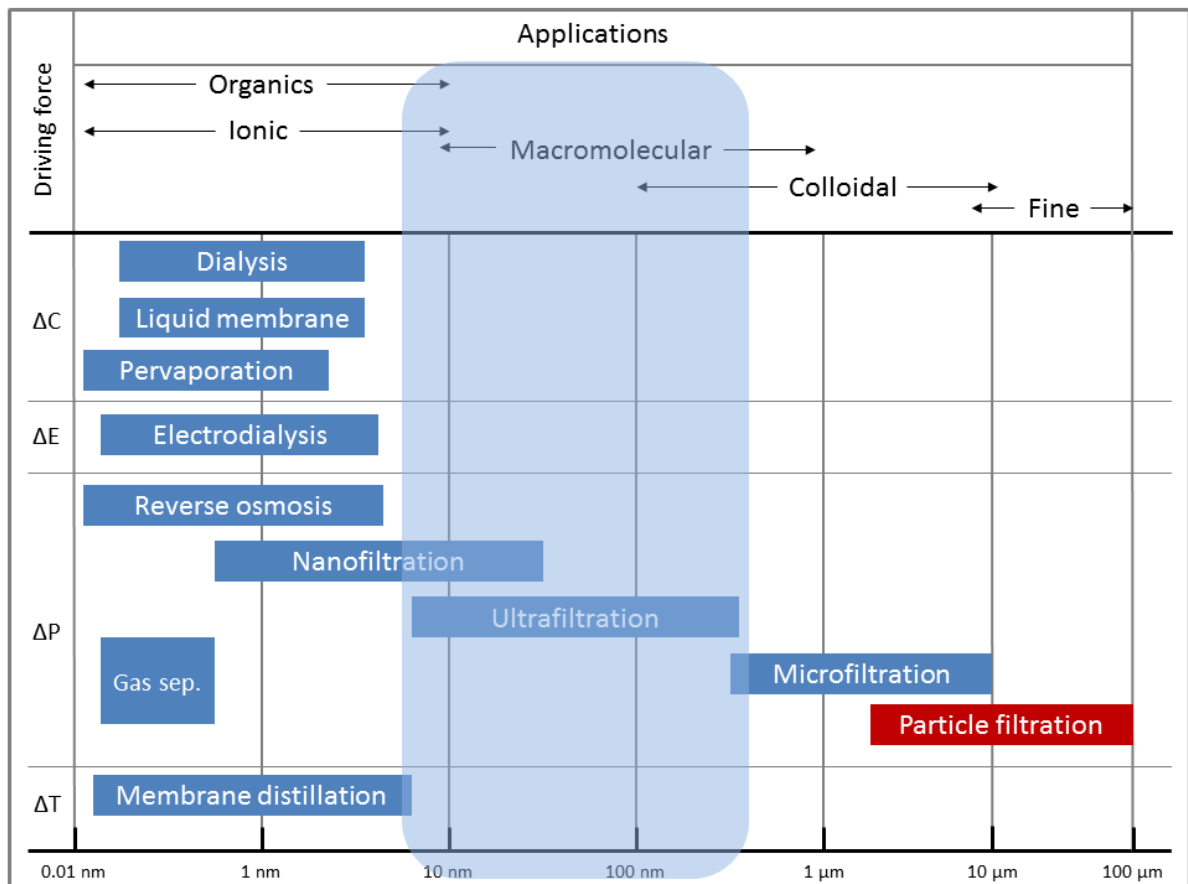
Figure 2.1 The family of membrane processes [Fane *et al.*, 2011]

UF process was mainly used to remove particles and macromolecules from industrial wastewater in the early days. With the rapid development of UF technology, it has expanded its application from wastewater and water treatment to the processing of biological macromolecules [Ghosh, 2009]. Bacteria, virus, colloids, and macromolecules in the molecular weight range of 1000 to 300,000 Da can be retained by UF membranes [Mulder, 1991; Fane *et al.*, 2011].
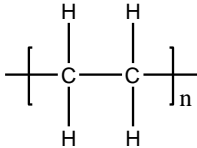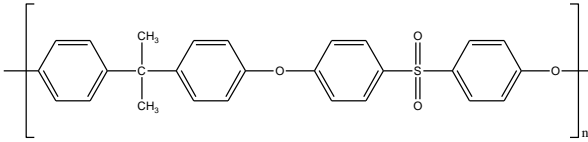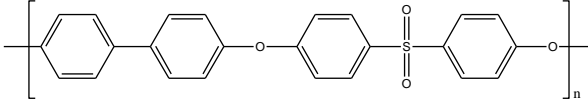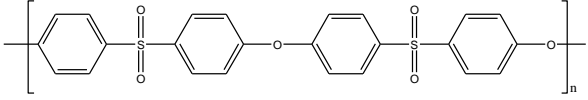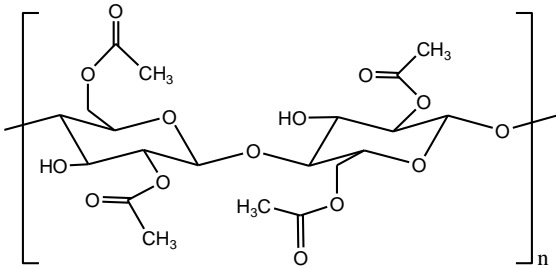
2.1.1 Membrane

The membrane, a selective barrier for separation, is the most important component in UF process. The permeability and selectivity are highly related to the membrane pore structure and materials. In general, the materials for UF membrane should possess high mechanical strength, chemical resistance, thermal stabilities, and the ability to form hollow fibre or flat sheet membranes easily [Fane *et al.*, 2011; Liu *et al.*, 2011]. UF is a relatively mature industrial separation process and UF membranes are produced commercially via the phase-inversion process, which is the primary process for membrane manufacturing.

Polymers are the most commonly used materials for fabricating UF membranes. Commercial UF membranes have been manufactured from various polymers, including hydrophobic polymers, (e.g., polyethylene (PE) [Bryjak and Gancarz, 1994], polysulfone (PS) [Tweddle *et al.*, 1983], polypropylene (PP) [Matsuyama *et al.*, 2000], polyethersulfone (PES) [Chaturvedi *et al.*, 2001]), and hydrophilic polymers (e.g., cellulose acetate [Kutowy and Sourirajan, 1975]). Table 2.1 lists some commercial polymeric membrane materials [Rivas *et al.*, 2003; Ghosh, 2009; Fane *et al.*, 2011]. The membrane materials, associated with the membrane surface properties (e.g., interfacial interaction, hydrogen bonding, charge transfer effect, and electrostatic effect) strongly influence the performance of ultrafiltration. Typically,
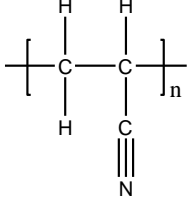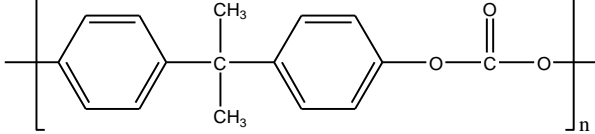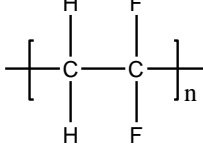
a hydrophilic membrane surface is less susceptible to fouling than a hydrophobic surface, but it often has the drawback of being less robust. Membrane modifications (e.g., blending, grafting, and the use of additives as pore formers) have been used to improve the performance of UF membranes [Yan *et al.*, 2005; Qiu *et al.*, 2008; Liu *et al.*, 2009].

Table 2.1 Commercial UF membrane materials and properties [Fane *et al.*, 2011]

Polymer	Molecular structure	Properties
Polyethylene (PE)		▪ Crystalline polymer ▪ Highly Hydrophobic ▪ Excellent chemical resistance that cannot be attacked by strong acids or bases
Polysulfone (PS)	 Udel polysulfone Radel polyphenylsulfone	▪ Amorphous polymer ▪ Great chemical, mechanical, hydrolytic, and thermal stability ▪ Also frequently applied in the formation of support layer for RO, NF, and some gas separation membrane
Polyethersulfone (PES)		▪ Wide temperature, pH, and chlorine tolerance ▪ High rigidity and dimensional stability ▪ Slightly less
Cellulose acetate (CA)		▪ Highly hydrophilic and crystalline ▪ Low chemical and oxidation resistances ▪ Vulnerable to hydrolysis microorganism attack ▪ Only stable over pH range from 4 to 6.5

(continued)

11

Table 2.1 (continued)

Polyacrylonitrile (PAN)		▪ Hard, rigid thermoplastic polymer ▪ Superior resistance to oxidation and hydrolysis ▪ Mainly used in UF membrane and composite membrane support
Polycarbonate (PC)		▪ Very good mechanical strength ▪ Transparent thermoplastic with high-performance properties ▪ Mainly used for track-etched membranes with well-defined structures ▪ Can be used to make UF and MF membranes by phase-inversion process
Polyvinylidene fluoride (PVDF)		▪ Semi-crystalline polymer with low glass transition temperature ▪ Excellent thermal and chemical stability ▪ The most popular hydrophobic material for UF membrane

2.1.2 Basic theory of ultrafiltration

Solvent transport through an UF membrane is related to the transmembrane pressure, often in the range of 0.1-0.5 MPa [Ghosh, 2009]. The mass transport through a membrane is usually expressed in terms of permeation flux, which is typically calculated by dividing the volumetric or mass flow rate by the effective membrane area. Various models have been developed to describe the mechanism of mass transport in UF [Porter, 1972; Bouchard *et al.*, 1994; Fane *et al.*, 2011]. On the basis of the irreversible thermodynamics model [Evans *et al.*, 2009; Fane *et*

al., 2011], which is one of the commonly used models in the analysis of UF, the volumetric

flux J_v is related to transmembrane pressure by [Evans *et al.*, 2009]:

$$J_v = L_p(\Delta P - \sigma \Delta \pi) \tag{2.1}$$

where L_p is the solvent permeability coefficient of the UF membrane, σ is the reflection

coefficient, ΔP is the transmembrane pressure difference, and $\Delta \pi$ represents the solute osmotic

pressure difference between the membrane walls on feed side and permeate side. In this model,

an assumption was made that there was no membrane fouling (including subsequent resistance

to permeate flow) and that the permeation flux was just a result of the trans-membrane pressure

gradient and the induced osmotic pressure difference [Denisov, 1994; Evans *et al.*, 2009].

Figure 2.2 illustrates the mass transport in UF.

The permeability coefficient L_p is the intrinsic property determined by the membrane and

the solvent in the feed involved (water in most cases), and it is a constant for given membrane

and feed solution systems. The reflection coefficient σ is however more complicated. It is a

representation of the retention ability of UF membrane to retain a solute while allowing passage

of the solvent, and it has a value in the range between 0 and 1. When the membrane shows no

rejection with respect to the solute in the feed solution, $\sigma = 0$. This means the solute molecules

can pass through the membrane freely, resulting in no concentration difference across the

membrane and thus the osmotic pressure difference $\Delta \pi$ in equation (2.1) is zero. The permeate

flux J_v is thus only a function of transmembrane pressure gradient ΔP. The pure water flux and

the rejection of small molecules (i.e., salts) in aqueous solutions by most UF membranes

belong to this case. On the other hand, if the membrane can reject all the solutes completely,

then $\sigma = 1$ and the osmotic pressure difference reaches maximum [Fane *et al.*, 2011]. In reality,

a typical value of σ between 0 and 1 indicates coupled transports of solvent and solute across the membrane [Bitter, 1991].
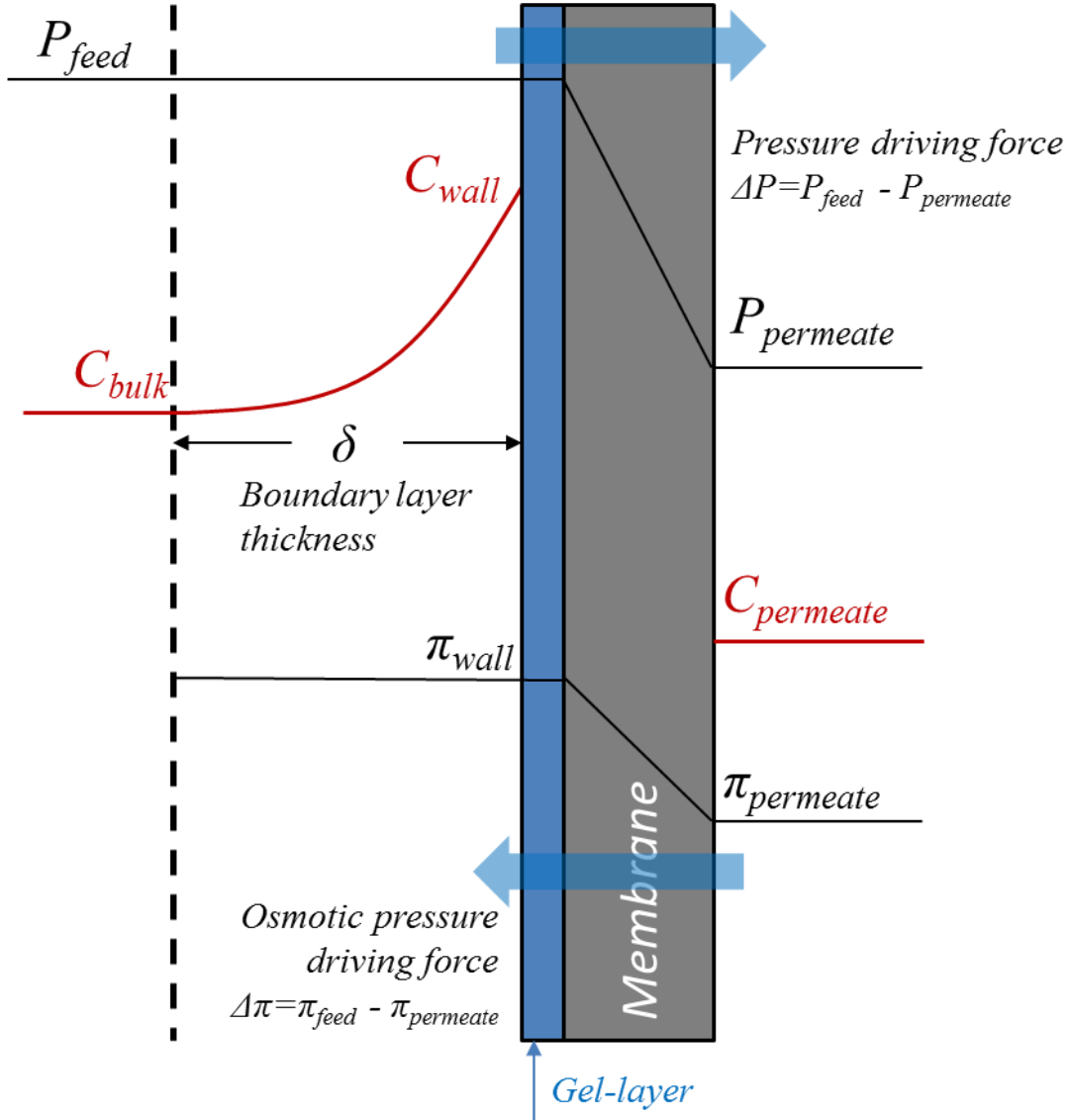
Figure 2.2 Schematic representation of mass transport in UF [Evans *et al.*, 2009]

In fact, the water flux through UF membranes can be described by empirical models on the basis of the Hagen-Poiseuille equation for membranes with cylindrical-pores:

$$J_v = \frac{\varepsilon r_p^2 \Delta P}{8 \eta \tau l_m} \tag{2.2}$$

or the Kozeny-Carman equation for membranes with pores formed by stacked spheres:

$$J_v = \frac{\varepsilon^3 \Delta P}{K(1-\varepsilon)^2 S^2 \eta l_m}$$ (2.3)

where η is the viscosity of the solvent, ε the membrane porosity, r_p the pore radius, τ the tortuosity of the pores, K the Kozeny-Carman coefficient, S the pore internal surface area, and l_m is the membrane thickness. Both equations shows that the solvent flux is proportional to the transmembrane pressure difference. It is actually a special case of the aforementioned irreversible thermodynamics model with $\sigma = 0$, and the proportionality constant is just a more detailed expression of the solvent permeability L_p taking into account of the membrane structure [Fane *et al.*, 2011].

The ability of UF membrane to reject a specific solute in the feed is usually expressed in terms of solute rejection, which is defined as [Ho and Sirkar, 1992; Fane *et al.*, 2011]:

$$R_{int} = 1 - \frac{C_{permeate}}{C_{wall}}$$ (2.4)

where C_{wall} and $C_{permeate}$ represent the solute concentrations at membrane surface and in the permeate, respectively. However, the concentration near the membrane surface is not readily available, and the apparent solute rejection R_{app} is often used in practice:

$$R_{app} = 1 - \frac{C_{permeate}}{C_{bulk}}$$ (2.5)

clearly, when membrane fouling or concentration polarization occurs, C_{wall} in equation (2.4) will be greater than the bulk concentration C_{bulk}, and the observed apparent solute rejection is thus lower than the actual solute rejection the membrane exhibits [Ho and Sirkar, 1992; Fane *et al.*, 2011].

As shown in Figure 2.2, the solute rejection by the membrane will lead to the accumulation of solute molecules near the membrane surface on the feed side, forming a boundary layer. This concentration build-up phenomenon adjacent to the membrane surface is called concentration polarization. It has been proved that a higher trans-membrane pressure gradient will result in more severe concentration polarization on the membrane surface for a given system [McDonogh *et al.*, 1995; Macedo *et al.*, 2011]. The detailed treatments about concentration polarization can be found elsewhere [Porter, 1972; Denisov, 1994; Zaidi and Kumar, 2004; Fane *et al.*, 2011].

2.1.3 Membrane fouling

Membrane fouling due to deposition of solutes on a membrane surface or inside membrane pores [Fane *et al.*, 2011], is another problem that results in a flux decline. The mechanism of membrane fouling can be different, depending on the nature of the foulants. Normally, four types of fouling can be distinguished: (1) adsorption of solute from feed solution to the membrane surface [Aimar *et al.*, 1988; Hanemaaijer *et al.*, 1989; Koltuniewicz and Noworyta, 1994], (2) clogging of the pores by colloids [Hanemaaijer *et al.*, 1989; Koltuniewicz and Noworyta, 1994; Fane *et al.*, 2011], (3) deposition of insoluble salts or solids due to chemical precipitation or crystallization [Gilron and Hasson, 1987; Koltuniewicz and Noworyta, 1994], and (4) gel-layer formed by macromolecules or microorganisms [Celik *et al.*, 2011; Fane *et al.*, 2011]. Membrane fouling will result in an increase in the mass transport resistance to solvent and thus a reduced solvent permeation flux at a given operating pressure; severe membrane fouling will also reduce the lifetime of the membrane [Koltuniewicz and Noworyta, 1994].
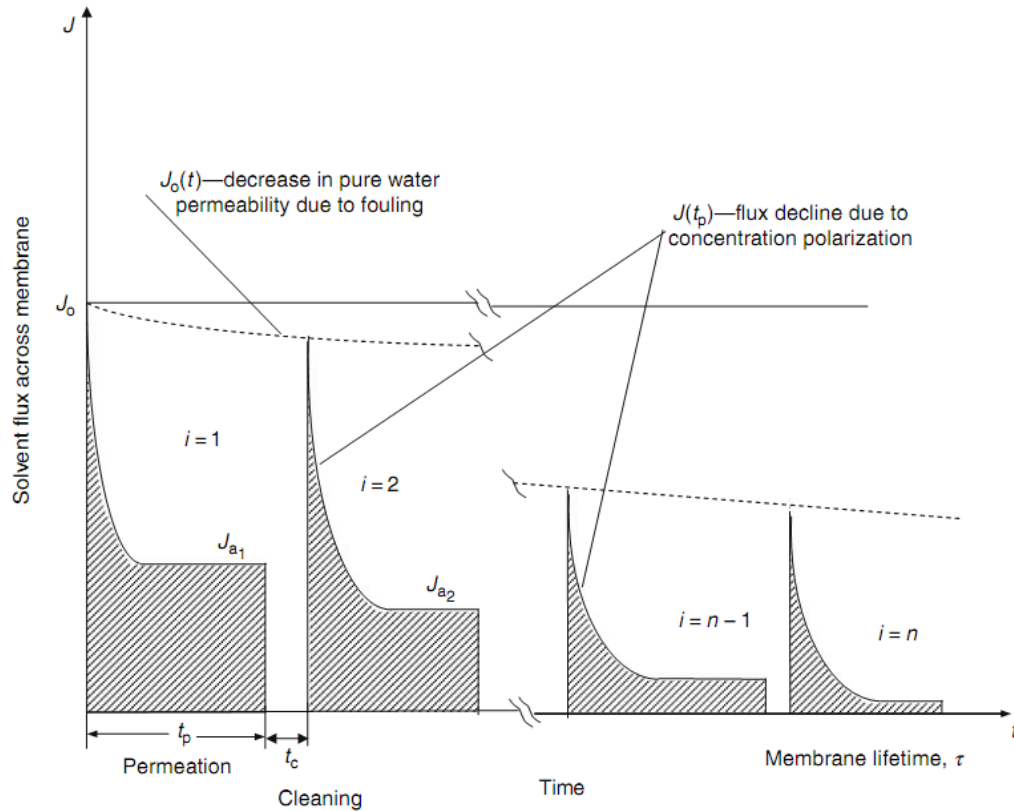
Figure 2.3 Typical flux–time plot during cyclic operation in large-scale ultrafiltration systems [Koltuniewicz and Noworyta, 1994; Goosen *et al.*, 2009]

Koltuniewicz and Noworyta [1994] have analysed concentration polarization and membrane fouling that are responsible for the flux decline during ultrafiltration operation. Figure 2.3 shows the flux variation of an UF membrane during its lifetime, including cyclic cleaning. In the initial period of each cyclic operation, the flux decreases dramatically due to concentration polarization, expressed as $J(t_p)$ in Figure 2.3. This happens in every cycle, since concentration polarization is an inherent phenomenon in UF and cannot be avoided. The flux decline between the cycles, $J_0(t)$, and the average flux decline under the steady-state, J_a (i.e., $J_{a1}>J_{a2}$) are shown to result from membrane fouling. In addition, the average flux decline J_a suggests that an irreversible fouling happens during the UF process [Goosen *et al.*, 2009].

17

Hermia developed four empirical fouling models that described the flux decline in ultrafiltration. The mathematical expressions of the four models are [Vela *et al.*, 2008]:

(a) Standard pore blocking

$$J = J_0(1 + \frac{1}{2}K_s AJ_0 t)^{-2} \tag{2.6}$$

(b) Intermediate pore blocking

$$J = J_0(1 + K_i AJ_0 t)^{-1} \tag{2.7}$$

(c) Cake layer formation

$$J = J_0[1 + 2K_c(AJ_0)^2 t]^{-\frac{1}{2}} \tag{2.8}$$

(d) Total pore blocking

$$J = J_0 \exp(-K_t t) \tag{2.9}$$

where K_s (L^{-1}), K_i (L^{-1}), K_c (h·L^{-2}) and K_t (h^{-1}) are the empirical fouling coefficients in the models, J_0 is the initial permeation flux and A is the membrane area.

Figure 2.4 demonstrates the proposed mechanisms for the four models. The standard pore blocking model considers that the solutes deposite over the pore walls. It is assumed that the pores of the membrane have a constant diameter and length along the whole membrane. The intermediate pore blocking model assumes that a solute molecule may block the pores when it approaches an open pore. The solutes can also stack onto another solute molecules that are readily settled. Unlike the former two models, the total pore blocking model considers that the membrane pores are completely blocked when the solutes reach the membrane surface. It does not consider the stack effect of solute on membrane surface. For cake layer formation, it is believed that all the solutes are deposited on the membrane surface and do not penetrate into the membrane, forming a cake layer of solutes [Vela *et al.*, 2008].
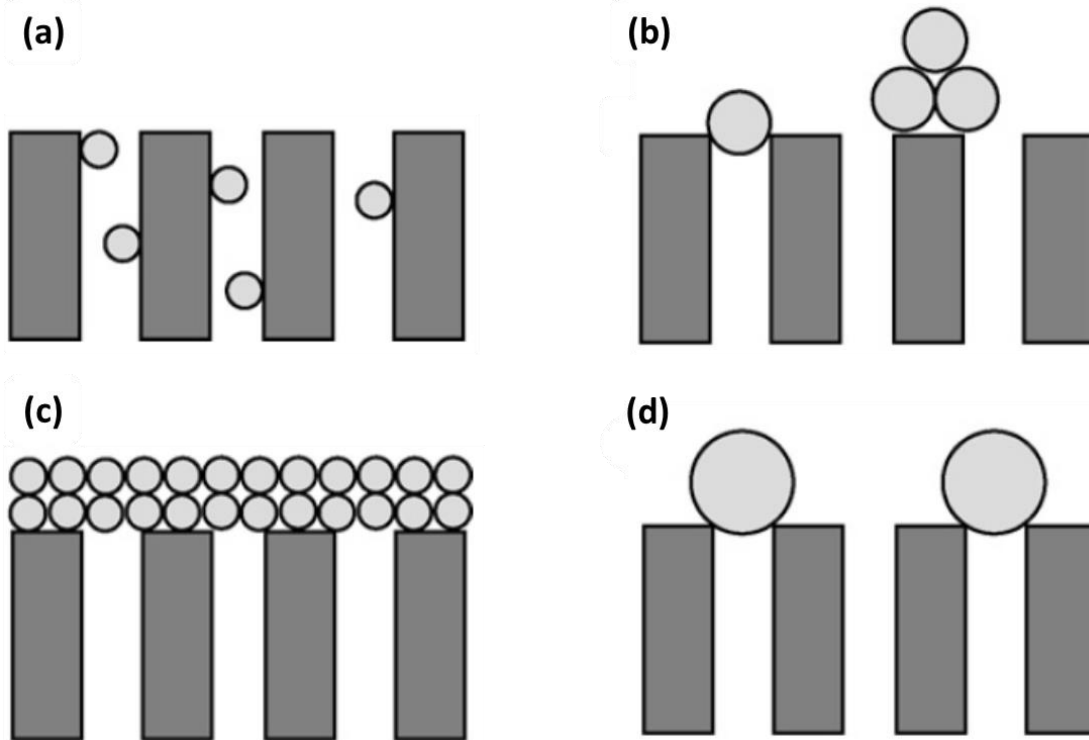
Figure 2.4 Illustration of the fouling mechanisms expressed by the models: (a) standard pore blocking, (b) intermediate pore blocking, (c) cake layer formation and (d) total pore blocking [Vela *et al.,* 2008]

A great deal of work has been done on proper selection of membrane materials and chemical pre-treatment of the membranes, in order to reduce membrane fouling. The details of reduction of membrane fouling are not discussed here, and more information can be found in literature.

2.2 Polymer-enhanced ultrafiltration

In PEUF, the properties of chelating polymers used will influence the UF performance. Here, the general principles of the PEUF, the water-soluble polymers used in the process and the polymer-metal interactions will be discussed.

2.2.1 Principles of PEUF

UF process used for separation of proteins or macromolecules are normally not capable of separating soluble metal ions from aqueous solutions. Almost all the soluble ions can pass through UF membranes because of the large pore sizes of the membranes. Thus in order to retain metal ions with UF membranes, other special technical aids should be used. According to the coordination chemistry, heavy metal ions can interact with ligand molecules in aqueous solutions to form coordination compounds or complexes. The strength of the interactions between the metal ions and ligands increase with an increase in the electron-accepting ability of the metal ion [Snceyink and Jenkins, 1980]. Such interactions can be exploited to bind the metal ions, followed by UF to filter water or other solvents, thereby achieving separation of metal ions from the solution.

Functional groups in water-soluble polymers, such as carboxyl, amine and sulfonic groups, can interact with heavy metal ions to form polymer-metal complexes [Radeva, 2001; Rivas *et al.*, 2003]. Such macromolecular complexes can be readily rejected by UF if the molecular weight of the polymer is greater than the MWCO of the UF membrane [Rivas *et al.*, 2003]. While the heavy metals attached to the polymer are rejected by the membrane, some un-bonded free ions can still pass through the membrane. A schematic diagram of this process, shown in Figure 2.5 [Palencia *et al.*, 2009], is called polymer-enhanced ultrafiltration [Doğanay *et al.*, 2011], polymer-assisted ultrafiltration [Molinari *et al.*, 2006; Cojocaru *et al.*, 2009], or polyelectrolyte-enhanced ultrafiltration [Li *et al.*, 2008] if ionic polymers are used, or simply enhanced ultrafiltration. Apparently, the stronger the interactions between the metal ions and the polymer, the better the performance of the ultrafiltration for separation of heavy metal ions from a solution. Many parameters, (e.g., metal species, polymer type, pH of the

20

solution and ionic strength of the metals in the solution) will influence the ultrafiltration performance.

The basic principle of PEUF is no different from conventional UF, except that water-soluble polymers are added in the feed to "bind" the metal ions. Generally, both cross-flow mode (where the feed fluid flows tangentially to the membrane surface) and dead-end mode (where the feed fluid is caused to move perpendicular to the membrane) can be utilized in PEUF. Since the interaction between metal ions and soluble polymers is the key factor that influences the UF performance, any factors (e.g., pH of solution, temperature and ionic strength of metals in the solution) that influence the polymer-metal interactions will have an impact on the performance of PEUF. Depending on molecular weights of the polymers used in PEUF, UF membranes with a MWCO of 1000-300,000 Daltons appear to be suitable for PEUF.
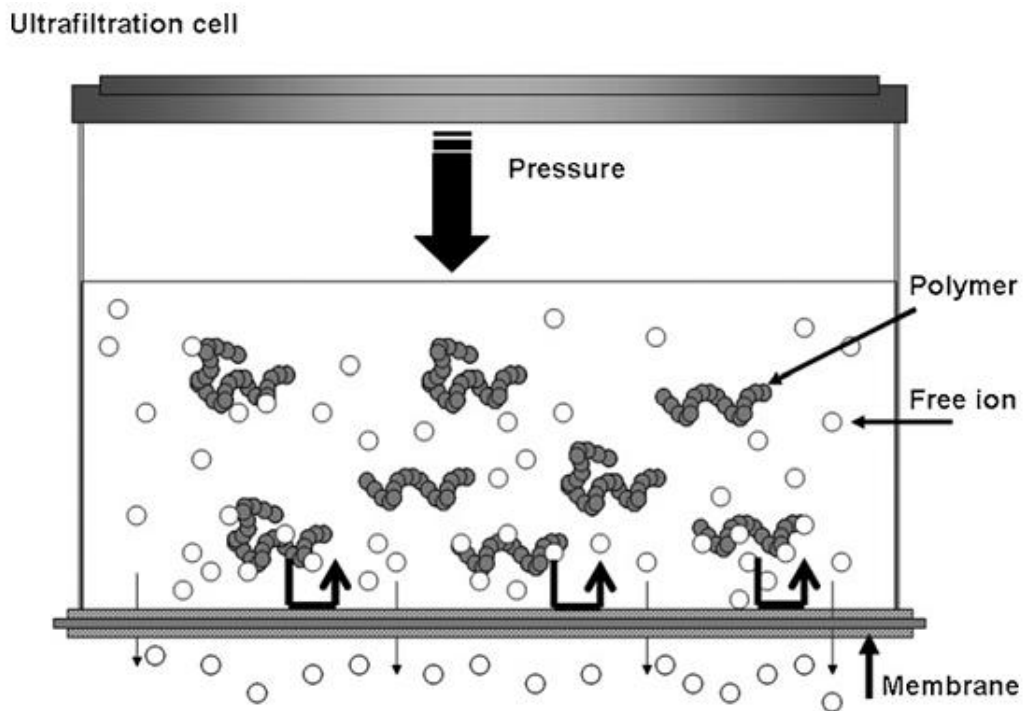
Figure 2.5 Polymer-enhanced ultrafiltration [Palencia *et al.*, 2009]
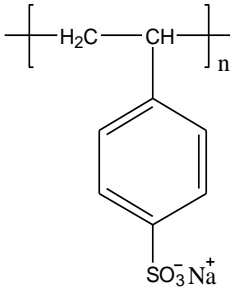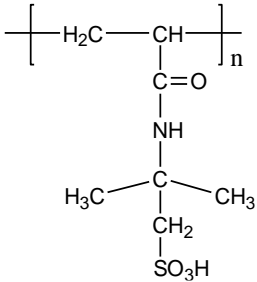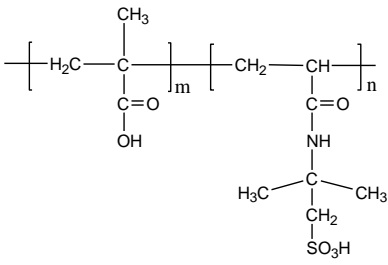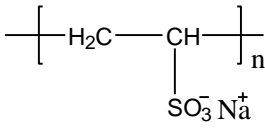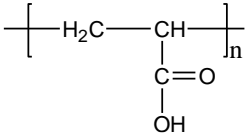
2.2.2 Water-soluble polymers used in PEUF

In general, water-soluble polymers can be classified into two categories: polyelectrolytes and polychelatogens (polymers containing chelating groups) [Rivas *et al.*, 2003]. Polyelectrolytes are the "polymers bearing ionisable groups, which, in polar solvents, can dissociate into charged polymer chains (macro-ions) and small counter-ions" [Barat and Joanny, 1996; Radeva, 2001], and polychelatogens are those which have functional chelating groups that can form coordination bonds with ions in aqueous media. Both types of polymers have the potential to be used in the removal of heavy metal ions by PEUF in view of their ion-exchange groups or chelating functions.

The functional groups in polyelectrolytes used in PEUF may include sulfonic acid, carboxyl and ammonium salt groups. These polymers are either commercially available or can be synthesized by copolymerization or grafting. In 1990, Scamehorn et al. [1990] used poly(sodium 4-styrenesulfonate) (PSS) as the functional polymer to remove Cu(II) by PEUF. The measured rejection reached 99%, and a relative high rejection (96%) was observed even after membrane fouling and concentration polarization occurred during the process. Recently, Korus [2012] and Palencia et al. [2011] further studied the performance of PSS to separate divalent ions (Cd(II), Zn(II), Ni(II)) using PEUF. A rejection of greater than 99% was obtained for Ni(II) and Zn(II) by adjusting the pH and polymer concentration [Korus, 2012], and a rejection of 80% for Cd(II) was obtained by Palencia *et al*. [2011]. Besides the commercial polymer PSS, several other lab-synthesized polymers containing sulfonic acid groups were also used to remove metal ions by PEUF [Rivas *et al.*, 2002]. Carboxyl group is another common functional group in polyelectrolytes. The possibility of using such polymers as poly(acrylic acid) (PAA), poly(methacrylic acid) (PMA) and poly(acrylic acid-co-maleic acid)
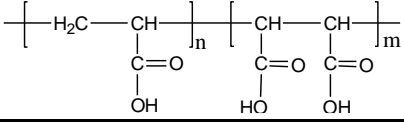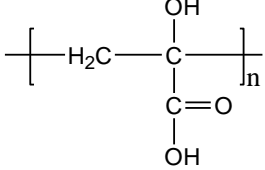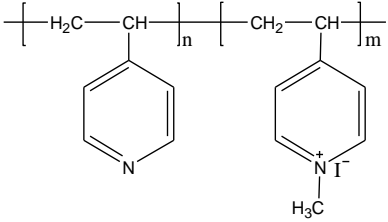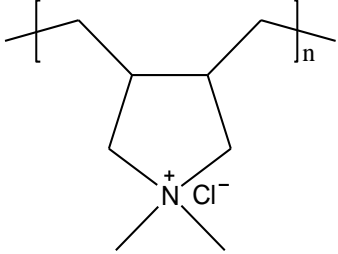
for the removal of heavy metal ions using PEUF has been also studied. Similar to the polymers containing sulfonic acid groups, polyelectrolytes containing carboxyl groups can interact with metal ions as well. It was shown that the copolymer of acrylic acid-maleic acid performed better than PAA for the removal of Ni(II) [Borbély and Nagy, 2009; Labanda *et al.*, 2009; Gao *et al.*, 2012]. The reason is still not very clear, but the larger number of carboxyl groups in the copolymer could be attributed to the better performance. In addition, polymers containing ammonium groups (e.g., quaternized polyethylenimine [Strathmann, 1980]) were also shown to be able to separate heavy metals from aqueous solutions using PEUF [Chaufer and Deratani, 1988]. The polymers used and metal ions separated using PEUF are summarized in Table 2.2. It needs to be pointed out that the counter-ions dissociated from the polyelectrolyte backbones may cause secondary pollution to the permeate stream obtained. This potential problem with the use of polyelectrolyte may affect its wide applications in PEUF if ion-free solvent (water) on the permeate side is needed.

Table 2.2 Water-soluble polyelectrolytes used in polymer-enhanced ultrafiltration

Polymer name and structure	Heavy metals	Membrane used Type	MWCO	Reference
Poly (sodium 4-styrenesulfonate)	Zn(II), Cu(II), Ni(II).	PS PAN	- -	[Korus, 2012]
	Cu(II), Cd(II).	PES	10 kDa	[Palencia et al., 2011]
Poly (2-acrylamido-2-methyl-1-propanesulfonic acid)	Cu(II), Cd(II), Co(II), Cr(II), Zn(II), Ni(II), Ag(I).	Filtron	5 or 100 kDa	[Rivas et al., 2000]
Poly (methacrylic acid-co-2-acrylamido-2-methyl-1-propanesulfonic acid)	Cu(II), Cd(II), Co(II), Hg(II), Zn(II), Ni(II), Ag(I).	-	5 kDa	[Rivas et al., 2001]
Poly (vinyl sulfonic acid)	Cu(II), Cd(II).	PES	10 kDa	[Palencia et al., 2011]
	Ni(II), Cu(II), Co(II), Zn(II), Cd(II), Pb(II).	PES	10 kDa	[Palencia et al., 2009]
Poly (acrylic acid)	Cu(II), Cd(II).	PES	10 kDa	[Rivas and Palencia, 2011]
	Ni(II).	PES	30 kDa	[Shao et al., 2013]
	Ag(I), Cu(II), Co(II), Cr(III).	-	-	[Rivas et al., 2002]

Table 2.2 (continued)

Poly (acrylic acid-co-maleic acid)	Cr(III).	CM[a]	15 kDa	[Labanda *et al.*, 2009]
	Ni(II).	PES	20 kDa	[Gao *et al.*, 2012]
Poly (α-hydroxyacrylic acid)	Cu(II), Fe(II).	Iris 3038	-	[Nguyen *et al.*, 1980]
Poly (1-vinylpyrrolidone-co-2-dimethylaminoethylmethacrylate quaternized)	Ag(I), Hg(II).	Filtron	5 kDa	[Rivas and Pereira, 2001]
Poly (diallyldimethyl ammonium chloride)	Arsenic anion	PES	10 kDa	[Pookrod *et al.*, 2004; Gallo *et al.*, 2006]

[a]CM: ceramic membrane

Polyethyleneimine, a polymeric amine, has been studied extensively as a chelating polymer in PEUF to remove heavy metal ions from aqueous solutions since Geckeler et al. [1980] first investigated the preparation and application of PEI and its derivatives. The approximate ratio of primary, secondary and tertiary amino groups present in PEI can be different (usually 1:1:1 or 1:2:1), depending on their manufacturers. Its good water solubility,

large amount of chelating amino groups and commercial availability make PEI an excellent chelating agent in PEUF. In addition, selective interaction with several uncommon metal ions (e.g., palladium, mercury, gold and platinum) can be achieved by introducing certain chelating groups such as thiourea, iminodiacetic acid, pyridine-2-aldimine, and hydroxyaniline to the PEI chains by copolymerization or grafting [Geckeler *et al.*, 1980]. The chelating abilities of PEI and its derivatives towards different metal ions have been tested and analyzed. [Bayer *et al.*, 1980; Geckeler *et al.*, 1980; Bayer *et al.*, 1985; Spivakove *et al.*, 1985; Geckeler *et al.*, 1986]. Besides PEI, a few other macromolecular chelating agents have also been developed via polymerization of monomers containing chelating groups or chemical modification of existing polymers. Geckeler and his research group have continued to synthesize new chelating polymers since 1991, including poly(N-hydroxyethyl ethyleneimine) (PHEI) and poly(N-acetyl ethyleneimine) (PAEI) which have hydroxyl and carbonyl groups on the polymer chains, respectively. These polymers have been tested for the retention of various inorganic ions through PEUF. In recent years, PEUF has been expanded to the removal of some semi-metalloid ions from aqueous solutions; for instance, Doganay et al. [2011] synthesized poly(glycidylmethacrylate) (PNS) to remove boron from aqueous media.
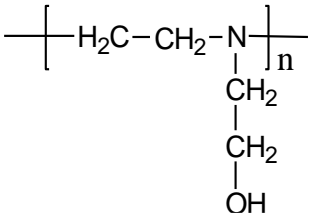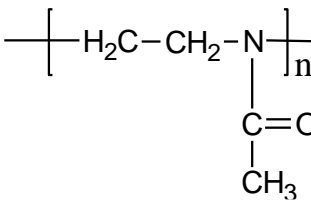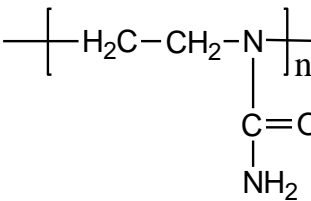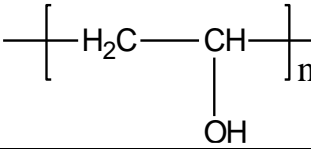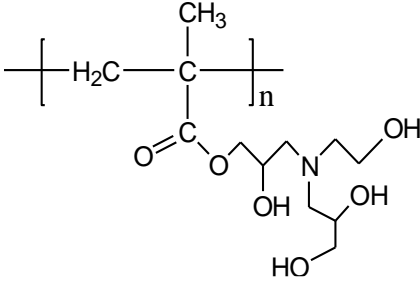
Table 2.3 Water-soluble chelating polymers used in polymer-enhanced ultrafiltration

Polymer name and structure	Heavy metals	Membrane used		Reference
		Type	MWCO	
Poly (ethyleneimine) and its derivatives:				
Poly (ethyleneimine) 	Co(II), Cu(II), Ni(II), Cd(II).	-	-	[Geckeler *et al.*, 1980]
	Cu(II), Ni(II), Zn(II), Cd(II).	-	-	[Rajesh *et al.*, 2011]
Poly (ethyleneimine N-methyl-N-thio-urea) 	Au(III), Pt(IV), Hg(II).	-	-	[Geckeler *et al.*, 1980]
Poly (ethyleneimine N-pyridine-2-aldimine) 	Fe(II).	-	-	[Geckeler *et al.*, 1980]
Poly (ethyleneimine acetic acid) 	Cu(II), Pd(II), Ag(I).	-	-	[Geckeler *et al.*, 1980]

(Continued)

Table 2.3 (Continued)

Other chelating polymers:
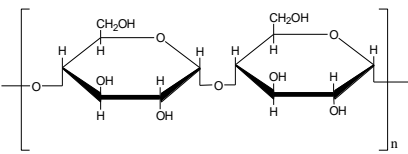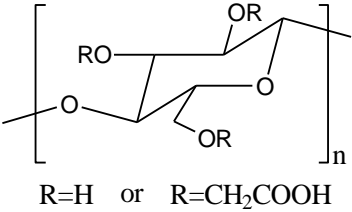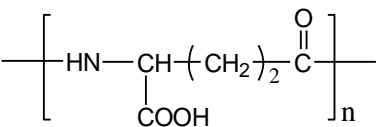
Poly (N-hydroxyethyl) ethyleneimine	Cu(II), Cd(II). Ni(II), Co(II), Zn(II), Cr(III), Fe(III), Pb(II).	UM-1[a]	1 kDa	[Geckeler et al., 1991]

Poly (N-acetyl) ethyleneimine	Cu(II), Cd(II). Ni(II), Co(II), Zn(II), Cr(III), Fe(III), Pb(II).	UM-1[a]	1 kDa	[Geckeler et al., 1992]

Poly (acrylamide)	Cu(II), Cd(II). Ni(II), Co(II), Zn(II), Cr(III), Fe(III), Hg(II).	Filtron	10 kDa	[Rivas and Villoslada, 1998]

Poly (vinyl alcohol)	Hg(II), As_2O_3.	CCM[b]	-	[Jana et al., 2011]
	Cr(III).	Tubular	15 kDa	[Labanda et al., 2009]
	Co(II).	PLCC[c]	5 kDa	[Uzal et al., 2011]

Poly (glycidylmethacrylate)	H_3BO_3.	PES	5 kDa	[Doğanay et al., 2011]

[a]UM-1: Amicon UM-1 membrane

[b]CCM: Self-prepared chitosan based ceramic membrane

[c]PLCC: PLCC04310 cellulose flat sheet membrane

Poly(vinyl alcohol) (PVA) is highly water soluble and seems to be able to chelate heavy metal ions because of the great number of hydroxyl groups. However, Uzal et al. [2011] and Labanda et al. [2009] showed that the rejections of Co(II) was merely 30% and there was no rejection to Cr(III) at all when PVA was used as the chelating agent in PEUF. However, after the PVA was modified by sulfonation by which the hydroxyl groups are converted into sulfonic acid groups, the rejection of Co(II) increased up to 99% [Uzal *et al.*, 2011]. Interestingly, PVA showed great retention ability for mercury and arsenic by PEUF [Jana *et al.*, 2011], indicating that the strength of coordination bond between a metal ion and a chelating polymer highly depends on the nature of the metal species and the chelating groups in the polymer. The chelating polymers used in PEUF are summarized in Table 2.3.

Several natural and synthetic bio-polymers with chelating groups have been investigated for the separation of metal ions by PEUF as well. In the early 1980s, Nguyen et al. [1980] exploited the interaction between iodine and amylose, a linear bio-polymer made up of D-glucose units to remove iodine from a solution. Later, cellulose polymers also attracted attention [Barakat and Schmidt, 2010] for the rejection of three metal ions (Ni(II), Cu(II), Cr(III)) where carboxy-methyl cellulose was used as the chelating polymer. The metal rejection reached around 95% at pH = 6. Another biodegradable polymer, poly(γ-glutamic acid) (γ-PGA), was recently used to capture lead ions by chelating interactions, followed by UF [Hajdu *et al.*, 2012]. Although the bio-polymers have unique properties in terms of biocompatibility and biodegradability, their variant structures and presence of other impurity molecules in the natural polymers may become an issue in the application unless they can be fractionated and purified substantially. Table 2.4 lists some representative bio-polymers used in PEUF.

Table 2.4 Water-soluble bio-polymers used in polymer-enhanced ultrafiltration

Polymer name and structure	Species	Membrane used		Reference
		Type	MWCO	
Amylose 	Iodine	Iris 3038	-	[Nguyen *et al.*, 1980]
Carboxy methyl cellulose R=H or R=CH₂COOH	Cu(II), Ni(II), Cr(III).	PES	10 kDa	[Barakat and Schmidt, 2010]
Poly-gamma-glutamic acid 	Pb(II).	-	10 kDa	[Hajdu *et al.*, 2012]
	Fe(III).	-	10 kDa	[Bodnar *et al.*, 2013]
Pectin	Cr(III).	-	-	[Aroua *et al.*, 2007]
Humic substance	Co(II).	-	-	[Kim *et al.*, 2005]

2.2.3 Polyvinylamine related research in PEUF

Polyvinylamine is one of the more recent commercially available amine polymers formed from monomer vinylamine, which can quickly self-react [Pinschmidt, 2010]. Research work on PVAm synthesis started in early 1940s [Jones *et al.*, 1944; Reynolds and Kenyon, 1947]. Scientists used other indirect stable polymerization precursors like N-vinylacetamide instead of unstable vinylamine to prepare the PVAm. Although the preparation in the lab scale was successful, it still took 40 to 50 years to achieve the commercial availability of PVAm.

In fact, before the large scale manufacturing of PVAm, Bayer et al. [1980] already started to study the possibility of using self-prepared PVAm for the removal of heavy metal ions via

PEUF. They utilized the PVAm as the basic material to synthesize different macromolecular chelating agents, similar to what they did in the modification of PEI mentioned before. Three chelating molecules (that is, 2-pyridinecarbaldehyde, chloroacetic acid and N-methylisothiocyanate) that were highly selective for Fe(II), Cu(II) and Hg(II), respectively, were incorporated into PVAm chains by reacting with the active primary amines. The modification reactions of PVAm are illustrated in Figure 2.6
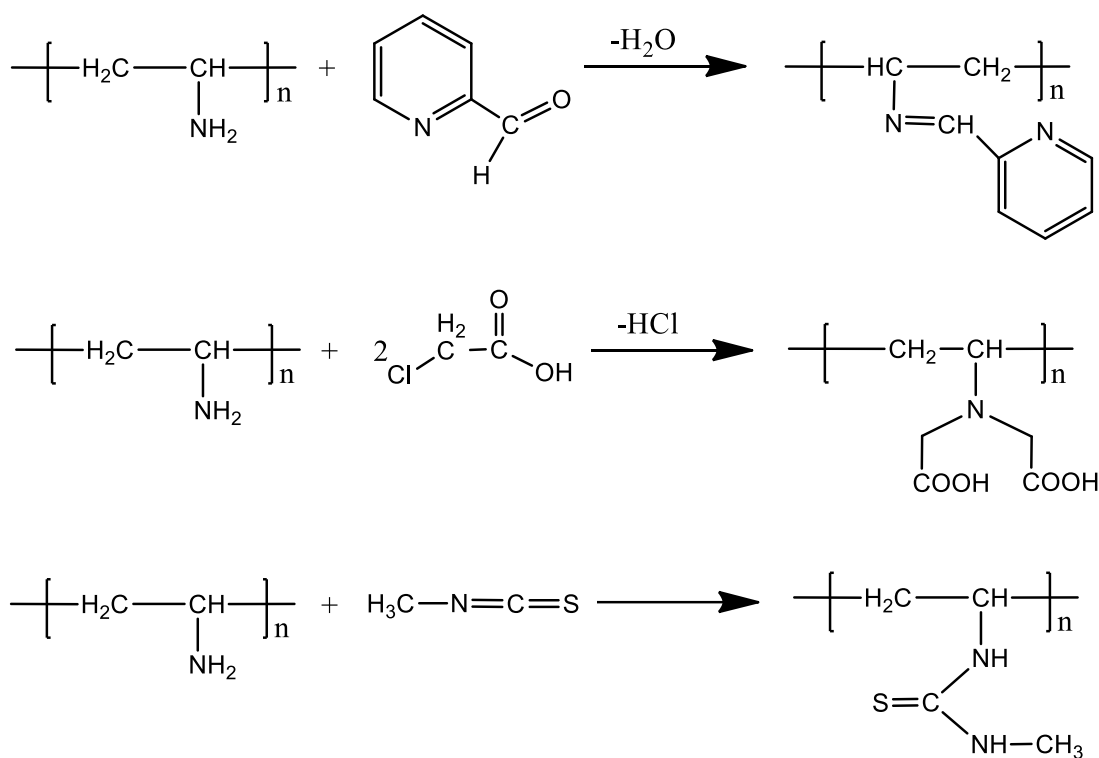
Figure 2.6 Modifications of PVAm [Bayer *et al.*, 1980]

However, the chemical modification by grafting specific functional groups onto PVAm chains will change its solubility in aqueous solution. The grafting reactions may consume the hydrogens on the primary amines and the grafted groups may have poor solubility in water. In addition, cross-linking reactions may also occur depending on the reagents used in the chemical modifications. The decrease in the polymer solubility can then make the modified PVAm

derivatives un-suitable for the PEUF process. However, the insoluble PVAm derivatives with specific functional groups may be used as a promising adsorbent for adsorption separation. Those grafted functional groups on PVAm still provide strong interactions, high binding capacity, and selectivity toward certain several heavy metals regardless of their water solubility. It actually expands the application of PVAm based materials in wastewater treatment.

2.2.4 Prospects for industrial application

Ultrafiltration is a relatively mature membrane separation process, and it has been used in industrial wastewater treatment or drinking water purification. However, the utilization of water-soluble polymers to remove heavy metals via PEUF makes the UF process much more complicated and large scale applications of PEUF are still not accomplished yet. Such operating parameters as temperature, pressure, presence of other contaminants, membrane lifetime and tangential velocity (cross-flow model), all influence the performance of the overall PEUF process. In fact, in order to optimize the operating conditions for practical applications, a pilot scale test is often needed. It is usually a cross-flow UF configuration with a recirculation loop. Technical variability and economic feasibility should be evaluated before a full-scale application can be commissioned. Figure 2.7 shows a schematic diagram of UF pilot set-up, where the main components of the process are illustrated.

Using PEI as chelating polymer, Uludag et al. [1997] investigated the effects of polymer concentration, feed pressure and feed flow rate on the performance of PEUF to remove mercury using a laboratory-scale continuous cross-flow UF system. It was shown that the operating pressure, feed flow and concentration of the added PEI had little effect on the mercury rejection, and it remained at a constant high value (98%) under the operating conditions tested. Later in another publication [Muslehiddinoglu *et al.*, 1998], a binary mixture

of mercury and cadmium was used as the model heavy metals in the wastewater, and a pilot scale UF system (Pilot scale SP20 UF system) and a laboratory-scale system were used. It was found that the rejection of mercury was not affected by the presence of cadmium in the feed solution, and the cadmium ions passed through the membrane while mercury ions were all retained, thereby separating mercury from cadmium.
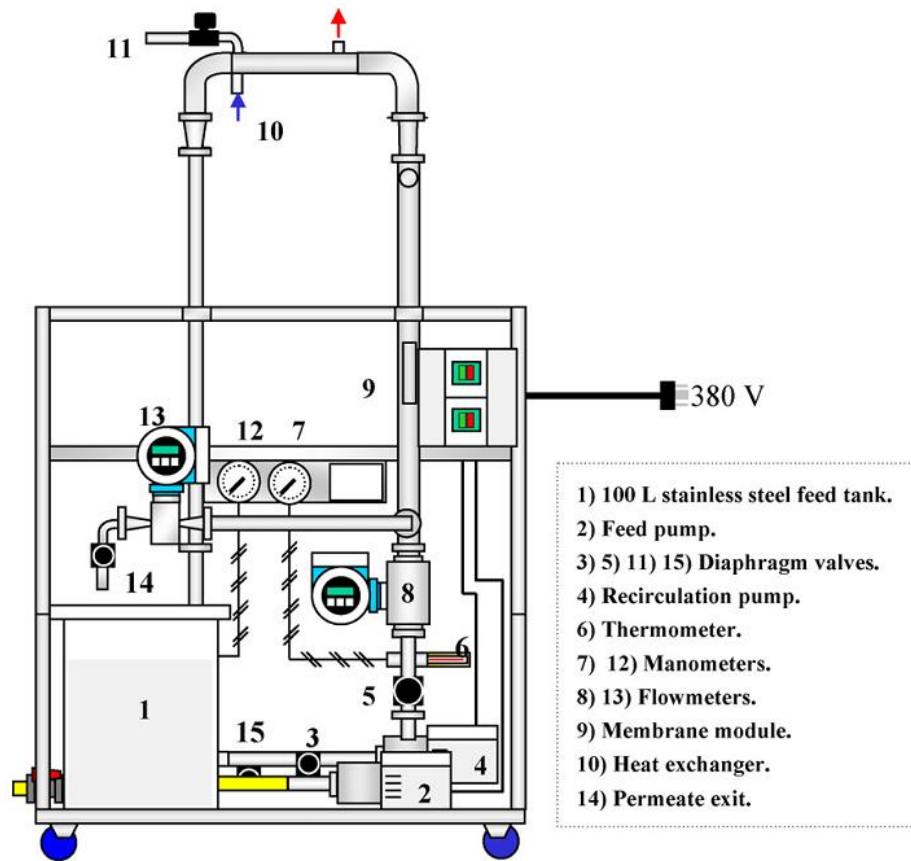
Figure 2.7 Schematic diagram of a UF pilot plant [Llanos *et al.*, 2009]

It may be mentioned that the composition of an industrial effluent wastewater can be quite complicated even after pre-treatments. All the components in the water will affect the performance of PEUF if the chelating interactions with the target components are affected. Thus, Schulte-Bockholt and Schuster [2008] used a PEUF to treat a real industrial phosphation

rinsing water to recover nickel, zinc and manganese phosphate with a two-stage pilot PEUF plant. Nickel and zinc were successfully enriched from around 20ppm to 1000ppm, and the concentrations of these two metals in the permeate stream never exceeded the discharge limits. Another team [Llanos *et al.*, 2009] also used a pilot scale set-up in a study to optimize their operating conditions (e.g., tangential velocity, trans-membrane pressure and temperature). A design equation relating the polymer bulk concentration and permeate flux was established, which can be used in the design of a specific PEUF operation. Besides heavy metal ions, the removal of semi-metalloid ions (i.e., arsenic and boron) via PEUF has also been studied in a pilot scale system [Dilek *et al.*, 2002; Gallo *et al.*, 2006], and the separation performance was not as good as for heavy metals removal.

These studies provide important information about the PEUF for a large scale of applications. However, much more work is needed for PEUF to develop to be a viable process because there are many variables (e.g., types of water-soluble polymer agents, different components in different industrial effluent water, and membrane type) involved.

2.3 Polymer-metal ion interactions

Generally, two major types of interactions between water-soluble polymers and metal ions in aqueous solutions can be distinguished: electrostatic forces and coordination bonds. There are also some weak interactions, including hydrogen bonding, Van der Waals force and trapping or wrapping of metal ions in the polymer bulk phase [Rivas *et al.*, 2003]. Apparently, only the former two types of strong interactions are dominant when water-soluble polymers are used to capture metal ions in PEUF. The following part will discuss the general properties of the two interactions between water-soluble polymers and metal ions.

2.3.1. Coordination

The theory of coordination between ligands and metal ions in aqueous phase is well developed. The basic nature of coordination bonds can be explained by the Lewis acid/base interactions. In the complex formation, the metal ions with empty electron orbits act as an electron acceptor whereas the ligands with free electron pairs act as an electron donor. The central metal ions may be classified as *A* and *B* categories [Martell and Hancock, 1996], based on the observation that certain ligands prefer coordination with metals like Ag(I), Zn(II), Hg(II), Pb(II), Pt(II) and Cu(I), while other ligands form stable complexes with Al(III), Ti(IV), Fe(III), Cr(III) and U(IV). The latter group of metals belongs to class *A* metals, which includes alkali, alkaline earth metals and some light transition metals. The former metal group, on the other hand, is classified as class *B* metals; They are mostly heavy transition metals[Snceyink and Jenkins, 1980; Martell and Hancock, 1996]. Similarly, the ligands can be also classified into *A* or *B* type depending on which class of central metal ions they prefer to coordinate. Table 2.5 summarizes the coordination trends and ligand preferences (the ligands are expressed by the atoms only). Generally, the coordination compounds formed by ligands and metal ions of the same class are most stable. These general observations provide a reference to the selection of appropriate water-soluble polymers for heavy metal removal by PEUF. In practical applications, almost all polymer ligands are those which have functional groups containing N, O or S. In addition, the ligand binding preference towards a specific metal can be used in the application of selective separation of that metal from an aqueous mixture containing different metal ions. For example, the polymers containing S-functional groups show strong interactions toward Hg(II), and thus it can be used in the selective separation and recovery of mercury.

Table 2.5 Stability trends of coordination compounds [Gispert, 2008]

Metal ion class	Stability trends with different ligands
Class A metal ions	N >> P > As > Sb > Bi
(Alkali, alkali earths, Fe(III), Al(III), Ti(IV), etc.)	O >> S > Se > Te
	F >> Cl > Br > I
Class B metal ions	N << P > As > Sb > Bi
(Pb(II), Hg(II), Ag(I), Pt(II), etc.)	O << S < Se ≈ Te
	F << Cl < Br < I

The equilibrium constants of the dissociation or formation of coordination compounds may be used to represent the thermodynamic stability of the complexes:

$$M^{n+} + L^- \leftrightarrow [ML]^{(n-1)+}; \qquad K = \frac{[[ML]^{(n-1)+}]}{[M^{n+}][L^-]} \equiv \frac{[ML]}{[M][L]} \qquad (2.10)$$
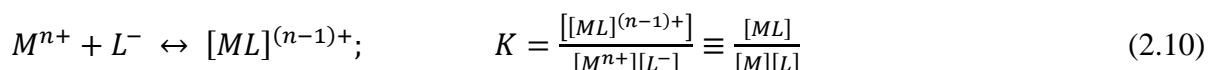
Most of the time, a single central metal ion can coordinate with more than one ligands (4, 5 or 6), forming coordination compound ML_m. Therefore, a series of coupled equilibria is introduced as follows:

$$M + L \leftrightarrow [ML]; \qquad K_1 = \frac{[ML]}{[M][L]} \qquad (2.11)$$

$$[ML] + L \leftrightarrow [ML_2]; \qquad K_2 = \frac{[ML_2]}{[ML][L]} \qquad (2.12)$$

$$\ldots \qquad\qquad \ldots$$

$$[ML_{m-1}] + L \leftrightarrow [ML_m]; \qquad K_m = \frac{[ML_m]}{[ML_{m-1}][L]} \qquad (2.13)$$
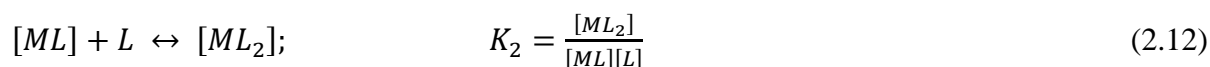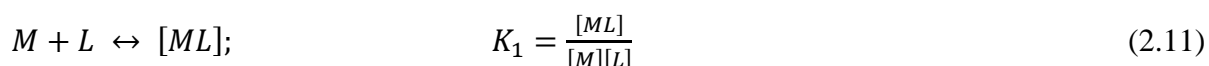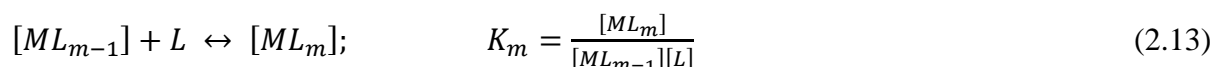
where the equilibrium constant K_m in each step measures the stability of individual ML_m compound, and m is the coordination number for that metal ion. When the overall coordination equilibrium is concerned, the global equilibrium constant β_m of the final product ML_m is then given by:

$$M + mL \leftrightarrow [ML_m]; \qquad \beta_m = \frac{[ML_m]}{[M][L]^m} = K_1 \cdot K_2 \cdot \cdots K_m \qquad (2.14)$$
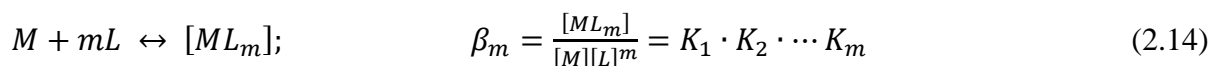
The ligands discussed above are unidentate. In the case of polymer-metal coordination, all the macromolecular ligands involved are multidentate. It means one single macromolecule can coordinate with more than one metal ions (see Figure 2.8). Accordingly, the overall equilibrium of polymer-metal coordination may be modified as:

$$\frac{l}{m}M + P \leftrightarrow \left[M_{\frac{l}{m}}P\right]; \qquad K = \frac{\left[M_{\frac{l}{m}}P\right]}{[M]^{\frac{l}{m}}[P]} \qquad (2.15)$$
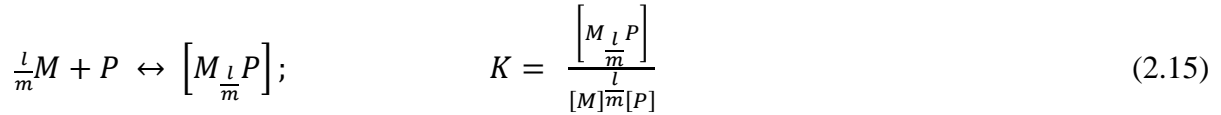
where P refers to the macromolecule, and l is the number of ligands on each single macromolecule (l equals to the degree of polymerization when each repeating unit in that macromolecule has only one ligand). Figure 2.8 illustrates the structure of the PVAm-metal macromolecular complexes. The discussion above is based on the following assumptions:

1. All the functional ligands on a macromolecular chain are equivalent. It means every ligand on that macromolecule has the same ability to coordinate with metal ions;

2. The end-group effects, interactions from the neighbourhood groups, and the intermolecular effects from another macromolecule are all ignored;

3. The macromolecular chain is highly flexible so that every functional ligand can coordinate with metal ions in the aqueous solution.

However, the real situation is much more complicated than the ideal equilibrium proposed above. As a matter of fact, in addition to the intramolecular coordination in one single macromolecule, the intermolecular coordination by which a metal ion links two nearby macromolecular chains together also exists in polymer complexes. Water-soluble polymers containing more than one functional groups show even more complicated coordination, because other functional groups which do not have the ability to coordinate metal ions may interfere with the coordination interactions. Figure 2.8 shows the possible structures of

macromolecular-metal complexes in aqueous solutions, where the polyvinylamine is used as a sample polymer.

Theoretical structure

Intermolecular structure

Intramolecular structure
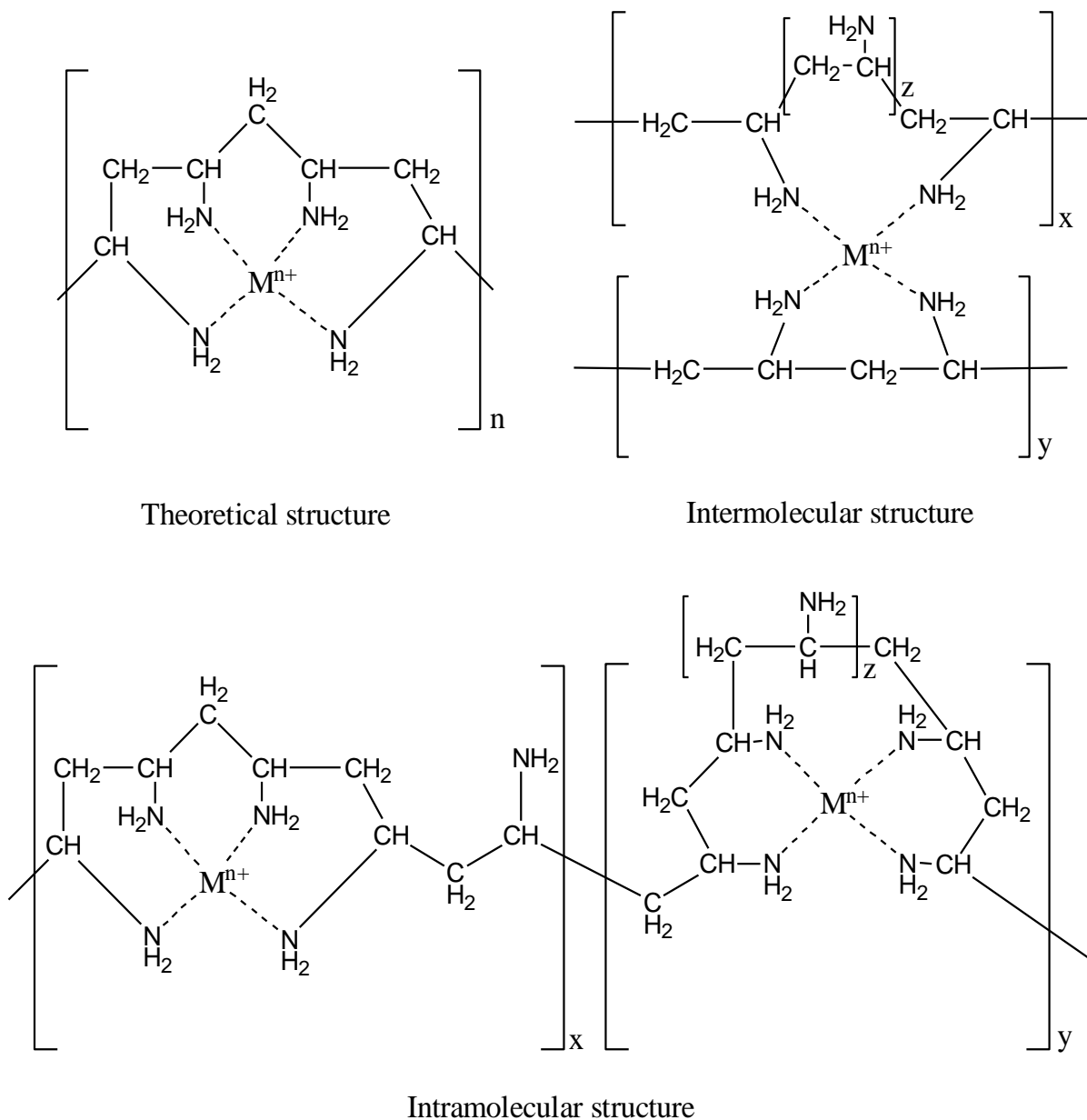
Figure 2.8 Structure of polyvinylamine metal complex [Teyssie *et al.*, 1965]

As a result, the equilibrium constant derived above remains only a simplified expression, and it is more difficult to determine than for small ligands. Previous research showed that all the tested equilibrium constants serve to give only a rough measure about qualitative stability

of polymer-metal complexes. Most of them are only suitable to a few specific water-soluble polymers.

2.3.2. Electrostatic interactions

Electrostatic forces exist mainly in polyelectrolytes, especially water-soluble polyelectrolytes with sulfonic acid groups. The target small contaminants will be restricted around the poly-ions by electrostatic attraction. The electrostatic interactions depend on the nature of the polyelectrolytes and the target species. The strength of the electrostatic interaction can still be different even for polyelectrolytes that contain the same functional groups. For example, the affinity of cations to polyacrylate is much greater than that of carboxy methyl cellulose, although they both have carboxy groups. It is believed to be due to different distances between carboxy groups on polymer chains (2.5 Å apart in polyacrylate, and 5 Å in carboxy methyl cellulose) [Tanford, 1961]. Organic counter-ions are also thought to bind polyelectrolytes more strongly than inorganic counter-ions because of their hydrocarbon nature [Rivas *et al.*, 2003].

It is difficult to establish a general description for the distribution and equilibrium between polyelectrolytes and heavy metals because there are so many exceptions. Nevertheless, many models and theories are proposed to describe the behaviour of heavy metals in the polyelectrolyte domain. Some models are based on long-range electrostatic interactions, in which heavy metals tend to be non-specifically restricted to the poly-ions chains. They can move along the axis of poly-ion chain. On the other hand, under short range interactions, the metals are bound to specific sites or areas of the poly-ions and fixed at that location [Rivas *et al.*, 2003]. On the basis of a two-zone model [Palencia *et al.*, 2011], as shown in Figure 2.9, in a close vicinity of the polyelectrolyte macromolecule, the metal ions are strongly bonded. This is referred to the polymeric domain, which is primarily responsible for retention of metal ions

during UF. There is an additional weaker external zone surrounding the polymeric domain (or internal zone), where the residual charges of the ionic polymer has a weak interaction with the metal ions. The free metal ions are located in the bulk liquid outside the external zone where the polyelectrolyte-metal interaction is sufficiently weak.
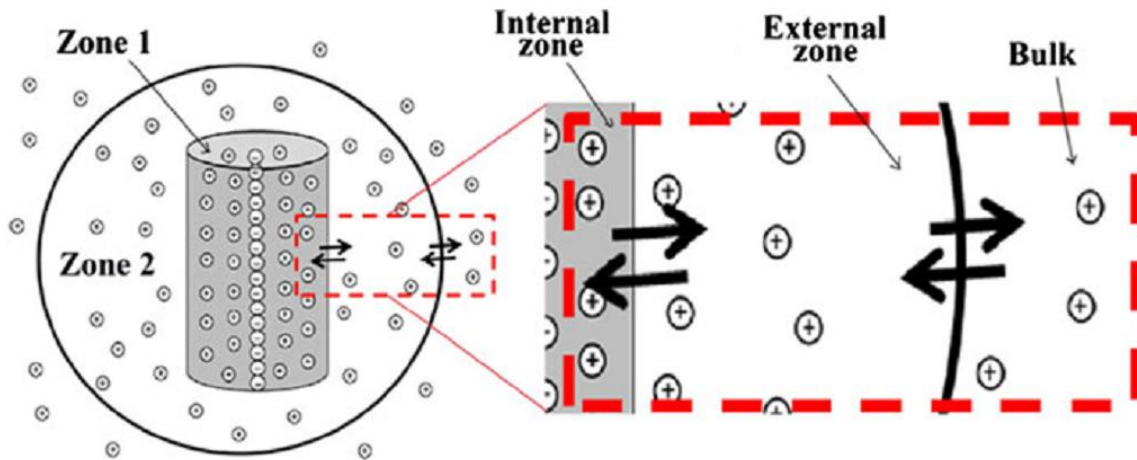
Figure 2.9 Two-zone model for the interpretation of mechanism between polyelectrolyte and heavy metal cation [Palencia *et al.*, 2011]

As a matter of fact, coordination and electrostatic interaction can exist simultaneously, because many water-soluble polymers contain more than one type of functional group. Even the negatively charged carboxy groups can form coordination compounds with metal ions due to the free electron pairs on oxygen atoms. Rivas et. al. [2003] explained that the metal ions can be attracted by the long-range electrostatic interactions at first, then the attracted ions can be fixed at that site by the coordination with ligands on the polymer chains as soon as the metal ions are condensed near to the polymers. Because of the complex polymer-metal ion interactions, evaluation or measurement of their equilibrium tends to be difficult.

2.4 Other separation techniques for removal of heavy metal ions

The separation of heavy metal ions from water is an important issue in the chemical and processing industry. Different techniques (e.g., adsorption, chemical precipitation and ion exchange) have been developed. Here, two other separation processes that are relevant to PEUF are briefly introduced. It will help understand the characteristics of PEUF and the relationship among them.

2.4.1 Coagulation and flocculation

Coagulation or flocculation is one of the wastewater treatment techniques for the removal of contaminants from water supplies to produce drinking water or to clean up the wastewater of domestic or industrial origin [Bolto, 1995]. The first step involved in this process is to destabilize the stable dispersion of pollutants in the water by addition of oppositely charged species to neutralize the charges on the impurities, forming small particles. Then a so-called flocculation step is applied to aggregate these small particles, producing larger flocs. In industrial applications, coagulation or flocculation is usually followed by separation steps in the form of flotation or sedimentation.

Strictly speaking, flocculation and coagulation are not synonymous. In addition, the original dispersion of impurity species is destabilized by overcoming the forces that maintain the stability of the dispersion, whereas in flocculation destabilized particles join together to form larger agglomerates [Hutchison and Healy, 1990; Bolto, 1995]. Aluminum ions are commonly used as coagulant, and they can neutralize the negative charges on some organic contaminants. In flocculation, water-soluble polymers are also normally used, which is similar to PEUF. According to the mechanism of flocculation, the soluble polymer in the feed solution

41

acts like a "bridge", which links the small particles or flocs formed by coagulation to build up and form larger aggregates. The interactions between the soluble polymer and the small flocs are essentially the same as those occurring in PEUF [Pivokonsky *et al.*, 2012; Wang *et al.*, 2013], if the impurities in water were heavy metal ions. In principle, all water-soluble polymers used in the PEUF can be also used in flocculation.

In spite of some common features of flocculation and PEUF, they are fundamentally different. The polymer-metal complexes in PEUF are soluble so as to minimize surface contamination of membrane, and thus the whole feed solution is homogenous. On the contrary, in flocculation the feed solution is heterogeneous because of the flocs formed. As one may expect, although water-soluble polymers are used in both processes, their functions are different, and thus they should be selected accordingly based on their functionality.

2.4.2 Adsorption process

Adsorption is one of the most common separation technique for heavy metal removal from waste effluents. Tons of adsorbent materials have been investigated and applied so far. The heavy metal ions in the aqueous solution can be captured by the adsorbent though the physical or chemical adsorption. Generally, the chemical adsorption is more popular for heavy metal removal because it has stronger interactions and higher adsorption capacity towards heavy metals. The special functional groups on the surface of the adsorbents provide significant interactions with heavy metals, resulting in the adsorptive separation of heavy metals from water. These interactions do not have intrinsic differences with the ones that occur in the coagulation/flocculation and PEUF process. All the functional groups that have been used in those two processes are also widely used in the adsorption process.

For example, in the removal of mercury species from wastewater, sulfurization is widely applied to enhance adsorption capacity and selectivity [Algarra *et al.*, 2014]. It is well-recognized that the sulfur-containing functional groups on the surface of adsorbents can increase the mercury uptake [Pillay *et al.*, 2013; Hadi *et al.*, 2015]. Many synthesised polymers or biopolymers with special functional groups (e.g., amine, carboxyl, and sulfonic acid) also show efficient adsorption capacity for heavy metal ions [Vieira and Beppu, 2005; Saber-Samandari and Gazi, 2013]. Those functional groups play a dominant role in the adsorptive removal of heavy metals.

Compared to PEUF, adsorption is a heterogeneous process where the adsorbents must be insoluble in the solution. The heavy metal ions absorbed by the adsorbent actually move from an aqueous phase onto a solid surface. This fundamental difference may determine their applications in the practical wastewater treatments.

2.5 Knowledge gap

With a high density of primary amine groups and good solubility in water, PVAm is expected to be a good chelating agent to remove heavy metals by PEUF. However, it received little attention before 1990s due to technical difficulty to produce it. Very little research has been done to investigate the performance of PVAm in PEUF process for heavy metal removal. Although the coordination between PVAm and heavy metals in aqueous solutions is thought to be the main reason that PVAm can capture the metals, the equilibrium of PVAm-metal complex system, the mechanism of complex formation and the effects of counter anions are still unclear. The interactions between PVAm and heavy metals influence the performance of PEUF significantly, and thus a systematic detailed investigation is required.

Although the PEUF process is essentially an ultrafiltration process, the additions of water-soluble polymers with various functional groups into the feed solution are believed to influence the membrane process. The effects of operating conditions (e.g., transmembrane pressure, temperature, membrane configuration and operating modes), concentration polarization and membrane fouling involved in the l ultrafiltration process on PEUF are complicated. In particular, membrane fouling in PEUF, which involves the water-soluble polymer and the UF membrane, is an important issue in practical application. The properties of the water-soluble polymers (e.g., molecular weight distribution, solubility, viscosity, branched or linear structures, and hydrophilicity) and the performance of UF membrane itself would affect membrane fouling and thus the permeation flux significantly. To achieve a considerable water production, a water-soluble polymer that leads to less membrane fouling while maintaining adequate metal rejections is preferred. To our knowledge, little attention has been paid to this area.

The PEUF process, nowadays, still remains a lab-scale process though several pilot-scale operations have been studied. Thus the prediction of permeation flux metal rejection in a typical PEUF process becomes important because it provides valuable information for process design when the PEUF process is scaled up to an industrial-scale application. Since almost all the flux functions in conventional UF fouling models are empirical, more work about the process modelling and calculation are then required.

In addition, the primary amine groups on PVAm chains are quite reactive. This provides opportunities to graft different functional groups onto PVAm. With the grafted groups, the modified PVAm may have stronger interactions with certain heavy metals, which is beneficial to further improve the metal removal efficiency and even to achieve selective separation of

different heavy metals with PEUF. However, cautions should be exercised when chemical grafting is used because it may consume the original amine groups and change the physiochemical properties (e.g., solubility in water)..

Therefore, the study in this thesis attempted to address the above isuuses and provide a clearer understanding about the PEUF process. The results will also give valuable references for the future practical applications.

Chapter 3

Preliminary Studies of PVAm as A Chelating Agent for Removal of Heavy Metals from Water via PEUF and Flocculation[*]

3.1 Introduction

As presented in Chapter 2, PEUF has exhibited various advantages for removing heavy metals from wastewater. Choosing a proper water-soluble polymer is very important for the performance of the PEUF process. With the highest content of primary amine groups of any polymer [Pelton, 2014], PVAm is expected to be a good chelating agent in PEUF. It is totally miscible with water in any proportion and can easily form stable complexes with many heavy metal ions [Kobayashi *et al.*, 1989].

The aqueous solutions to be treated by PEUF are preferably homogeneous [Rivas *et al.*, 2003]. While the polymer-metal complexes are often soluble in water, they do precipitate under specific conditions for certain metals [Navarro *et al.*, 2005; Jellinek and Luh, 1969]. This will significantly affect the PEUF process. As a matter of fact, when the polymer-metal complexes precipitate out of a homogeneous solution, the whole process is essentially a hybrid flocculation-filtration process [Zhao *et al.*, 2015], rather than a PEUF process. Many water-soluble polymers used in PEUF, including PEI, sulphonic acid and carboxylic acid polymers,

---

[*] Portions of this chapter have been published in ***Sep. Purif. Technol.***, 158 (2016) 124-136. The first author contributed to the experments, data analysis and drafting of manuscript. The co-authors involed in discussion and analysis of the experimental data and revision of the manuscript.

may also serve as good flocculants in coagulation/flocculation systems for certain metals [Bolto, 1995]. The dissolved macromolecular complexes with attached metal ions can enhance floc growth because of the polymer bridging effect [Bolto and Gregory, 2007].It appears that the two different separation techniques using the same water-soluble polymer for heavy metal removal actually take advantage of the different states of the polymer-metal complexes in aqueous solutions. However, it is not yet clear how the performance of PEUF or coagulation/flocculation process is affected by the state change of the polymer-metal complexes in aqueous solutions.

Therefore, in this chapter, PVAm was used to capture heavy metal ions by forming complexes, followed by UF. Several heavy metal ions, Co(II), Cu(II), Ni(II), Pb(II), Fe(III), Cd(II), Zn(II), and Mn(II), were selected as the representative metals in water. Their interactions with PVAm were characterized by UV spectrophotometry and conductometric titration. The possible precipitation of the polymer-metal complexes and its effects on PEUF performance were also investigated for PVAm-Cu(II) and PVAm-Co(II) systems, and an attempt was made to correlate PEUF and coagulation/flocculation for such systems.

3.2 Experimental

3.2.1 Materials

The UF membrane used was based on polyethersulfone supplied by Sepro Membranes with a nominal MWCO of 10 kDa (PES-10). Polyvinylamine (Lupamin 9095, Mw 340,000) was supplied by BASF Corporation. In order to make sure that the low molecular weight fractions of PVAm and other small residue molecules (e.g., initiators or catalysts left in PVAm) would not pass through the membrane, the polymer was subjected to pre-filtration with the same UF

membrane before it was used as a chelating agent in PEUF. The concentrations of PVAm in the feed and permeate solutions were analyzed by a UV-Vis Spectrophotometer. Eight salts of heavy metal, namely $CoSO_4 \cdot 7H_2O$ (The British Drug Houses Ltd.), $CuSO_4 \cdot 5H_2O$ (J.T. Baker Chemical Co.), $NiCl_2 \cdot 6H_2O$ and $FeCl_3$ (B.D.H. Laboratory Supplies), $Pb(NO_3)_2$ (Sigma-Aldrich), $CdCl_2$ (Poly Research Corp.) and $MnCl_2 \cdot 4H_2O$ (B.D.H. Inc.) were used to prepare the feed solutions. All aqueous solutions were prepared using deionized water with conductivity lower than 1 μs/cm.

3.2.2 Ultrafiltration process

The UF experiments were carried out using a dead-end UF cell, with an effective feed volume of 300 mL and an effective membrane area of 36 cm^2. The trans-membrane pressure was provided using a pressurized nitrogen gas, and the gas pressure was monitored using an on-line pressure gauge (Cole Parmer). A schematic diagram of the UF system is shown in Figure 3.1. All experiments were carried out at a constant transmembrane pressure of 200 kPa and at room temperature (25 ℃), unless specified otherwise. The PES-10 membrane was soaked in deionized water overnight and then pre-pressurized at 200 kPa gauge by deionized water for at least 1 h prior to the UF experiments. The feed solution containing pre-determined amounts of heavy metal and PVAm was well mixed under agitation for 2 h before UF to ensure that there was sufficient time for PVAm to interact with the heavy metals. During the course of PEUF process, the permeate samples were collected and analyzed.

The metal rejection R_m and water permeation flux J were calculated by following:

$$R_m = \frac{C_f - C_p}{C_f} \times 100\% \tag{3.1}$$

$$J = \frac{m}{A \times t} \tag{3.2}$$

where C_f and C_p are the concentrations of heavy metal ions in the feed solution and the permeate sample, respectively, and m is the weight of the permeate sample collected over a period of time t through a membrane area A. The experiments were repeated 3 times, and the experimental error for the UF experiment was found to be within 6%.
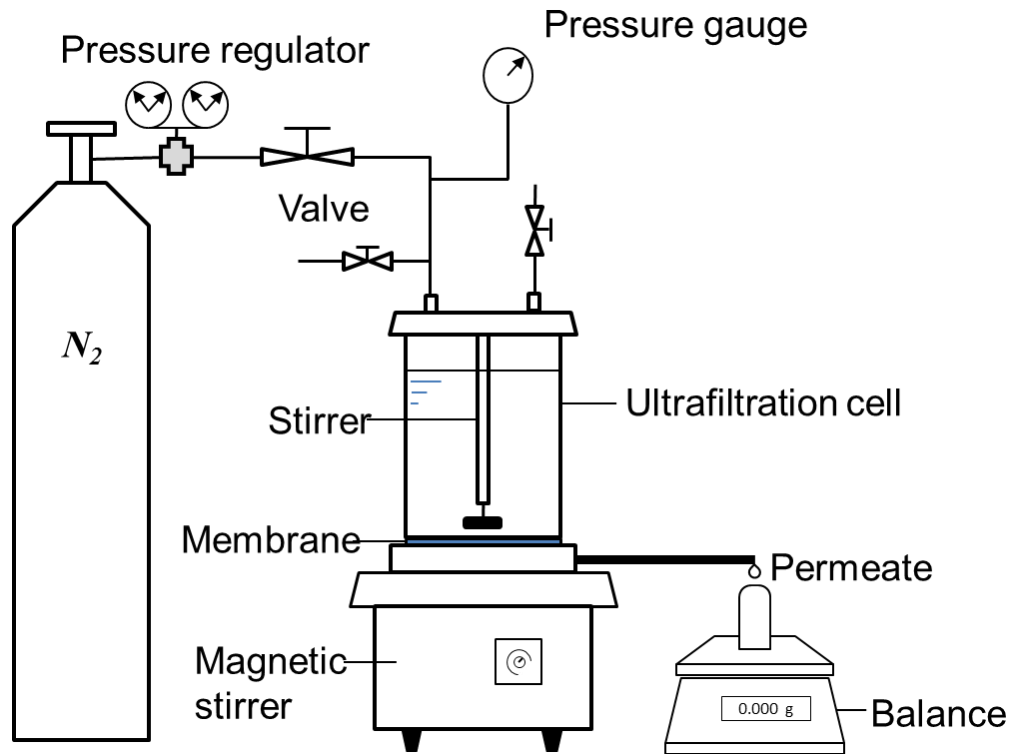
Figure 3.1 Schematic diagram of ultrafiltration set-up

The concentrations of the heavy metals in the feed and permeate solutions were determined using a Prodigy radial inductively coupled plasma optical emission spectrometry (ICP-OES) (Teledyne-Leeman). The system was standardized for each metal analyte through a series of standard solutions over a concentration range of 0 to 160 ppm, prepared from certified commercial stock solutions. Yttrium was used as an internal standard at a fixed concentration of approximately 10 ppm. Each sample was analyzed 3 times to get an average concentration value, and drift corrections of the instrument were performed every 12 samples.

In order to investigate the fouling and precipitation behavior of PVAm-metal complexes during UF, aqueous PVAm-Co(II) complex solutions were selected as a model system. The permeation fluxes at different concentrations of Co(II) were determined while maintaining a constant PVAm concentration (0.1 wt%) in the aqueous solution. The metal concentrations reported in the study were based on the mass concentrations of the metal ions.

3.2.3 Characterization

To investigate the interactions between PVAm and heavy metal ions in the aqueous solution, their UV-vis absorbance was determined using a Shimadzu UV-Vis Spectrophotometer (UV mini-1240) over a wavelength range of 200-450 nm. The absorption spectra were obtained with solutions containing 25 ppm of a heavy metal ion and 1000 ppm of PVAm. In addition, the absorption spectrum of PVAm-Cu(II) complex solution with different PVAm concentrations ranging from 40 to 250 ppm was also determined.

The conductometric titration experiments were conducted to study the formation of PVAm-metal complexes and the capability of PVAm to bind the different heavy metals. This information was used to elucidate the UF result with respect to metal rejection and water flux. For this series of experiments, 100 mL of PVAm solution at a given concentration was "titrated" dropwise with a heavy metal solution at a concentration of 1,000 ppm, and the conductivity of the titrand solution was evaluated continuously using an inoLab Cond Level 2 Presicion Conductivity Meter. All measurements were carried out at room temperature.

3.2.4 Flocculation analysis

Flocculation was found to occur in PVAm-CuSO$_4$ and PVAm-CoSO$_4$ aqueous mixture at a proper PVAm-to-metal ratio. To look into the mechanism of PVAm-metal flocculation, an additional titration experiment along with UV-vis analysis was performed. First, five different

heavy metal salt solutions, namely $CoSO_4$, $CuSO_4$, $CuCl_2$, $Cu(CH_3COO)_2$ and $Cu(NO_3)_2$ with a metal concentration of 1,000 ppm, were added dropwise into 100 mL of a PVAm titrand solutions (0.1wt%) using a buret, respectively. Then the absorbance of the titrand solutions was determined using the UV-vis spectrometer at different wavelengths (190 to 700 nm). The UV spectra and the characteristic peaks of the PVAm-metal system were obtained. In addition, the effects of PVAm concentration in the titrand on flocculation formation were also investigated.

Moreover, a typical flocculation test was performed in this study as well. A series of PVAm aqueous solutions with fixed concentrations (0.5, 1 and 2 wt%) were prepared and stirred, and then different pre-determined amounts of $CuSO_4$ salts were added quickly to the PVAm solutions. The resulting mixtures were stirred vigorously for 5 min, followed by slow stirring for 20 min, and then the mixture was allowed to stand for 20 min. Samples of clean solutions were taken up from the top, and after filtration through a micron filter paper, the samples were analyzed for copper concentration using the ICP-OES.

3.3 Results and discussion

3.3.1 Ultrafiltration performance

3.3.1.1 Pre-filtration of PVAm

There is a molecular weight distribution in polymers. They are comprised of molecules with a range of molecular weights. Typically, the number average (M_n), weight average (M_w) or the z-average (M_z) of molecular weight can be used to characterize the average molecular weight of a polymer. The polyvinylamine used in this study is a linear polymer. Though the average molecular weight of the PVAm is much larger than the molecular weight cut-off of the

ultrafiltration membrane, it was decided to pre-filtrate the low molecular weight fractions of PVAm and any other small molecules (e.g., residual initiators or catalysts left over in PVAm) that could not be completely retained by the membrane during subsequent PEUF processes. This would prevent secondary contamination to the permeate water due to possible passage of these small molecules during the PEUF.

The aforementioned concerns were confirmed by the less than 100% rejection of the UF membrane to PVAm in the first few minutes, as shown in Figure 3.2a, indicating that some small molecules from the PVAm polymer did penetrate through the membrane, though the amount of these small molecules was not very significant. Nonetheless, such small molecules, if not removed, will enter the permeate stream, imposing a potential problem for water treatment (e.g., drinking water purification). As expected, as the pre-filtration continued to proceed, the observed rejection to PVAm increased and a very high retention (99.6%) was eventually obtained after about 1 hour (see Figure 3.2a). The PVAm retention data of pre-filtration were further supported by the UV absorbance of the permeate sample as well as the purified PVAm, as shown in Figure 3.2b. The distinct peak around 210 nm resulting from the UV-absorbing chromophore on PVAm chains in the feed solution dropped dramatically after ultrafiltration to remove the small molecules. The pre-filtrated PVAm would be completely retained by the membrane when subjected to PEUF.
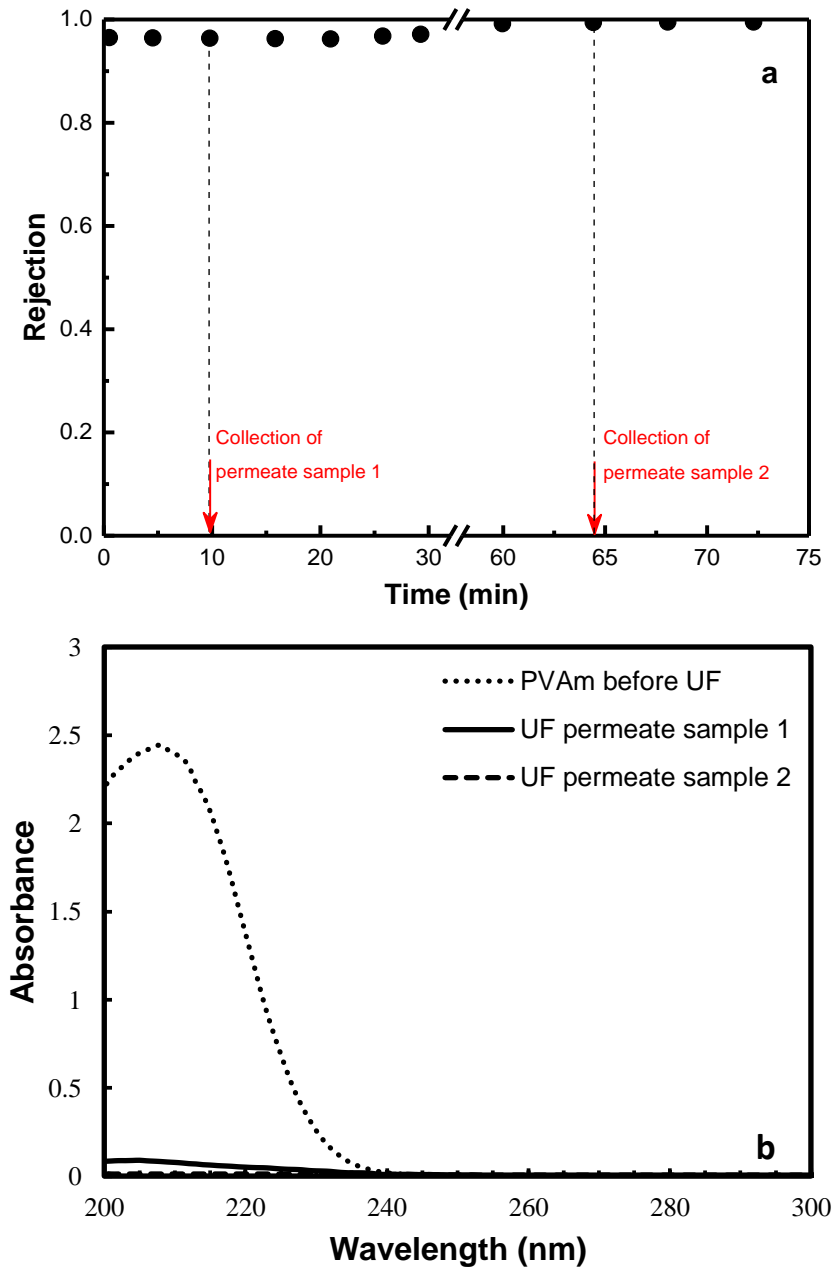
Figure 3.2 Pre-filtration of PVAm, a) PVAm retention versus filtration time, b) UV absorbance. Initial PVAm concentration: 1000 ppm, transmembrane pressure: 200 kPa

It should be pointed out that the secondary contamination problem in micellar-enhanced ultrafiltration is a significant issue. The un-micelled surfactant monomers are able to pass through the membrane. The problem is readily resolved in PEUF using a simple pre-filtration

of PVAm before it was added to the feed solution as a complexation agent for PEUF to remove heavy metal from water.

3.3.1.2 Removal of heavy metal by PEUF using PVAm

In view of the fact that i) heavy metal ions can form complexes easily with many amine compounds [Gispert, 2008] and ii) PVAm has a large quantity of primary amines that can coordinate with many heavy metal ions [Teyssie *et al.*, 1965], it is reasonable to anticipate a good retention with PEUF using PVAm as a chelating agent. As shown in Figure 3.3, the UF membrane, which is not able to reject soluble ions, successfully retained the heavy metal ions in the presence of PVAm. Obviously, it was the binding of heavy metal ions by PVAm that led to retention of heavy metals from aqueous solutions by UF. As expected, PEUF has different capabilities of rejecting different heavy metal ions. Among the eight heavy metal ions tested here, Cu(II), Fe(III) and Pb(II) showed the highest rejections (nearly 100%), while the rejections for Ni(II), Mn(II), Co(II), Cd(II) and Zn(II) were much lower at the same operating conditions. This seems to suggest that how strongly PVAm interact with the heavy metals has a significant impact on the metal rejection. The values of metal rejections and permeation fluxes varied within $\pm 6\%$ for the replicate experiments. This experimental error shown here was very much the same for all the experimental datain this study, and thus error bars were not shown in the followingfigures

In addition to the intrinsic properties of the polymer-metal interactions, the operating parameters involved in the UF process (e.g., initial concentrations of PVAm and heavy metal ions) also affects the performance of PEUF for heavy metal removal. This is shown in Figure 3.4, where the metal rejections at different PVAm dosages were presented as function of the

54

amount of filtrate. As shown in Figure 3.4a, cobalt rejection was enhanced with an increase in PVAm concentration or decrease in cobalt concentration in the feed. With 0.1 wt% of PVAm, Co(II) rejection was 40% at a feed Co(II) concentration of 25 ppm; cobalt rejection was only 5% at 100 ppm of Co(II) in the feed. On the other hand, when the initial PVAm dosage was increased to 1wt%, a much higher cobalt rejection was achieved. Similar results were also observed for the rejection of Cu(II), Ni(II) and Pb(II), as shown in Figures 3.4b to 3.4d, where a PVAm dosage of 1 wt% resulted in a very high metal rejection over the entire metal concentration range tested. At a given PVAm dosage, the quantity of PVAm in the feed was fixed during the course of PEUF, and so was the number of the metal coordination sites in the polymer. At a low metal concentrations, the heavy metal ions would start to bind the most favorable coordination sites in the PVAm. With an increase in the metal concentration, the coordination sites in PVAm become gradually saturated, and thus the number of coordination sites available to bind additional metals was reduced. Similarly, a lower PVAm dosage meant fewer coordination sites accessible to the heavy metal ions. As the metal ions that are not bonded by PVAm will leak through the membrane, the relative amount of the PVAm and the metal is expected to influence the heavy metal rejection significantly.

Figure 3.4 also showed that the instantaneous heavy metal rejection during the initial period of PEUF was not at a constant value. This time-variant metal rejection observed in PEUF is believed to be caused by the concentration polarization. As discussed earlier, the amount of PVAm relative to the amount of heavy metal ions in the feed solution is an important parameter to the percentage retention of heavy metal ions by the PVAm. During the filtration process, the concentration polarization began to develop on the feed side adjacent to the membrane surface, which would increase the local concentration of PVAm on the membrane

surface, and to a lesser extent, the concentration of heavy metal ions not bounded by PVAm as well since the UF membrane exhibited a low degree of rejection to the heavy metal ions in the absence of PVAm. While the PVAm macromolecules were retained by the UF membrane, the increased local concentration of unbounded heavy metal ions on the membrane surface would lead to an increased permeation rate of metal ions and thus a lower metal rejection.

This explains the initial decline in the observed rejection of the membrane to Co(II), Cu(II) and Pb(II). As the filtration proceeded with time, the gradually concentrated PVAm macromolecules near the membrane surface would help retain the unbounded heavy metal ions. As a result, a constant heavy metal rejection was eventually reached (for instance, Co(II) and Cu(II)), and sometimes it could became slightly increased (e.g., Pb (II)). However, there was no obvious initial decline in Ni(II) rejection (see Figure 3.4c), presumable due to the presence of Cl^- in the $NiCl_2$ feed solution. Different from the polyatomic anion (i.e., SO_4^{2-} and NO_3^-) the chloride may also have weak coordination interactions toward heavy metal ions [Gispert, 2008]. This characteristics may help increase the Ni(II) rejection at the early stage of the filtration process. On the other hand, if the initial PVAm concentration in the feed was already high enough to bind almost all the heavy metal ions in the feed, the occurrence of concentration polarization would enhance the metal binding by PVAm (see Figures 3.4b-2, c-2, and d-2).
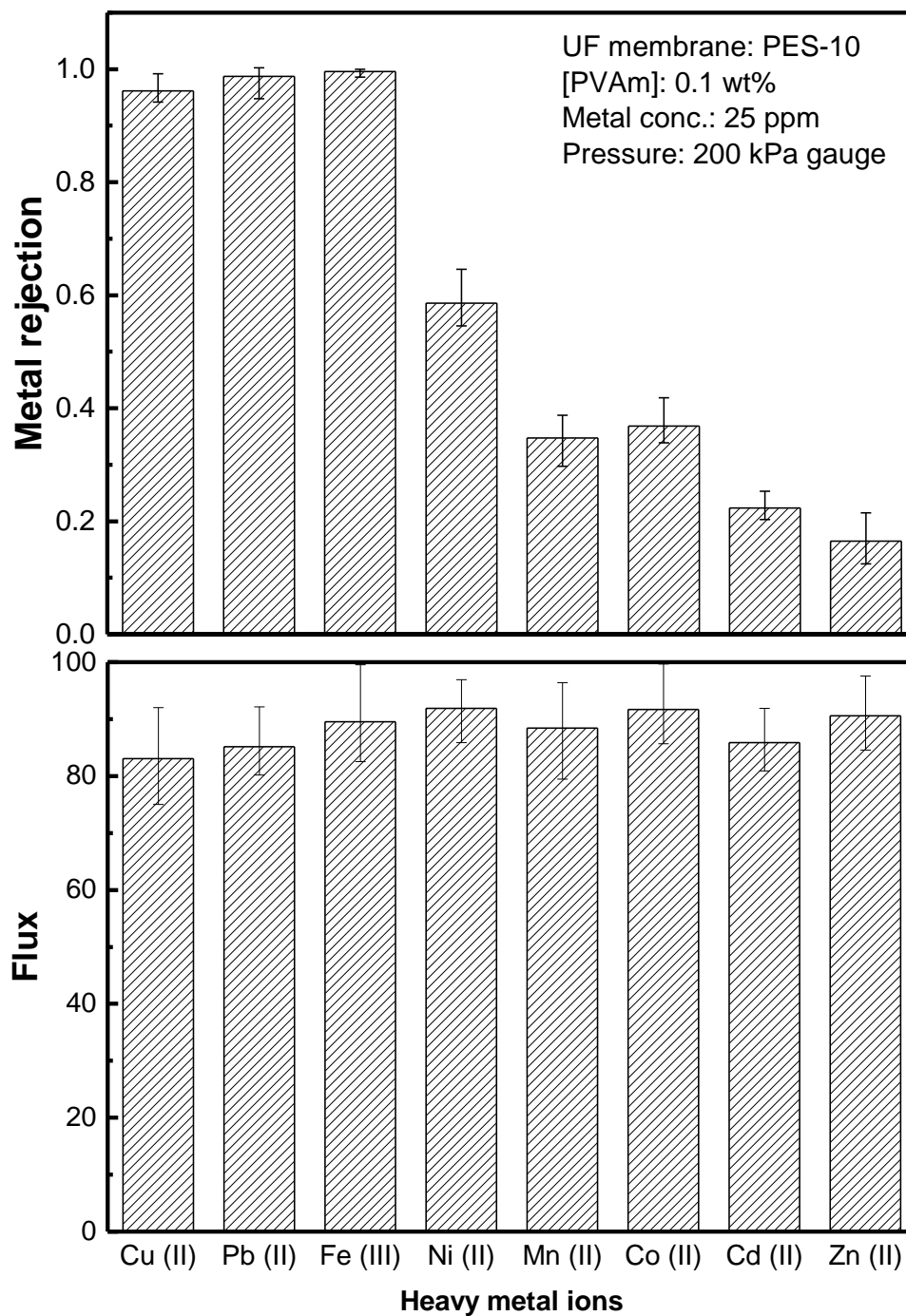
Figure 3.3 Heavy metal rejections and permeation fluxes using PVAm in PEUF, the data was obtained after the first 40 g filtrates were discarded.
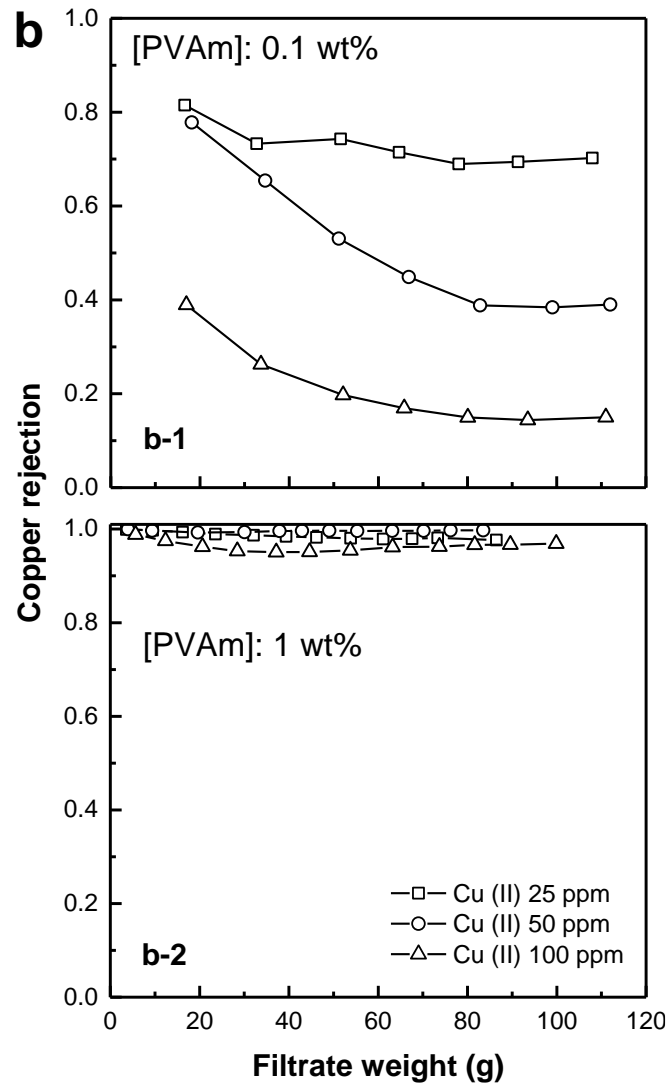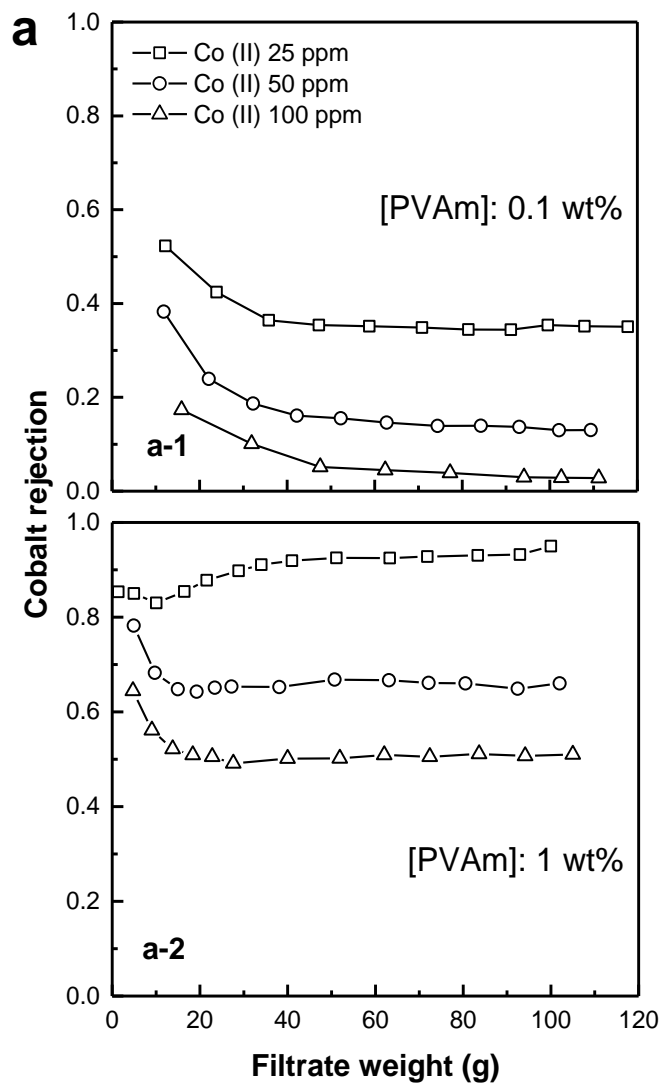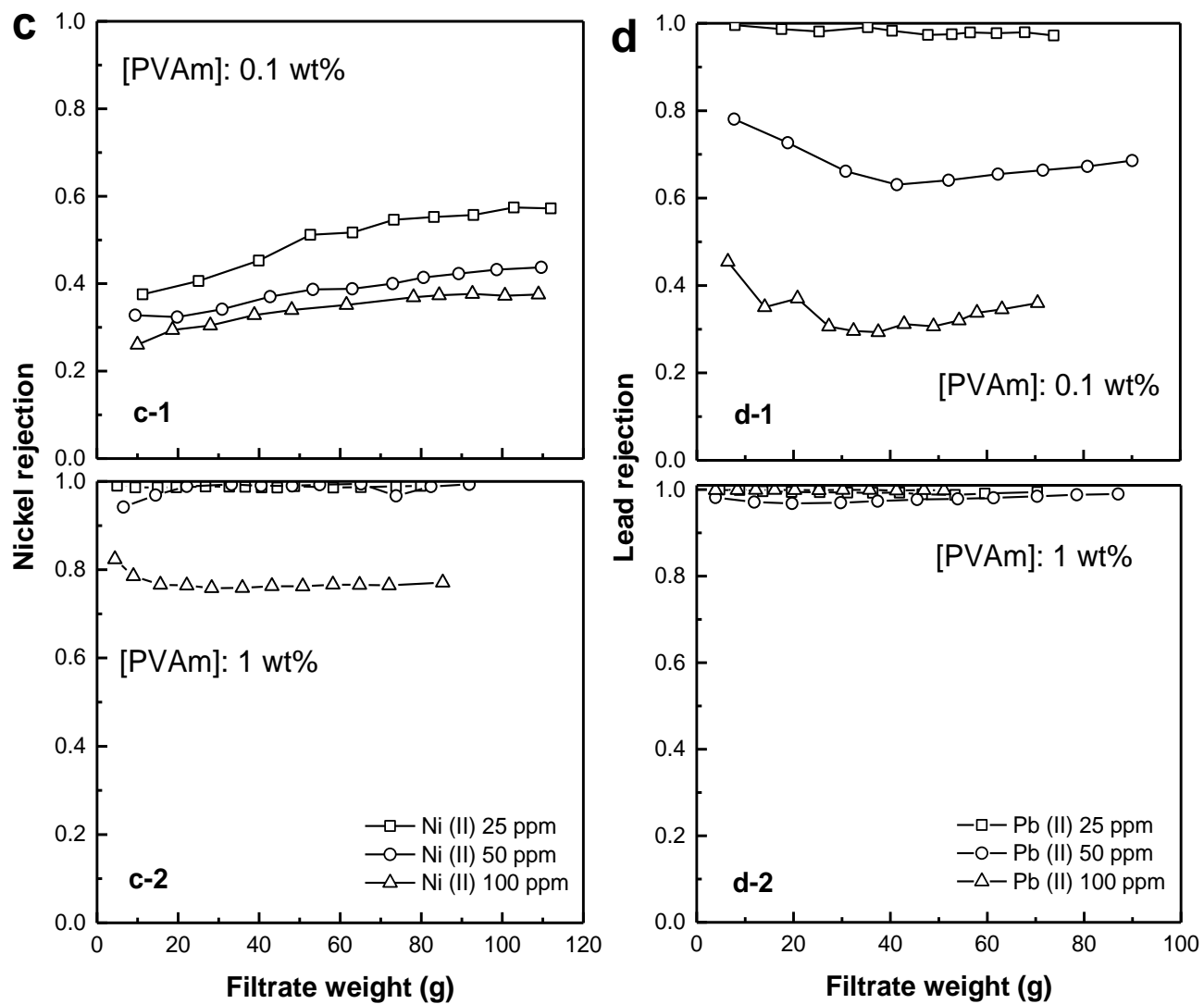
Figure 3.4 Rejections of four metals at different metal and PVAm concentrations as a function of filtrate weight, a) Co(II), b) Cu(II), c) Ni(II) and d) Pb(II), transmembrane pressure: 200 kPa.

Although an increase in PVAm dosage can improve the metal rejection in PEUF, there will be a decrease in water flux. This is shown in Figure 3.5, where a significant reduction in the permeation flux was noticed when the initial PVAm dosage increased from 0.1wt% to 1wt%. This is not unexpected because of the intensified concentration of polarization and membrane fouling. Interestingly, the permeation flux was shown to be independent of the types of heavy metals involved. This suggests that the PVAm dosage is a primary factor influencing the permeation flux. Therefore, an appropriate PVAm dosage should be used in practice in order to achieve a good metal rejection without significantly lowering the permeation flux.
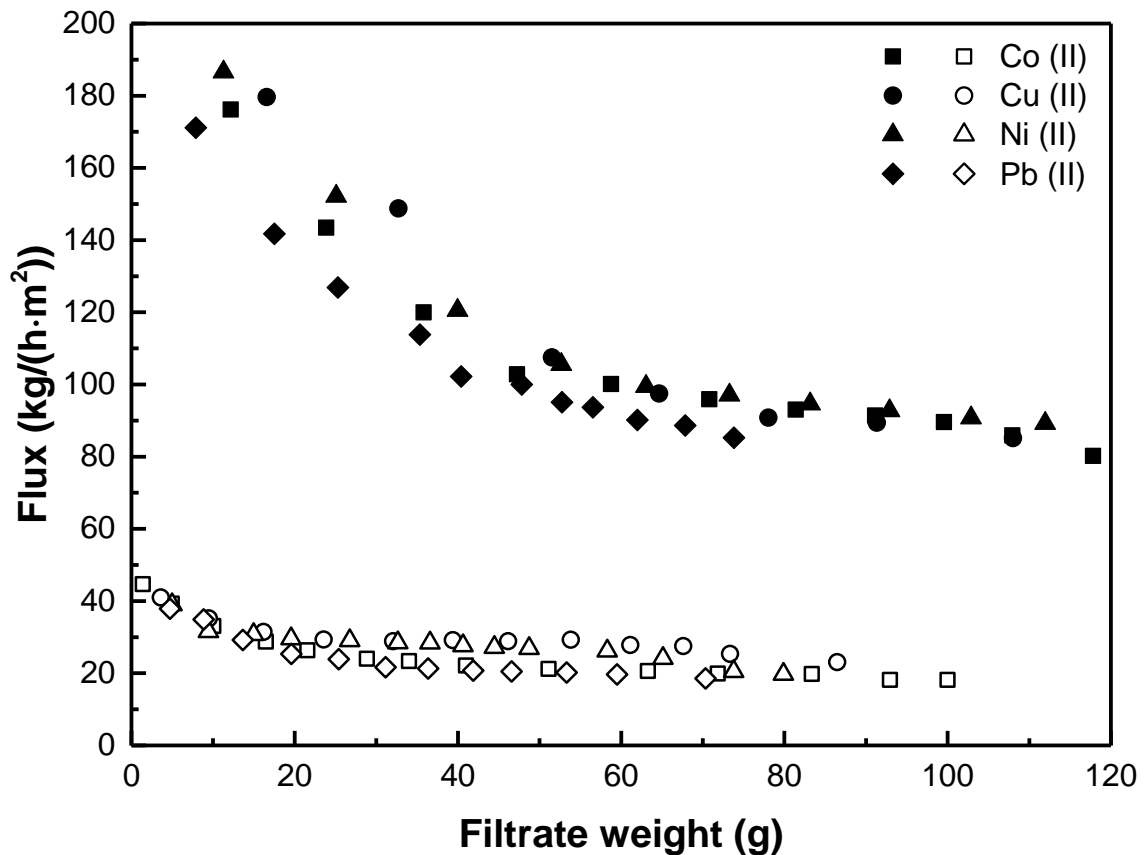
Figure 3.5 Effect of feed PVAm concentration on flux in PEUF, open keys: [PVAm] = 1 wt%, solid keys: [PVAm] = 0.1 wt%; concentrations of metals: 25ppm; transmembrane pressure: 200 kPa.

3.3.1.3 Effect of operating pressure and temperature

The effects of operating pressure and temperature on the PEUF performance for metal rejection were studied. Figure 3.6 shows the metal rejection and water flux at different pressures. At a given PVAm dosage, there was little change in the rejection of heavy metals over a wide pressure range of pressures (from 40 to 800 kPa gauge). This is easy to understand because the pressure did not have a significant influence on the interaction between the chelating polymer and the metal ions and it only provided a driving force for mass transport across the membrane. As observed in typical UF processes [Porter, 1990], the permeation flux increases with an increase in the pressure applied, but the increase in the flux is less than proportional. When the pressure is relatively low, the permeation flux increases almost linearly with the transmembrane pressure. The pressure dependence of the flux becomes less significant as the pressure increases. When the pressure is high enough, the permeation flux will reach a limiting flux when the concentration of the macromolecular solute accumulated on the membrane surface is high enough to form a grey layer [Porter, 1990; Macedo *et al.*, 2011]. The gel-layer thickness will grow until the rate of solute transport by convection towards the membrane surface from the solution (driven by the pressure) is equal to the rate of solute transport by back diffusive (driven by the concentration gradient), thereby reaching a steady state. At this point, a further increase in the pressure will not affect the permeation flux because of the "gel-polarization" [Porter, 1990]. For the heavy metal solutions studied, the permeation flux appears to be essentially the same at a given PVAm dosage, irrespective of what heavy metals are present in the feed.
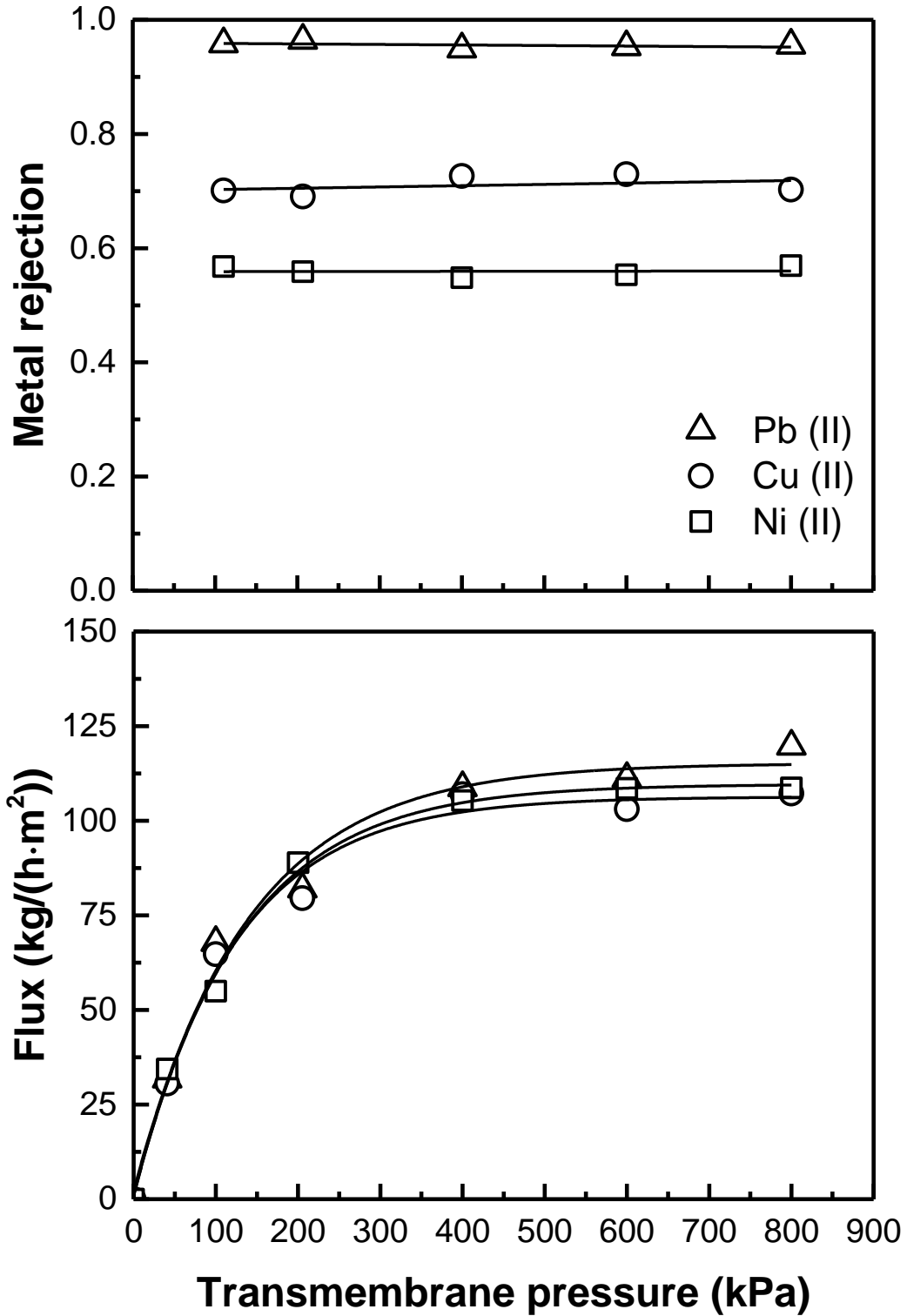
Figure 3.6 Effect of transmembrane pressure on flux and metal rejection in PEUF, PVAm concentration: 0.1 wt%, metal concentration: 25 ppm. All experiments were operated at room temperature (25 °C).

Figure 3.7 shows how the pressure affected the permeation flux when different dosages of PVAm were used; for purpose of comparison, the permeation flux of pure water and the water flux of an aqueous PVAm solution in the absence of heavy metals were also plotted. As expected, at a given pressure, a higher PVAm concentration in the feed resulted in a lower permeation flux. In addition, at a higher PVAm concentration, the permeation flux begins to level off at a lower pressure. This is consistent with the commonly observed trend in the threshold pressures that the limiting flux is lower for higher solute concentrations [Porter, 1990].
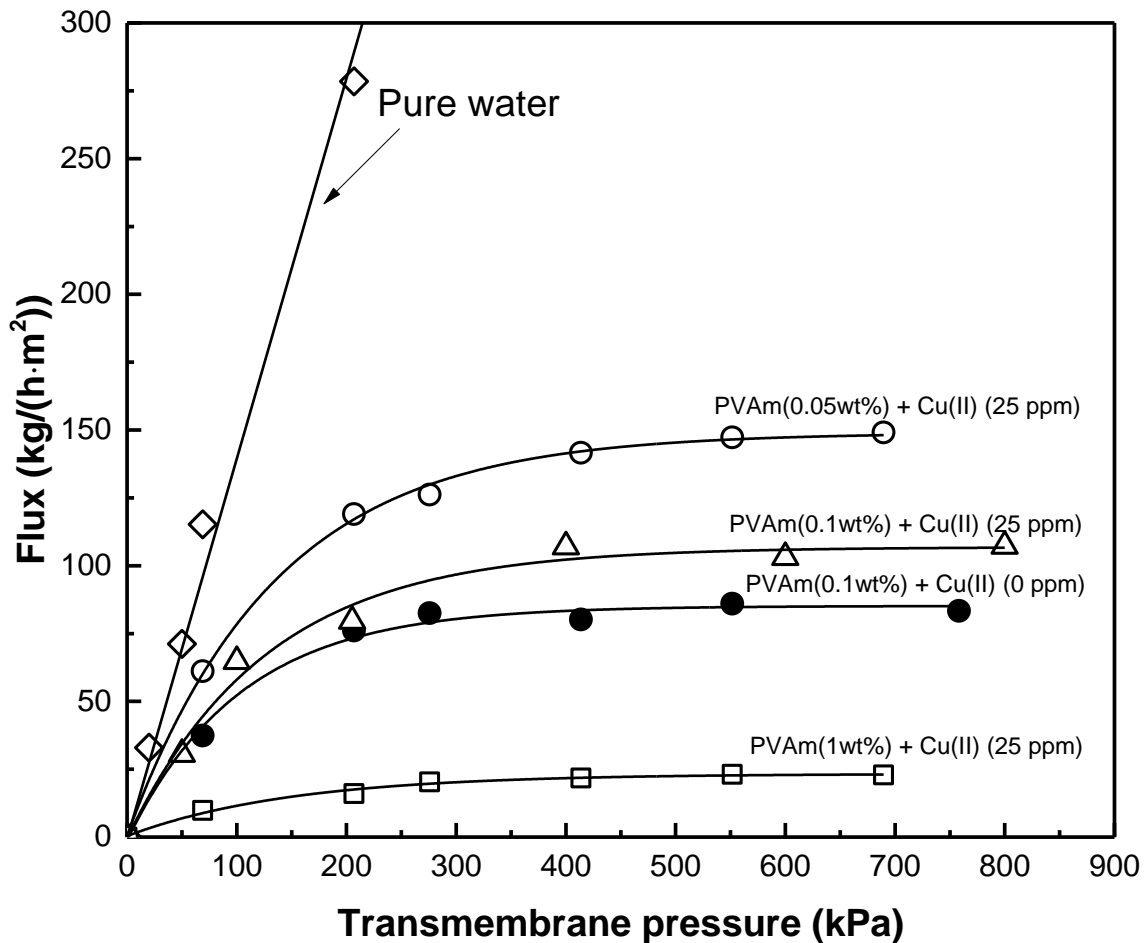
Figure 3.7 Permeation flux changes at different dosages of PVAm. All experiments were operated at room temperature (25 ℃).

Interestingly, at a given PVAm concentration (e.g., 0.1 wt%), the UF flux for PEUF of the copper solution is higher than the UF flux of the aqueous PVAm solution in the absence of copper ions. This can be explained as follows. The chelation of heavy metal cations by PVAm is considered to be primarily intramolecular, and the polymer chains of PVAm will be less stretched upon chelation when the metal ions are present [Bolto and Gregory, 2007], resulting in significant changes in the shape and configuration of the macromolecules. This helps reduce its viscosity and adhesivity, which favors the permeation rate during the UF of the feed solutions.

To investigate the effects of temperature on the performance of PEUF for metal rejection, the PVAm-$CuSO_4$ system was selected for studies at different copper concentrations, and the results are shown in Figure 3.8. It can be seen that at a given copper concentration, there was no or little change in the rejection of Cu(II) over the temperature range tested (25 - 60 ℃), whereas the permeation flux increased significantly with an increase in the temperature. The increased permeation flux is easy to understand because an increase in temperature will reduce the viscosity of the solution. The effects of temperature on copper rejection may be considered from two aspects: On the one hand, an increase in temperature tends to weaken the intermolecular interactions for chelate formation that is used to retain the metal, which is unfavorable for copper rejection in the PEUF. On the other hand, like many other salts, there is a considerable increase in the solubility of the copper salt in water when temperature increases, which increases the activity of the copper for binding into the PVAm macromolecules. When the two opposing effects are balanced, the metal rejection will not be significantly influenced by temperature.
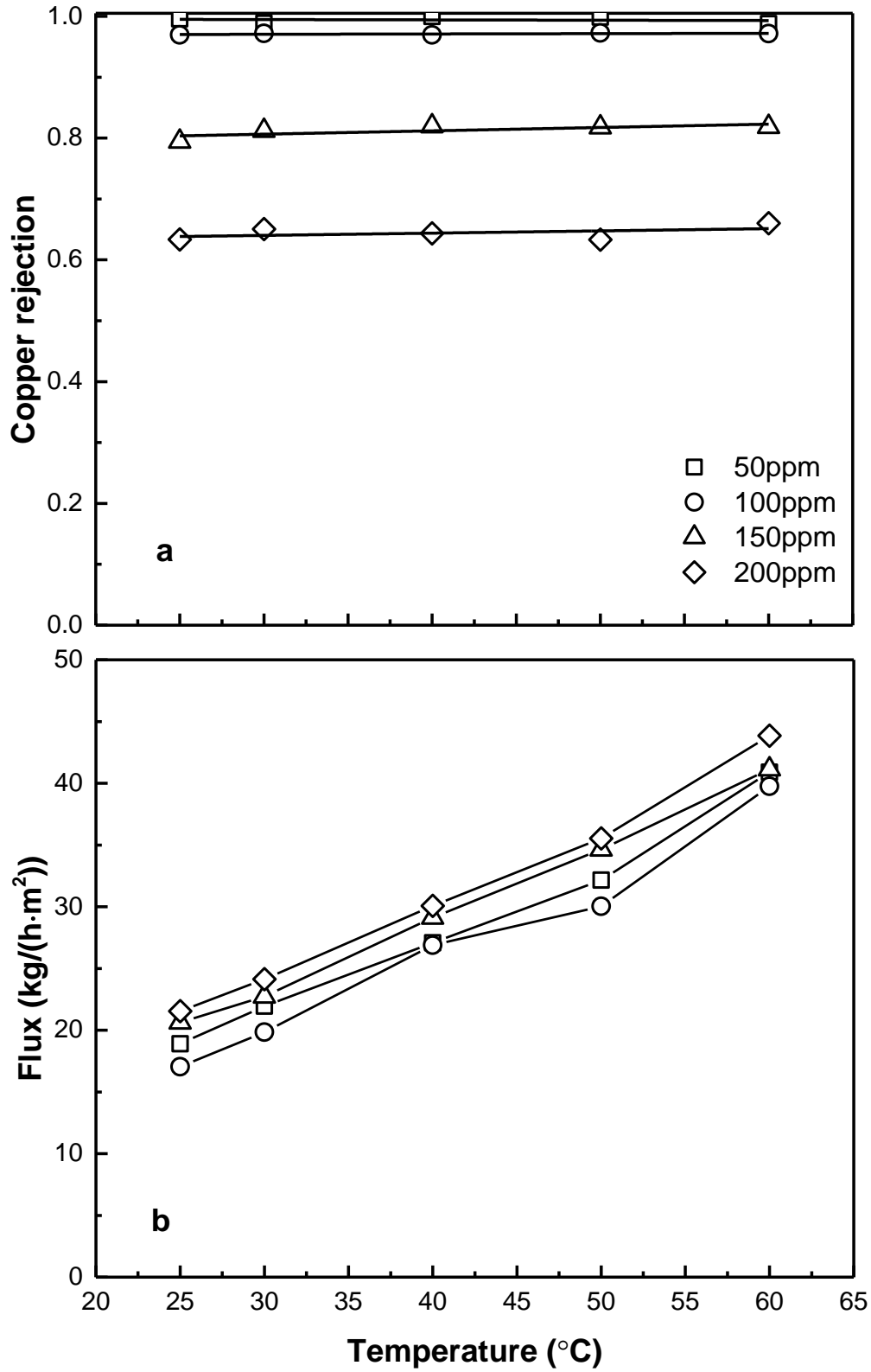
Figure 3.8 Effect of temperature on Cu rejection and flux at different copper concentration in PEUF. CuSO$_4$ was used, [PVAm] = 1 wt%, transmembrane pressure = 200 kPa.

3.3.2 Coordination of PVAm with heavy metal ions

3.3.2.1 Characterization

Such characterization methods as UV-Vis spectrometry and conductometric titration may be employed to study polymer-metal complexes [Teyssie *et al.*, 1965; Jia *et al.*, 2014]. The UV-vis absorbance of various PVAm-metal complex solutions was examined. As shown in Figure 3.9, at a metal concentration of 25 ppm, there were no obvious new characteristic peaks for the PVAm-metal complexes except for PVAm solutions containing Co(II) and Cu(II), where two absorption peaks were observed at about 306 nm and 250 nm for PVAm-Co(II) and PVAm-Cu(II) complexes, respectively. This confirms the coordination between PVAm macromolecules and Co(II) and Cu(II) in the aqueous phase. Although no new peaks were observed for the PVAm solutions in the presence of Fe(III), Cd(II) and Pb(II), their peaks corresponding to the primary amine groups in PVAm (at 210 nm in the absence of the metals) became broadened and shifted to a longer wavelength, indicating interactions between these metal ions and PVAm macromolecules. For the other heavy metal ions studied here (i.e., Ni(II), Mn(II) and Zn(II)), no obvious changes in the absorbance peak shifting were noticed except that the peak at 210 nm was intensified by these heavy metal ions. It should be pointed out that although the UV-vis spectrometry was not adequate to reveal the coordination interactions for the aqueous PVAm-Ni(II), Mn(II) and Zn(II) complex systems, a significant enhancement in rejections of these three metals did occur in the PEUF due to PVAm. In addition, the characteristic peaks for the PVAm-metal complexes were quite sensitive to the PVAm concentration in the solution. As shown in Figure 3.10, an increase in the PVAm concentration tends to not only intensify the peak strength but also shift the peak to a shorter wavelength.

66
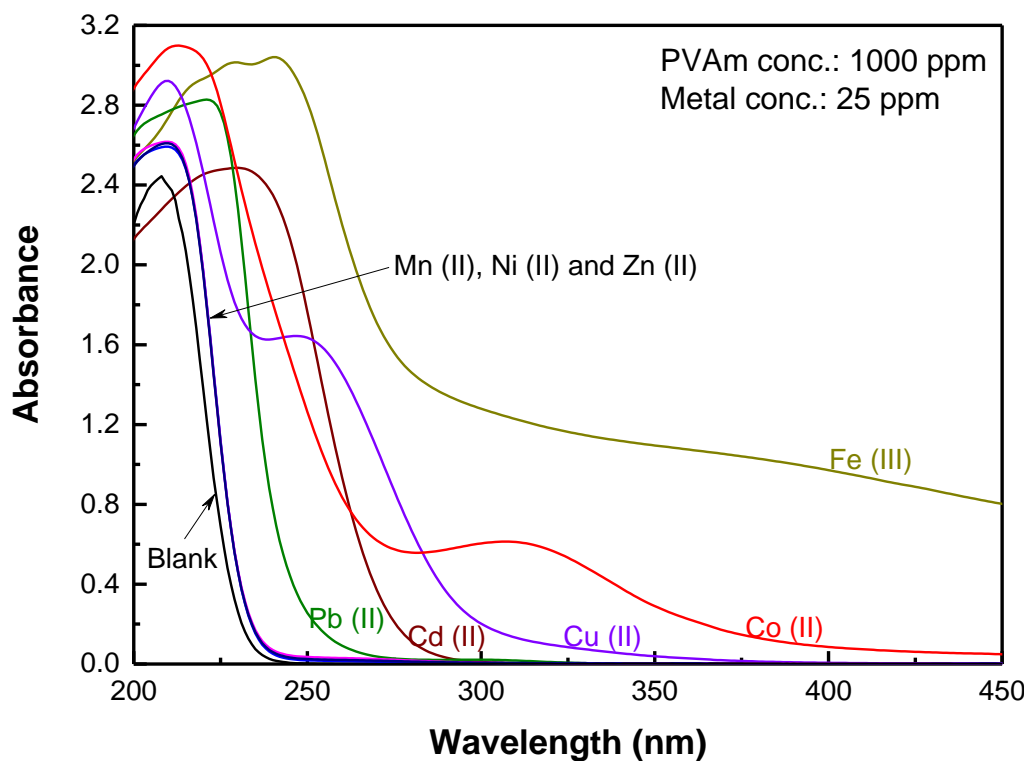
Figure 3.9 UV adsorption spectrum of PVAm coordinated with each heavy metal ion.
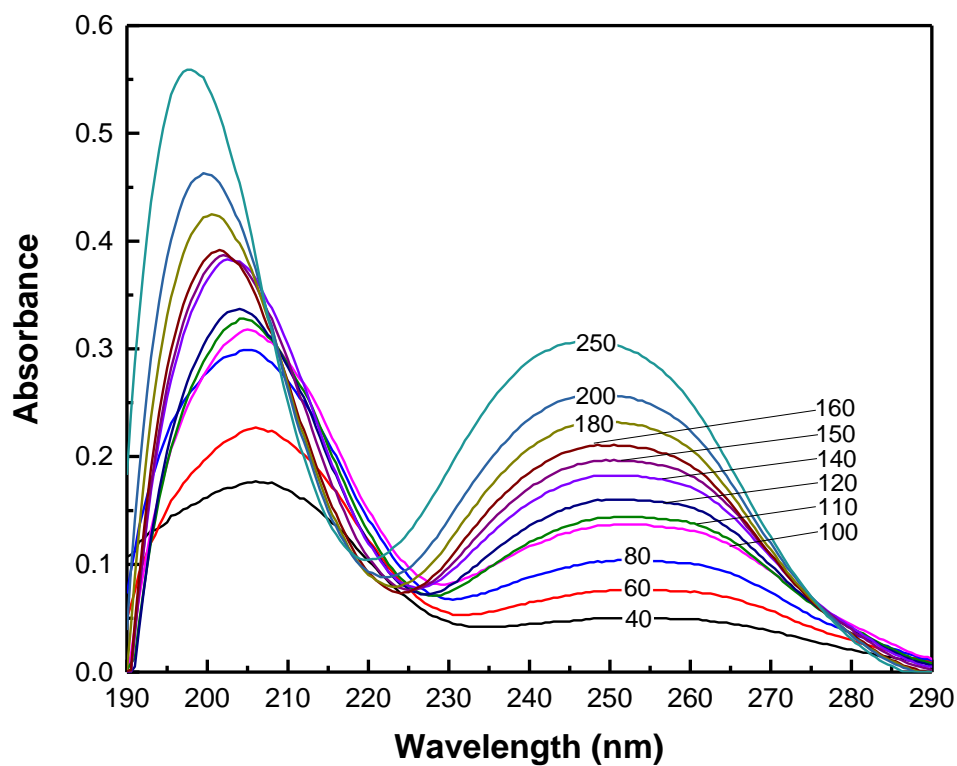
Figure 3.10 Effect of PVAm conc. on the adsorption spectrum of PVAm-Cu(II) coordination. $CuSO_4$ was used, [Cu]: 50 ppm, [PVAm] increased from 40 to 250 ppm as labelled.
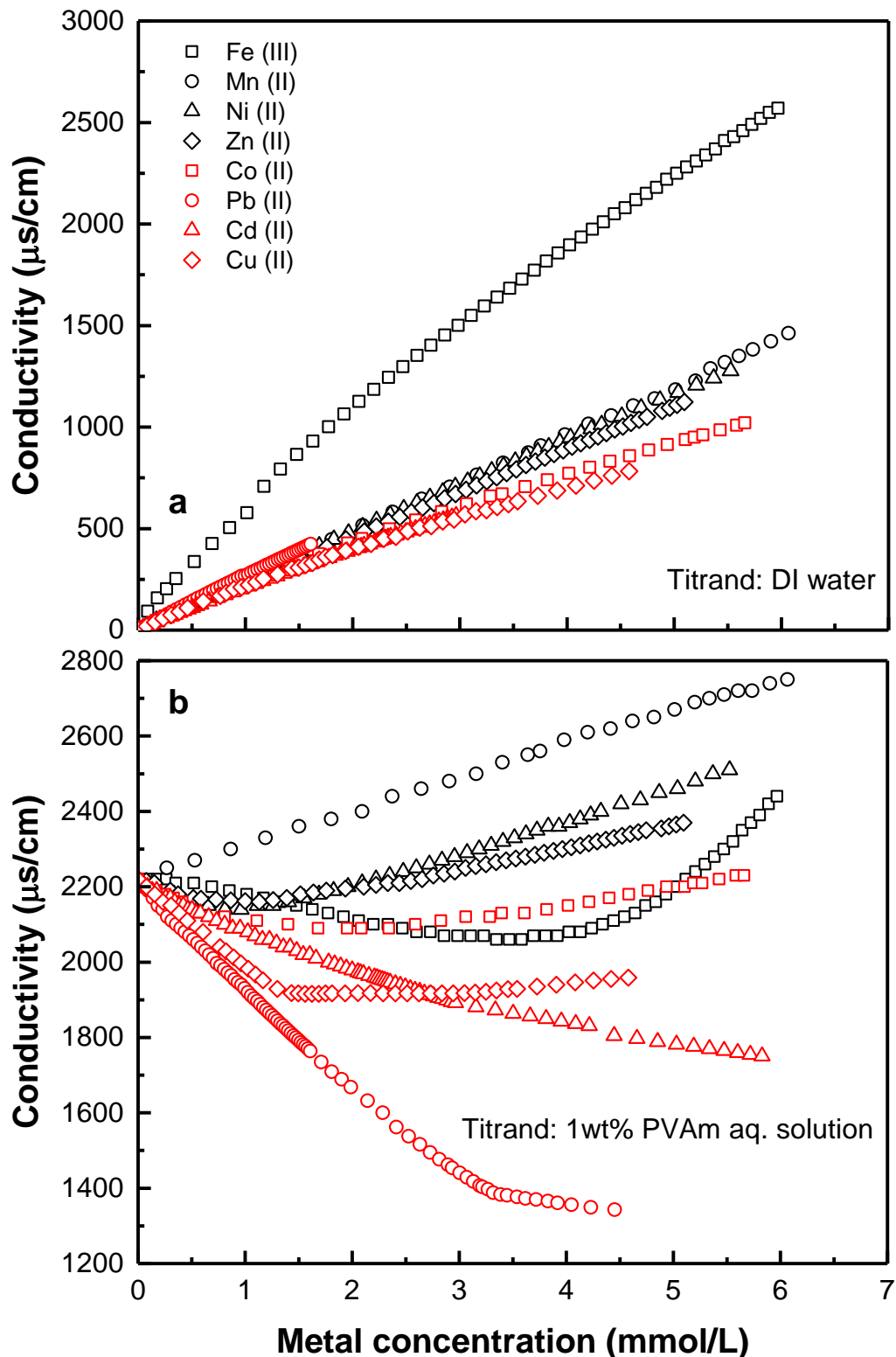
Figure 3.11 Conductometric titrations where metal ion solutions of 1000 ppm titrate 100 mL
1 wt% PVAm aqueous solution or DI water.

In order to further investigate the properties of PVAm-metal complexes and to get a clearer picture about the interactions of PVAm-Ni(II), PVAm-Zn(II) and PVAm-Mn(II) complexes, conductometric titration experiments were conducted. The results of the titration experiments are presented in Figure 3.11, where the conductivity of the resulting (titrand + titrant) solution mixture was plotted as a function of the metal ion concentration in the solution. Normally, the addition of an ionic compound into an aqueous solution will increase the conductivity of the solution due to increased concentration of free ions. As expected, when the metal salt solution was added to deionized water, the conductivity of the solution increased because of the increased ion concentrations in the solution mixture, as shown in Figure 3.11a. However, when the titrand was originally an aqueous solution of PVAm (1 wt%) in water, the conductivity of the (titrand + titrant) solution mixture experienced a decrease initially as the salt solutions were added to the PVAm solution, except for the Mn(II) salt. The decreased conductivity may be attributed to successive formation of metal-PVAm complexes, which reduced the number of free ions in the solution and restrained the mobility of bonded ions in the complexes. When sufficient quantities of titrants Fe(III), Cu(II), Zn(II), Co(II), and Ni(II), were added to the PVAm solution, the conductivities of the solution mixtures began to increase with further addition of such titrants. For titrants Pb(II) and Cd(II), the conductivities of (titrand + titrant) solutions kept decreasing with an increase in the metal content in the solution. Interestingly, the conductometric titration curve of Mn (II) showed a different trend. The conductivity of the aqueous solution of (PVAm + $MnCl_2$) increased with an increase in the metal content. It is believed that conductivity of an ionic species will be lowered if a complex with the PVAm is formed. The above results seem to suggest that different metals have different strengths of interactions with PVAm and there is an equilibrium between the PVAm-

metal complexes and the un-bonded ions in the aqueous system. Both the UV-vis spectrometry and conductometric titration results show that there are considerable interactions between PVAm and Co(II), Cd(II) and Zn(II). However, the rejections of these metals in PVAm-enhanced UF are relatively low (see Figure 3.3). It suggests that the strength of the interaction between PVAm and heavy metals in aqueous phase is just a necessary condition for a high metal rejection in PEUF.

3.3.2.2 Correlation with the metal rejections in PEUF

Prior research has shown that for a given amount of a water-soluble polymer, the amount of metal ions that can be retained by the polymer in PEUF is limited [Uludag *et al.*, 1997; Muslehiddinoglu *et al.*, 1998; Qiu and Mao, 2013; Shao *et al.*, 2013]. This is, the metal rejection cannot maintain a high level if the metal-to-polymer ratio is sufficiently high. This was also confirmed by the conductometric titrations and the UF experiments carried out in this study. For the sake of illustration, the conductivity and metal rejection in PEUF are plotted in Figures 3.12 and 3.13 at different metal-to-PVAm mass ratios for PVAm-Cu(II) and PVAm-Ni(II) systems, respectively. The sharp changes in the conductivities of the PVAm-metal complex solutions with a change in the metal-to-PVAm mass ratio corresponded well to the drastic changes in the metal rejections in PEUF. Below a certain level of the metal-to-PVAm mass ratio, a rather high value of metal rejection (>98%) was achieved, and the conductivities of PVAm-metal complex solutions decreased continuously with an increase in the metal-to-PVAm mass ratio. For a given amount of PVAm, when the quantity of the metal in the solution was large enough that the PVAm was no longer sufficient to adequately bind additional metal ions, an increase in the metal-to-PVAm mass ratio would increase the conductivity of the

solution and reduce the metal rejection of PEUF because of the un-bonded free metal ions in the solution. In addition, as shown in Figure 3.12, where copper(II) salts with different counter anions were selected in the study, the metal-to-PVAm mass ratio at which the metal rejection and solution conductivity experienced sharp changes was not affected by the counter anions of copper(II). However, among the four copper(II) salts tested, the highest copper rejection was observed with copper acetate, and this system also exhibited the lowest conductivity. This is not surprising because the carboxyl groups are good coordinating sites themselves. The oxygen atom on carboxyl groups with free electron pairs is also a good electron donor, and can coordinate with Cu(II). Since the feed solution must be neutral, PVAm actually will capture the Cu(II) cations along with the accompanying carboxyl anions, forming a complicated metal complex. The synergic effects of carboxyl and amine groups may result in the higher rejection of Cu(II).

To summarize, the interactions between PVAm and heavy metals in aqueous solutions are shown to be correlated to the metal rejections in PEUF. The properties of the PVAm-metal complexes are different for different heavy metals, and this subsequently influences the efficiency of PVAm as a chelating agent for the removal of heavy metals by PEUF. The complexation of heavy metals with macromolecular amines is known to be much more complicated than complexation with small molecular chelating agents (e.g., ethylenediamine, nitrilotriacetic acid and ethylenediaminetetraacetic acid) in aqueous solutions. More research is required to get an insight into the mechanisms of the polymer-metal complexation. Nonetheless, PVAm was shown to be a good chelating agent for the removal of such heavy metals as Cu(II), Pb(II), Ni(II) and Fe(III) from water using PEUF.
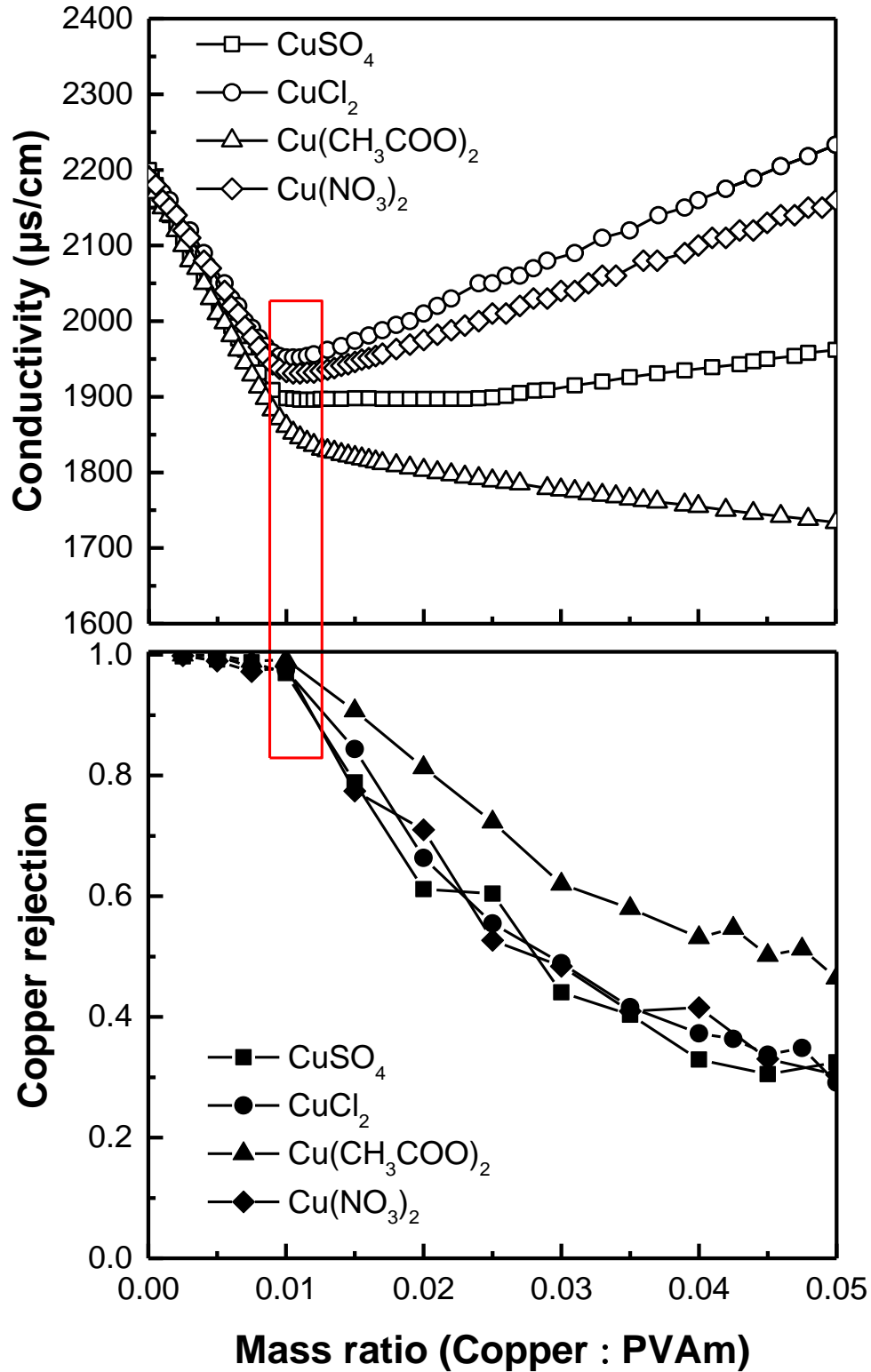
Figure 3.12 Behaviour of copper rejection and conductivity in function of the mass ratio, four kinds of copper salts with different anions were used.
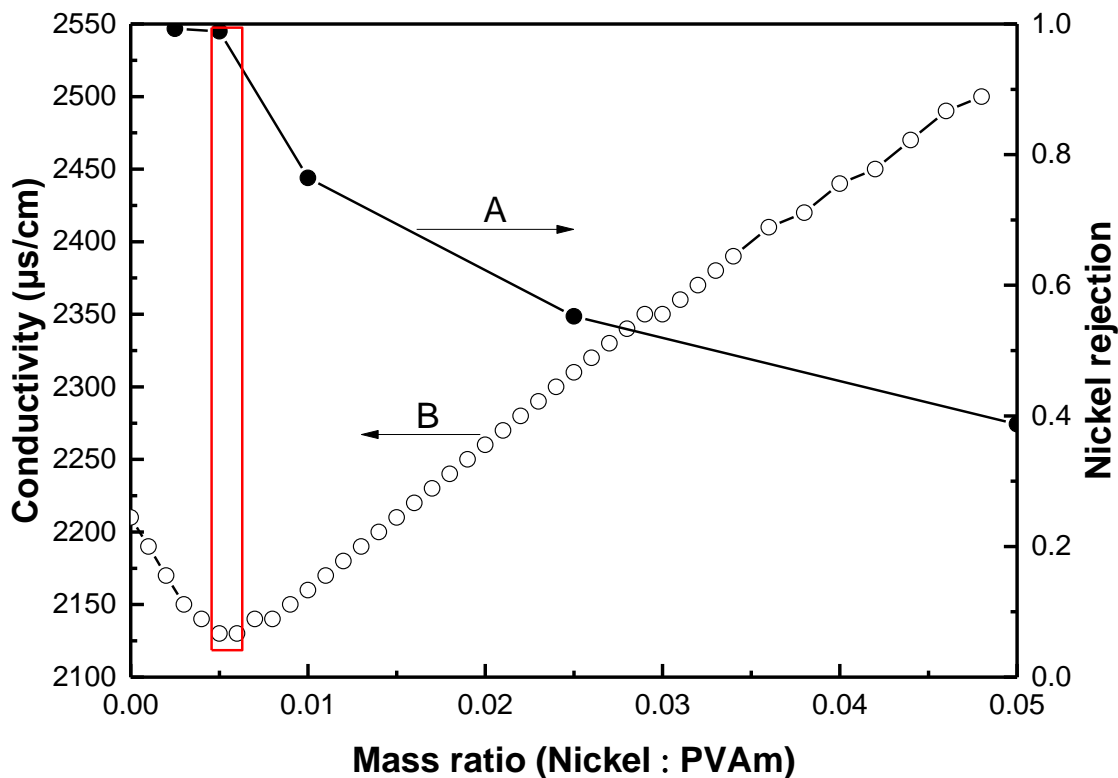
Figure 3.13 Behaviour of nickel rejection and conductivity in function of the mass ratio

Curves A: plots of metal rejection vs mass ratio in PEUF experiment

Curves B: plots of conductivity of PVAm-Ni(II) soln. vs mass ratio in titration experiment

3.3.3 PVAm-metal Equilibrium in aqueous solutions

3.3.3.1 Precipitation

It is now still difficult to establish a simple equilibrium model to describe polymer-metal complex systems, although a great deal of work has been done in an attempt to look into the complexation mechanisms [Geckeler *et al.*, 1980; Golovanov *et al.*, 1993; Rivas *et al.*, 2003; Palencia *et al.*, 2011; Shao *et al.*, 2013; Zerze *et al.*, 2013]. In this study, an attempt was made to investigate the PVAm-metal equilibrium in aqueous solutions. Besides the polymer-metal complex formation, a further phase separation between PVAm-metal complexes and their

constituents in aqueous solutions occurred under certain conditions. This will change the mechanism of heavy metal removal from PEUF to traditional coagulation/flocculation. This aspect, to our knowledge, has not been investigated in the literature.

In the titration experiments, it was found that when the heavy metal ions were added dropwise to the PVAm solution, some precipitates would appear beyond a certain amount of metal added. The occurrence of precipitation of PVAm-metal complexes is confirmed by UV-vis spectrophotometric analysis. Figure 3.14 shows the changes in the absorbance of the aqueous PVAm solution containing different amounts of the Cu(II) and Co(II), and PVAm-metal precipitates are also visible to human eyes (see inserts in Figure 3.14). When $CuSO_4$ was gradually added to the aqueous PVAm solution, the intensity of the characteristic peak of PVAm-Cu(II) complex at 250 nm initially increased and then levelled off, followed by a dramatic drop when the metal content in the solution was high enough to induce precipitation the PVAm-Cu(II) complex. As a result, there are two equilibria in the solution system: one is complexation between Cu(II) and PVAm in the aqueous phase to form water-soluble complex, and the other is phase equilibrium between insoluble PVAm-Cu(II) complex and the constituents in the liquid phase (i.e., copper salt and PVAm-Cu(II) complex dissolved in the aqueous phase) when the metal content is sufficiently high. Similar results were also observed for the characteristic peaks of PVAm-Co(II) complexes at 306 nm when $CoSO_4$ was added to the aqueous PVAm solution (Figure 3.14b). In addition, two new characteristic peaks appeared; one was at a wavelength of 365 nm, and the other was at ca. 445 nm. Both absorbance peaks were intensified when Co(II) was added, and the spectral peaks at around 445 nm also showed a hypsochromic shifting.
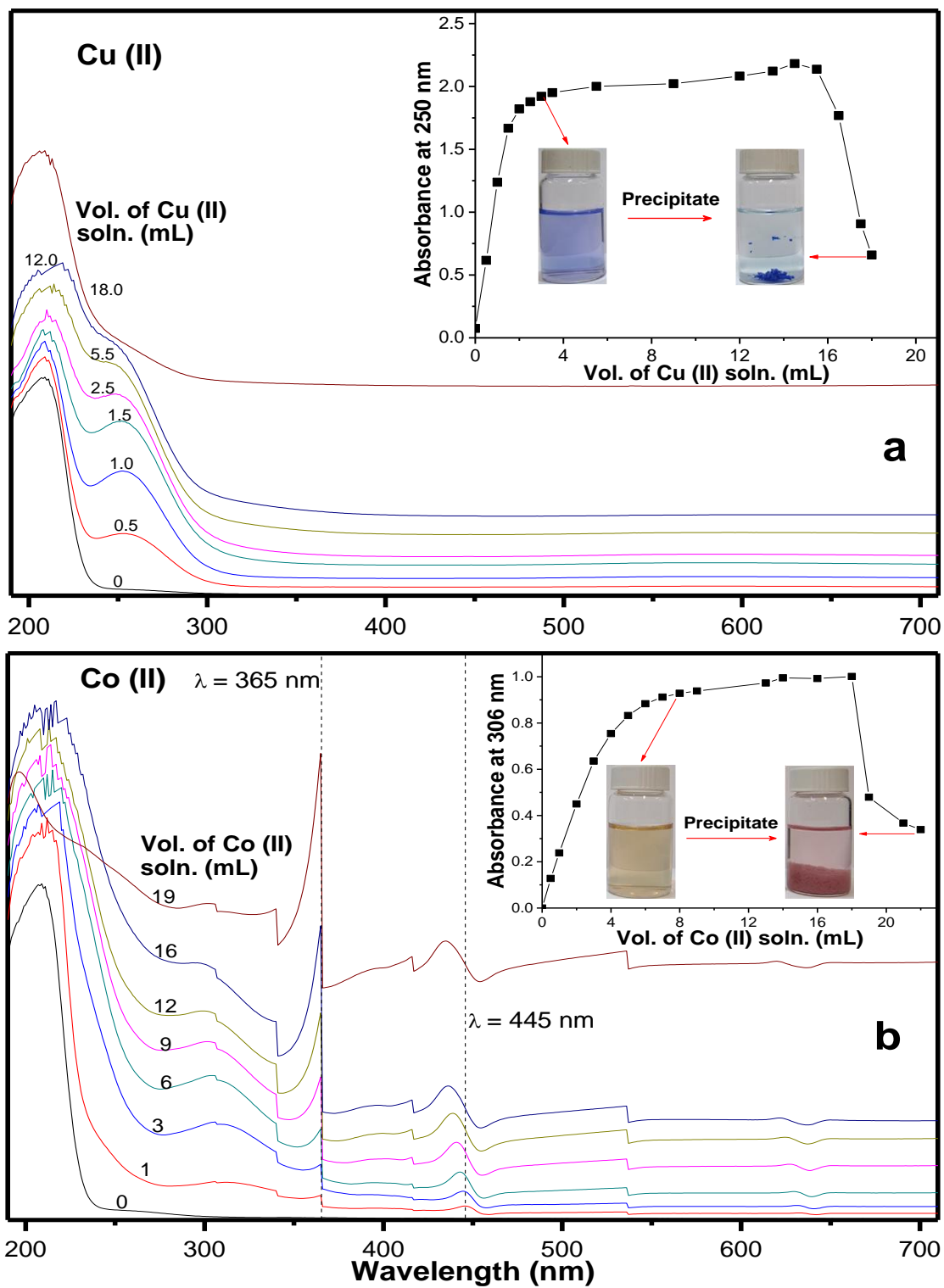
Figure 3.14 UV-spectra to illustrate formation of PVAm-metal complexes and precipitations
a) 100 mL of PVAm solution (0.1wt%), titrated by $CuSO_4$ solution with 1000 ppm Cu(II)
b) 100 mL of PVAm solution (0.1wt%), titrated by $CoSO_4$ solution with 1000 ppm Co(II)
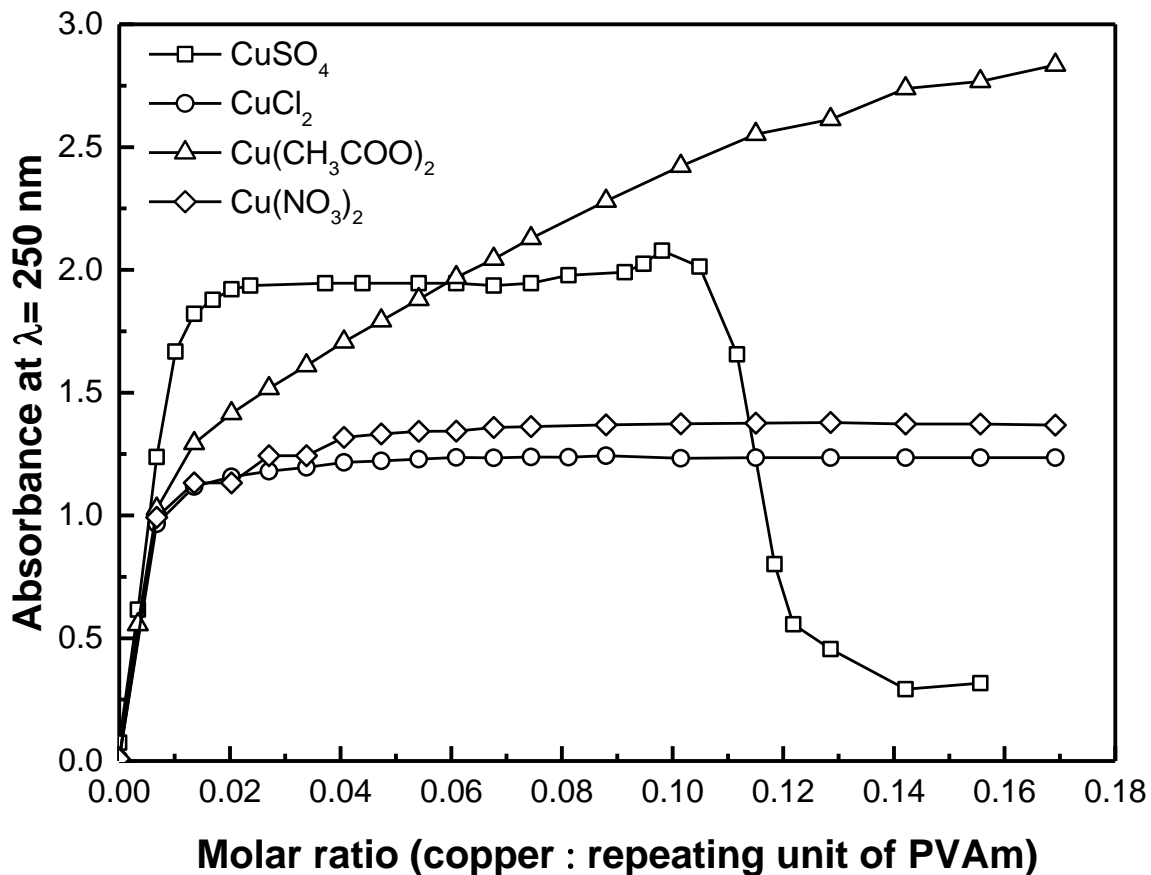
Figure 3.15 Effects of anions on the UV-vis absorption peak strength of PVAm-Cu(II) complex in aqueous solutions, obtained by titrating 100 mL 0.1 wt% PVAm aqueous solution with different copper salt solutions ([Cu] = 1000 ppm)

In view that the PVAm-metal complexes need to be electroneutral, it is of interest to further investigate whether the precipitation of PVAm-metal complexes from an aqueous solution is influenced by the counter anions of the metal salts. Figure 3.15 shows the absorbance of aqueous PVAm with different copper salts at a wavelength of 250 nm. There was no sharp decrease in the intensity of the spectral bands at 250 nm for the PVAm-Cu(II) systems with the exception of the PVAm-CuSO$_4$ solution. For the copper salts with monovalent anions, the PVAm-Cu(II) complexes were water soluble and no precipitate was observed. It is thus hypothesized that the divalent sulfate anions may have caused ionic cross-

linking of the linear PVAm macromolecules via the amine sites. The function of sulfate anions here may be similar to polyacids that can cause polybase-metal complexes to flocculate [Jellinek and Luh, 1969; Jellinek and Sangal, 1972].
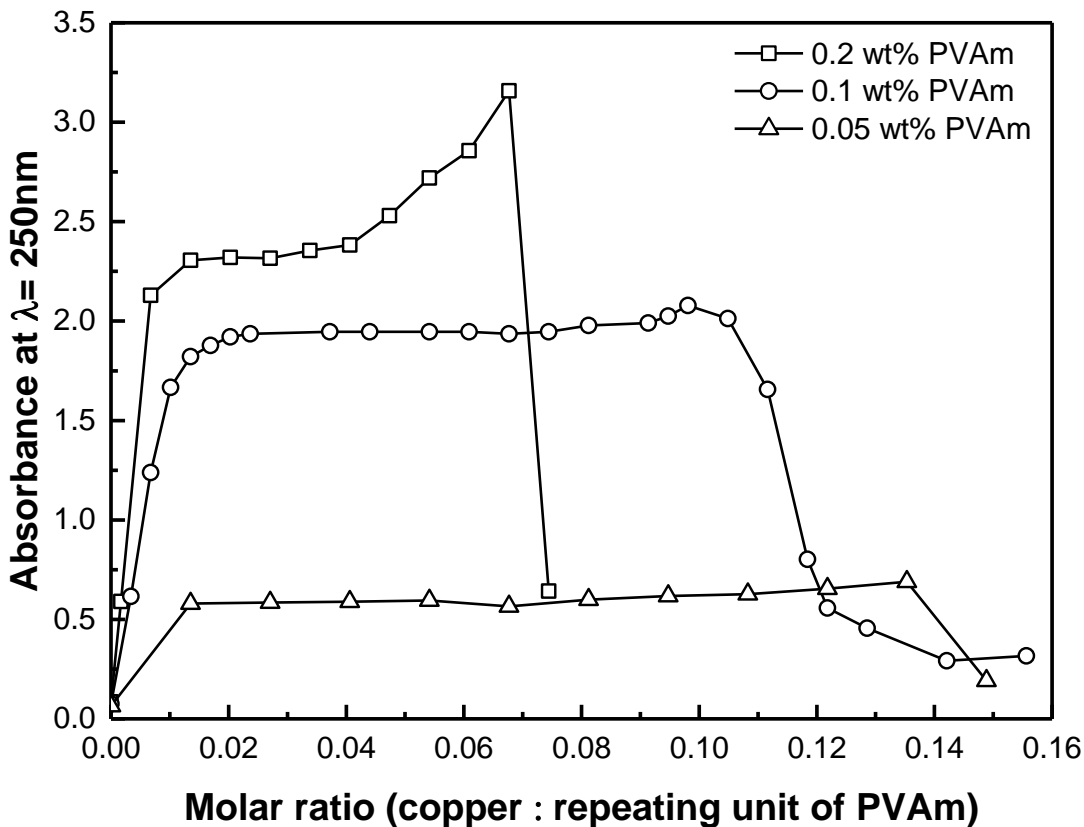
Figure 3.16 Copper sulfate solution with 1000 ppm Cu titrate 100 mL PVAm solution with different initial concentrations

It is apparent that PVAm may be used as a flocculant to remove $CuSO_4$ from water. However, the formation of PVAm-Cu(II) precipitate in aqueous solutions did not follow a simple stoichiometric relation. Figure 3.16 shows that the precipitation occurred at different copper-to-PVAm molar ratios for different PVAm concentrations. In addition, the flocculating capacity of PVAm at a given copper concentration was affected by the PVAm concentration used, as shown in Figure 3.17. A high concentration of PVAm in the solution tends to result

in a lower capacity for copper removal by flocculation in terms of the quantity of copper captured per unit mass of PVAm. When the concentration of PVAm is high, more SO_4^{2-} will be needed for the PVAm macromolecules to crosslink and form precipitates. . Therefore, the flocculation capacity per unit mass of PVAm is decreased because of the increased concentration of Cu(II) in the aqueous solution.
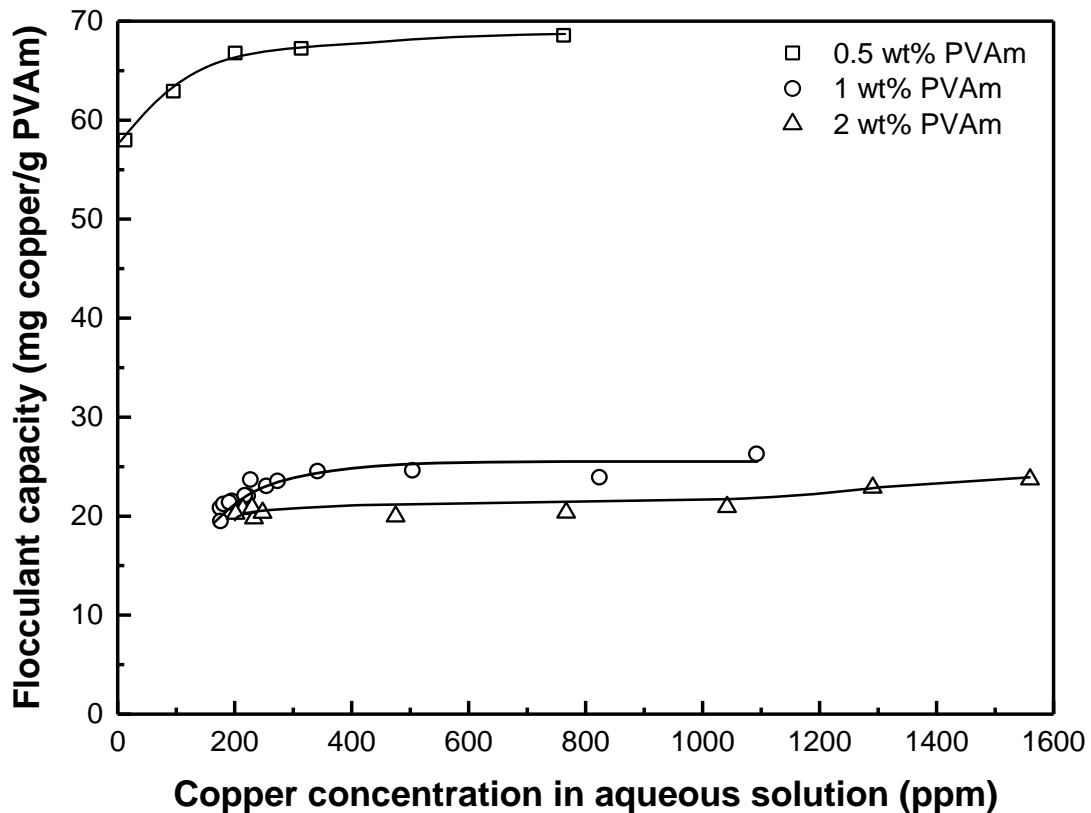
Figure 3.17 Effect of PVAm conc. on the flocculant capacity per unit amount of PVAm

3.3.3.2 The nature of polymer-metal complex and its flocculation

From a coordination chemistry point of view, there will be a reaction equilibrium for the formation of PVAm-metal complexes. Prior work has shown that it was difficult to quantify the equilibrium for the polymer complex formation [Juang and Liang, 1993; Juang and Chen,

1996; Jia *et al.*, 2014; Yang *et al.*, 2014]. For the system studied here, the PVAm coordinates with a heavy metal M to form PVAm-metal complex M(PVAm)$_n$, where *n* is the coordination number. It cannot be expressed by a simple chemical formula because of intramolecular chelation and to a lesser extent intermolecular chelation as well.
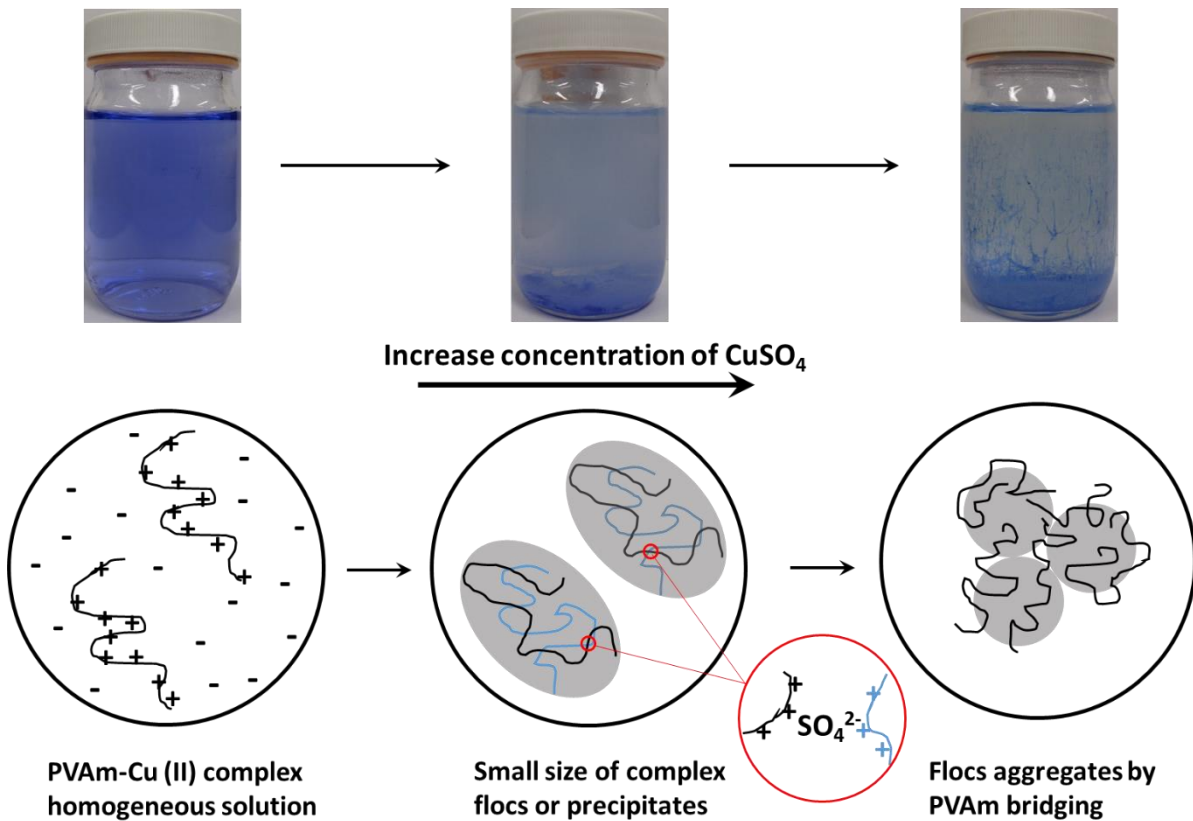
Figure 3.18 Growth of PVAm-Cu(II) complex flocculation, induced by SO_4^{2-}.

The stable water-soluble polymer-metal complex system can be broken by adding a suitable coagulating agent. Previous work showed that polyethyleneimine (PEI)-metal complexes could be flocculated out of a solution when a negatively charged water-soluble polymer (e.g., polyacrylic acid and phosphonomethylated PEI) was added [Jellinek and Luh, 1969; Navarro *et al.*, 2005], and the precipitation was attributed to charge neutralization and metal bridging [Bolto, 1995; Bolto and Gregory, 2007; Wang *et al.*, 2013]. As shown above,

a small amount of divalent sulfate anion in the solution is also able to induce precipitation of PVAm-Cu(II). This process, which is essentially a coagulation/flocculation process, can be illustrated in Figure 3.18. The copper cations are easily attached onto PVAm chains by coordination with the primary amine groups in PVAm to form water-soluble PVAm-Cu(II) complexes in the homogeneous liquid phase. As the sulfate concentration increases, the PVAm-Cu(II) complexes may be connected together under electrostatic forces between sulfate anion and the positively charged sites on PVAm-Cu(II). Such ionically cross-linked complexes will grow and aggregate, and eventually precipitate out of the solution. Then, the small light-weight precipitates are further connected under the bridging effect, forming large sized flocs eventually. The pictures presented in Figure 3.18 shows the typical transition from an initial flocs formation to complete flocculation. During this process, the liquid phase is a homogeneous solution comprising of copper salt, PVAm and PVAm-Cu(II) complexes dissolved in water, which was confirmed experimentally with a PVAm-CuSO$_4$ solution. For the sake of illustration, a PVAm/CuSO$_4$/H$_2$O mixture containing 1.07 wt% of PVAm and 465 ppm of Cu(II) was filtered using a UF membrane (MWCO: 10k Da), a microfiltration membrane (MWCO: 100k Da) and a filter paper (pore size: 2.5 μm), and the copper concentration in the filtrate was 248, 285, and 298 ppm, respectively. Note that all macromolecules (including PVAm and PVAm-Cu complexes) were retained by the UF membrane, and that only the insoluble flocculates were retained by the filter paper. The copper contents in the filtrates suggest that a total of ca. 40% of the copper present in the solution was bonded to PVAm and that 67% of the PVAm-Cu(II) complexes were precipitated.

It may be pointed out that the sulfate induced phase separation of PVAm-metal complexes cannot be described by a simple solubility product constant based on an equilibrium

between the dissolved/dissociated compounds and the undissolved solid. For a typical solubility equilibrium, increasing either reactant concentration will increase the amount of the precipitate. Additional experiments in this study showed that continuously adding PVAm into the above mentioned PVAm/CuSO$_4$/H$_2$O mixture (which contained insoluble flocculates) would eventually dissolve the flocculates. This means that the flocculates were converted back to the water-soluble PVAm-Cu(II) complexes by the PVAm.

3.3.3.3 Implications for practical wastewater treatment

This study shows that the PVAm-metal complex may flocculate out of the solution by sulfate, and there is a potential to use PVAm for metal removal with PEUF or flocculation. However, the two processes are based on different properties of the PVAm-metal systems. In PEUF, the heavy metals are captured by the polymer as a water-soluble polymer-metal complex, followed by UF to retain the macromolecules. On the other hand, the flocculation process requires the polymer-metal complexes to precipitate out of the solution, followed by separation of flocs from the solution by, for example, centrifugation or sedimentation. In PEUF, the concentration of the polymer-metal complexes gradually increases as the process proceeds with time, and thus the precipitation of the polymer-metal complexes is a potential issue that should be addressed.

Figure 3.19 shows the permeation flux of PEUF for feed solutions containing different concentrations of CoSO$_4$ while at a constant PVAm concentration (0.1 wt%). The UV absorbance of the feed solution at 306 nm was also shown in Figure 3.19 where the sharp decrease in the UV absorbance corresponds to precipitation of PVAm-CoSO$_4$ complexes. Interestingly, contrary to the common perception that the permeation flux will be reduced

when the membrane is contaminated by a solid deposit layer on the membrane surface, there is a significant increase in the permeation flux when the macromolecular complexes start to precipitate on the membrane surface. This is because the precipitation will lower the concentration of the macromolecular solutes in the feed solution, resulting in a significant reduction in the solution viscosity. In addition, instead of forming a gel-layer uniformly covering the membrane surface that will significantly affects the permeation flux, the aggregated flocs randomly deposited on the membrane surface are not densely packed. This can be seen from the membrane surfaces fouled with a homogeneous PVAm-CoSO$_4$ solution and PVAm-CoSO$_4$ flocs (Figure 3.20). In spite of good permeation flux (which is close to the pure water flux) and metal rejection when flocs form in the solution, the accumulation of solid deposits on the membrane surface is by no means advantageous for practical applications because 1) they need to be removed for disposal or subsequent further treatment and 2) the membrane surface needs cleaning to prevent blockage of the feed channel in the membrane module. Sulfate is a common ion in wastewater, and thus caution should be exercised in the PEUF process for wastewater treatment using amine polymers as chelating agents.

On the other hand, when flocculation is to be used for heavy metal removal using the amine polymers (e.g., PVAm and PEI) as flocculants, the commonly used polyacids (e.g., polyacrylic acid and polyacrylic acid-co-maleic acid) to aid flocculation may no longer be needed when multivalent anions (e.g., sulfate and phosphate) are present in the wastewater. This will help reduce the process cost as well as the secondary waste produced.
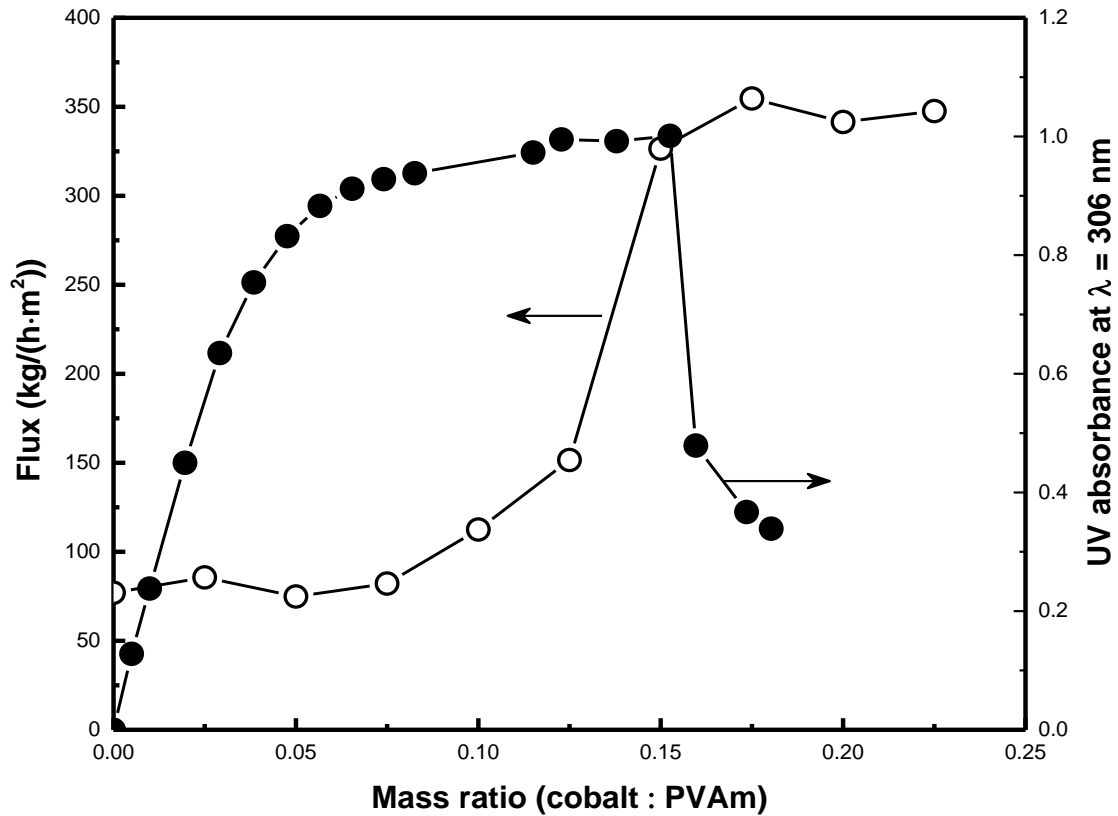
Figure 3. 19 Effect of PVAm-Co(II) flocculation on permeation flux in PEUF, flux data is tested at the steady state, transmembrane pressure: 200 kPa; UV absorbance at $\lambda = 306$ nm is taken from Figure 3.14.
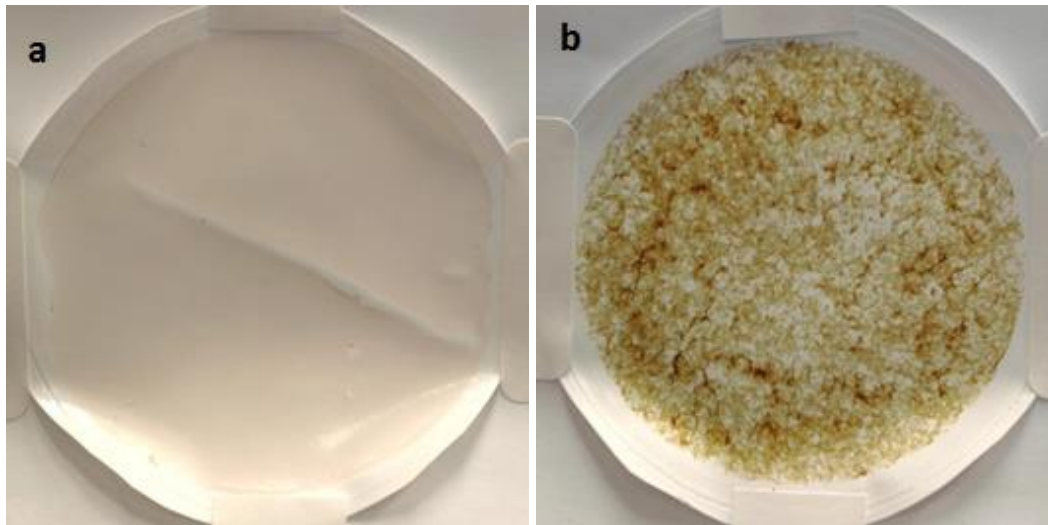
Figure 3. 20 Fouled membrane surfaces by a) soluble PVAm-Co(II) complex and b) PVAm-Co(II) flocculant

In view that the coagulation/flocculation works best to remove heavy metals at high concentrations while PEUF works best at low metal concentrations, the two processes may be integrated to form a hybrid process so as to take full advantage of the complementary features of the two steps

3.4 Conclusions

The removal of heavy metals from water with PEUF was investigated using PVAm as a chelating agent. At a PVAm dosage of 0.1wt%, the metal rejections for Pb(II), Cu(II), and Fe(III) reached 99%, 97% and 99%, respectively. Although an increase in the PVAm dosage would increase the metal rejections, the permeation flux would be compromised. The pressure and temperature had little effect on metal rejection in the operating ranges tested, whereas the permeation flux was significantly affected. The PVAm-metal interactions in aqueous solutions were studied using UV-vis spectrometry and conductometric titration, and it was shown that the metal rejection in PEUF was highly correlated to the coordination properties between the polymer and the metals.

The presence of sulfate anions in the solution would cause ionic cross-linking of PVAm, resulting in phase separation of the PVAm-metal complexes when the metal concentration was sufficiently high. Both PVAm and sulfate concentrations had significant influence on the formation of precipitates. It was shown that PVAm could be used as a flocculant for heavy metal removal by flocculation. While the flocculation worked best at high metal concentrations, the PEUF performed well in removing heavy metals at low concentrations. The two processes may be integrated to take full advantage of their complementary performance characteristics.

Chapter 4

Removal of Mercury(II) from Wastewater by Polyvinylamine-Enhanced Ultrafiltration*

4.1 Introduction

Mercury pollution has attracted significant attention worldwide since the first major case of mercury poisoning occurred in Japan (Minamata Bay, 1956) [Jiang *et al.*, 2006; Li *et al.*, 2009]. Among the various anthropogenic mercury emission sources, industrial wastewater from chlor-alkali and battery industries are presently the primary contributors to mercury releases to aquatic environment, and mercury emissions and releases are continuing to increase [Wang *et al.*, 2004; Di Natale *et al.*, 2011]. HgCl$_2$ is the most common form of Hg(II) compound. Mercury(II) in aqueous solutions can be transformed biologically or chemically into an organic form of methylmercury, which is the most toxic, persistent and bioaccumulative form of mercury in nature [Say *et al.*, 2008; Driscoll *et al.*, 2013]. Thus, there are increasingly stringent regulations on mercury levels allowed in drinking water from natural sources and the discharge limits of mercury from wastewater.

Previous research was shown that the PEUF process could be an alternative for Hg(II) removal from waste effluents, if proper water-soluble polymers were used [Swanson *et al.*,

---

1973; Uludag *et al.*, 1997; Rivas and Pereira, 2001; Barron-Zambrano *et al.*, 2004]. While prior studies focused mainly on the complexing interactions between the polymer ligands and Hg(II), which are influenced by the polymer composition, feed pH and ionic strength [Rivas *et al.*, 2003], other parameters involved in the UF process (e.g., transmembrane pressure, cross flow rate, and membrane properties) are also important as they are directly related to the concentration polarization, membrane fouling, and eventually the cleaning strategies and membrane service life for industrial-scale applications. While the increased polymer concentration on the membrane surface due to concentration polarization generally lowers the permeation flux, the opposite is often true for solute rejection by UF. In micellar-enhanced ultrafiltration (MEUF), the accumulation of surfactants on the membrane surface can lead to the formation of micelles even at a surfactant concentration in the bulk feed that is below its critical micellar concentration, which is advantageous for reducing the surfactant usage [Fillipi *et al.*, 1999; Beolchini *et al.*, 2006]. Membrane fouling caused by the accumulation or adsorption of the "solutes" (including the water-soluble polymers or surfactants) on the membrane will impose a hydrodynamic resistance to mass transport through the membrane, resulting in a gradual flux decline with time. Normally, membrane fouling can be minimized by proper management of the fluid hydrodynamics via control of the cross flow rate and the transmembrane pressures [Porter, 1990]. In addition to the operating parameters, both the properties of the water-soluble polymers (or surfactants) and the UF membranes used also have profound effects on membrane fouling [Jönsson and Jönsson, 1995], and they should be considered in selecting suitable cleaning agents. especially in long term operation [Porter, 1990; Fane *et al.*, 2011].

This chapter describes the investigation of the use of PVAm to remove mercury(II) from

86

wastewater by PEUF. The complexing interactions between mercury(II) and PVAm in aqueous streams were characterized by UV-vis spectrometry and conductometric titration. Both dead-end and cross-flow operating modes were used to elucidate the effects of concentration polarization in the PEUF process. The effects of PVAm concentration in the feed, transmembrane pressure, and cross-flow rate on water permeation flux and mercury rejection were studied. The "gel-polarization model" commonly used for UF was applied to explain the flux behaviour, and the membrane cleaning to remove the foulants for restoration of the permeation flux was also investigated. Finally, the potential use of the PEUF to capture mercury(II) from aqueous solutions was tested with simulated wastewater that is relevant to chlor-alkali wastewater.

4.2 Experimental

4.2.1 Ultrafiltration experiments

Mercury(II) chloride ($HgCl_2$) was purchased from Sigma-Aldrich and was analytical reagent grade with a purity of 99%. All other chemicals and UF membrane used were the same as described in Chapter 3. Both dead-end and cross-flow PEUF runs were performed in this chapter. The dead-end module was the same as described in Chapter 3. The cross-flow runs were performed using a tangential flow lab unit, which was equipped with two pressure gauges installed up- and down-stream of the UF module to monitor the transmembrane pressure during the filtration process. A schematic diagram of the cross-flow module was shown in Figure 4.1. The membrane cell equipted with a flat sheet membrane had an effective membrane area of 18.1 cm^2. The feed solution was pumped to the membrane module at a given pressures, and the residue stream was circulated back to the feed tank.
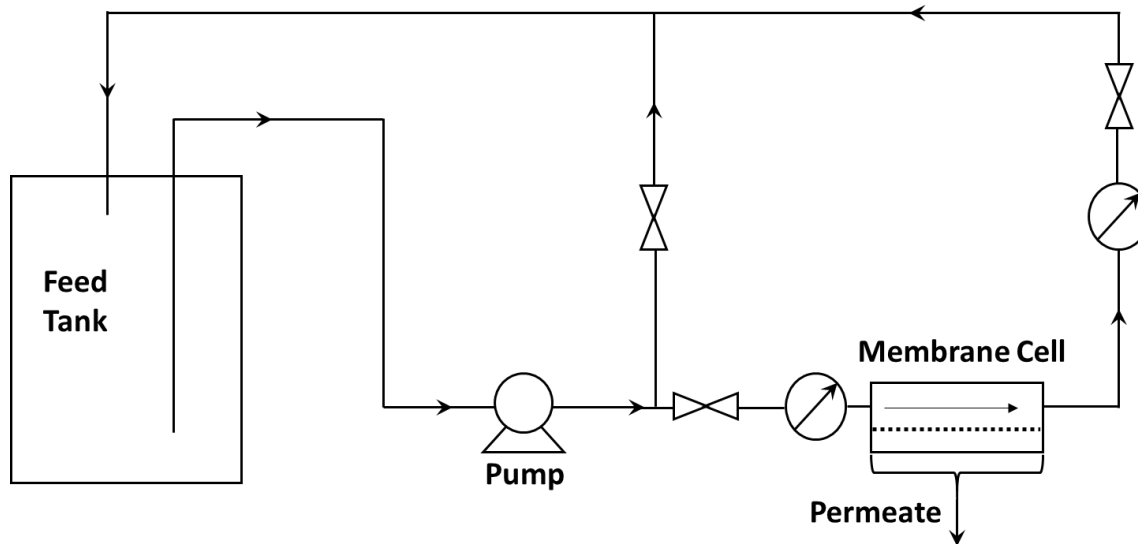
Figure 4.1 A schematic illustration of the cross-flow lab unit

For the dead-end UF runs, the feed solution containing mercury(II) and a given amount of PVAm were stirred for 2 h before being charged into the UF cell, and vigorous agitation of the feed continued with the magnetic stirrer fitted inside the permeation cell. The composition and pH of the feed solutions are shown in Table 4.1. To study the effects of concentration polarization and membrane fouling during the filtration process, a batch operation was performed as follows: first, 200 mL of the feed solution containing mercury and PVAm was filtrated through the pristine UF membrane continuously at a constant transmembrane pressure of 0.2 MPa, and permeate samples (sizes 5 to 10 mL) were collected over time. When the final volume of the feed solution in the UF cell was less than 50 mL, the membrane was removed from the cell and rinsed with deionized water or dilute hydrochloric acid (0.1 wt%) for 24 h. Then, the cleaned membrane was mounted in the permeation cell for ultrafiltration tests with the same feed solution under the same operating conditions. The same membrane cleaning and filtration tests were continued for five cycles for the batch filtration experiments. During the course of the experiments, the pure water permeability of the membrane was measured prior

to the filtration with the feed solutions. The dead-end UF was also carried out using a simulated chlor-alkali wastewater containing mercury and sodium chloride and sulfate at different pHs.

In cross-flow UF, 2 L of the feed solution was used. In one series of experiments, the feed solutions contained different amounts of PVAm (0.05 - 1 wt%), and the UF runs were carried out at a constant feed flow rate of 60 L/h. Another series of experiments was carried out at different feed flow rates (20 to 100 L/h) with a constant PVAm concentration (0.5 wt%) in the feed solutions. The transmembrane pressure was varied in the range of 0.1 to 0.8 MPa. All the retentate and permeate streams were collected and analyzed. In addition, a continuous operation over a period of 6 days in the cross-flow mode was also performed to evaluate the flux decay caused by membrane fouling, and both the permeate flux and mercury rejections were monitored during the course of cross-flow UF.

During the experiments, the concentrations of mercury and PVAm in the feed and permeate solutions as well as the separation performance calculations were similar as described in Chapter 3. Unless specified otherwise, the mercury concentration reported was based on concentration of mercury(II) in the solution.

4.2.2 Characterizations

The interactions between PVAm and mercury(II) in aqueous solutions were characterized using UV-vis spectrometry and conductometry as described in Chapter 3. The viscosities of the aqueous PVAm-Hg(II) solutions at different pHs were measured at room temperature (25 ℃) using a Brookfield digital viscometer to help understand the fouling control of acid cleaning of the foulants on the membrane surface. The solution pH was adjusted using 1 M hydrochloric acid.

The cross-section of the PES membrane was examined under a scanning electron

microscopy (SEM) (JEOL Ltd.). The membrane samples were fractured in liquid nitrogen and they were sputter-coated with palladium for morphological analysis.

4.3 Results and discussion

4.3.1 PVAm-mercury interactions

In view of the fact that i) mercury(II) can form complexes easily with many amine compounds [Uludag *et al.*, 1997] and ii) PVAm has a large quantity of primary amines that can coordinate with many heavy metals [Teyssie *et al.*, 1965], it is reasonable to anticipate a coordination between mercury(II) and PVAm will occur in aqueous solutions. In this study, their coordination interactions were confirmed experimentally by using conductometric titration and spectrometric characterizations.

Figure 4.2 shows the conductivity of the PVAm titrand solution as a function of the amount of mercury(II) chloride solution added. It should be pointed out that $HgCl_2$ is generally considered to be a covalent compound that exists mainly in molecular state, and only a very small amount may be dissociated into $HgCl^+$ and Cl^- in aqueous solutions. This is supported by the low conductivity of $HgCl_2$ solution even at a high concentration (see insert of Figure 4.2). PVAm is cationic in water due to its high density of primary amine. The titration data in Figure 4.2 shows that when the $HgCl_2$ titrant solution was added to the PVAm titrand solution, the conductivity of the mixture decreased. The reduction in the conductivity could be attributed to two factors: One was the dilution of PVAm that lowered its concentration, and the other was the coordination between PVAm and mercury. In order to exclude the effect of dilution, a "blank" titration with deionized water was also conducted for comparison purposes. The two titration curves did not overlap, and the presence of $HgCl_2$ lowered the conductivity of the

90

resulting solution mixture. This means that the ionization of the polymeric amine was restrained by coordination with mercury. Thus, there existed amine-mercury interactions, although detailed information about the interaction was unavailable.
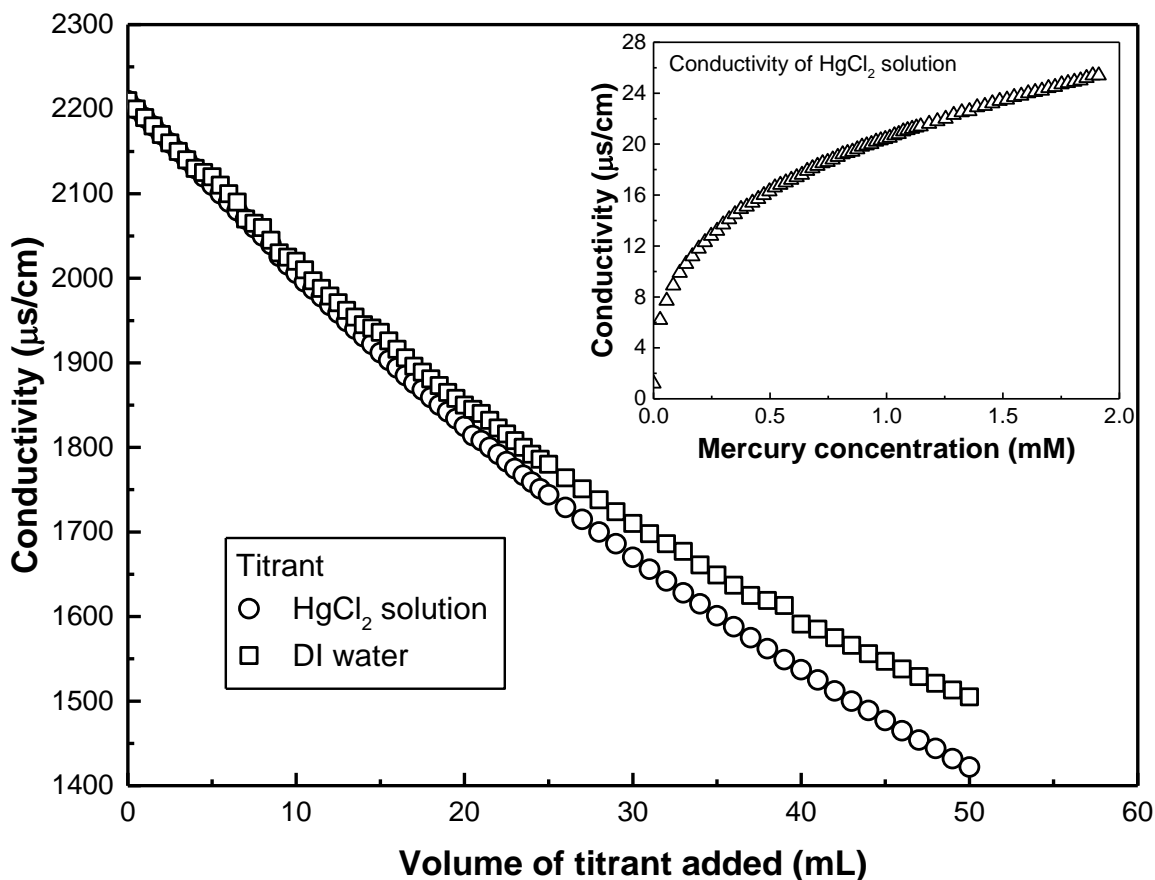
Figure 4.2 Conductometric titration curves, titrand: 100 mL aqueous solution of PVAm at a concentration of 1 wt.%; titrant: aqueous solution of $HgCl_2$ at a Hg(II) concentration of 1000 ppm, deionized water was used as a blank titrant. Insert: conductivity of aqueous $HgCl_2$ solution at concentrations.
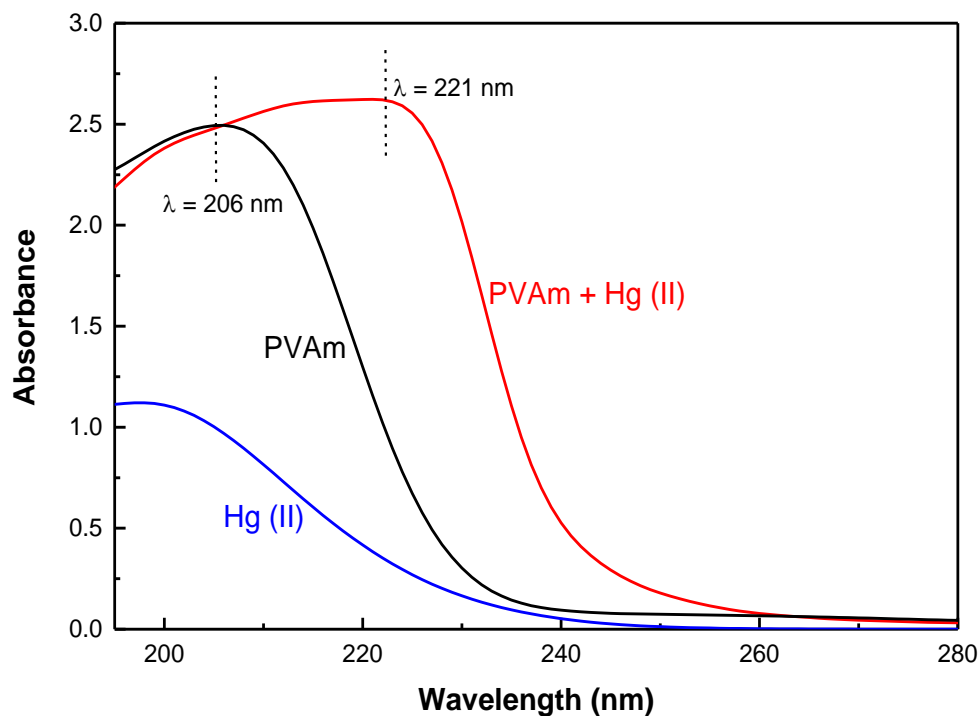
Figure 4.3 UV-vis absorption spectra of PVAm coordinated with Hg(II) (PVAm concentration: 0.1 wt.%, mercury concentration: 10 ppm). The absorbance of an aqueous PVAm solution (0.1 wt%) and an aqueous $HgCl_2$ solution (mercury conc. 10 ppm) were also shown for comparisons.

The coordination interaction between PVAm and mercury(II) in aqueous solutions was also characterized by the UV-vis spectrum shown in Figure 4.3. There was shift in the absorption peak from 206 to 221 nm when mercury(II) chloride was added to the PVAm solution, which may be attributed to the electron transition due to the coordination interaction between the amine functionalities and mercury(II) molecules.

4.3.2 Using PVAm to enhance mercury rejection by PEUF: Proof of concept

Eleven sets of permeability tests were carried out in dead-end filtration mode (Table 4.1) to study the effects of the concentrations of PVAm and mercury in the feed solution on the permeation flux and mercury rejection. The initial pH of the feed solution was monitored. The

nearly neutral pH of the aqueous PVAm-mercury feed solutions indicated that the majority of the amine groups on PVAm were not protonated, and they were expected to function as good coordination sites for Hg(II). In the absence of PVAm, the membrane rejection to mercury was also measured. As one may expect, when PVAm was absent in the feed solution, the UF membrane was unable to retain the mercury adequately. The limited mercury rejection obtained was believed to be caused partially by mercury adsorption onto the membrane due to sulfur atoms in polyethersulfone. Clearly, it was the capture of mercury by PVAm that resulted in the high mercury rejection by the PEUF, where the mercury was bounded to the PVAm macromolecules that were effectively retained by the UF membrane. For all the tested concentration conditions, the concentrations of mercury and PVAm in the feed solution had little effect on the mercury rejection, and a high mercury rejection (up to 99%) was achieved even at a high mercury concentration (e.g., 20 ppm) using only ~0.1 wt% of PVAm.

As expected, the permeation flux was influenced by the concentration of PVAm added to the feed, but independent of the concentration of mercury in the feed. At a given transmembrane pressure, the addition of PVAm to the aqueous mercury(II) solution significantly reduced the permeation flux through the membrane. The reduction in the permeation flux due to PVAm was more significant at a higher PVAm content in the feed. The presence of PVAm in the feed increased the viscosity of the feed and also produced an additional hydrodynamic resistance to water permeation due to the boundary layer effects developed on the membrane, thereby lowering the permeation flux. In addition, membrane fouling by the macromolecular solute will be more significant at high PVAm dosage. Therefore, for practical applications, a low PVAm concentration in the feed should be used as long as a sufficiently high mercury rejection can be achieved at a given mercury(II)

concentration.

Table 4.1 Mercury removal by PVAm-enhanced ultrafiltration. (Transmembrane pressure: 0.2 MPa, dead-end filtration)

Test set	Test identifier	Mercury conc. in feed (ppm)	PVAm conc. in feed (wt%)	Solution pH	Flux (L/h m^2)	Mercury rejection
1	P1	1.0	1.01	7.5	7.5	0.99
	P2	1.1	0.99	7.4	8.1	0.98
2	P3	4.6	1.11	7.6	7.6	0.97
	P4	4.4	1.02	7.5	6.4	0.96
3	P5	9.2	0.98	7.3	7.7	0.98
	P6	8.8	0.99	7.4	6.9	0.99
4	P7	23.2	1.01	7.4	7.2	0.97
	P8	22.3	1.05	7.4	6.8	0.98
5	P9	45.0	1.00	7.5	8.8	0.99
	P10	46.5	1.04	7.6	7.7	0.98
6	P11	1.2	0.09	6.8	95.4	0.99
	P12	0.9	0.10	6.8	99.5	0.99
7	P13	3.4	0.11	6.9	86.2	0.98
	P14	3.6	0.13	6.8	79.3	0.99
8	P15	8.6	0.10	6.8	83.1	0.97
	P16	7.9	0.14	6.8	85.9	0.98
9	P17	20.5	0.09	6.7	77.2	0.99
10	P18	36.1	0.11	6.9	69.4	0.95
11	P19	5.0	0	7.1	259.2	0.19
	P20	5.5	0	7.0	257.4	0.16
	P21	19.8	0	6.9	247.3	0.09

4.3.3 Effect of concentration polarization

During the course of UF, the permeation flux normally decreases with time due to the concentration polarization on the membrane surface [Denisov, 1994; Zaidi and Kumar, 2004]. The solute molecules retained by the membrane accumulate on the membrane surface, resulting in a higher solute concentration on the membrane surface than the solute concentration in the bulk feed stream. When the concentration of the solute retained on the membrane surface is high enough, a gel layer may be formed. This will lower the permeation flux of solvent (i.e., water in this case). Because of the macromolecular solute (e.g., PVAm)

used in the PEUF, a significant boundary layer effect is expected. Thus, the average flux over a given period of filtration time is sometimes used to characterize the throughput of PEUF in some studies [Beolchini *et al.*, 2006; Khosa *et al.*, 2014]. However, the time-averaged flux cannot objectively represent the instantaneous performance of the PEUF because the flux decline over time was not at a constant rate.
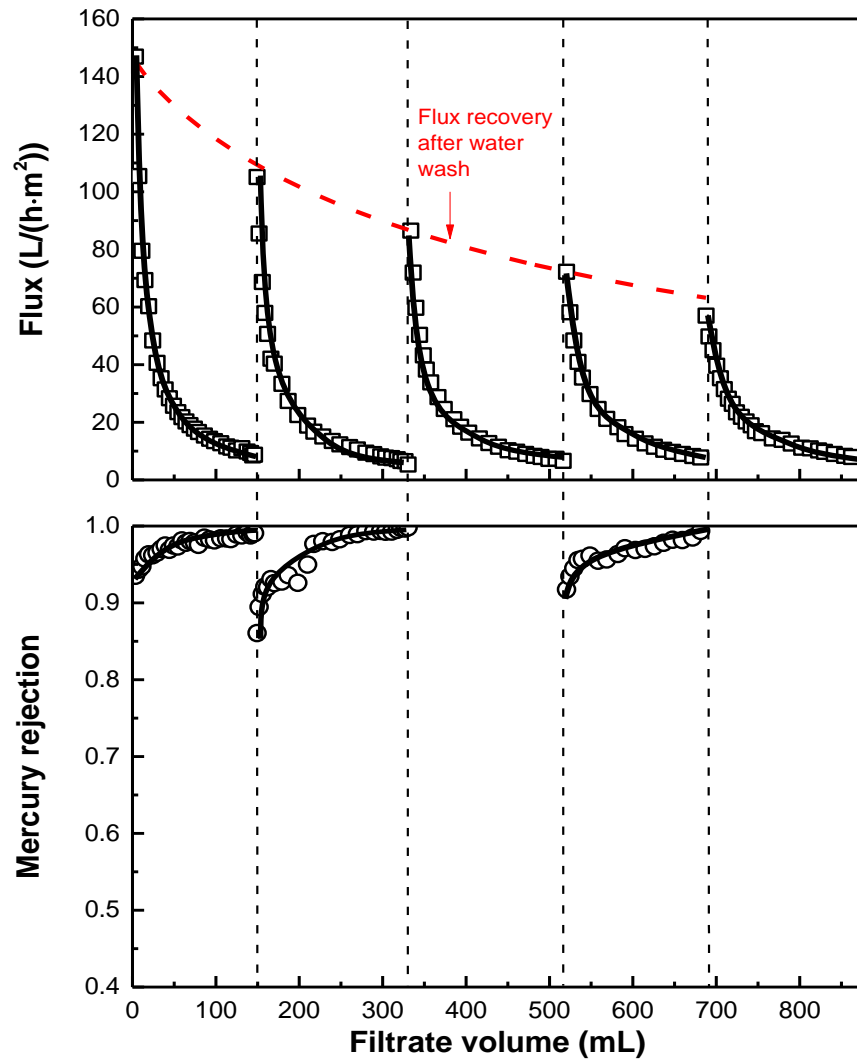
Figure 4.4 Water flux and rejection with dead-end PEUF when water wash applied between each cycle of operation. Mercury concentration in feed: 10 ppm, PVAm content: 0.1 wt%, transmembrane pressure: 0.2 MPa).

Thus in this study, the instantaneous flux and mercury rejection were measured as a

function of the volume of the filtrate collected. Figure 4.4 shows the permeation flux and mercury rejection during the dead-end PEUF process. The water flux decreased as the filtration proceeded with time, while mercury rejection increased. During the filtration process, the PVAm was concentrated, which favored the binding of mercury(II) molecules. As one may expect, the amount of PVAm relative to the amount of mercury in the feed is an important parameter related to the percentage of mercury that can be captured by the PVAm. This is supported by the mercury rejection data in Figure 4.5 for which significantly different PVAm concentrations (i.e., 0.1 and 1 wt%) were used for a feed mercury concentration of 74 and 97 ppm, respectively. At a relatively high mercury concentration, if the PVAm content present in the feed was low, mercury would have a good chance to "leak" through the UF membrane at the early stage of filtration, resulting in a low mercury rejection. However, as the filtration proceeded, the concentration polarization began to develop on the membrane surface, which would increase the concentration of PVAm on the membrane surface, and to a lesser extent, the concentration of mercury not bound by PVAm as well since the UF membrane also exhibited a low degree of rejection to mercury in the absence of PVAm. While the PVAm would be retained by the UF membrane, the increased local concentration of unbound mercury molecules on the membrane surface would lead to an increased permeation rate and thus a lower rejection. This explains the initial decline in the observed membrane rejection to mercury. On the other hand, the locally concentrated PVAm on the membrane surface helped to retain unbound free mercury molecules in the feed. As a result, the mercury rejection eventually increased over time. The initial reduction of mercury rejection was not observed when a high dosage of PVAm was used. This is understandable because when the initial PVAm concentration in the feed is already high enough, almost all the mercury molecules will be

96

bound to the polymer, and the concentration polarization will further help mercury to bind onto PVAm. The advantageous effect of concentration polarization on solute rejection has also been observed in MEUF, where surfactant micelles may form near the membrane surface at a bulk surfactant concentration below its critical micellar concentration [Fillipi *et al.*, 1999; Beolchini *et al.*, 2006].
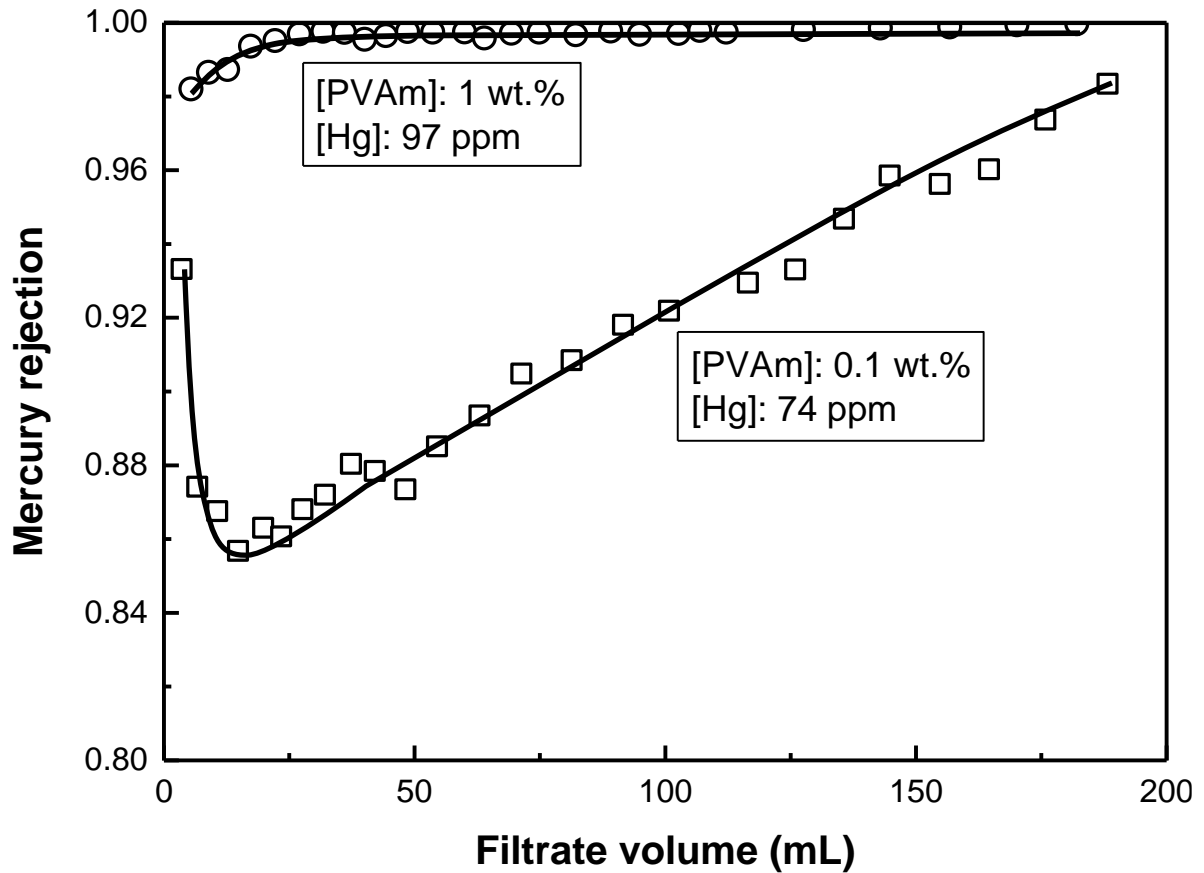
Figure 4.5 Different behavior in mercury rejection in dead-end filtration when significantly different dosages of PVAm were used. Transmembrane pressure: 0.2 MPa.
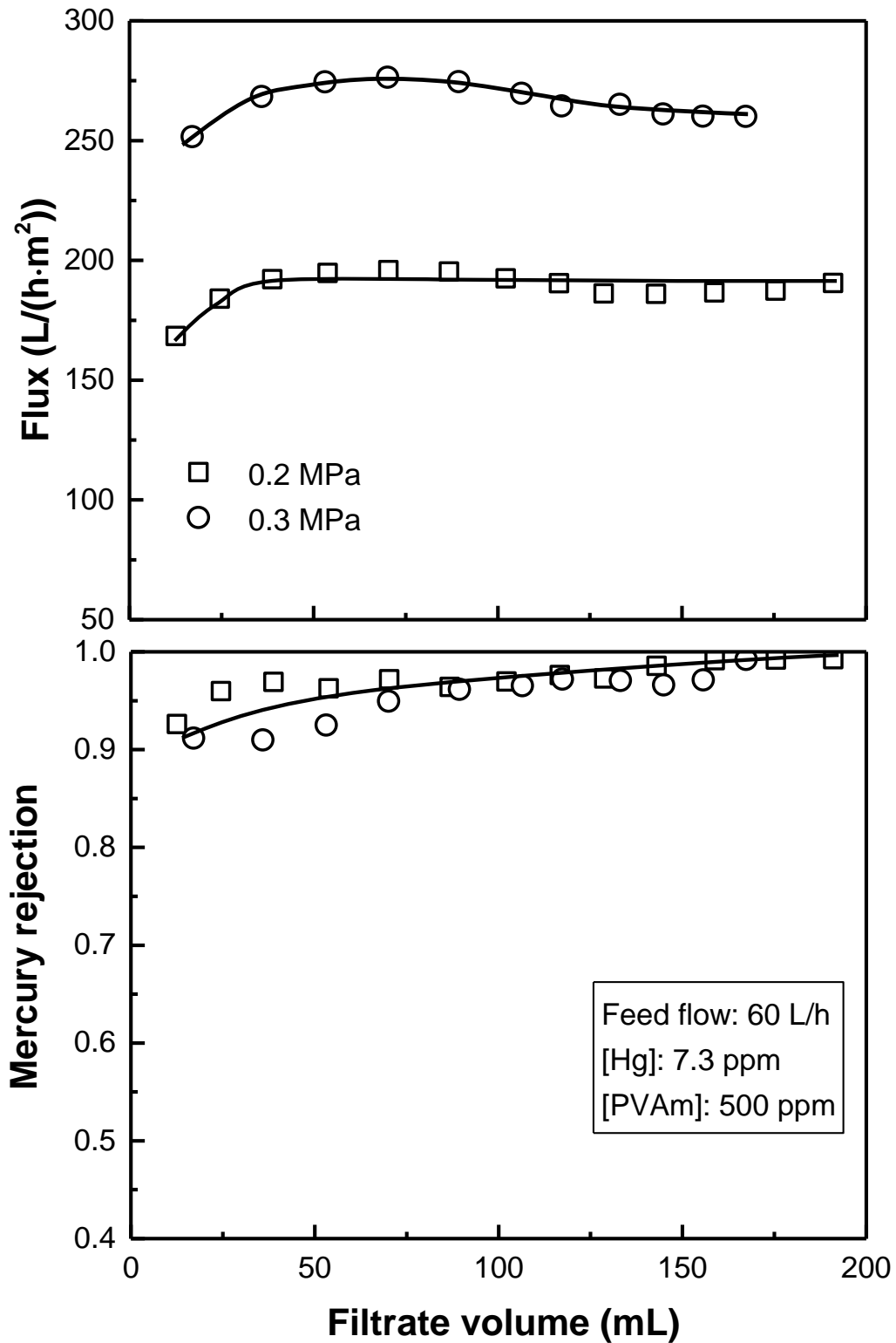
Figure 4.6 Water flux and mercury rejection at different pressure in cross-flow filtration. Feed flow rate: 60 LPH, mercury conc. in feed: 7.3 ppm, PVAm content: 0.05 wt.%.

Generally speaking, the concentration polarization is undesired in practical applications because of the reduced flux throughput. Concentration polarization can be controlled and reduced by module design and proper fluid flow management. In this regard, the cross-flow filtration mode is preferred, which allows the PVAm accumulated on the membrane surface to be swept away by the tangential flow [Porter, 1990]. Increasing the feed flow velocity tends to reduce the boundary layer effect and increase the permeation flux. As shown in Figure 4.6, the permeation flux in cross-flow filtration can maintain a value for a much longer time than deal-end filtration, indicating that the concentration polarization is indeed reduced significantly by the tangential flow of the feed solution on the membrane surface. The permeation flux obtained is around 170-190 L/(h·m^2) at only 0.2 MPa transmembrane pressure. Such a permeate flux is much higher than the typical permeate flux in traditional nanofiltration and reverse osmosis. It is anticipated that the permeation flux can be increased further by increasing the transmembrane pressure or using an UF membrane with larger pore sizes as long as the macromolecules are adequately retained. The good mercury rejection demonstrates the effectiveness of using the PEUF process to capture mercury from wastewater.

4.3.4 Effect of pressure

The data in Figure 4.6 show that the mercury rejection in cross-flow filtration is not significantly affected by the transmembrane pressure, but the permeation flux is highly pressure dependent. Although some prior work on PEUF and MEUF showed a linear change in flux with respect to the transmembrane pressure [Canizares *et al.*, 2004; El-Abbassi *et al.*, 2011], such a relationship is not representative for common UF processes [Wijmans *et al.*, 1984; Nabetani *et al.*, 1990; Porter, 1990].
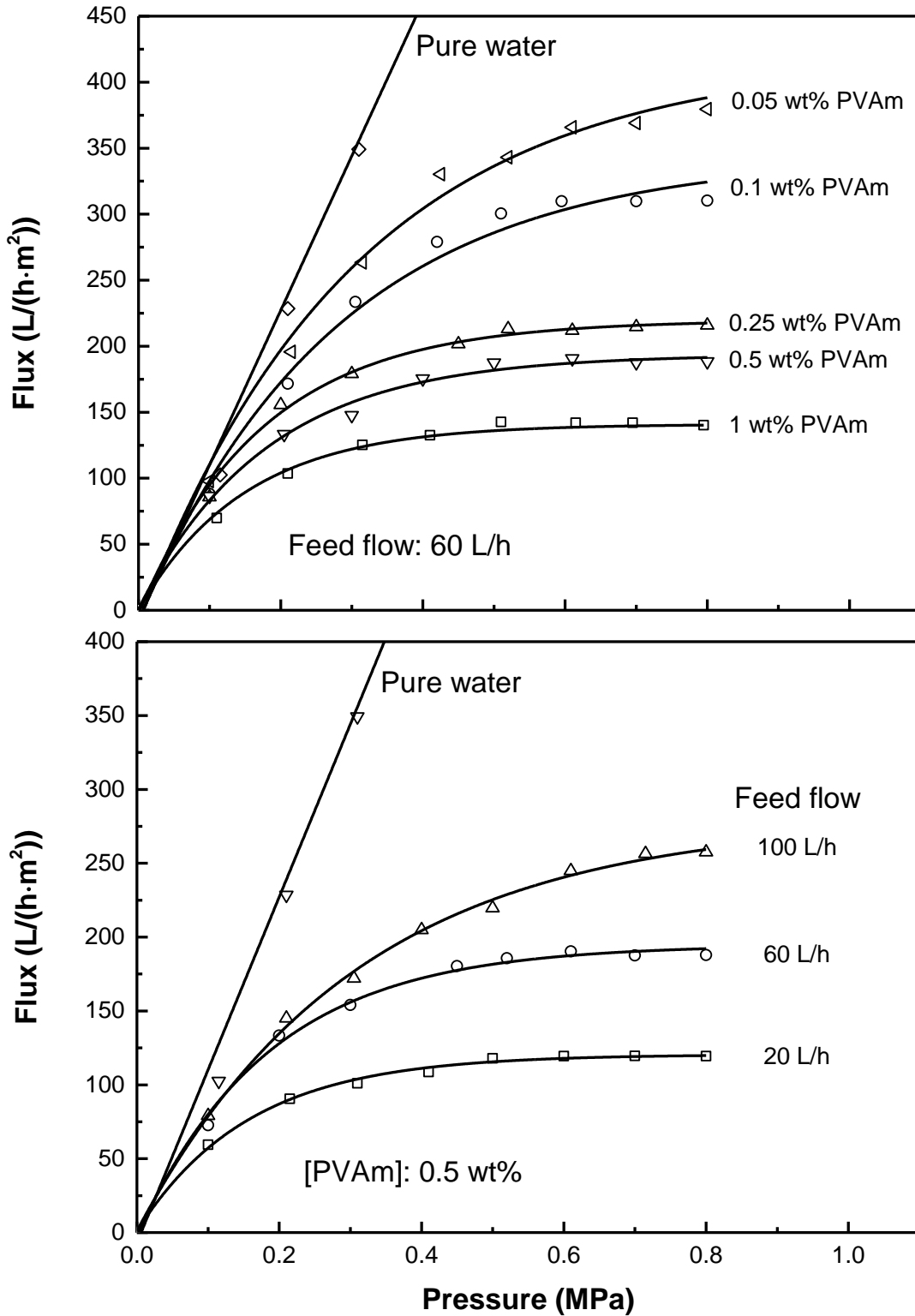
Figure 4.7 Effect of transmembrane pressure on water flux in PEUF under cross-flow filtration mode. Mercury concentration in feed: 10 ppm.

The pressure dependence of permeation flux for mercury rejection using PVAm-enhanced ultrafiltration is shown in Figure 4.7, where a typical flux curve for UF was observed. The pure water permeation flux was shown to be proportional to the transmembrane pressure. However, the permeation flux in the PEUF increased with an increase in the transmembrane pressure and it began to level off when the transmembrane pressure was sufficiently high. This is typical of conventional UF which can be explained by concentration polarization and gel layer formation. At low pressures, the permeation rate is low and the boundary layer effect on mass transport is insignificant, and thus the water flux increases almost linearly with the transmembrane pressure. However, when the permeation flux becomes large enough that the concentration polarization is no longer negligible, the external mass transfer resistance will be increasingly important, and in this case the water flux will continue to increase with the transmembrane pressure but the increase in the flux is less than proportional. In an extreme case of concentration polarization in the boundary layer where the solute concentration on the membrane surface is high enough to form a gel layer, the mass transfer resistance in the gel layer becomes dominant over the resistance of the membrane itself, and an increase in the pressure applied will increase the thickness of the gel layer due to increased solute accumulation on the membrane. When a gel layer is formed, the flux reaches a limiting value. As expected, at a given feed flow rate, the limiting flux is lower at a higher concentration of the macromolecular solute (i.e., PVAm); at a given solute concentration in the feed, the limiting flux is higher at a higher feed flow rate. This is indeed shown in Figure 4.7 for the PEUF system studied here.
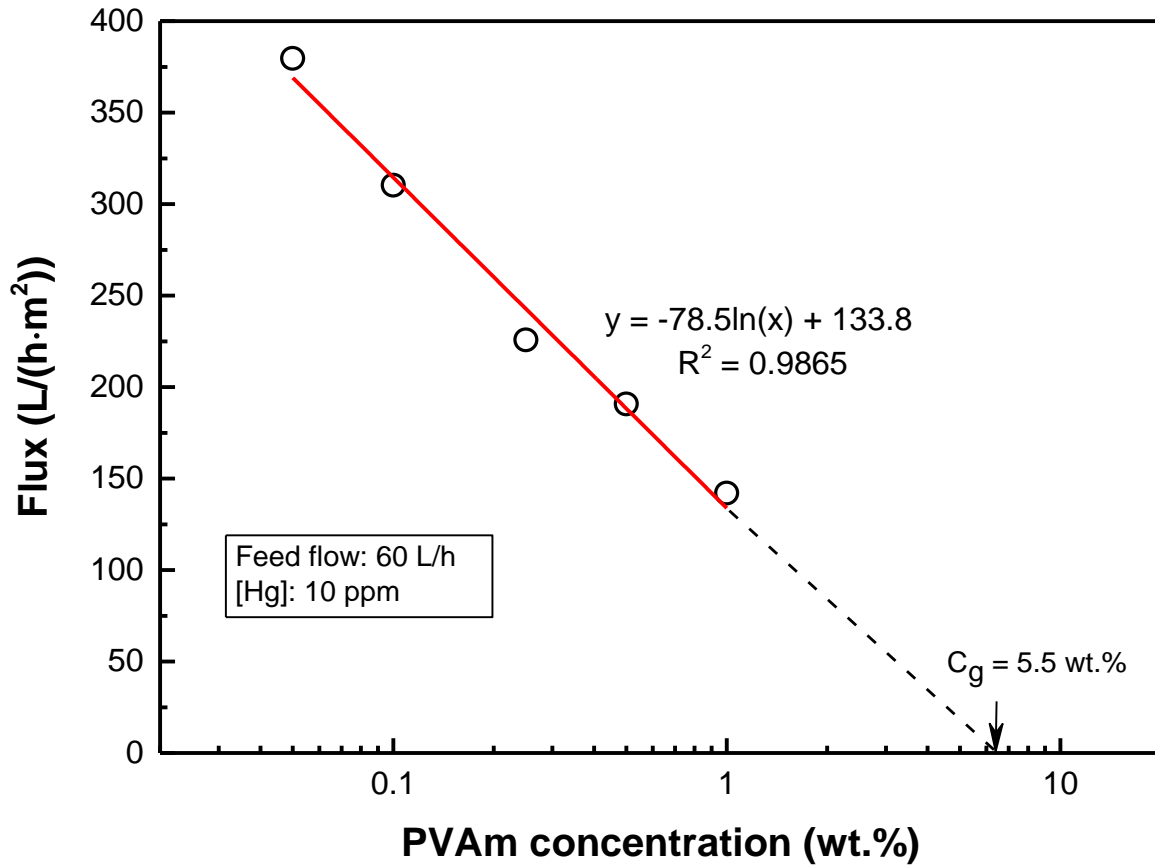
Figure 4.8 Semi-log plot of limiting flux at different PVAm concentration.

Theoretically, the limiting flux is related to the solute concentration in the feed by the following equation [Nabetani *et al.*, 1990; Porter, 1990]:

$$J_\infty = k \cdot \ln\frac{C_g}{C_b} \tag{4.1}$$

where J_∞ is the limiting flux through the membrane, k is the mass transfer coefficient, C_b is the solute concentration in the bulk feed, and C_g is the gel concentration (i.e., the solute concentration at which the solute forms a gel). Equation (4.1) suggests that if the feed flow hydrodynamic conditions are fixed (and thus k is constant), a plot of the limiting flux versus the logarithm of C_b will yield a straight line, which extrapolates to the gel concentration at zero flux. The flux data for the PVAm-enhanced ultrafiltration to remove mercury from water

appears to fit the model quite well, as shown in Figure 4.8; the gel concentration of the macromolecular PVAm (or more strictly speaking, the PVAm-Hg(II) complexes) is estimated to be 5.5 wt%. It may be mentioned that there are several other models that can be used to describe the flux in UF. In spite of some shortcomings with the gel layer model [Wijmans *et al.*, 1984; Nabetani *et al.*, 1990], it was shown to be adequate to describe experimental data about the limiting flux for the PEUF system studied.

4.3.5 Flux decline and restoration

Although the concentration polarization can be controlled to some extent by proper fluid management, the flux may still decline gradually with time due to membrane fouling. The solute and other foulants present in the wastewater (e.g., bacteria, proteins, or microorganism) will accumulate or absorb on the membrane, resulting in pore blocking in the membrane and boundary layer effect on the membrane surface. As a result, the flux through the membrane decreases over time at a given operating pressure [Porter, 1990; Fane *et al.*, 2011]. The surface of the PES membrane used in this study is negatively charged [Jawor and Hoek, 2010; Wu *et al.*, 2014], which makes it vulnerable to fouling by positively charged solutes. On the other hand, PVAm (which have primary amine groups) may be slightly protonated, and a small amount of $HgCl_2$ can also be dissociated into $HgCl^+$ and Cl^- in aqueous solutions. The accumulation or adsorption of positively charged PVAm-Hg(II) onto the negatively charged PES membrane surface was unlikely to be insignificant. Figure 4.9 shows the flux and mercury rejection over a period of 6 days. Although membrane fouling reduced the flux, an average mercury rejection of greater than 90% was achieved over the entire course of PEUF operation.
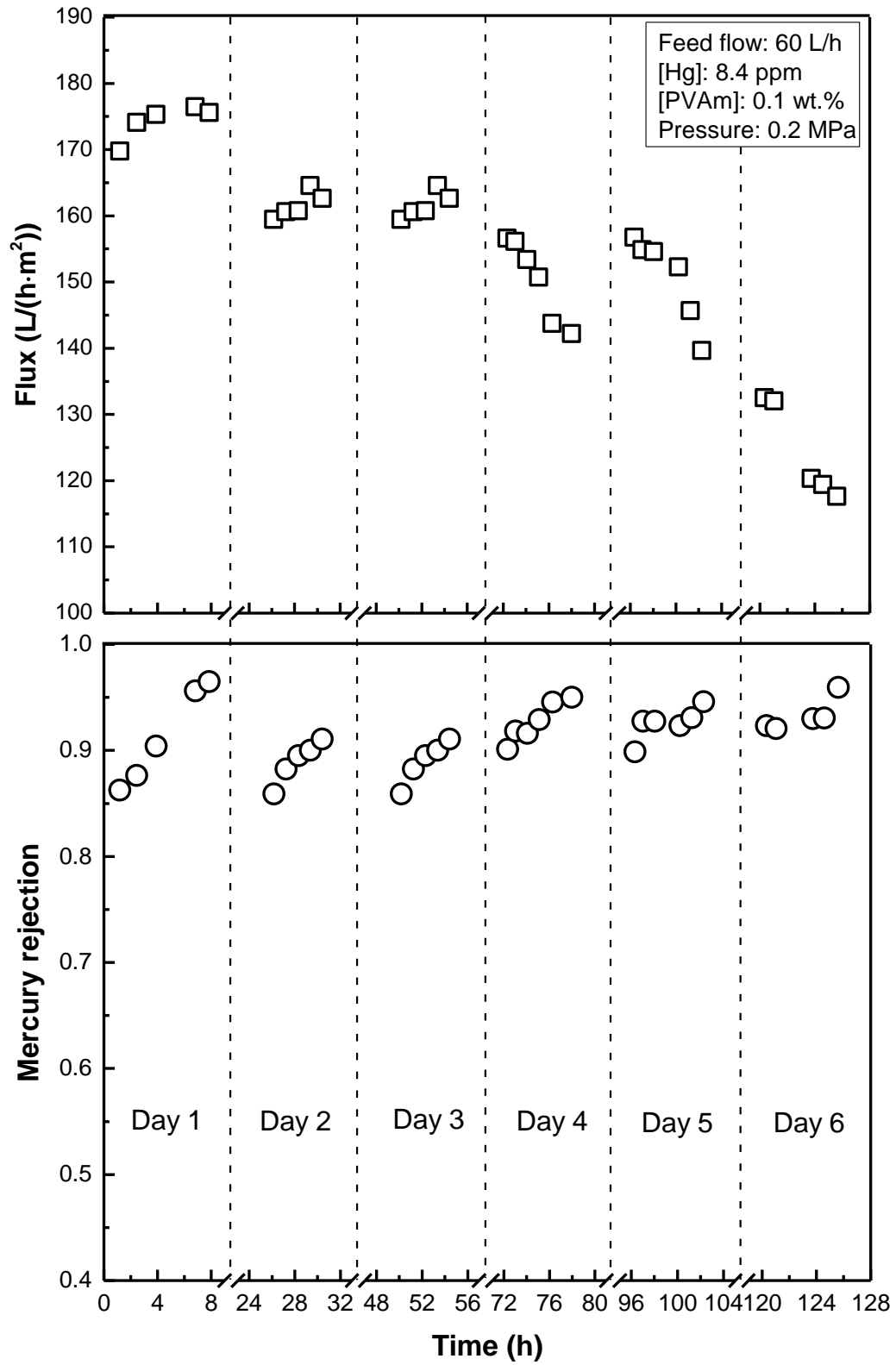
Figure 4.9 Flux and mercury rejection in cross-flow PEUF over a period of 6 days.
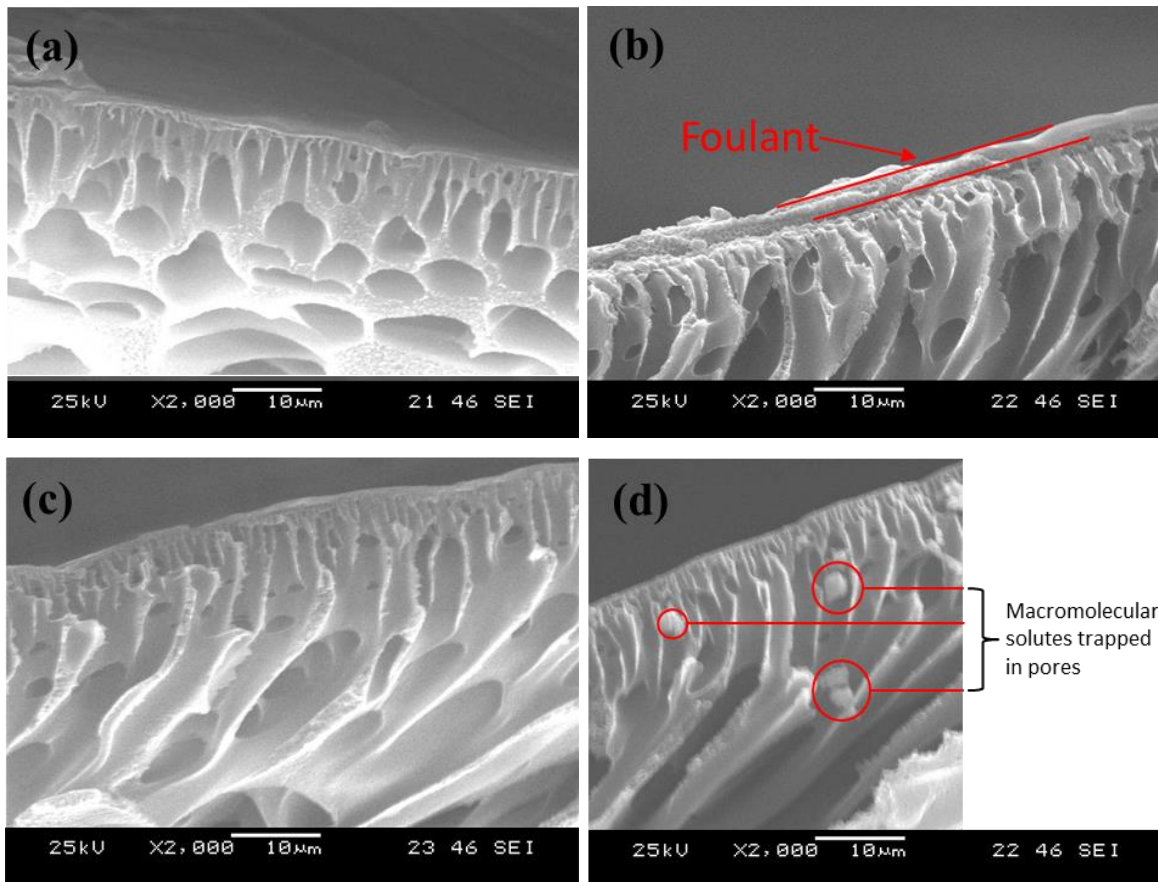
Figure 4.10 SEM images of membrane cross-sections. (a) pristine PES membrane, (b) fouled membrane, (c) membrane after cleaning with hydrochloric acid, and (d) membrane after cleaning with deionized water.

Periodic cleaning of the membrane with clean water and other suitable cleaning agents is often used to reduce membrane fouling. In addition to water, a dilute hydrochloric acid was also used to clean the membrane in this study in consideration that it can remove the PVAm deposits effectively without damaging the PES membrane. Figure 4.10 shows the cross sections of the membranes; a fouling layer was clearly observed on the membrane surface after PEUF runs. The figure also shows that the foulants can be removed when the membrane is cleaned with water or dilute hydrochloric acid, but the SEM images cannot tell how well the flux will be restored. Therefore, a series of PEUF experiments were conducted with periodic cleaning of the membrane.

105
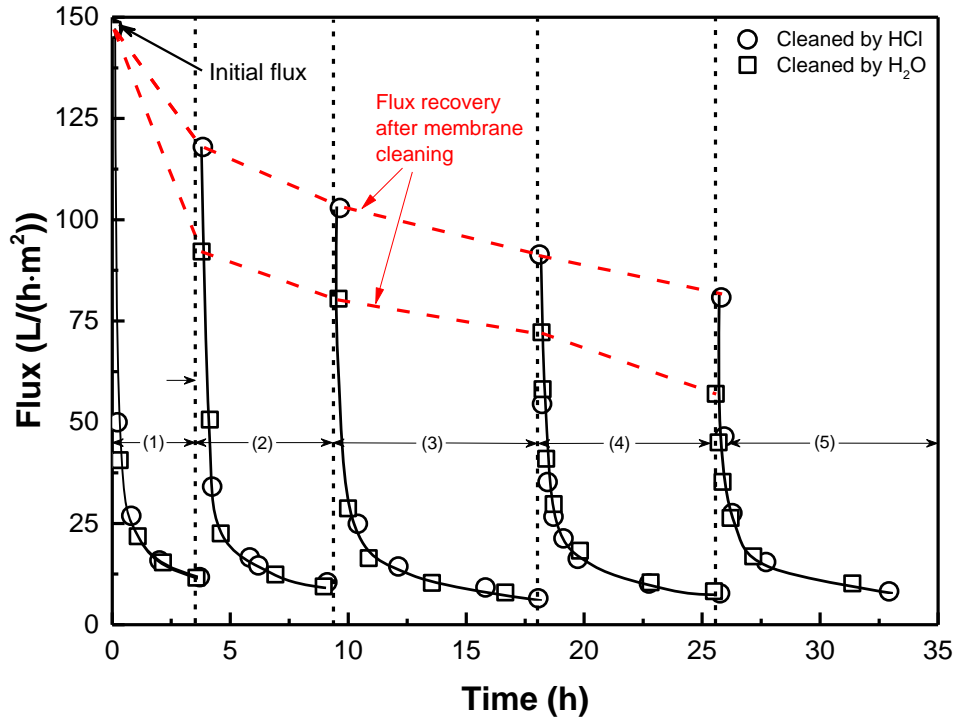
Figure 4.11 Flux restoration by membrane cleaning, tested in dead-end filtration module. Feed solution: PVAm: 0.1 wt%, mercury 10 ppm, transmembrane pressure 0.2 MPa.
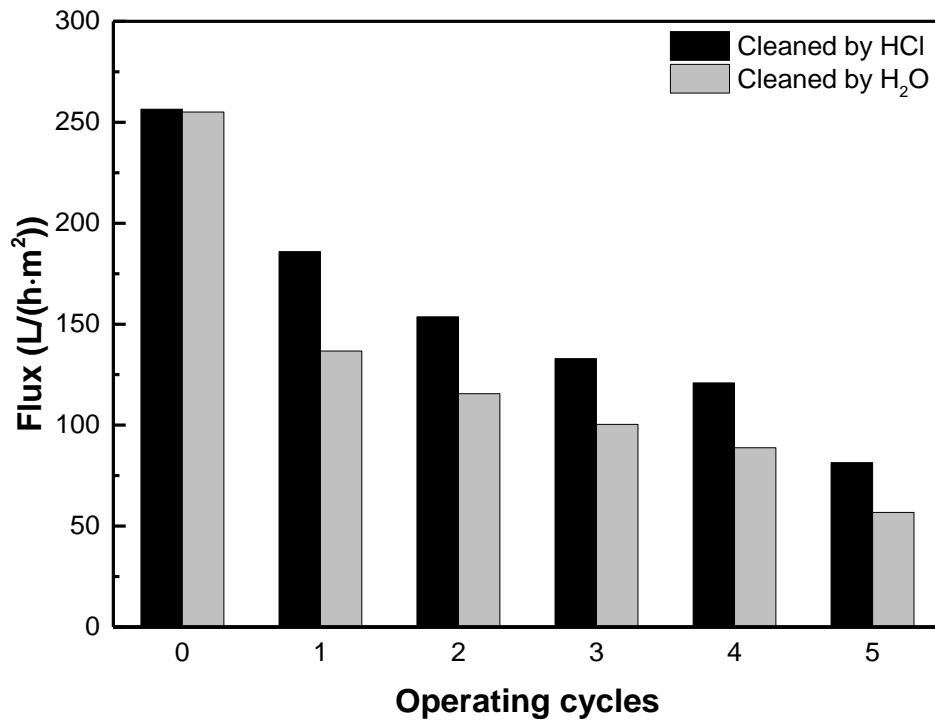
Figure 4.12 Pure water flux after membrane cleaning at the beginning of each operating cycle, tested in dead-end filtration mode, transmembrane pressure 0.2 MPa.

The flux restoration by membrane cleaning is shown in Figure 4.11; the changes in membrane permeability are more clearly shown by the pure water fluxes at the beginning of each operating cycle presented in Figure 4.12. Using the dilute hydrochloric acid to clean the membrane yielded a better flux recovery than using water as a cleaning agent. This is not surprising since (1) the hydrochloric acid can readily dissolve the PVAm gel layer, and (2) the viscosity of PVAm-Hg(II) solutions at an acidic pH will be decreased, as illustrated in Figure 4.13 where the viscosities of the solutions at a high PVAm content (8 wt%) were measured at different solution pH. Thus, the foulants can be detached from the membrane surface and flushed away with the aid of the hydrochloric acid. However, the acid cleaning of the membrane was unable to restore the flux to its original value, and the flux recovery became worse when the membrane was subjected to additional filtration-cleaning cycles. This is presumably due to irreversible membrane fouling caused by pore blockage, which is common in ultrafiltration [Hanemaaijer *et al.*, 1989; Hashino *et al.*, 2011]. In fact, some macromolecular foulant aggregates were found to be trapped in the finger pores (see Figure 4.10d). The pore blocking by macromolecular solutes is difficult to resolve, and this is likely the main reason for the declining trend of flux over time even with periodic cleaning. In addition, it may be pointed out that except within a very short period immediately after membrane cleaning, the membrane flux was essentially the same regardless whether water or dilute hydrochloric acid was used in the membrane cleaning, although membrane cleaning with dilute hydrochloric acid produced a better flux recovery than cleaning with water. Nonetheless, a valuable feature of using hydrochloric acid as a cleaning agent is that it can break the coordination bonds between PVAm and mercury(II) due to enhanced ionization of the polymeric amine at acidic conditions so that the mercury can be released from the polymer for regeneration and reuse in

PEUF. However, it should be mentioned that the flux reduction was not fully recovered after membrane cleaning with the dilute hydrochloric acid under the conditions (e.g., concentration, cleaning time) used in the study, and cleaning protocols that are more effective for the flux recovery are needed.
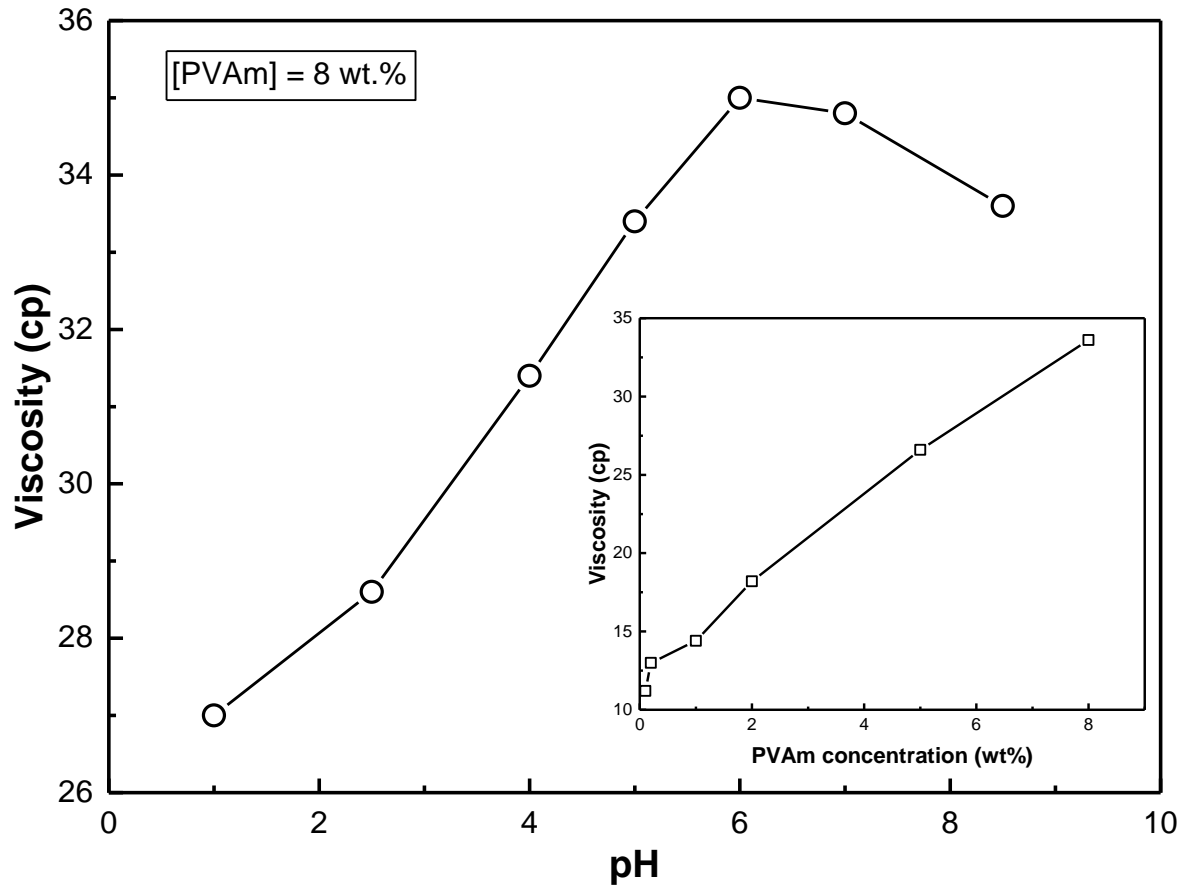
Figure 4.13 Effect of solution pH on the viscosity of PVAm-Hg solution with 8 wt% of PVAm and 10 ppm of mercury(II). Insert: viscosities of aqueous PVAm solution in the absence of mercury(II). Temperature = 25 °C.

4.3.6 Treatment of simulated industrial effluents

In practice, mercury(II) is often present in industrial effluents along with other compounds, and their interactions may influence the separation performance. The chlor-alkali electrolysis wastewater is an example of mercury-containing wastewater, which is a major aqueous mercury emission source [Reis *et al.*, 2009]. The typical mercury concentration in chlor-alkali wastewater is around 10 ppm [Canstein *et al.*, 1999]. The wastewater also contains a certain amounts of sodium chloride and sulfate, depending on the specific process.

Therefore, a further test on PEUF was performed using a simulated chlor-alkali wastewater containing mercury(II) in the presence of NaCl and Na_2SO_4 at different pHs. The pH of the solution was adjusted using sodium hydroxide or hydrochloric acid. As shown in Figure 4.14, the mercury rejection was indeed affected by the accompanying compounds in the feed. At a neutral pH condition, a 90% mercury rejection was obtained when the sodium chloride and sodium sulfate concentrations in feed solution were 5,000 and 650 ppm, respectively. However, with an increase in the sodium chloride concentration to 25,000 ppm, the mercury rejection was reduced to about 50%. One of the reasons for the reduction in mercury rejection was the formation of mercuro-chloro complexes (e.g., $HgCl_3^-$ and $HgCl_4^-$) [Canstein *et al.*, 1999], which would weaken the coordination interaction between mercury and the amine polymer. At an acidic (pH = 3.4) condition, the mercury rejection became lower. This was easy to understand because protonation of the amine groups in the polymer would reduce and eventually lose its power to coordinate with mercury. On the other hand, when the feed solution was at an alkaline pH, a high mercury rejection of around 90% was obtained even at a considerably high chloride concentration. This suggests that the interference from accompanying compounds on mercury rejection can be mitigated by changing the solution pH,

as pH adjustment in advance is a common procedure in most wastewater treatment processes. Obviously, an alkaline pH condition is preferred to remove mercury from chlor-alkali wastewater by the PVAm-enhanced UF. At a given pH, the permeation flux was not influenced significantly by the presence of sodium salts, as shown in Figure 4.15, but it was affected by the changing of solution pH. The flux will be higher at an acidic pH and lower at an alkaline pH. As one may expect, when the solution pH changes, the PVAm-mercury(II) complexation and the conformation of PVAm chains will be affected, and therefore the flux varies at different pHs [Cañizares *et al.*, 2005].

The PVAm-enhanced UF is shown to be a promising process to capture mercury from wastewater. However, additional work is needed to look into the fouling issues involved in the filtration process due to the use of the macromolecules as well as the regeneration of the water-soluble polymer for reuse. One possible approach for the polymer regeneration is to use a chelating agent (e.g., ethylenediaminetetraacetic acid) to strip mercury from PVAm-mercury complexes, followed by UF concentration and alkaline treatment. This is a subject of further studies.
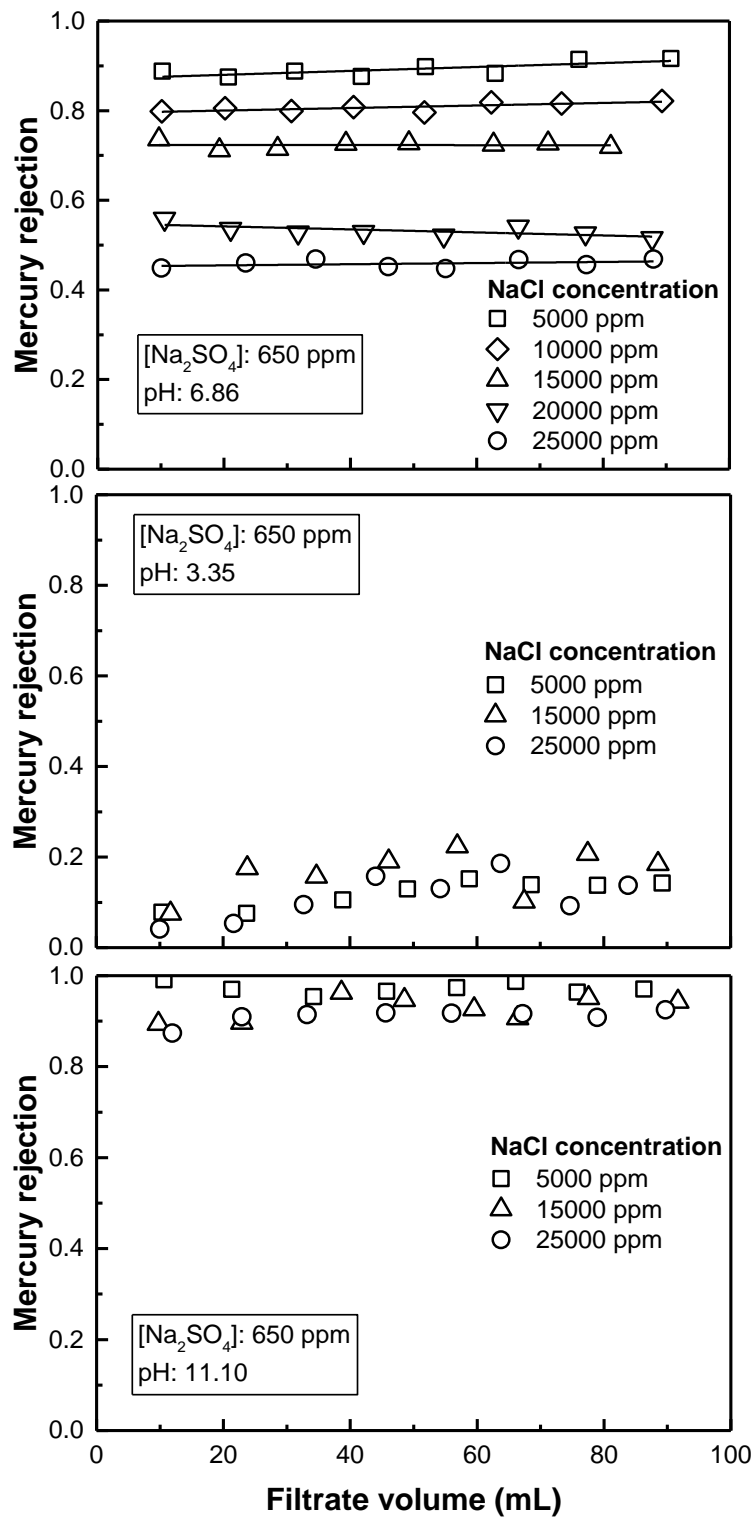
Figure 4.14 Mercury rejections of PVAm-enhanced UF in treating simulated chlor-alkali wastewater under dead-end filtration mode. Mercury concentration in feed: 10 ppm, PVAm dosage: 0.1 wt.%, transmembrane pressure: 0.2 MPa.
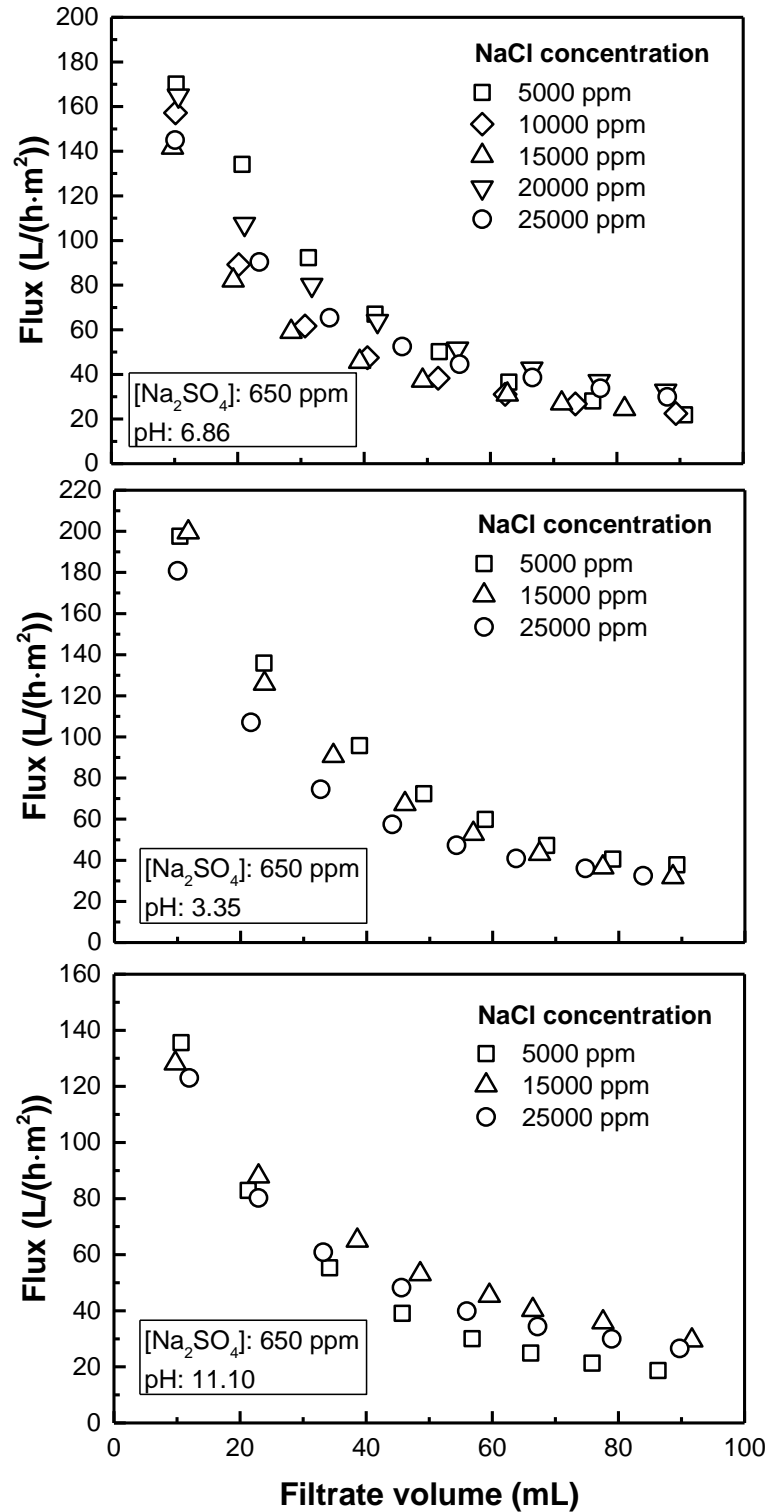
Figure 4.15 Water flux of PVAm-enhanced UF for treating simulated chlor-alkali wastewater. Operating conditions same as in Figure 4.14.

4.4 Conclusions

This study dealt with the concentration and capture of mercury(II) from wastewater by PEUF using PVAm as the mercury-binding polymer. It was shown that a mercury removal as high as 99% could be achieved, which was otherwise impossible with an UF membrane in the absence of PVAm. The PVAm dosage did not affect the mercury rejection considerably in the mercury concentration range tested, but it had a significant effect on the water flux. Due to the macromolecular nature of the "solutes" in the feed solution, a typical flux vs pressure relationship was observed, which appeared to follow the concentration polarization and gel layer formation model. Periodic cleaning of the membrane surface with dilute hydrochloric acid was effective to recover the membrane permeability, but the flux decline over time due to membrane fouling was an issue yet to be resolved. Mercury removal with the PEUF was also tested with a simulated chlor-alkali wastewater where other chemicals (i.e., sodium chloride and sulphate) were present as well, and the composition of the feed solution was shown to affect the performance for mercury removal. Regeneration of PVAm for reuse in the PEUF process, which is important for practical applications, will be a subject in further studies.

Chapter 5

Batch PEUF Processes for Hg(II) Recovery from Wastewater

5.1 Introduction

This chapter deals with the recovery of mercury(II) from wastewater by batch PEUF. Three water-soluble polymers, PEI, PVAm and PAA were used as the chelating agents. The experiments were conducted in two different operating modes. First, a lab-scale cross-flow was used in a total recirculation mode, where the permeate flowed back to the feed tank. This allowed for checking if the properties of the water-soluble polymers had any significant influence on mercury rejection and membrane fouling in PEUF. The relationship between the permeation flux and the polymer concentration in the feed in a typical UF system was investigated, as well. This would provide information needed for further modeling studies.

Next, the PEUF was carried out in a batch process. Batch operation of the PEUF process, by which the permeate was collected and removed continuously, was easy to control and suitable for metal ion recovery when varying quantities of feed water with different metal concentrations were encountered. For a given feed solution containing a low concentration of metal ions, the batch operation of PEUF can concentrate the feed and increase the metal concentration to a higher level for subsequent further treatment. The mathematical modelling of the batch PEUF operation is another objective of this project. A set of equations describing

the batch PEUF process were developed and their applicability was validated with experimental data.

5.2 Theoretical

Feng and Huang [1992] studied batch operation of pervaporation. They developed a mathematical model which could match the experimental results very well, showing promising potential in prediction separation performance of a given batch pervaporator. In this study, this model was used with appropriate modifications for batch operation of PEUF process.

M_a, M_b, M_c – Instantaneous concentrations of mercury ions in retentate, permeate and cumulated product, respectively.

P_a, P_b, P_c – Instantaneous concentrations of water-soluble polymers in retentate, permeate and cumulated product, respectively.

V_f and V_p – Total amount of retentate and cumulated product, respectively.
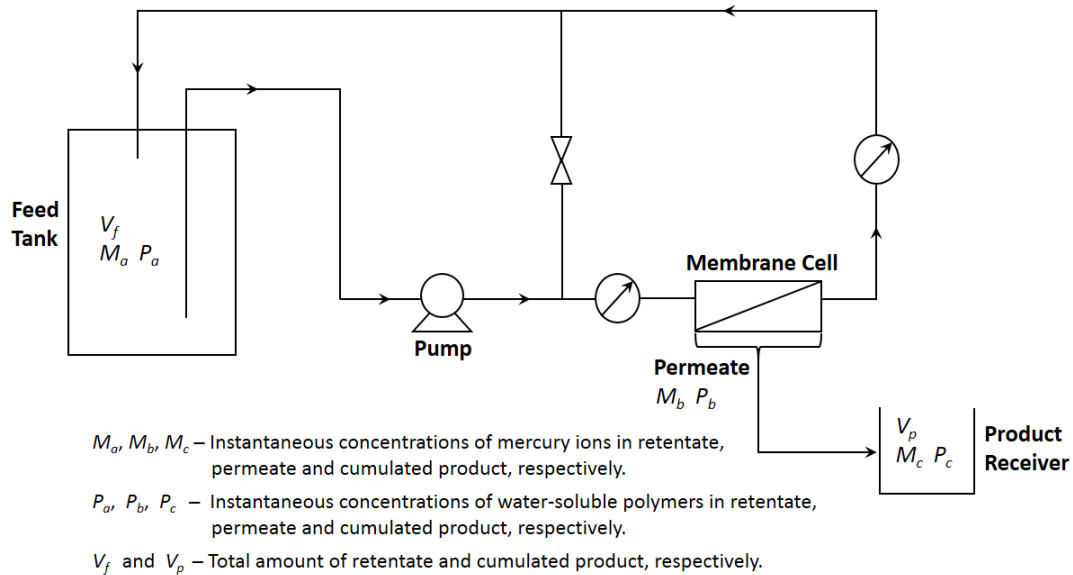
Figure 5.1 A schematic of batch PEUF

Consider the batch process of PEUF shown in Figure 5.1. The feed solution containing a water-soluble polymer and metal ions (mercury(II) in this study) is initially pumped into the cross-flow UF module, and the permeate is continuously collected as a product or discharged directly. The solution in the feed tank is thus concentrated gradually. The batch operation is an unsteady process because the polymer and metal concentrations in the feed change with

time and the membrane is gradually fouled. The feed solution can be assumed as a well-mixed system at any time. For a given instant, let M_a, M_b and M_c be the instantaneous concentrations of metal ion, and P_a, P_b and P_c be the instantaneous concentrations of water-soluble polymers, in the retentate, permeate and cumulated product, respectively. Also, let R_m and R_p be the rejections of the membrane to the metal ion and water-soluble polymers respectively, and J be the instantaneous total permeation flux. V_f and V_p represent the total amount (in volume) of the retentate and accumulated product respectively at that instant. Considering both the metal and polymer as solutes in the feed for the permeation purpose, on the basis of mass balances, the permeation rate can be described by the following three equations:

$$-\frac{dV_f}{dt} = J \cdot A \tag{5.1}$$

$$-\frac{d(V_f \cdot M_a)}{dt} = J \cdot A \cdot M_b \tag{5.2}$$

$$-\frac{d(V_f \cdot P_a)}{dt} = J \cdot A \cdot P_b \tag{5.3}$$

Equations (5.2) and (5.3) are derived from the mass balances of the metal ion and water-soluble polymer, respectively. At relatively low metal concentrations, the concentration of metal ion is assumed to have no influence on total flux, and thus J is an unique function of feed concentration of water-soluble polymer P_a. For metal ion, equation (5.1) and (5.2) lead to:

$$\frac{dV_f}{V_f} = \frac{dM_a}{M_b - M_a} \tag{5.4}$$

At $t = 0$, $V_f = V_{f0}$ and $M_a = M_{a0}$. By integrating equation (5.4), the following relationship can be obtained.

$$\ln\frac{V_f}{V_{f0}} = \int_{M_{a0}}^{M_a} \frac{dM_a}{M_b - M_a} \tag{5.5}$$

or

$$V_f = V_{f0} \exp(z_1) \tag{5.6}$$

where

$$z_1 = \int_{M_{a0}}^{M_a} \frac{dM_a}{M_b - M_a} \tag{5.7}$$

Similarly, considering the mass balance of water-soluble polymer, a similar expression can be obtained using equation (5.1) and (5.3):

$$\frac{dV_f}{V_f} = \frac{dP_a}{P_b - P_a} \tag{5.8}$$

With the initial condition for water-soluble polymer ($t = 0$, $V_f = V_{f0}$ and $P_a = P_{a0}$), integrating equation (5.8) leads to:

$$V_f = V_{f0} \exp(z_2) \tag{5.9}$$

where

$$z_2 = \int_{P_{a0}}^{P_a} \frac{dP_a}{P_b - P_a} \tag{5.10}$$

Note that equation (5.7) and (5.10) have similar mathematical expressions, and from equations (5.6) and (5.9), one has:

$$\frac{V_f}{V_{f0}} = \exp(z_1) = \exp(z_2) \tag{5.11}$$

This is not surprising, because the total residual volumes of feed solution that is calculated based on mass balance of metal ion should be equal to the value that is calculated on the basis of mass balance of the solute polymer. Applying the mass balance for the overall batch process, we obtain:

$$V_{f0} = V_f + V_p \tag{5.12}$$

$$V_{f0} \cdot M_{a0} = V_f \cdot M_a + V_p \cdot M_c \qquad (5.13)$$

$$V_{f0} \cdot P_{a0} = V_f \cdot P_a + V_p \cdot P_c \qquad (5.14)$$

From equation (5.11), let $z_1 = z_2 = z$. Substituting into (5.12), (5.13) and (5.14) gives:

$$V_p = V_{f0} \cdot [1 - \exp(z)] \qquad (5.15)$$

$$M_c = \frac{M_{a0} - M_a \cdot \exp(z)}{1 - \exp(z)} \qquad (5.16)$$

$$P_c = \frac{P_{a0} - P_a \cdot \exp(z)}{1 - \exp(z)} \qquad (5.17)$$

Thus the retention rates of metal ion (r_1) and water-soluble polymer (r_2) in feed solution can be expressed as:

$$r_1 = \frac{V_{f0} \cdot M_{a0} - V_p \cdot M_c}{V_{f0} \cdot M_{a0}} = \frac{V_f \cdot M_a}{V_{f0} \cdot M_{a0}} = \frac{M_a}{M_{a0}} \exp(z) \qquad (5.18)$$

$$r_2 = \frac{V_{f0} \cdot P_{a0} - V_p \cdot P_c}{V_{f0} \cdot P_{a0}} = \frac{V_f \cdot P_a}{V_{f0} \cdot P_{a0}} = \frac{P_a}{P_{a0}} \exp(z) \qquad (5.19)$$

Note that the relationship between P_a and P_b (polymer concentration in feed and permeate) is determined by the UF membrane and the water-soluble polymer used, while the relationship between M_a and M_b (metal concentration in feed and permeate) is determined by the interactions between metal ion and water-soluble polymer. They directly influence the difficulty in integrating equations (5.7) and (5.10). From previous research work on PEUF, it has been shown that the metal rejection R_m will not change for a given UF membrane and initial concentration of the water-soluble polymer [Shao *et al.*, 2013; Zeng *et al.*, 2014]. In addition, the rejection of water-soluble polymer R_p by the membrane can also be assumed to be constant if the molecular weight of the polymer is above the MWCO of the UF membrane. From the definition of solute rejection in UF:

$$R_m = \frac{M_a - M_b}{M_a} \tag{5.20}$$

$$R_p = \frac{P_a - P_b}{P_a} \tag{5.21}$$

These are the functional forms of M_b vs. M_a, and P_b vs. P_a. Unlike the pervaporation model derived by Feng and Huang [1992], the PEUF actually involves a mixture of three components (i.e., water, metal compound and water-soluble polymers), but the permeation flux is independent of the metal present. From the PEUF experiments with different water-soluble polymers in this study (i.e., PEI, PVAm and PAA), the separation data (R_m and R_p) and permeation data (J vs. P_a) are obtained. In order to facilitate the mathematical treatment, regression equations fitted to the experimental data may be used as an approximation if the real functional expressions are difficult to find. With equation (5.11), equations (5.15), (5.16) and (5.17) correlate respectively the accumulated amount of permeate product, and the permeate concentrations with feed concentrations (both metal ions and water-soluble polymer), which change with the ultrafiltration time. The latter three equations demonstrate that for a given concentrating task (i.e., to increase the concentration of V_{f0} litters of metal ion solution from M_{a0} to M_a), the feed concentration and the quantity of the metal depend on the relationship between M_a and M_b (i.e., R_m). In addition, the feed concentration of water-soluble polymer, which may be obtained from equation (5.17), also provides significant information on further recovery of water-soluble polymer. It is currently a major issue that hinders PEUF as a competitive technique in practical applications [Geckeler and Volchek, 1996].

To find the batch time and membrane area needed to treat a given concentrating task, rearranging equation (5.2) and (5.3) and substituting equation (5.1) give:

$$dt = \frac{V_f}{J \cdot A \cdot (M_a - M_b)} dM_a \tag{5.22}$$

$$dt = \frac{V_f}{J \cdot A \cdot (P_a - P_b)} dP_a \tag{5.23}$$

Integrating the above two equations with the aid of equation (5.11), we obtain:

$$t = \frac{V_{f0}}{A} \int_{M_{a0}}^{M_a} \frac{\exp(z)}{J \cdot (M_a - M_b)} dM_a \tag{5.24}$$

$$= \frac{V_{f0}}{A} \int_{P_{a0}}^{P_a} \frac{\exp(z)}{J \cdot (P_a - P_b)} dP_a \tag{5.25}$$

Those equations show the relation between time and membrane area in a batch operation of PEUF process. The permeation flux remains in the terms to be integrated, because in general it changes with the concentration of water-soluble polymer as the PEUF proceeds. Equations (5.24) and (5.25) have similar expressions to the well-known equation in batch pervaporation [Feng and Huang, 1992], and have very similar meanings. Here, the equations show that for a given concentrating task in PEUF where the membrane, water-soluble polymer, target metal ions to be separated, and the initial and final feed concentrations are specified, the time required in a batch operation is proportional to (V_{f0}/A), the total initial amount of feed solution to be treated per unit membrane area. This provides very useful information for process design as the scale up of batch PEUF from a lab-scale to an industrial-scale is quite straight forward. However, two important assumptions used in deriving the general equations cannot be overlooked: (1) the feed solution is well mixed; (2) the flux decrease caused by the potential membrane fouling from the water-soluble polymer itself is assumed to be negligible. However, membrane fouling by polymeric solute may be significant, and a more accurate equation describing the permeation flux will be required. It should be noted that equations (5.24) and (5.25) also provide information about the feed concentration (metal ion and water-soluble

polymer) in relation to batch time. It means that such quantities as V_f, V_p, M_c, P_c, r_1 and r_2 can be predicted as well.

5.3 Experimental

All chemicals used were the same as described in Chapter 3. Ethylene glycol (BDH Chemicals) and diiodomethane (Sigma-Aldrich) were used as received. Table 5.1 lists the water-soluble polymers used in this chapter. The cross-flow mode and the UF membrane used for PEUF experiments were the same as used in Chapter 4.

The experiments were conducted in two different modes of operation. The first one was carried out in the total recirculation mode where the permeate flowed back to feed tank, to maintain constant feed concentrations of water-soluble polymer and metal ions. This operating mode allows for determination of the separation characteristics of the PEUF process at given feed polymer concentrations. In addition, it also allows us to check the fouling trend of the water-soluble polymers used in a long-term operation, which provides information about the flux that is needed in the modelling studies. Next, the batch operation of PEUF with the different water-soluble polymers were conducted. Permeate was collected continuously and did not recycle to the feed tank after flux and rejection were analysed. A very small amount of sample in each batch operation was also collected continuously from the feed tank to monitor the change of concentration in feed. The total volume of the collected samples was kept below 5% of the initial volume of the feed solution. For both operation modes, the well-mixed feed solutions containing pre-determined concentrations of mercury(II) and water-soluble polymer with given initial feed volumes were charged into the feed tank and fed to the membrane module. In all the experiments the transmembrane pressure, flow rate and temperature were

kept at 0.2 MPa, 65 L/h and room temperature, respectively. The permeation flux was determined gravimetrically, and the concentrations of mercury(II) in the feed and permeate solutions were determined using the ICP as described in Chapter 3.

Table 5.1 Water-soluble polymers used in PEUF

Polymer	Molecular weight (Da)	Description	Source
Polyvinylamine (PVAm)	$\overline{M_n} = 340,000$	Lupamin 9095, linear structure, liquid form	BASF Corporation
Polyethyleneimine (PEI)	$\overline{M_n} = 60,000$ $\overline{M_w} = 750,000$	Branched structure, 50 wt.% in H_2O	Sigma-Aldrich
Polyacrylic acid (PAA)	$\overline{M_w} = 240,000$	Partial sodium salt, 25 wt.% in H_2O	Sigma-Aldrich

The interfacial properties of the PES UF membrane and the mercury-polymer complexes were evaluated from the contact angles by a contact angle meter (Cam-plus Micro, Tantec Inc.). To characterize the interfacial properties of the mercury-polymer complexes, the mercury-polymeric aqueous solutions were deposited onto the PES UF membrane, and contact angles were measured after air drying for 24h at room temperature (25 ℃). At least seven contact angle measurements from different surface locations were performed, and the average values were reported after discarding the largest and smallest values. In order to obtain the interfacial free energies and surface tensions of a solid surface, the contact angles were measured using three probe liquids with well-known surface tensions [Brant and Childress, 2002; van Oss, 2007; Jawor and Hoek, 2010]. The detailed information about the surface tensions, including the total surface tensions and the components of each probe liquid used in this chapter is listed in Table 5.2.

Kinematic viscosities of the three water-soluble polymer aqueous solutions at different concentrations were measured by a Cannon-Fenske Routine Viscometer, size 75. All measurements were made at room temperature (25 ℃).

Table 5.2 Surface tensions of probe liquids at 20 ℃

Liquid	γ^{LW} (mJ/m^2)	γ^+ (mJ/m^2)	γ^- (mJ/m^2)	γ^{AB} (mJ/m^2)	γ_L (mJ/m^2)
Water	21.8	25.5	25.5	51.0	72.8
Ethylene glycol	29.0	1.9	47	19	47.9
Diiodomethane	50.8	0	0	0	50.8

Data taken from van Oss [van Oss, 1993]

5.4 Results and discussion

5.4.1 Effectiveness of water-soluble polymers in PEUF

Figure 5.2 shows the mercury rejection and the corresponding water permeation fluxes in PEUF using three different water-soluble polymers as binding agents. From this figure, it can be seen that both permeation fluxes and mercury rejections are influenced by the feed polymer concentrations for all three water-soluble polymers. In general, the mercury rejections in PEUF with all three polymers were very high (>90%) even at a relatively low feed polymer concentration, and it increased slightly with an increase in the concentrations of the water-soluble polymers in the feed. Similar results for mercury rejection using PEI and PAA in PEUF have been observed in previous research [Uludag *et al.*, 1997; Pastor *et al.*, 2002; Barron-Zambrano *et al.*, 2004; Kuncoro *et al.*, 2005; Zeng *et al.*, 2009].
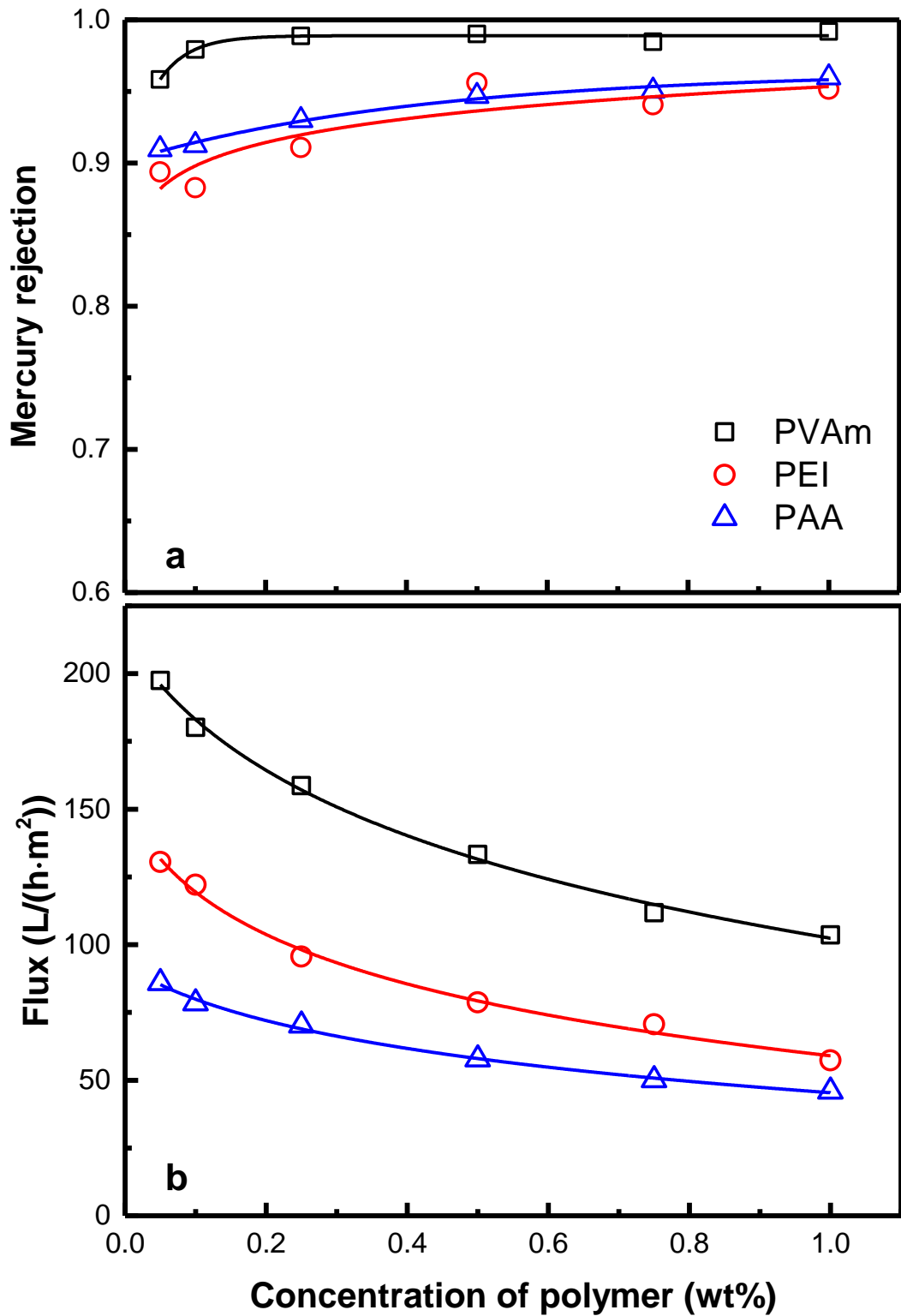
Figure 5.2 Mercury rejection and permeation flux in PEUF using different water-soluble polymers. Mercury concentration: 11 ppm, ΔP: 0.2 MPa, feed flow rate: 65 L/h.

It confirms that the amine and carboxyl groups in these water-soluble polymers are good binding sites for mercury(II) in aqueous solutions, resulting in a high mercury rejection in the PEUF process. Further, the slight change in mercury rejections over a relatively wide range of feed polymer concentrations justifies the aforementioned assumption in mathematical modelling that the metal rejection R_m does not change significantly with feed polymer concentration if the initial loading of the polymer relative to metal is high enough. It should be noted that when PVAm is used as the chelating agent, the mercury rejection is higher than what is obtained with the other two polymers. This is believed to be due to the abundant primary amine groups in the PVAm chains that result in a strong interaction with mercury(II).

However, as shown in Figure 5.2, the permeation flux decrease significantly as the concentration of the water-soluble polymers in the feed increases. This trend is consistent with conventional UF of proteins or other macromolecular solutes [Porter, 1990]. A higher polymer concentration in the feed may cause more severe concentration polarization and possible membrane fouling, reducing the flux subsequently. In addition, Figure 5.2 shows that water permeation fluxes in PEUF with the three water-soluble polymers decrease in the order PVAm > PEI > PAA at a given feed polymer concentration. It is believed that the interfacial properties of the water-soluble polymer and the membrane have an influence on permeation flux [Jawor and Hoek, 2010]. Table 5.3 shows the water contact angles on the PES membrane and the membrane fouled with a deposited layer of the mercury-polymeric complexes. The contact angle of water on the PES membrane is 79°, showing a wetting but moderately hydrophobic surface. It drops to 60° and 70°, after depositions with PVAm-Hg(II) and PEI-Hg(II) complexes, respectively. Interestingly, the water contact angle increases to 86° after PAA-Hg(II) deposition onto the PES membrane. PAA with carboxylic acid functionality is the most

hydrophobic material, among the three water-soluble polymers characterized. It is expected to exhibit the highest hydrodynamic resistance, which is confirmed by the lowest permeation flux observed for PAA as shown in Figure 5.2.

Table 5.3 Contact angles on the membrane and the mercury-polymer complexes

	Water	Ethylene glycol	Diiodomethane
PES membrane	$79\,^{\circ}\pm5\,^{\circ}$	$47\,^{\circ}\pm4\,^{\circ}$	$37\,^{\circ}\pm3\,^{\circ}$
PAA-Hg(II)	$86\,^{\circ}\pm3\,^{\circ}$	$52\,^{\circ}\pm5\,^{\circ}$	$59\,^{\circ}\pm1\,^{\circ}$
PEI-Hg(II)	$70\,^{\circ}\pm2\,^{\circ}$	$42\,^{\circ}\pm3\,^{\circ}$	$50\,^{\circ}\pm3\,^{\circ}$
PVAm-Hg(II)	$60\,^{\circ}\pm3\,^{\circ}$	$25\,^{\circ}\pm3\,^{\circ}$	$37\,^{\circ}\pm4\,^{\circ}$

In addition to the hydrophilicity difference, another intrinsic property, i.e., the viscosity, of the water-soluble polymer solutions is also expected to affect the permeation flux. It has been experimentally verified that the permeation flux decreases as the solution viscosity increases for a large number of UF membrane systems [Porter, 1990]. As shown in Figure 5.3, the PAA solution has a much higher kinematic viscosity than the other two amine polymers, and also shows a greater concentration dependency. A higher viscosity of the feed solution will lead to a lower permeation flux. It should be noted that the kinematic viscosity of PVAm solution is larger than that of PEI solution, but the permeation flux in PEUF with PVAm is also higher, as shown in Figure 5.2. That may be caused by the highly branched structure of PEI that will have inevitable effects on the flux decrease as compared to the linear PVAm. In addition, PVAm appears to be more hydrophilic than PEI based on its lower water contact angle. It may be mentioned that the concentrations of the soluble polymers shown in Fig. 5.2 were in wt%. There are different numbers of repeat units for a given amount of mass. Nevertheless, PVAm was shown to have better performance on mercury separation by PEUF

than the other two water-soluble polymers in terms of both water flux and mercury rejection at a given mass dosage of the polymers used.
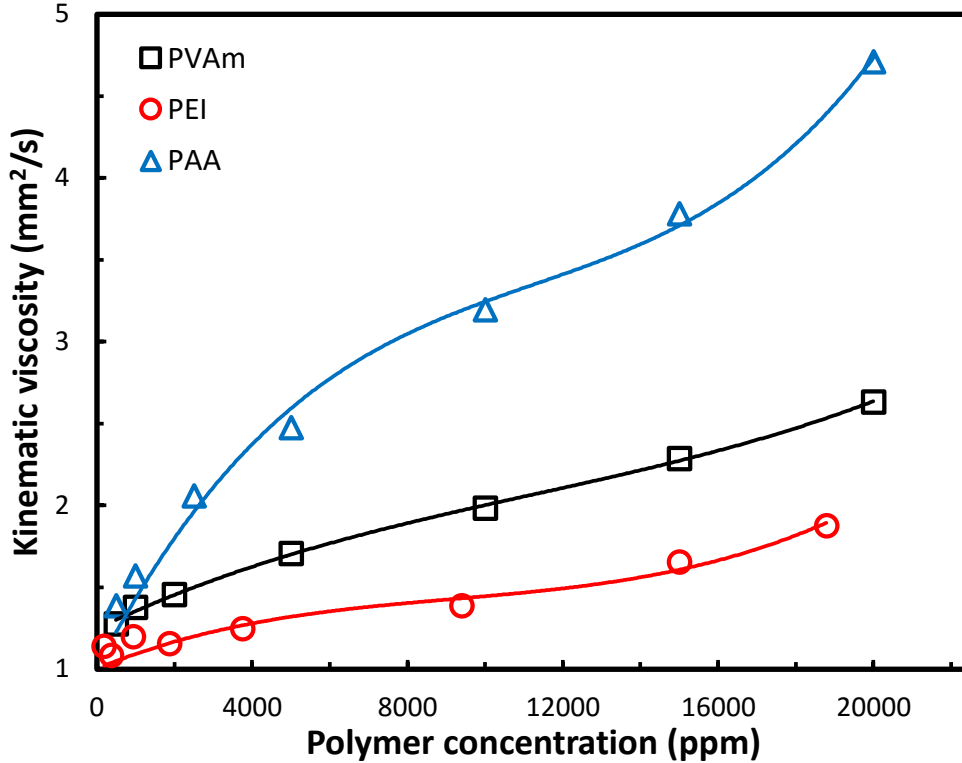
Figure 5.3 Kinematic viscosity as a function of concentration of water-soluble polymers in aqueous solution. T = 25 ℃.

5.4.2 Membrane fouling by the water-soluble polymers

One of the assumptions made in developing the mathematical batch model in section 5.2 was that the flux decrease caused by membrane fouling in a cross-flow module at a low concentration of water-soluble polymer was negligible. However, sometimes the membrane fouling by the water-soluble polymers in PEUF was significant. To understand the fouling trends of different water-soluble polymers on the UF membrane, a total recirculation operation mode was conducted over a prolonged period of time. As shown in Figure 5.4, the permeation fluxes were nearly constant for PVAm and PEI after PEUF operating for 50 h, while the

permeation flux in PEUF using PAA as the chelating agent decreased with time. The concentrations of all three water-soluble polymers in the feed solution were constant. This indicates that the flux decrease in PEUF with PAA was caused by the membrane fouling. The different fouling propensies of water-soluble polymers on the PES membrane may be explained by the interfacial free energy of adhesion (i.e., interaction energy at contact) between PES membrane and water-soluble polymers in water.

Table 5.3 lists the contact angles of three probe liquids on the PES membrane and the three water-soluble polymers (PAA, PEI and PVAm) in the presence of mercury(II). Using this information as well as the known surface tensions of the probe liquids (Table 5.2), one can calculate the surface tension parameters for the PES membrane and the fouling layers according to the extended Young-Dupré equation [van Oss, 2007; Jawor and Hoek, 2010]:

$$-\Delta G_{SL} = (1 + cos\theta)\gamma_L = 2\left(\sqrt{\gamma_S^{LW} \cdot \gamma_L^{LW}} + \sqrt{\gamma_S^+ \cdot \gamma_L^-} + \sqrt{\gamma_S^- \cdot \gamma_L^+}\right) \tag{5.26}$$

where ΔG_{SL} represents the free energy of interaction when a solid "S" is immersed in a liquid "L", γ^{LW} is the apolar part of the total surface tension of solid or liquid (γ_S or γ_L), and γ^+ and γ^- are two parameters representing the electron-acceptivity and electron-donicity, respectively, of the polar part (γ^{AB}) of the total surface tension. θ is the contact angle of the probe liquid on the solid surface, which was measured experimentally. The individual surface tension parameters of solids (PES membrane and the dry deposit of mercury-polymer complexes on PES in this study) can be determined by solving a set of three equations based on equation (5.26). Once the surface tension parameters of the individual solid material are known, one can further determine the interfacial free energy of adhesion between two solid materials at contact when immersed in water "W" (ΔG_{SWM}), using the following equation [van Oss, 2007]:

$$\Delta G_{SWM} = 2\left[\left(\sqrt{\gamma_W^{LW}} - \sqrt{\gamma_S^{LW}}\right) \cdot \left(\sqrt{\gamma_M^{LW}} - \sqrt{\gamma_W^{LW}}\right) + \sqrt{\gamma_W^+}\left(\sqrt{\gamma_S^-} + \sqrt{\gamma_M^-} - \sqrt{\gamma_W^-}\right) + \right.$$

$$\left. \sqrt{\gamma_W^-}\left(\sqrt{\gamma_S^+} + \sqrt{\gamma_M^+} - \sqrt{\gamma_W^+}\right) - \sqrt{\gamma_S^+ \gamma_M^-} - \sqrt{\gamma_S^- \gamma_M^+}\right] \qquad (5.27)$$

where the subscripts S and M refer to mercury-polymer complexes and the membrane, respectively.

The free energy of adhesion (ΔG_{SWM}) is the interaction free energy per unit area when the mercury-polymer complexes and the PES membrane are immersed in water and brought to contact at their surfaces [Brant and Childress, 2002; Jawor and Hoek, 2010]. It provides a means to quantitatively describe the affinity between the macromolecular complexes and the membrane. A positive value of ΔG_{SWM} indicates that the membrane is adhesion-resistant to the polymer complexes, and a negative value implies an adhesive tendency between them [Jawor and Hoek, 2010]. If the PES membrane is fully covered by the polymer complexes after a long-term operation, the fouling propensity at that time can thus be described by the interfacial free energy of cohesion (ΔG_{SWS}), which represents the free energy of interaction of the same polymer complexes when contacted in water. It relates to the adhesion and aggregation to deposited fouling layer on the membrane surface.

Table 5.4 Surface tensions and surface energies of membrane and mercury-polymeric complexes

	γ^{LW} (mJ/m^2)	γ^+ (mJ/m^2)	γ^- (mJ/m^2)	γ^{AB} (mJ/m^2)	γ_s (mJ/m^2)	ΔG_{SWM} (mJ/m^2)	[a]ΔG_{SWS} (mJ/m^2)	[b]-ΔG_{SW} (mJ/m^2)
PES membrane	41.1	0.2	5.1	1.8	42.9	-	-51.6	86.7
PAA-Hg (II)	29.2	1.2	2.7	3.6	32.8	-63.1	-60.7	77.9
PEI-Hg (II)	34.3	0.7	11.9	5.6	39.9	-46.7	-50.0	97.7
PVAm-Hg (II)	41.1	0.7	16.6	6.7	47.8	-44.1	-53.9	109.2

[a]ΔG_{SWS}: Interfacial free energy when the two same solids "S" are immersed in water "W" and brought to contact at their surfaces;

[b]ΔG_{SW}: Free energy of interaction when a solid "S" is immersed in water "W".
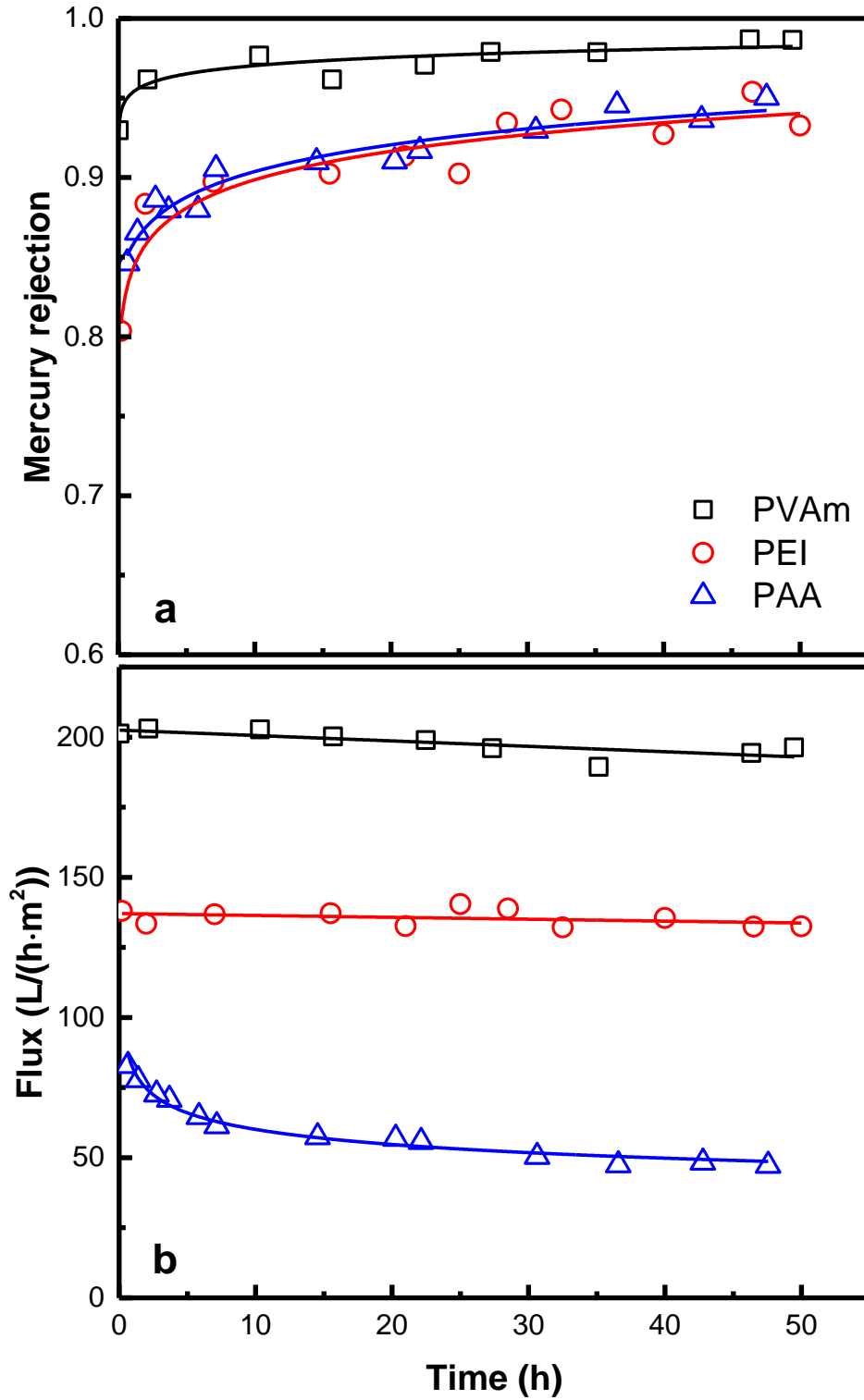
Figure 5.4 Mercury rejection and permeation flux in PEUF under the total recirculation mode. Polymer concentration: 0.05wt%, mercury concentration: 10 ppm, ΔP: 0.2 MPa, feed flow rate: 65 L/h.

Table 5.4 lists the surface tension parameters of the four solid entities and the interfacial free energies of adhesion and cohesion between the three polymer complexes and the membrane in water. In general, all three polymer complexes are likely to foul the PES membrane in aqueous media as shown by their negative interaction free energies, and the PAA-Hg(II), which has the largest absolute value, is expected to exhibit the highest fouling tendency. The interfacial free energy of cohesion of PAA-Hg(II) is also the largest, which implies that the fouling trend of PAA-Hg(II) is still the highest even after the membrane surface is deposited with a layer of PAA-Hg(II) complex. In practice, the membrane surface may be partially covered by the foulants, and therefore the fouling propensity is governed by the free energies of adhesion and cohesion jointly. Nevertheless, the expected flux decline based on the surface thermodynamic analysis corresponds well with the observations that showed the highest flux decline occurred for PAA- Hg(II) as shown in Figure 5.4. In addition, the PAA used in this chapter was a partial sodium salt. The positive sodium ions and the mercury(II) may be served as a cation bridge [Jawor and Hoek, 2010] between carboxyl functionalized PAA and the negatively charged PES membrane [Wu *et al.*, 2014], which will further increase the fouling propensity of PAA.

Interestingly, the interfacial free energies of adhesion between the two amine polymer complexes (i.e., PEI-Hg(II) and PVAm-Hg(II)) and the PES UF membrane are negative, indicating a fouling trend. However, the permeation fluxes in PEUF do not show a significant decrease over a period of 50 hours, as shown in Figure 5.4. This is because the surface thermodynamic analysis is based on a thermodynamic equilibrium without considering the high shear rate along the membrane surface in a cross-flow UF mode. The high flow velocity near the membrane surface can wash away the deposited water-soluble polymers from the

membrane surface, which will significantly reduce the concentration polarization and fouling. In addition, the fluid kinematic viscosity of the feed solution at such a low polymer concentration (0.05 wt%) is close to pure water viscosity. Therefore, the permeation flux in PEUF involving PEI-Hg(II) and PVAm-Hg(II) maintained a relatively constant value. In fact, even for PAA-Hg(II), the flux decrease was less significant after a long enough operating time. It appears reasonable to use flux regression equations obtained from Figure 5.2b for the modeling of batch PEUF. However, attention should be exercised for PEUF with PAA, because the flux decrease due to membrane fouling in this case may be significant enough to affect the model predictions.

5.4.3 Batch operation of polymer-enhanced ultrafiltration

5.4.3.1 Batch operation for PEUF with PEI and PVAm, where membrane fouling is insignificant

All three water-soluble polymers, PEI, PVAm and PAA, were used in a batch PEUF study, but the significant membrane fouling in the case of PEUF with PAA makes the batch process modeling complicated. It was thus decided to look into modeling of PEUF with PAA separately from PEUF with PEI and PVAm. The experimental results of instantaneous feed concentration of mercury (M_a) and the permeation flux (J) for PEUF with PEI and PVAm are shown in Figures 5.5 and 5.6, respectively. The instantaneous mercury concentration in the feed solution was measured directly. The characteristics (flux and rejection) of the PEUF process for the two water-soluble polymers as a function polymer concentration obtained experimentally in advance were represented by equations listed in Table 5.5. The permeation flux versus polymer concentration in feed and the mercury rejection for each polymer were obtained from Figure 5.2. Note that the flux equation used here was just an empirical

132

expression of the relationship between flux and feed polymer concentration, which was obtained by a simple data regression as mentioned in section 5.2. In theory, the PES-10 membrane had a rejection of close to 1 to PEI and PVAm, and a rejection value of 0.96 was taken on the basis of previous research [Geckeler and Volchek, 1996; Llanos et al., 2009]. Using the equations in Table 5.5, the values of Ma and J for PEUF with PEI and PVAm were calculated on the basis of equations (5.24) and (5.25). The results are shown in Figures 5.5 and 5.6. The agreement between calculated and experimental data indicates that the equations developed for the modeling of the batchwise operation of PEUF process are applicable.

Table 5.5 Curve fitting equations for permeation flux as a function of polymer concentration, and membrane rejections to mercury and the polymer in PEUF

Water-soluble polymer	Equations	Unit
PEI	$J = -24.48 \ln(P_a) + 61.218$	(L/h·m^2)
	$R_m = 0.923$	(-)
	$R_p = 0.96$	(-)
PVAm	$J = -26.79 \ln(P_a) + 113.25$	(L/h·m^2)
	$R_m = 0.982$	(-)
	$R_p = 0.96$	(-)
PAA	$J = -13.46 \ln(P_a) + 47.511$	(L/h·m^2)
	$R_m = 0.935$	(-)
	$R_p = 0.96$	(-)
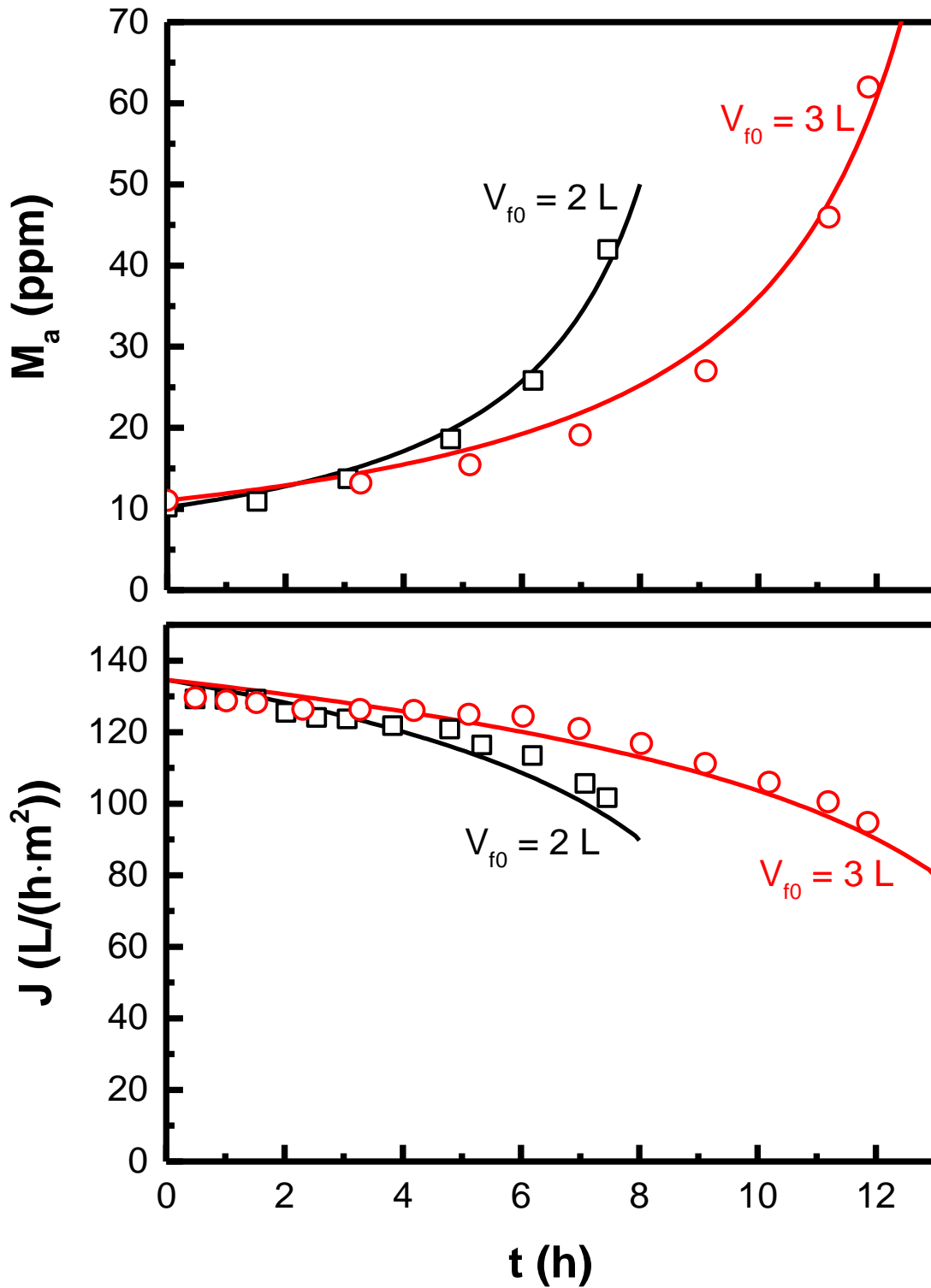
Figure 5.5 Comparison of calculated (lines) and experimental (keys) data for batch PEUF. Water-soluble polymer: PEI, ΔP: 0.2 MPa, feed flow rate: 65 L/h, M_{a0}: 11 ppm, P_{a0}: 0.05 wt%, A: 1.81×10^{-3} m^2.
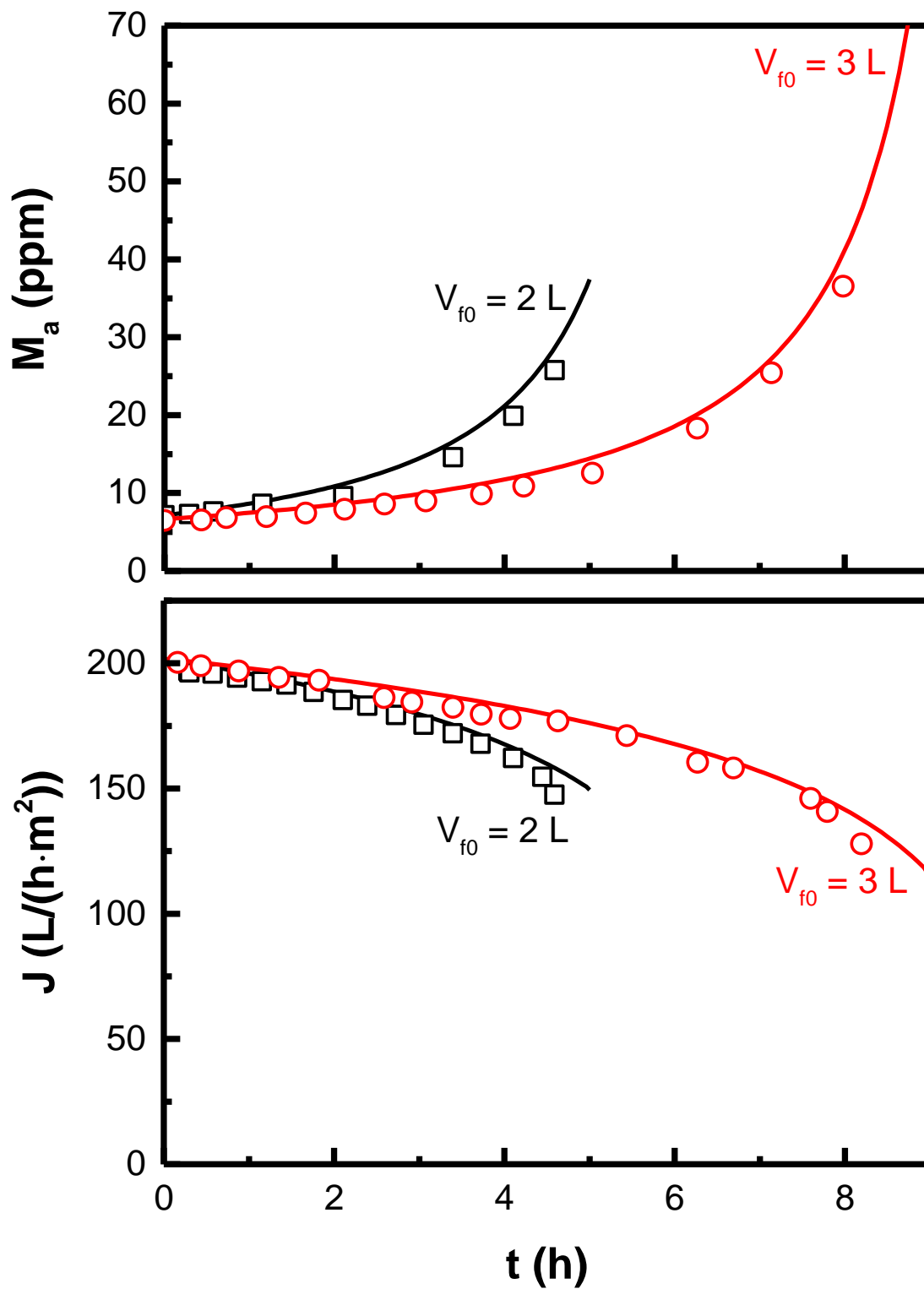
Figure 5.6 Comparison of calculated (lines) and experimental (keys) data for batch PEUF. Water-soluble polymer: PVAm, ΔP: 0.2 MPa, feed flow rate: 65 L/h, M_{a0}: 7 ppm, P_{a0}: 0.05 wt%, A: 1.81×10^{-3} m².
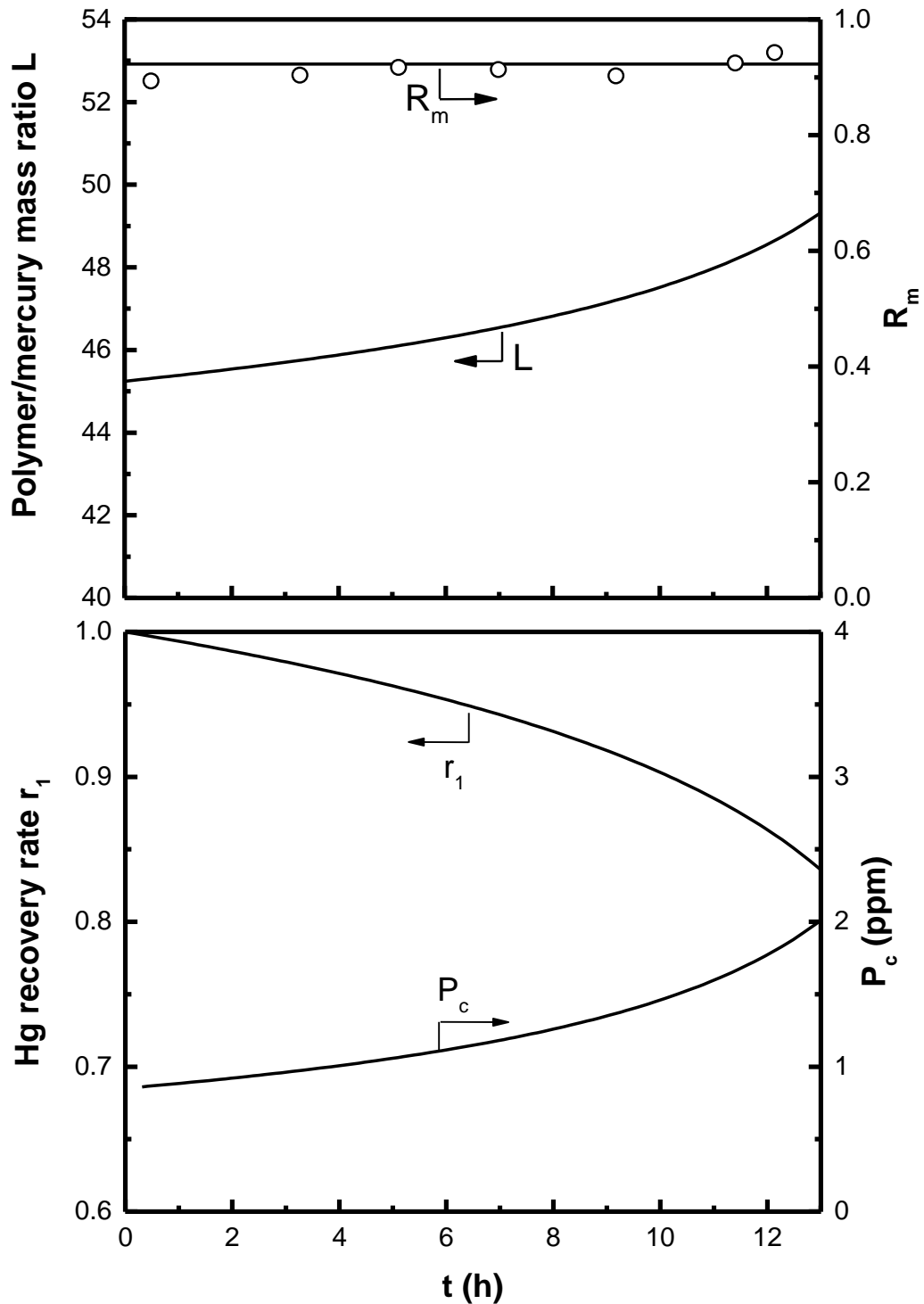
Figure 5.7 Cumulated product concentration of mercury, recovery rate of mercury, and the mass ratio (polymer/mercury) in feed, calculated for $V_{f0} = 3$ L, $M_{a0} = 11$ ppm, $P_{a0} = 0.05$ wt%, $A = 1.81 \times 10^{-3}$ m^2, water-soluble polymer: PEI. Open circles represent the experimental data of mercury rejection.
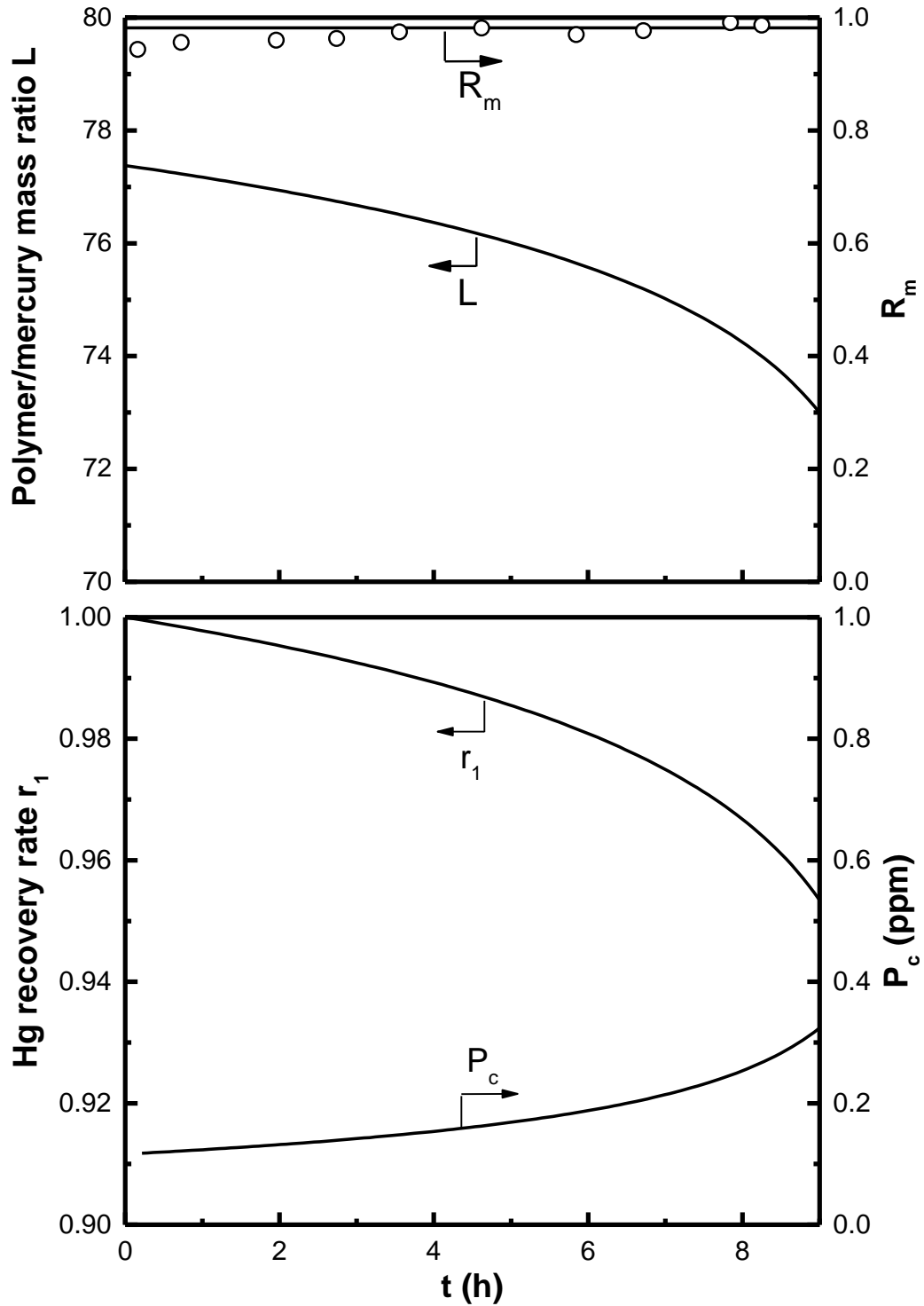
Figure 5.8 Cumulated product concentration of mercury, recovery rate of mercury, and the mass ratio (polymer/mercury) in feed, calculated for $V_{f0} = 3$ L, $M_{a0} = 7$ ppm, $P_{a0} = 0.05$ wt%, $A = 1.81 \times 10^{-3}$ m^2, water-soluble polymer: PVAm. Open circles represent the experimental data of mercury rejection.

Figures 5.7 and 5.8 illustrate the mercury concentration in cumulated permeate product (P_c), mercury recovery rate (r_1) and the instantaneous mass ratio of water-soluble polymer to mercury(II) in feed solution (L) as batch PEUF proceeds with time. The experimental results of mercury rejection (R_m) vs. time were also shown in the Figures. There was no significant variation in the polymer/mercury mass ratio (either decrease or increase, $< 8\%$), which explains why the mercury rejection did not decrease even though the mercury concentration in the feed increased with time. The mercury rejection will not change in PEUF as long as the polymer/mercury mass ratio in the feed solution maintains at a constant value. This is consistent with observations for separations of many other heavy metals using the PEUF technique with different water-soluble polymers [Uludag *et al.*, 1997; Muslehiddinoglu *et al.*, 1998; Islamoglu Kadioglu *et al.*, 2009; Qiu and Mao, 2013]. Note that the recovery rates of mercury decreased while the mercury concentration in cumulated permeate products increased with time. This is reasonable because the total amount of mercury passing through the membrane into the permeate increased with time as the polymers did not retain the metal completely.

5.4.3.2 Batch operation of PEUF with PAA, where membrane fouling is not negligible

As mentioned in the preceding sections, the flux decrease caused by membrane fouling will affect model predictions if membrane is not taken into account. It is not surprising that the calculated data for PEUF with PAA using the equations in Table 5.5 diverges considerably from the experimental data, as shown in Figure 5.9. The mercury concentration in the feed calculated with the model without considering the fouling is much higher than the actual values. This is because the flux in PEUF used in the model calculation was overestimated, and the

138

increased PAA concentration in the feed during the PEUF also reduced the flux. Therefore, if membrane fouling is not negligible, appropriate permeation flux equations that takes into account of the concentration increase and membrane fouling are needed for a better model representation.

In traditional UF, various fouling models have been used to predict the flux decline. The permeation flux data for PEUF with PAA in this study was represented based on the four fouling models as discussed in chapter 2. Their linear expressions are [Daufin *et al.*, 1998; Llanos *et al.*, 2009; Polyakov and Zydney, 2013]:

(a) Standard pore blocking

$$\frac{1}{J^{\frac{1}{2}}} = \frac{1}{J_0^{\frac{1}{2}}} + \frac{1}{2}K_s A J_0^{\frac{1}{2}} t \tag{5.28}$$

(b) Intermediate pore blocking

$$\frac{1}{J} = \frac{1}{J_0} + K_i A t \tag{5.29}$$

(c) Cake layer formation

$$\frac{1}{J^2} = \frac{1}{J_0^2} + 2K_c A^2 t \tag{5.30}$$

(d) Total pore blocking

$$lnJ = lnJ_0 - K_t t \tag{5.31}$$

where K_s (L^{-1}), K_i (L^{-1}), K_c (h·L^{-2}) and K_t (h^{-1}) are the empirical fouling coefficients in the models, J_0 is the initial permeation flux and A is the membrane area.
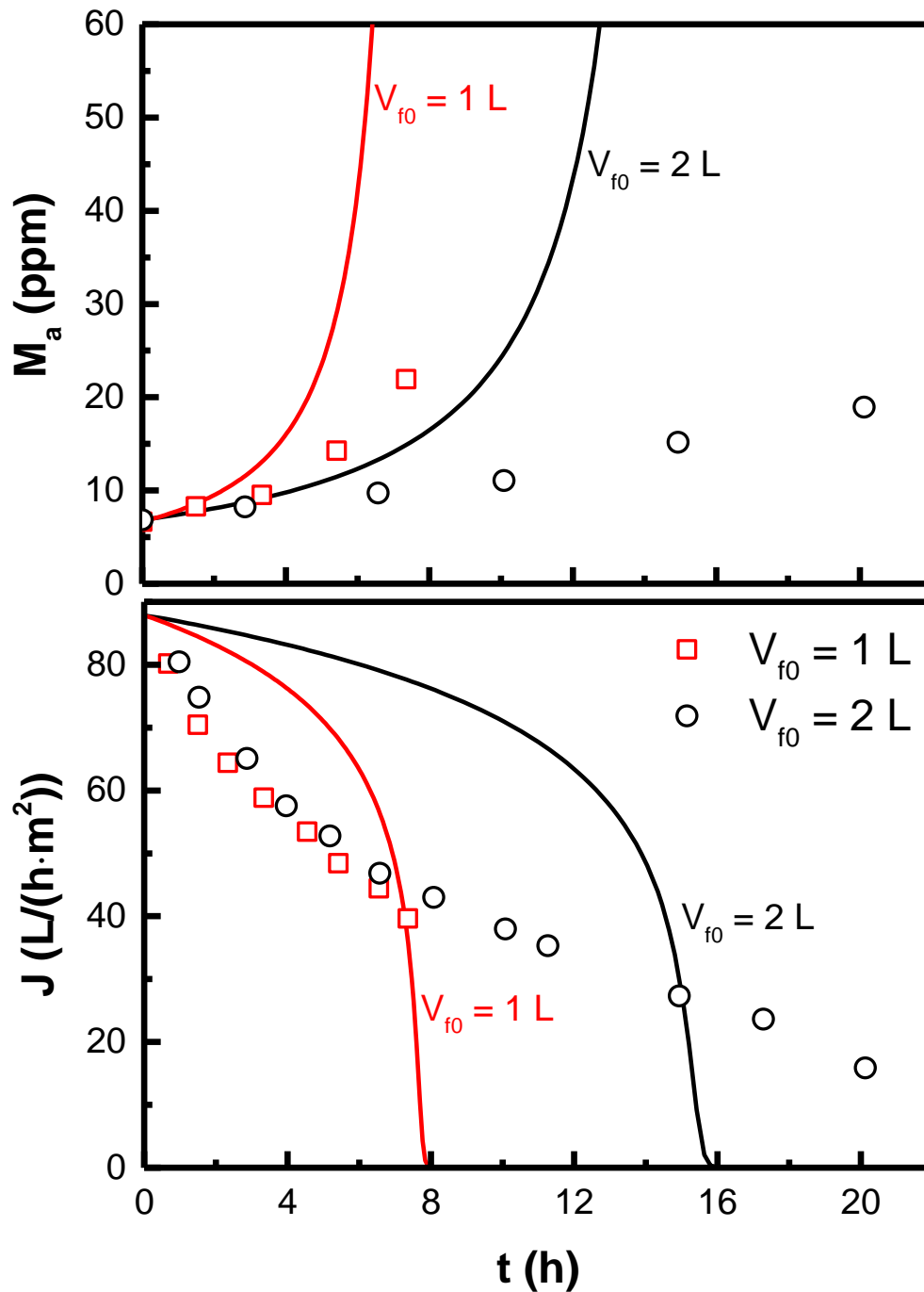
Figure 5.9 A comparison of model calculations (lines) and experimental data (keys) for PEUF with PAA. Water-soluble polymer: PAA, ΔP = 0.2 MPa, flow rate = 65 L/h, M_{a0} = 7 ppm, P_{a0} = 0.05 wt%, A = 1.81 $\times 10^{-3}$ m^2.
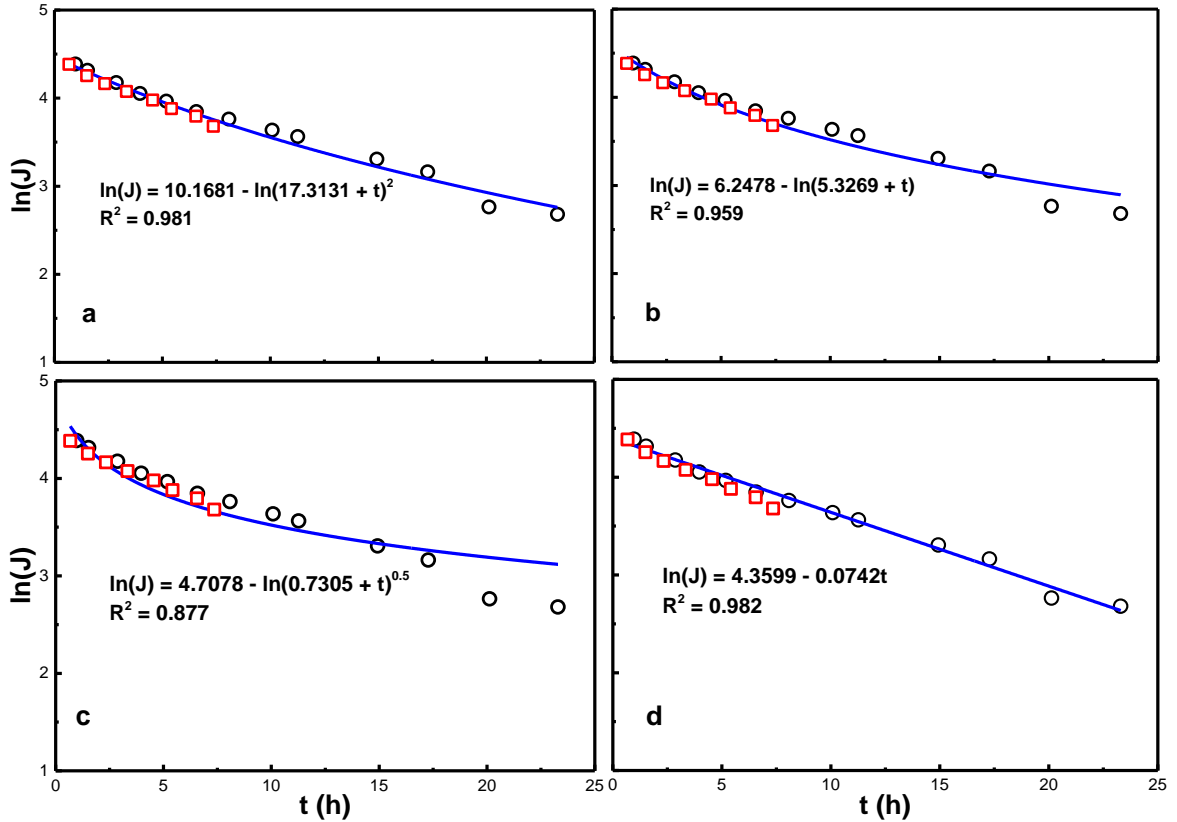
Figure 5.10 Comparison between experimental data (keys) and model calculations (lines) using different fouling models, a) standard pore blocking, b) intermediate pore blocking, c) cake layer formation, and d) total pore blocking models. Water-soluble polymer: PAA, $\Delta P = 0.2$ MPa, flow rate = 65 L/h, $M_{a0} = 7$ ppm, $P_{a0} = 0.05$ wt%, $V_{f0} = 1$ L ($\square$), 2 L ($\circ$), $A = 1.81 \times 10^{-3}$ m^2.

Figure 5.10 shows the permeation flux fitted to fouling models, and Table 5.6 lists the model parameters characterize the membrane fouling behavior. All the four fouling models can describe membrane fouling adequately for the PEUF with PAA, which confirms that the membrane fouling caused the flux decline. To facilitate mathematical treatment , the total pore blocking model that is represented with a simple flux equation was chosen as a semi-emprical equation for use in this study for the batch model calculation.

141
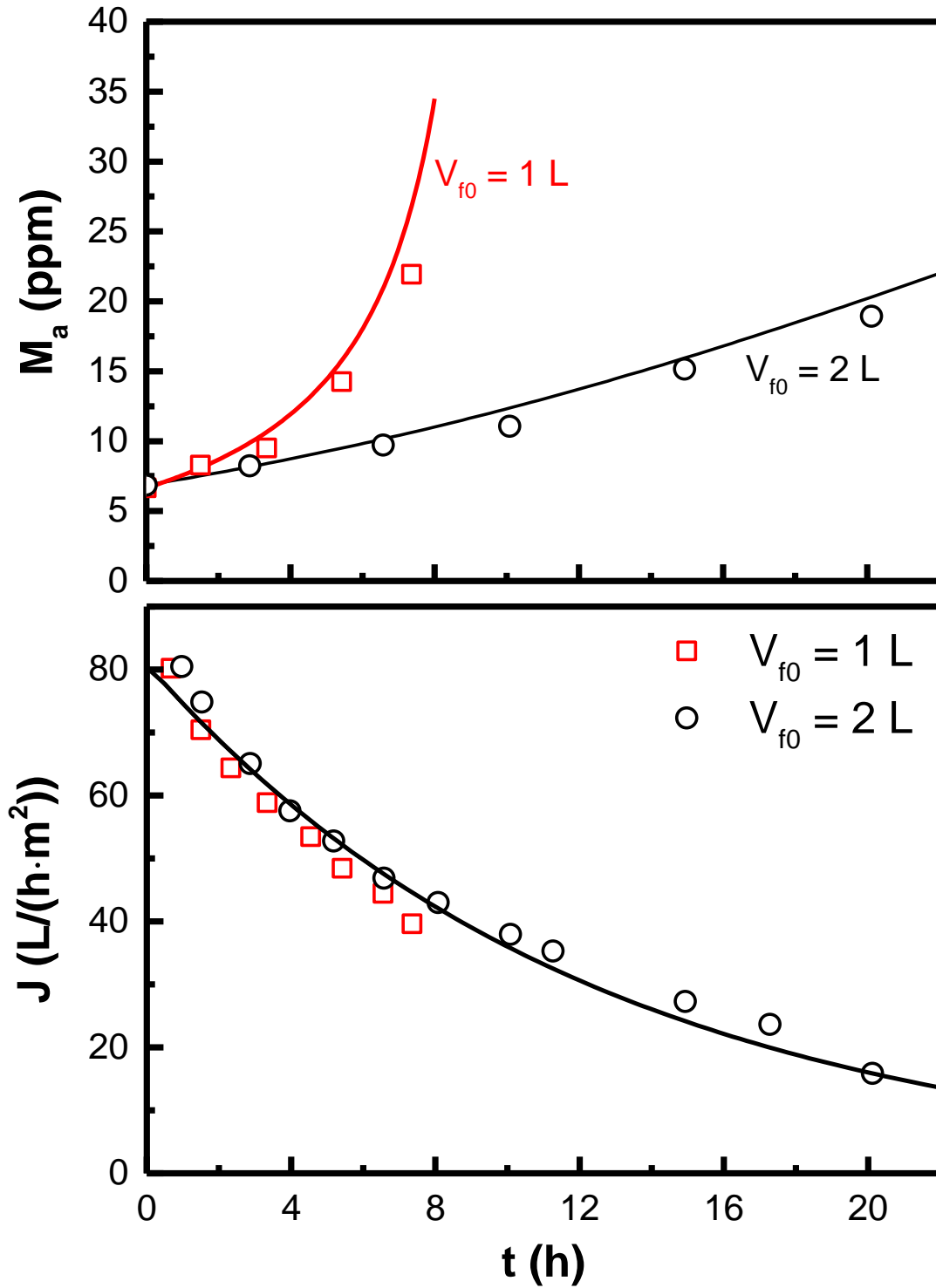
Figure 5.11 Comparison of model calculations (lines) and experimental (keys) data after taking into account of membrane fouling for batch PEUF with PAA. Water-soluble polymer: PAA, $\Delta P = 0.2$ MPa, flow rate = 65 L/h, $M_{a0} = 7$ ppm, $P_{a0} = 0.05$ wt%, $A = 1.81 \times 10^{-3}$ m^2.

Figure 5.11 shows the re-calculated flux and mercury concentration in the feed for the batch PEUF with PAA after membrane fouling was accounted for. The model predictions for batch PEUF process now agree well with the experimental data. It should be noted that the total pore blocking fouling model used was just a semi-empirical expression of the relation between flux and time. The other three fouling models shown in Figure 5.10 with relatively high coefficient of determination may also give acceptable agreements for the batch PEUF process. The result further testifies the applicability of the model equations developed for batch PEUF for circumstances where membrane fouling is not negligible.

Table 5.6 Parameters of the fouling models that describe membrane fouling for PEUF with PAA

	J_0 (L/(h·m²))	K	R^2
Standard pore blocking	86.93	$K_s = 0.7342$ L^{-1}	0.981
Intermediate pore blocking	97.03	$K_i = 1.0689$ L^{-1}	0.959
Cake layer formation	129.65	$K_c = 12.43$ h·L^{-2}	0.877
Total pore blocking	78.25	$K_t = 0.0742$ h^{-1}	0.982

In summary, the flux behaviour in the PEUF is highly related to the properties of the UF membrane and the water-soluble polymer used. The flux decline caused by membrane fouling in PEUF, may have a significant influence on the model predictions of batch PEUF performance, though membrane fouling is not always significant for certain membrane/polymer pairs used in the PEUF systems.

5.4.3.3 Implication of model predictions for practical PEUF applications

One important potential application of the developed batch model for PEUF process in practical water treatment or metal recovery is the prediction of the operating time or membrane area needed to concentrate a metal solution to a target value when the membrane and the water-

soluble polymer are selected. For a given membrane module (A is fixed), the operating time required depends on the quantity of feed solution to be treated and the properties of the membrane and water-soluble polymer used. The effects of (V_{f0}/A) value, which is the quantity of feed solution to be treated per unit membrane area, on the mercury concentration in the concentrated feed solution and the total mercury recovery rate were calculated for PEUF with PEI and PVAm, as shown in Figures 5.12 and 5.13, respectively. This allows for prediction of operating time needed to concentrate an aqueous mercury solution from its initial concentration to a desired value. For a given operating time, the lower the (V_{f0}/A) value, the higher the mercury concentration in the feed and the lower the total mercury recovery. The calculation results also show that if a relatively large amount of feed solution was to be treated in a short period of time, a larger membrane area will be needed. Comparing Figures 5.12 and 5.13, it can be seen that the effects of (V_{f0}/A) on the batch separation depend on characteristics of the used polymers for given UF membranes.

It has to be mentioned that if membrane fouling from the water-soluble polymer during PEUF is significant, as is the case for PEUF with PAA, the flux equation in the batch model equations should take into account of membrane fouling. In addition, changing the UF membrane may also change the flux behaviour for the same water-soluble polymer. Although the batch model for PEUF process developed in the present study is based on a cross-flow filtration, its applicability in a dead-end filtration mode is also expected, though concentration polarization and membrane fouling are more significant in the dead-end mode. Further, the batch model derived from the mercury/polymer system also applies to the recovery of other heavy metals from wastewater using the PEUF, provide that the perm-selectivity of the membrane/water-soluble polymer pair is known.
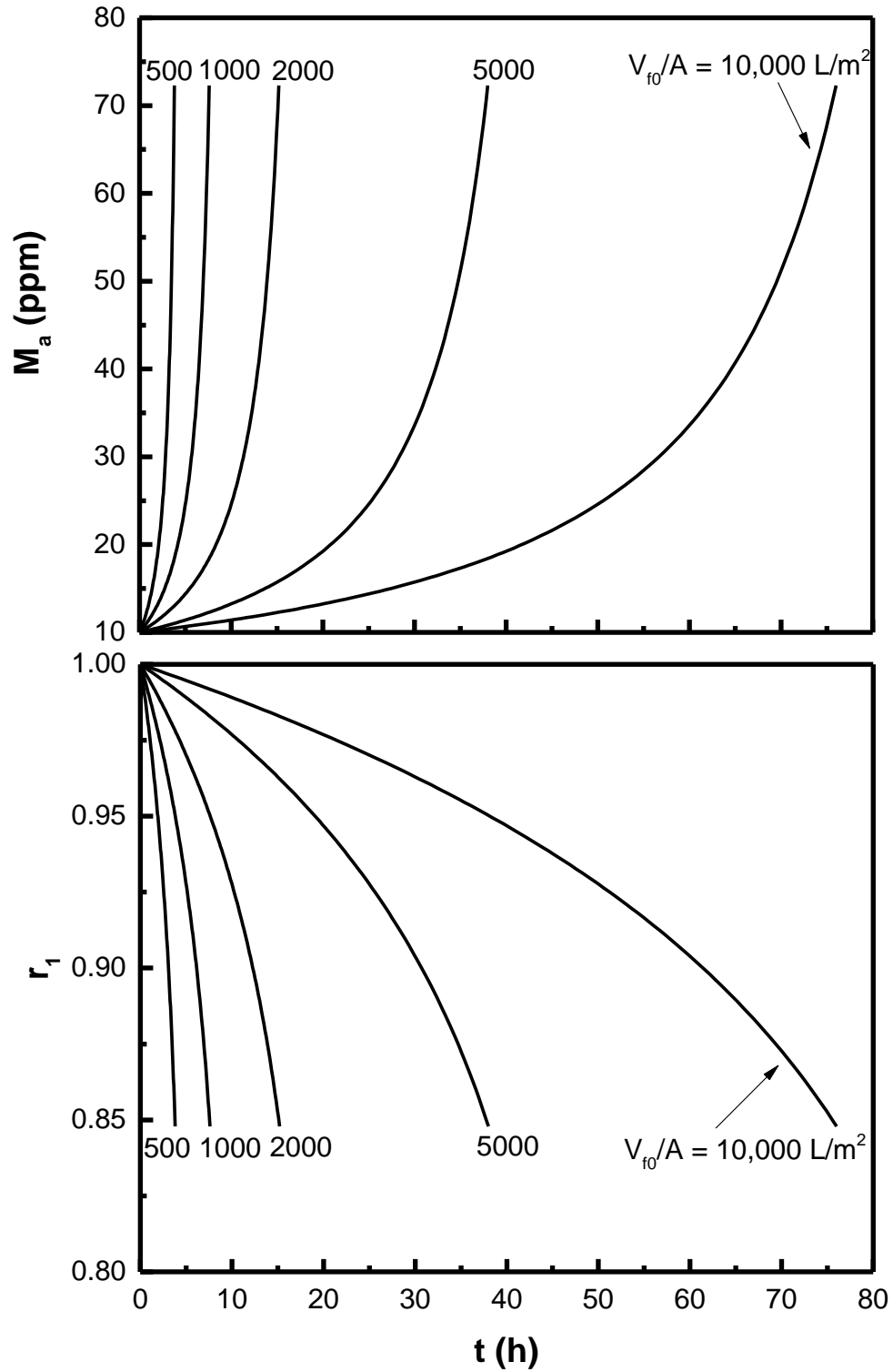
Figure 5.12 Calculated mercury concentration in the concentrated feed solution and mercury recovery rate for different V_{f0}/A values. Water-soluble polymer: PEI, membrane: PES, $\Delta P =$ 0.2 MPa, flow rate = 65 L/h, $M_{a0} = 10$ ppm, $P_{a0} = 0.05$ wt%.
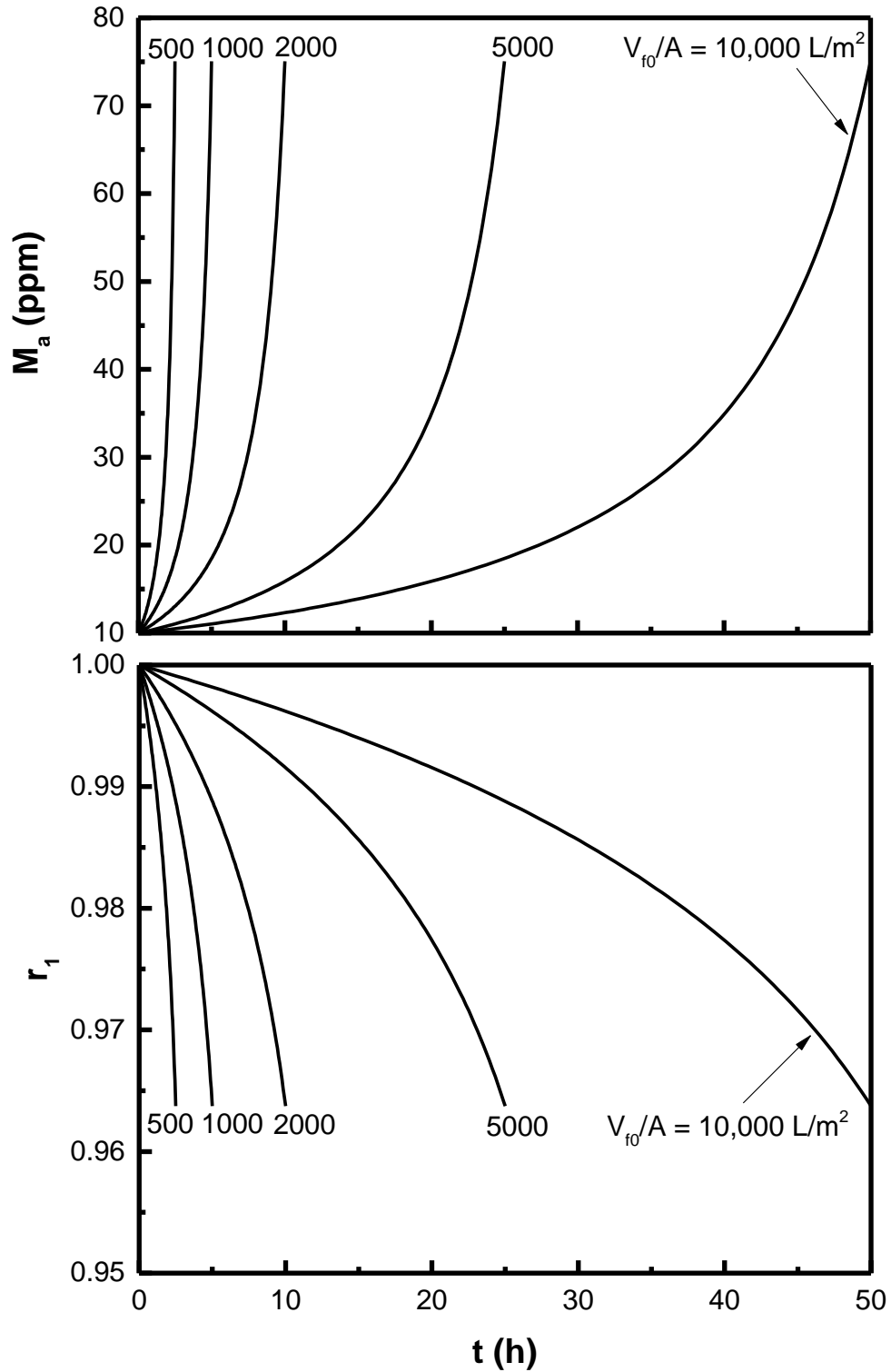
Figure 5.13 Calculated mercury concentration in the concentrated feed solution and mercury recovery rate for different V_{f0}/A values. Water-soluble polymer: PVAm, membrane: PES, ΔP = 0.2 MPa, flow rate = 65 L/h, M_{a0} = 10 ppm, P_{a0} = 0.05 wt%.

5.5 Conclusions

The recovery of mercury(II) from wastewater by PEUF using three water-soluble polymers was investigated, and a mathematical model describing batch operation of PUEF process was developed. The following conclusions can be drawn from this study:

1. Among the three polymers used for PEUF, PVAm showed the best performance in separating mercury(II) from water by PEUF, and a high permeation flux and mercury rejection were obtained at a low polymer concentration.

2. The dosage of the water-soluble polymers used in PEUF affected the permeation flux significantly, while it had little effect on mercury rejection under the tested concentration range. A correlation between permeation flux and feed polymer concentration was established semi-empirically.

3. The membrane fouling for PEUF with PVAm and PEI in cross-flow mode at low polymer dosage was insignificant. There was a considerable flux decline due to membrane fouling for PEUF with PAA, and the total pore blocking model was shown adequate to represent the flux decline in PEUF with PAA.

4. The batch operation of PEUF to recover mercury(II) from wastewater could be modelled by a set of equations, derived based on the mass balance. The information required in the model was the concentration dependences (both water-soluble polymers and heavy metal ions) of permeation flux and solute rejection, which can be obtained experimentally. Membrane fouling caused by the water-soluble polymer used in the PEUF affected the separation performance, and appropriate fouling control strategies were needed to minimize the possible fouling of the UF membrane by the polymer used.

Chapter 6

Polyvinylamine Bearing Thiol Groups for Removal of Mercury(II) from Wastewater by Adsorption

---

6.1 Introduction

As discussed in Chapter 2, many efforts have been made to incorporate functional groups into water-soluble polymer chains by chemical grafting. The chemical modified water-soluble polymers will obtain stronger interactions with heavy metals, and thus have better performance in PEUF process. In addition, the incorporated functional groups with high selectivity for specific heavy metals can help to achieve selective separation. Therefore, the attempt to introduce functional groups into PVAm chains was made to further enhance its performance for mercury separation in PEUF.

In the last two decades, sulfur-containing materials with good affinity and capacity for mercury removal have been investigated [Manohar *et al.*, 2002; Lo *et al.*, 2012]. Sulfurization of traditional adsorbent materials (e.g., activated carbon and carbon nanotubes) can drastically enhance the mercury removal efficiency [Pillay *et al.*, 2013; Hadi *et al.*, 2015]. Several polymeric adsorbents with sulfur-containing functional groups have been developed by chemical grafting as well. Saad *et al*. [UNEP] and Algarra *et al.* [2014] successfully grafted thiol groups onto polyethyleneimine and diaminobutane-based polypropyleneimine dendrimer, respectively. The modified amine polymers can then be used either as an efficient adsorbent

148

or as an additive for preparation of functionalized membranes. The sulfur-containing groups substituted in the backbone of polyamines act as strong adsorption sites for removing mercury species in aqueous solution.

Therefore, it was proposed to graft sulfur-containing groups onto PVAm chains via the reactive primary amines in view of the fact that PVAm has the highest density of primary amine groups in any amine-based polymers. These amine groups will serve as reaction sites for substituting sulfur-containing groups. Compared with polyethylenimine and polyallylamine, PVAm is much less understood in terms of its applications in the environmental industry. However, the preliminary experiment showed that the new synthesized PVAm with thiol groups after grafting become insoluble in water, which is obviously not acceptable in PEUF process. Therefore, the adsorption process was selected as an alternative for mercury separation in this chapter.

The objective of this study was to chemically graft thiol groups onto PVAm chains so as to produce an efficient polymeric adsorbent for removal of Hg(II) from wastewater. A series of batch sorption tests were conducted under a range of water chemistry conditions to investigate the kinetics and thermodynamics of Hg(II) adsorption on sulfurized PVAm. Desorption of mercury adsorbed on the polymeric adsorbent was also investigated to assess the sorbent regeneration and reusability.

6.2 Experimental

6.2.1 Synthesis and characterization of thiolated polyvinylamine (PVAm-SH)

Polyvinylamine and mercury chloride used were the same as described in Chapter 4. All other reagents and solvents were purchased from Sigma-Aldrich (Canada). The synthesis of

thiolated PVAm was carried out in two stages following a procedure similar to that described in the literature [Connolly *et al.*, 2000]. At first, N-hydroxysuccinimide (NHS, 3 g) was dissolved in CH_2Cl_2 solution (500 mL) under magnetic stirring to form a clear solution. Then 3-mercaptopropionic acid (2.766 g) dissolved in 10 mL of CH_2Cl_2 was added. After the mixture was stirred for 30 min, 1,3-Dicyclohexylcarbodiimide (DCC, 5.385 g) dissolved in 50 mL of CH_2Cl_2 was added dropwise to the reaction mixture over a period of 50 min. The mixture was further stirred for 24 h. Afterward, the solid formed was separated from the solution by filtration, and the solvent was removed under reduced pressure to obtain the product of NHS ester. For the final thiolation of PVAm, 1.5 g of PVAm in 125 mL of CH_3OH was well mixed with 500 μL of triethylamine. NHS ester (3.532 g) dissolved in 125 mL of CH_3OH was added dropwise over a period of 5 h. Then the mixture was stirred for 24 h. The obtained light yellow solid was washed several times with deionized water and finally dried in the oven (T = 40 ℃) for further use. Figure 6.1 shows a scheme of the thiolation reaction and the structure of PVAm-SH.

Both FT-IR and UV-vis spectroscopy were used to characterize the thiolated derivative of PVAm before and after adsorption of Hg(II). For FT-IR analysis, the samples were treated by the potassium bromide pellet technique, and scanned by the infrared spectroscopy (Thermo Nicolet 3600). For UV-vis analysis, the solid samples were ground to powder and then dispersed into N-methyl-2-pyrrolidone solvent by sonication. The synthesized PVAm-SH was partially dissolved. After sedimentation for 24 h, the upper supernatant was collected by a syringe and then scanned using a UV-vis spectrophotometer (Shimadzu UVmini-1240).
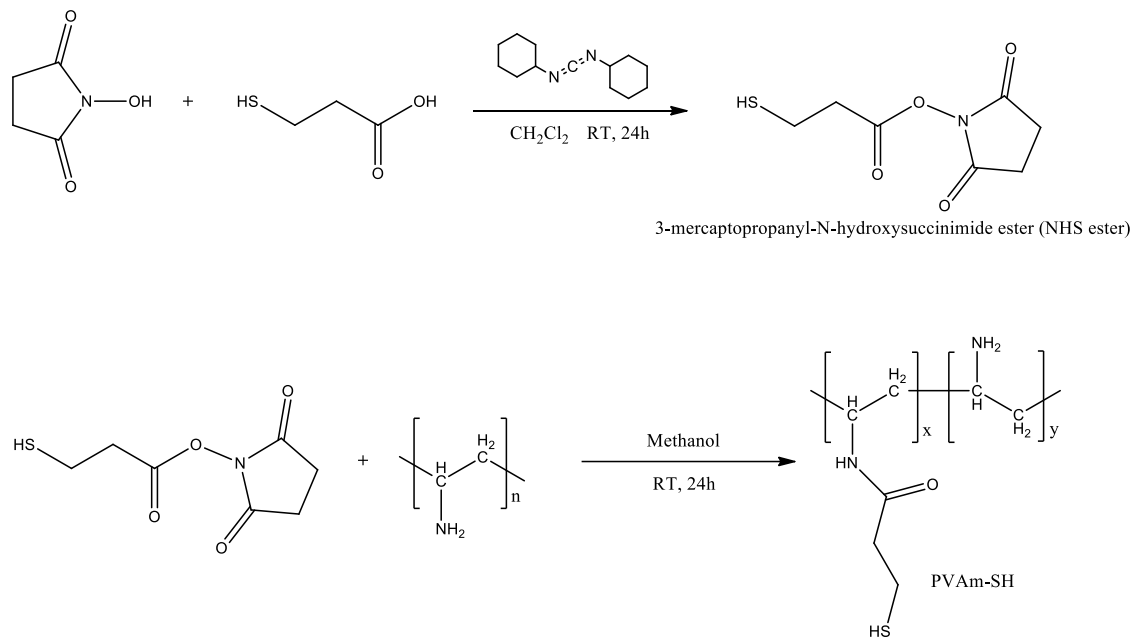
Figure 6.1 A schematic of thiolation of PVAm

6.2.2 Water solubility test

The solubility of PVAm-SH in water was tested by an indirect method described as follows: a known amount of PVAm-SH was immersed in deionized water of 500 mL. Then, the conductivity of the solution was monitored by inoLab Cond Level 2 Presicion Conductivity Meter continuously. In addition, the solution was also scanned by an UV-vis spectrophotometer (Shimadzu UV mini-1240). The experiment was operated at room temperature (25 ℃).

6.2.3 Batch adsorption experiments

The adsorption equilibrium of Hg(II) on PVAm-SH was reached within approximately 12 h under the experimental conditions according to a preliminary test. Therefore, an equilibrium time of 24 h was selected for all batch adsorption experiments. A mercury stock solution with 1000 mg/L prepared from $HgCl_2$ was used to prepare the working solutions with various initial

151

mercury concentrations by serial dilution. A pre-determined amount of PVAm-SH was mixed with 20 mL of an aqueous Hg(II) solution. After reaching sorption equilibrium, the solution was filtered immediately and the Hg(II) concentrations in the filtrate was analyzed using an Inductively Coupled Plasma Optical Emission Spectroscopy (ICP-OES). Each sample was analyzed three times. The effects of temperature, aqueous pH (1−11), and presence of other water constituents (e.g., NaCl, Na$_2$SO$_4$ and MgCl$_2$) on the Hg(II) sorption were also studied. The amount of Hg(II) adsorbed per unit mass of PVAm-SH (Q_e, mmol/g) was calculated on the basis of mass balance of mercury before and after the adsorption.

The adsorption kinetics was determined in a 1 L vessel with a sealed cover. 1 L of mercury solution at 50 mg/L Hg(II) was added into the vessel, and then, 0.4 g of PVAm-SH adsorbent was quickly added. Immediately after the addition of PVAm-SH, the adsorption time was monitored. 1 mL of the sample solution was collected by a syringe at pre-determined time intervals, and filtered with a 0.45 μm membrane. The sample solutions were then diluted 10 times before analysis for mercury concentration. During the entire course of the adsorption kinetic study, the total amount of solution removed from the 1 L initial mercury solution was approximately 20 mL, which was less than 2% of the initial solvent volume. This means the concentration variation of mercury in the solution due to sampling was negligible. The temperature of vessel was controlled by a water bath.

6.2.4 Desorption

To study the regeneration of mercury-loaded PVAm-SH, desorption experiments were conducted by using 0.5% thiourea in 0.5 M HCl as the stripping agent [Pillay *et al.*, 2013]. The previously loaded PVAm-SH was mixed with the stripping solution and stirred for 24 h. Then, the solution was filtered using a filter paper (pore size: 2.5 μm) and the polymer obtained

was washed thoroughly with deionized water and dried prior to reuse. The adsorption capacity of the regenerated polymer was studied for batch adsorption as described in section 6.2.3. The desorption study was repeated for 4 cycles under the same experimental conditions, and the mercury removal efficiency (R_e) was calculated for each cycle:

$$R_e = \frac{M_0 - M_e}{M_0} \times 100\% \tag{6.1}$$

where M_0 is the initial mercury(II) concentration, and M_e is the mercury(II) concentration at equilibrium.

6.3 Results and discussion

6.3.1 Characterization of PVAm-SH

As shown in Figure 6.1, the thiolation of PVAm was achieved in two steps. The 3-mercaptopropyl acid first reacted with N-hydroxysuccinimide to produce 3-mercaptopropanyl-N-hydroxysuccinimide ester (NHS ester). The NHS ester is an amine-specific functional group that can easily react with primary amines to yield stable amide bonds. The FTIR spectrum for NHS ester in Figure 6.2 clearly shows three characteristic bands at 1750, 1787, and 1816 cm^{-1}, which are attributed to the stretching of C=O in the COO-NHS ester moiety [Wang *et al.*, 2011; Liu *et al.*, 2014]. The other two bonds at around 3055 and 2940 cm^{-1} are related to C-H stretching from carbon backbone (CH$_2$) [Wu *et al.*, 2014]. The FTIR spectrum of PVAm-SH before and after Hg(II) adsorption showed two peaks at 1540 cm^{-1} (amide-II N-H bend) and 1675 cm^{-1} (amide-I C=O stretching), which confirms the amide bond in the polymer as indicated in Figure 6.1 [Wu *et al.*, 2014]. The weak peak occurring around 2390 cm^{-1} is due to the thiol S-H stretching. It should be mentioned that the FTIR analysis was operated under the N$_2$ protection, and thus the absorbance around 2390 cm^{-1}

153

cannot be contributed to carbon dioxide which also had an absorbance near 2400 cm^{-1} [Liao *et al.* 2002].
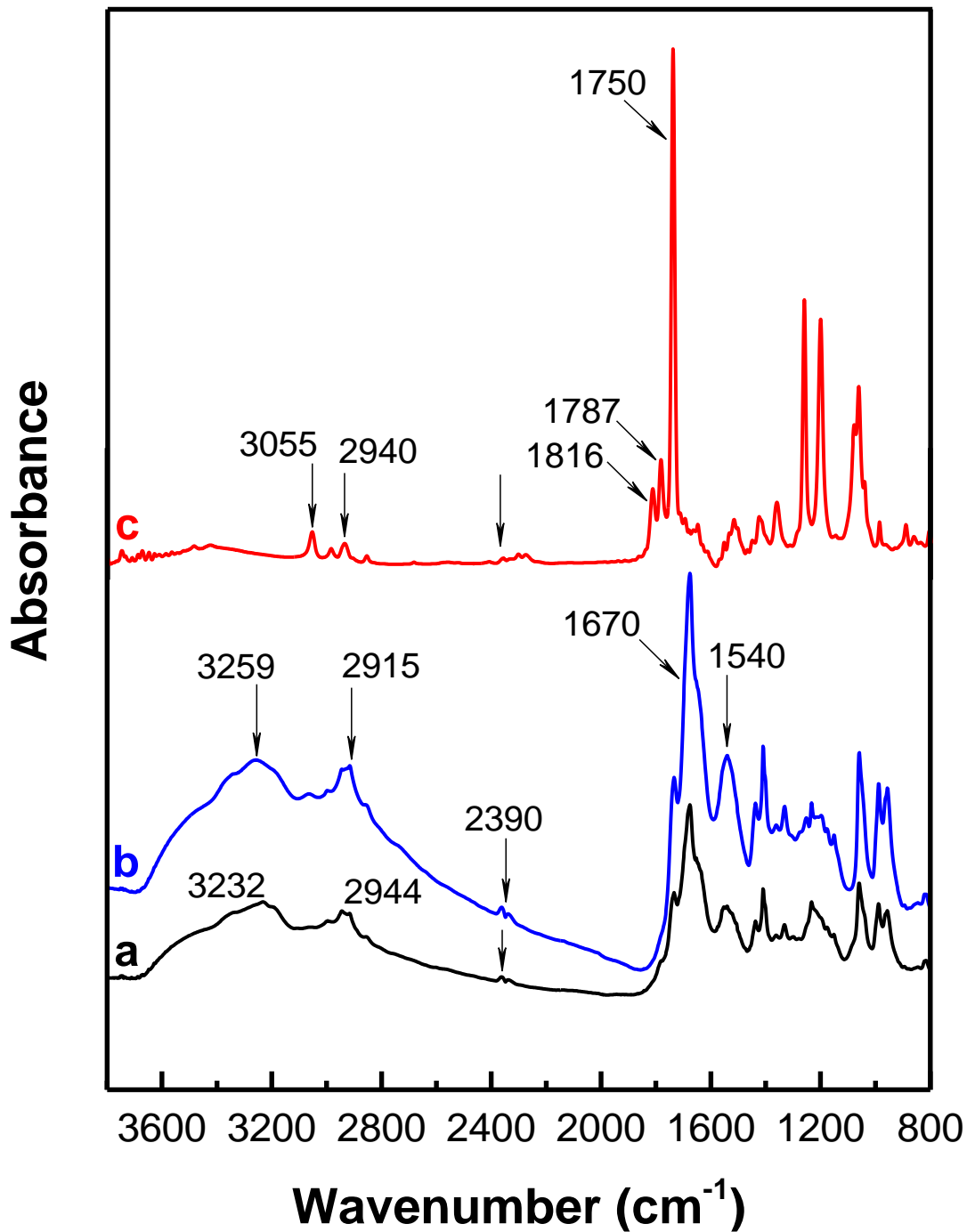
Figure 6.2 FTIR of a) PVAm-SH, b) PVAm-SH after Hg(II) sorption, c) NHS ester

The two characteristic bonds at 2944 and 3232 cm^{-1} are ascribed to the primary N-H$_2$ stretching, which indicates that only a portion of the amine groups in PVAm have been reacted. The FTIR results confirm the successful grafting of thiol groups onto the PVAm chains by forming the amide bonds. After Hg(II) was sorbed into PVAm-SH, there was a change in the shapes of the primary N-H$_2$ stretching peaks, and the peak positions were shifted, as well. It implies that Hg(II) adsorption took place through chelate or coordinate interactions between Hg(II) and the functional groups of the PVAm-SH adsorbent.

The grafting of thiol onto PVAm was further confirmed by the UV-vis spectra. As shown in Figure 6.3, there was new peak observed at around 270 nm after grafting, which was ascribed to the thiol group [Pretsch *et al.*, 2009]. When Hg(II) is sorbed onto PVAm-SH, the characteristic absorption peak experienced a blue-shift and broadening.
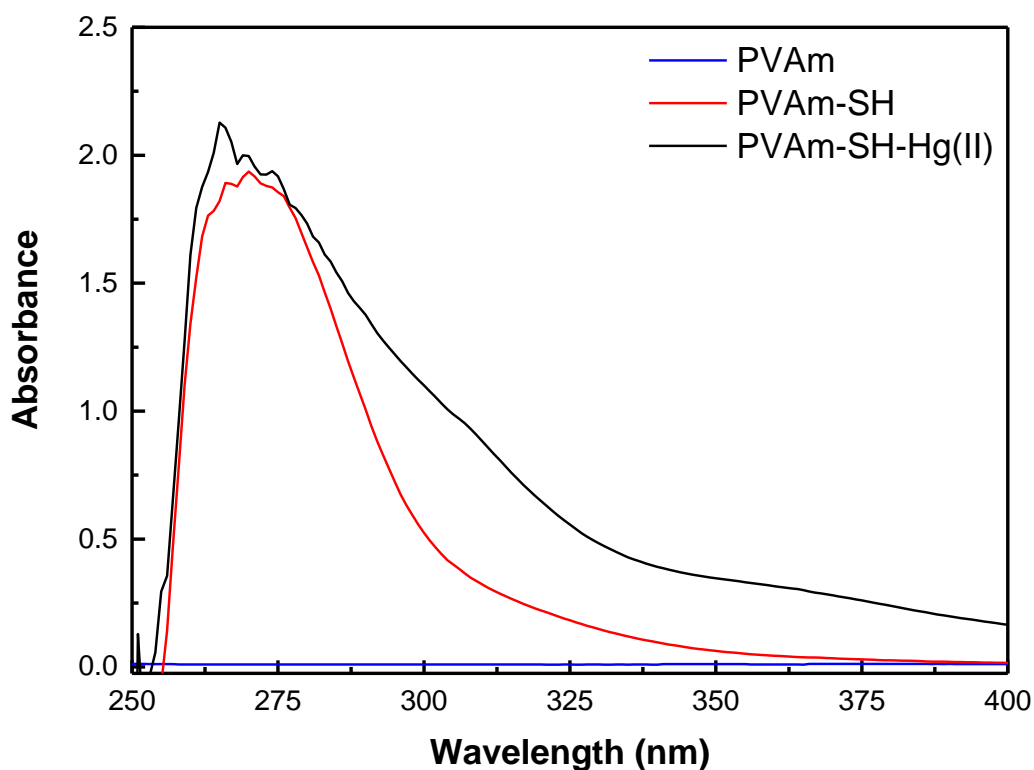
Figure 6.3 UV-vis spectra of pristine PVAm, thiol grafted PVAm (PVAm-SH) and PVAm-SH after Hg(II) sorption

6.3.2 Water solubility of PVAm-SH

As shown in Figure 6.4, the conductivity of the PVAm-SH suspension over 2 days almost remained a constant value close to that of deionized water (~1.0 μs/cm), indicating that the PVAm-SH did not dissolve in the water. The fluctuation shown in the figure may be caused by the temperature change in the environment. The spectra obtained by UV-vis spectrophotometer also showed no obvious signal in the wavelength from 190 to 710 nm. The result confirmed that the PVAm-SH synthesized in this study was insoluble in water, and thus can be used as an adsorbent for Hg(II) removal.
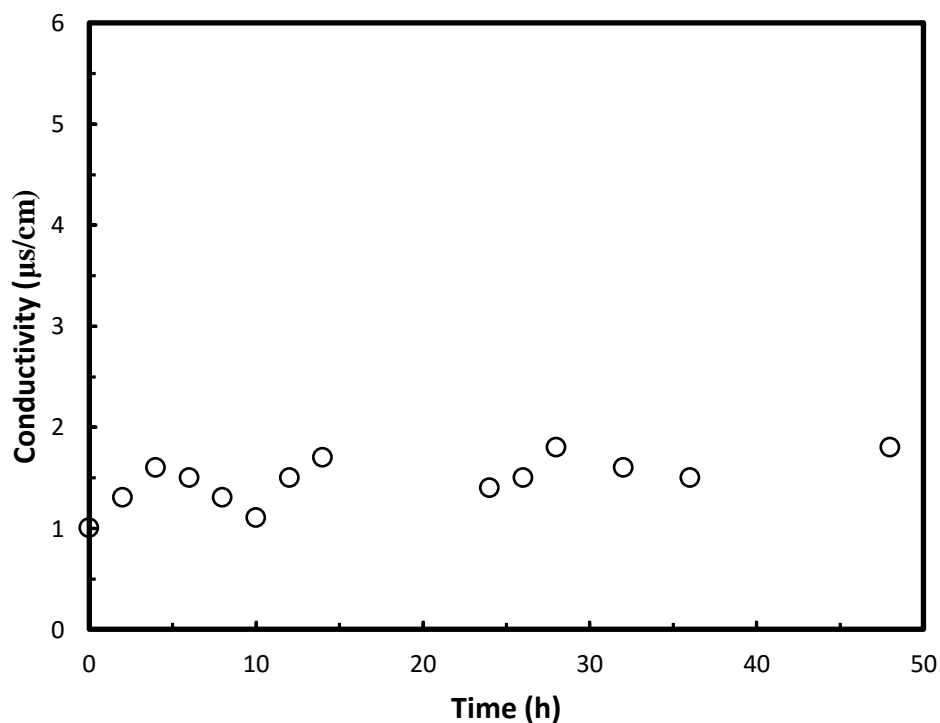
Figure 6.4 Conductivity of PVAm-SH suspension. T: room temperature (25 ℃)

6.3.3 Adsorption isotherm

The adsorption isotherm of Hg(II) onto PVAm-SH at neutral pH and different temperatures are shown in Figure 6.5. The saturated sorption amount of Hg(II) in PVAm-SH increased with an increase in temperature, suggesting the endothermic nature of the sorption.

156
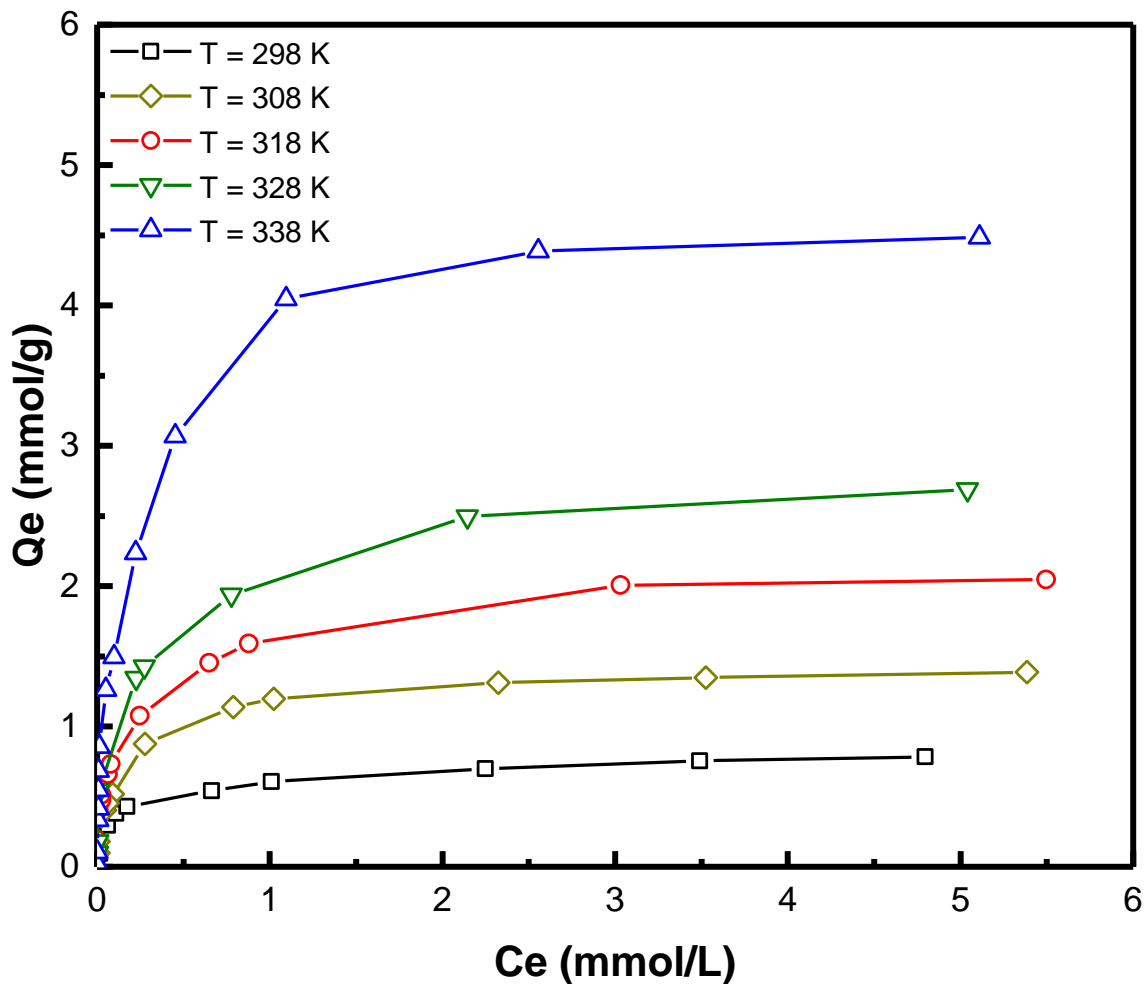
Figure 6.5 Isotherms for the sorption of Hg(II) in PVAm-SH

The experimental sorption uptake data are fitted by two sorption equilibrium models. The Langmuir model, which was developed by Langmuir [Langmuir, 1916], is the most widely used expression for physical sorption from aqueous solution. The sorption model has three important assumptions: a) adsorbate molecules are absorbed at well-defined localized states, b) all the sorption sites on adsorbent are identical, and each site accommodates one adsorbate molecule only, and c) no lateral interactions take place in the sorption process. The linearized form of Langmuir model can be expressed as follows [Tu *et al.*, 2012]:

$$\frac{C_e}{Q_e} = \frac{C_e}{Q_m} + \frac{1}{Q_m K_L} \tag{6.2}$$

where C_e and Q_e represent the equilibrium concentration of mercury in the solution and equilibrium sorption uptake, Q_m refers to theoretical maximum adsorption capacity, and K_L is the Langmuir constant.

In many cases, sorption of adsorbates in polymers might not fit Langmuir model. In that case, another purely empirical model: Freundlich isotherm is used. The linear expression of Freundlich model can be written as [Geng and Zebolsky, 2002]:

$$ln\, Q_e = ln\, K_F + \frac{ln\, C_e}{n} \tag{6.3}$$

where K_F is the Freundlich constant reflecting the adsorption capacity and has a unit of $(mmol)^{(1-1/n)}(L/g)^{1/n}$, and $1/n$ is the heterogeneity factor.

The sorption uptake data was re-plotted in Figure 6.6 and the model parameters were determined from the slopes and intercepts. Table 6.1 summarizes the parameters as obtained. In general, the adsorption isotherms of Hg(II) onto PVAm-SH are represented much better by the Langmuir model than by the Freundlich model. This observation is similar to a number of other studies about heavy metal sorption [Chiron *et al.*, 2003; Tu *et al.*, 2012; Liu *et al.*, 2013]. This appears to suggest that the Hg(II) sorption onto PVAm-SH tends to follow monolayer adsorption. It is understandable because the main driving forces for Hg(II) sorption onto PVAm-SH is the chemical interactions between Hg(II) and the thiol or unreacted amine groups. Once the adsorption sites on the surface of PVAm-SH are occupied by Hg(II), additional sorption of Hg(II) to form multilayers will be difficult. Table 6.1 also shows that both the Langmuir constant K_L and the maximum adsorption capacity Q_m increase with an increase in the temperature. It indicates the Hg(II) sorption onto PVAm-SH is endothermic.
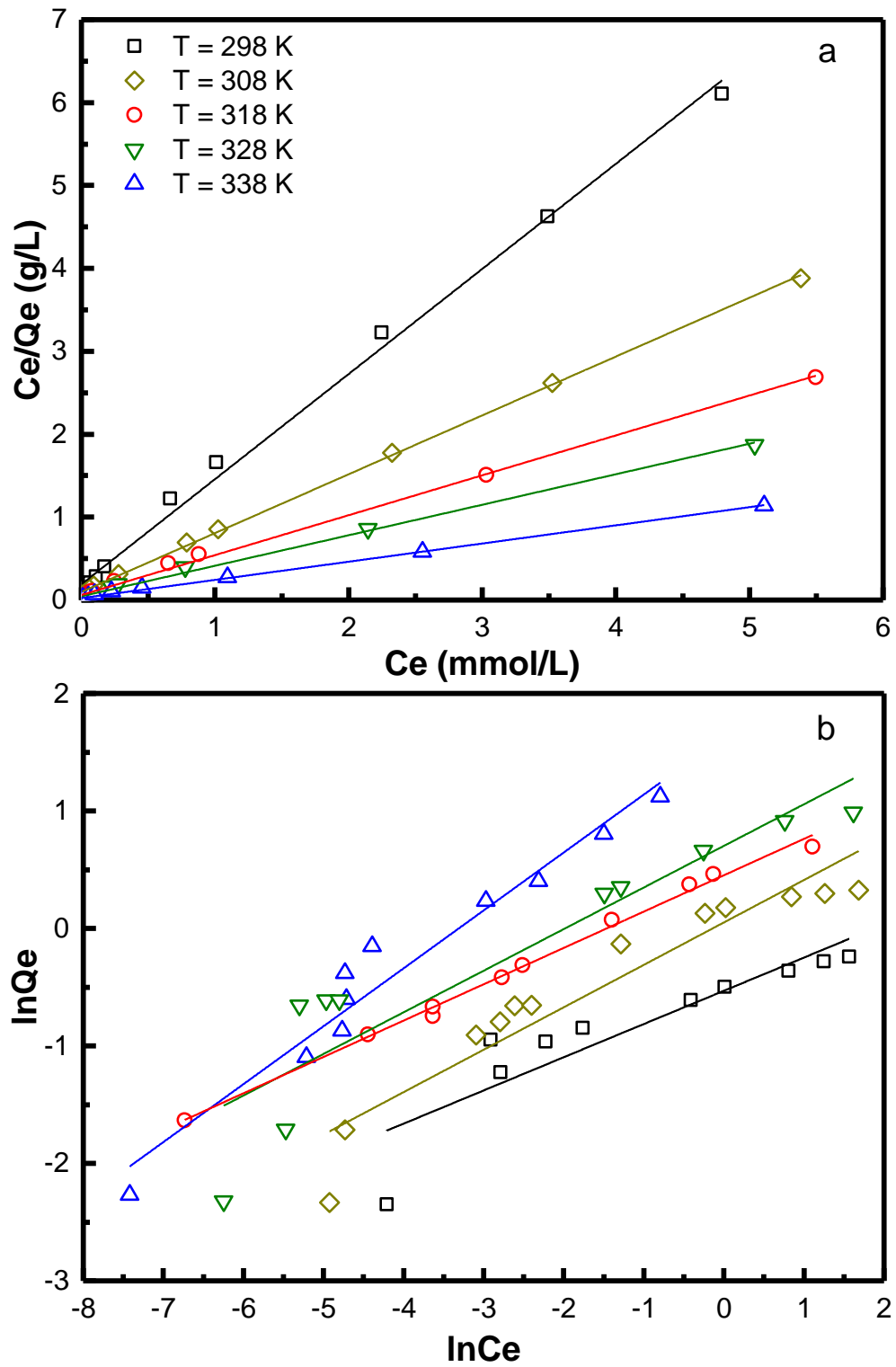
Figure 6.6 a) Langmuir and b) Freundlich model for the adsorption of Hg(II) on PVAm-SH at different temperatures

Table 6.1 The Langmuir and Freundlich constants for Hg(II) adsorption on PVAm-SH

Adsorbent	T (K)	Langmuir model			Freundlich model		
		$*Q_m$ (mmol/g)	$*K_L$ (L/mmol)	R^2	$*K_F$ $(mmol)^{(1-1/n)}(L/g)^{1/n}$	$*n$	R^2
	298	0.797 ± 0.045	6.14 ± 3.26	0.996	0.59 ± 0.13	3.54 ± 2.36	0.904
	308	1.427 ± 0.028	6.39 ± 1.21	0.993	0.87 ± 0.19	3.49 ± 0.83	0.812
PVAm-SH	318	2.101 ± 0.052	7.54 ± 2.88	0.998	1.44 ± 0.09	3.21 ± 0.21	0.961
	328	2.733 ± 0.083	8.17 ± 2.91	0.998	1.85 ± 0.74	2.99 ± 1.42	0.861
	338	4.560 ± 0.141	9.37 ± 2.12	0.997	3.95 ± 1.59	2.09 ± 0.43	0.925

*At 95% confidence level, the confidence bounds for parameters are shown in the table

6.3.4 Adsorption kinetics

The studies on adsorption kinetics were carried out to determine the Hg(II) adsorption rate on PVAm-SH. It will provide an insight into the mechanism of the adsorption process as well. Figure 6.7 shows the adsorption kinetics of PVAm-SH for Hg(II) at various temperatures. As expected, the adsorption time influenced the Hg(II) adsorption. The sorption was fast initially and then gradually leveled off. At the beginning, Hg(II) could easily access the surface of PVAm-SH because of the abundant binding sites available for Hg(II) sorption. However as the sorption proceeded, the sorption sites were gradually saturated, leading to a decreased adsorption rate. The relatively high initial adsorption rate suggests that Hg(II) sorption took place mainly through the surface binding [Das *et al.*, 2007]. Figure 6.7 also shows that temperature has significant effects on the adsorption rate as well as the equilibrium adsorption capacity. The increased adsorption capacity with an increase in temperature has been observed in the sorption isotherm studies. The adsorption rate increased with temperature as well. In general, metal ion adsorption on an adsorbent can be divided into two consequent processes: fast diffusion, and slow surface complexation [Liu *et al.*, 2013]. When the temperature is

increased, both the rate of Hg(II) diffusion from bulk solution to adsorbent surface and the rate of complexation with sorption sites in PVAm-SH.
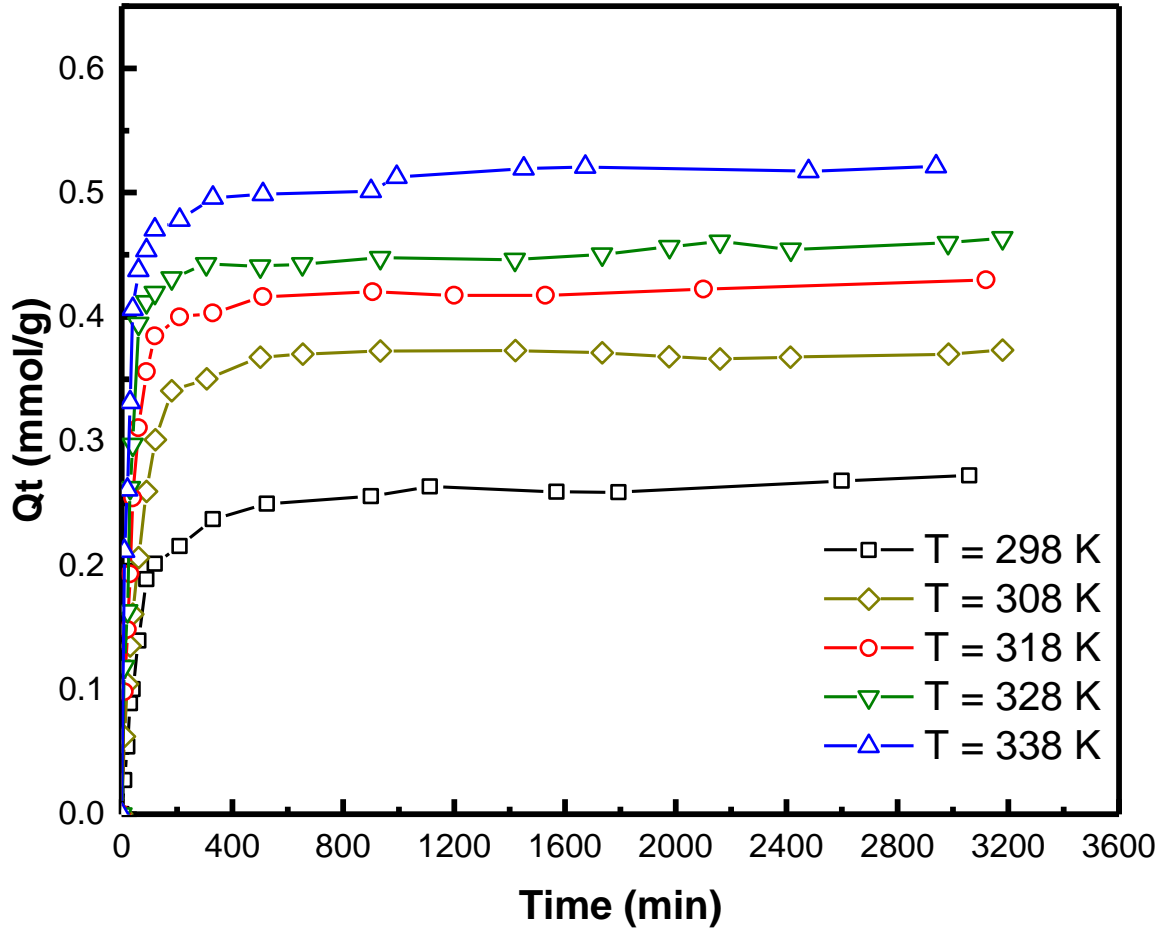
Figure 6.7 Adsorption kinetics of Hg(II) on PVAm-SH at different temperatures

To further explain the Hg(II) sorption kinetics, two commonly used kinetic models, namely the pseudo-first- and pseudo-second-order models, were applied to fit the experimental data. The pseudo-first-order model was developed by Lagergren [Lagergren, 1898], and it assumed that the adsorption rate was proportional to the adsorption capacity. The equation can be expressed as follow [Lee *et al.*, 2011]:

$$\frac{dQ_t}{dt} = k_1(Q_e - Q_t) \tag{6.4}$$

where Q_e and Q_t are the solute uptake at equilibrium and time t, respectively, and k_1 is the pseudo-first-order rate constant. Integration of equation (6.4) gives the following linearized equation:

$$ln(Q_e - Q_t) = ln\, Q_e - k_1 t \qquad (6.5)$$

Plotting $ln(Q_e - Q_t)$ vs. time t will result in a straight line. The rate constant k_1 can be then determined from the slope and intercept.

The pseudo-second-order kinetic model, on the other hand, was first proposed to describe the divalent metal sorption onto peat. It assumed that the adsorption was caused by the valence force through sharing electron pairs between peat and divalent metals as covalent forces [Ho, 2006]. Apparently, the pseudo-second-order model appears to be more suitable for the Hg(II) sorption onto PVAm-SH by its very nature in this study. The rate expression is given by [Ho and McKay, 1998]:

$$\frac{dQ_t}{dt} = k_2(Q_e - Q_t)^2 \qquad (6.6)$$

where k_2 is the pseudo-second-order rate constant of adsorption. By integration and rearrangement, a linear form of equation (6.6) can be obtained [Ho and McKay, 2000]:

$$\frac{t}{Q_t} = \frac{1}{k_2 Q_e^2} + \frac{t}{Q_e} \qquad (6.7)$$

Similar to pseudo-first-order model, the rate constant k_2 can be obtained by plotting t/Q_t vs. time t as well.

Figure 6.8 shows how the models were fitted to the sorption data, and the model parameters were calculated and listed in Table 6.2. It is quite obvious that the pseudo-second-order model was fitted to the data much better than the pseudo-first-order model. Previous studies have reported that polar amines and thiol groups can be involved in chemical

interactions and act as adsorption sites for Hg(II) [Das *et al.*, 2007; Wang *et al.*, 2009; Cai and Jia, 2010]. Thus the Hg(II) adsorption onto PVAm-SH may be represented by:

$$2P+ Hg(II) \leftrightarrow P_2Hg(II)$$
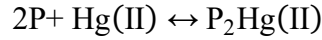
where P represents the adsorption site on the PVAm-SH adsorbent [Ho, 2006].

As can be seen in Table 6.2, the uptake capacity at equilibrium ($Q_{e, cal}$) calculated from the model deviates from the one determined experimentally ($Q_{e, exp}$). It suggests that the pseudo-second-order model did not precisely describe the adsorption kinetics in this study. One important assumption in pseudo-second-order model is that the uptake capacity at equilibrium (Q_e) as shown in equation (6.6) is constant and only related to the solute concentration at equilibrium. However, the data in Table 6.2 and other studies [Singh *et al.*, 2001; Taty-Costodes *et al.*, 2003] showed that Q_e was not constant, and it may change with time during sorption process. Therefore, a precise estimation of Q_e in pseudo-second-order kinetic model is needed.

Table 6.2 The adsorption kinetic parameters for Hg(II) adsorption on PVAm-SH

Adsorbent	T (K)	$Q_{e, exp}$ (mmol/g)	*Pseudo-first-order			*Pseudo-second-order		
			k_1 (min)$^{-1}$	$Q_{e, cal}$ (mmol/g)	R^2	k_2 (g/mmol·min)	$Q_{e, cal}$ (mmol/g)	R^2
PVAm-SH	298	0.264	0.0045	0.182	0.884	0.049	0.287	0.996
	308	0.370	0.0082	0.263	0.957	0.043	0.414	0.994
	318	0.421	0.0062	0.201	0.819	0.074	0.444	0.999
	328	0.455	0.0054	0.162	0.636	0.102	0.467	0.998
	338	0.518	0.0049	0.162	0.741	0.142	0.514	0.999

*The confidence bounds for the parameters are shown in the Appendix
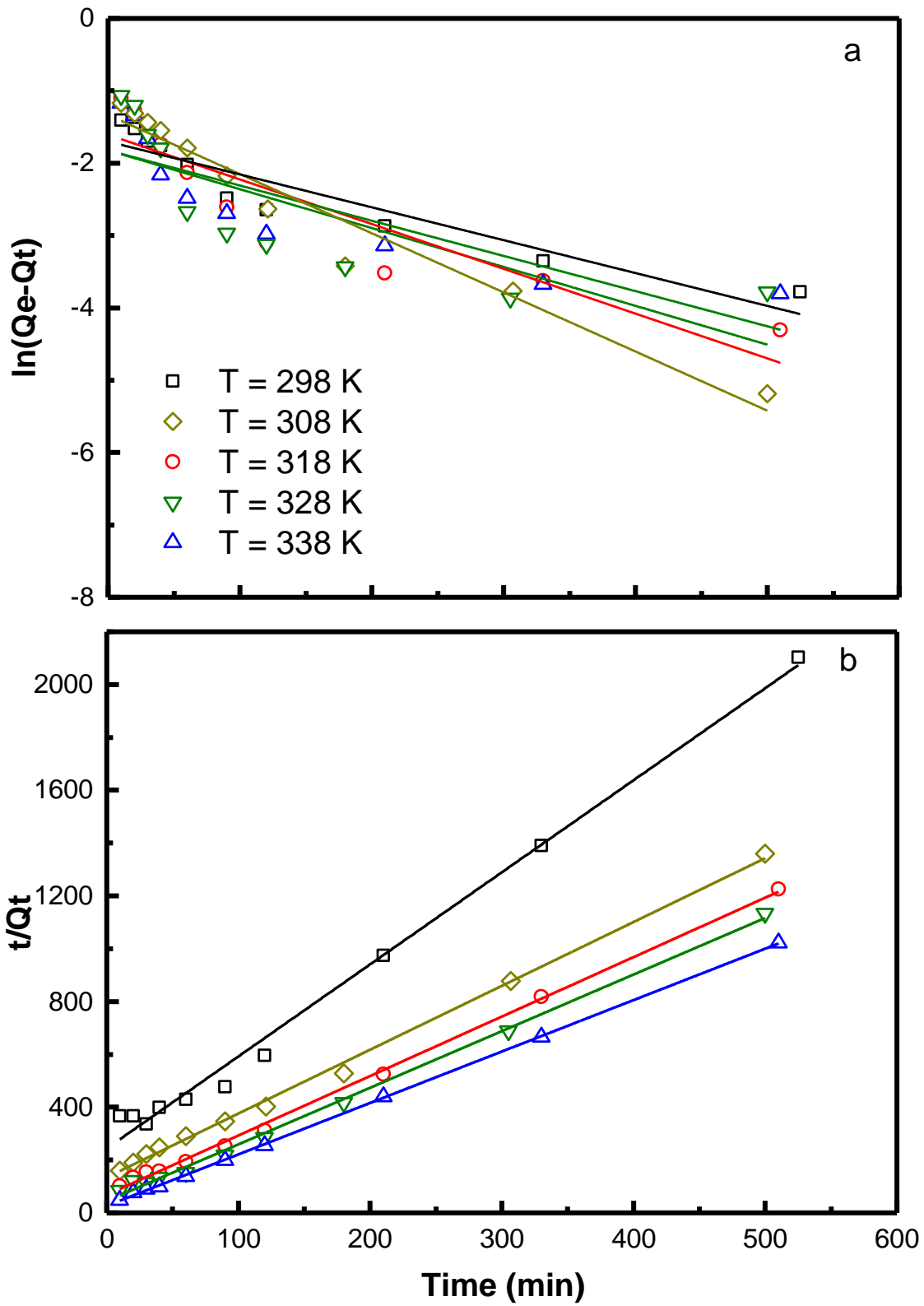
Figure 6.8 a) The pseudo-first- and b) pseudo-second-order kinetic models fitted to sorption data of Hg(II) adsorption on PVAm-SH

In fact, the term Q_e in equation (6.6) should be the equilibrium uptake corresponding to the instantaneous solute concentration at time t. It can be modified as a function of instantaneous solute concentration. For the Hg(II) adsorption on PVAm-SH, the relationship between Q_e and C_e can expressed by the Langmuir model:

$$Q_e = Q_m \frac{K_L C_e}{1 + K_L C_e} \tag{6.8}$$

The mass balance equation of a batch adsorption process gives:

$$Q_t = \frac{(C_0 - C)V}{M} \tag{6.9}$$

where Q_t is the uptake of Hg(II) at time t, M is the mass of PVAm-SH used, V is the volume of the aqueous solution, C_0 is the initial Hg(II) concentration and C is the instantaneous Hg(II) concentration. Equation (6.9) can be rearranged to:

$$C = C_0 - \frac{Q_t M}{V} \tag{6.10}$$

Because the uptake capacity at equilibrium Q_e should be related to the instantaneous Hg(II) concentration C at any time t, the term Q_e can be then calculated by combining equations (6.8) and (6.10):

$$Q_e = Q_m \frac{K_L \left(C_0 - \frac{Q_t M}{V}\right)}{1 + K_L \left(C_0 - \frac{Q_t M}{V}\right)} \tag{6.11}$$

By substituting equation (6.11) into equation (6.6), the pseudo-second-order equation can be modified as:

$$\frac{dQ_t}{dt} = k_2 (Q_m \frac{K_L(C_0 - \frac{Q_t M}{V})}{1 + K_L(C_0 - \frac{Q_t M}{V})} - Q_t)^2 \tag{6.12}$$

where the constant term Q_e in equation (6.6) is now substituted by a function of Q_t, changing as adsorption proceeds. Parameter Q_m and K_L can be determined by the equilibrium isotherm in section 6.3.3.
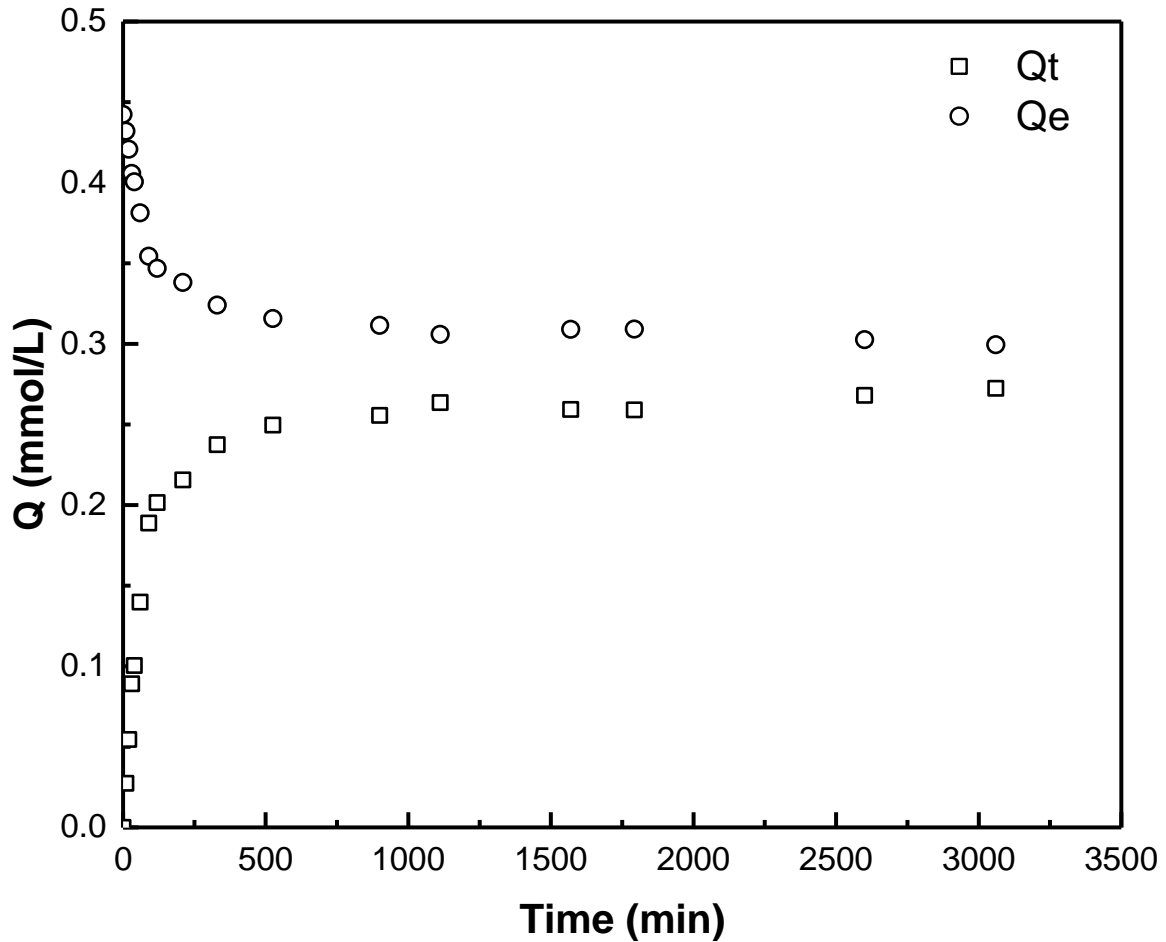
Figure 6.9 Illustration of instantaneous equilibrium uptake of Hg(II) Q_e (calculated from Langmuir model and mass balance) changing with time during sorption process. T = 25 ℃

Figure 6.9 shows how the term Q_e (calculated by the Langmuir model and mass balance) changes as adsorption proceeds. It decreases with an increase of time, and is always bigger than the Q_t. It is reasonable because the difference between Q_e and Q_t provides the driving force for the adsorption as described in the pseudo-second-order model. With the decrease of Q_e and the increase of Qt, the driving force will drop and the adsorption rate will level off. At

an infinite time t, both Q_e and Q_t will approach the same constant value, and the adsorption will finally stop.

By fitting the kinetic data to equation (6.12), the rate constant k_2 was recalculated by a numerical solution program developed in Matlab. To check the validity of the modified pseudo-second-order model, the fitting data was compared to the experimental data as shown in Figure 6.10. It shows that the fitting data regenerated from modified kinetic model seems to be in good agreement with the experimental data. The modified pseudo-second-order model works well to describe the kinetic data of Hg(II) adsorption onto PVAm-SH.
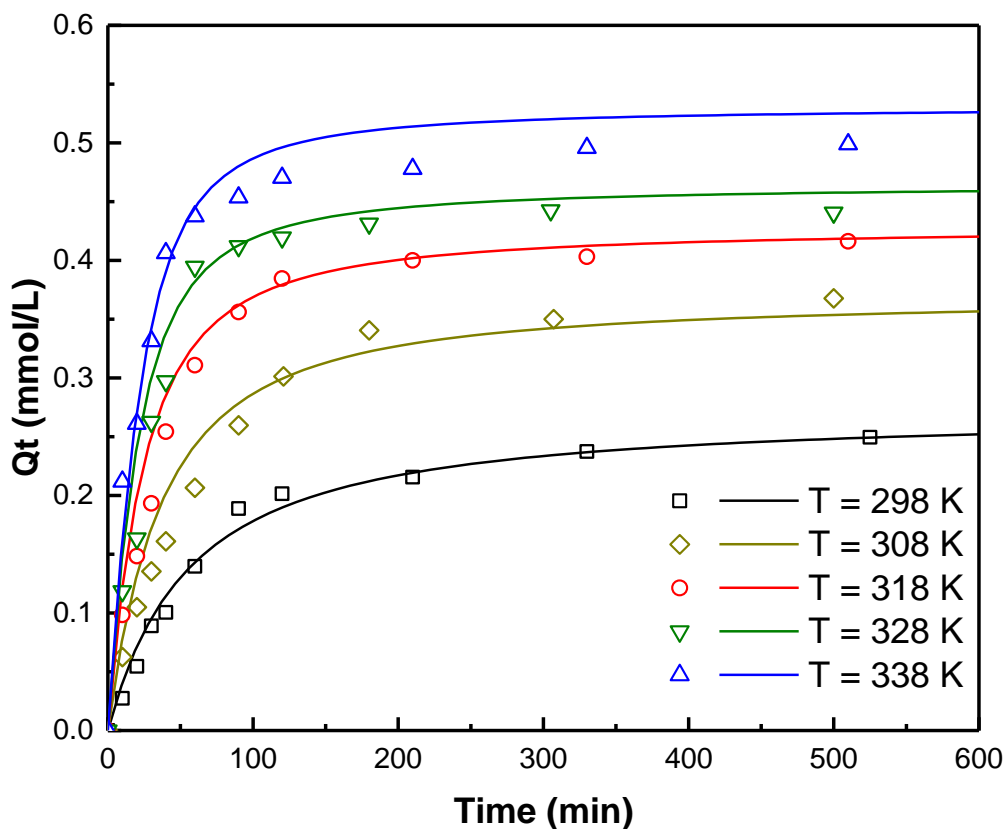
Figure 6.10 Comparison of experimental data (keys) for the Hg(II) adsorption on PVAm-SH with regenerated data (lines) from modified pseudo-second-order kinetic model.

Table 6.3 lists the recalculated rate constant $k_2{}^*$ for the Hg(II) sorption onto PVAm-SH from modified pseudo-second-order model. Comparing with the values calculated from the original pseudo-second-order model, $k_2{}^*$ calculated from the modified model is roughly 10 times lower. It is reasonable because the term Q_e assumed to be constant in the original pseudo-second-order model at the early stage of the adsorption, is actually changing with time and larger than the estimated constant value, which means that the driving force for Hg(II) sorption onto PVAm-SH is also underestimated in the original pseudo-second-order model. Thus, the underestimation of the driving force (i.e., the term $(Q_e - Q_t)$ in equation (6.6)) will be compensated by having a larger rate constant when the data is fitted by the original model.

Table 6.3 Recalculated rate constant $k_2{}^*$ for the Hg(II) sorption on PVAm-SH

Adsorbent	T (K)	Modified pseudo-second-order $k_2{}^*$ (g/mmol·min)	Pseudo-second-order k_2 (g/mmol·min)
PVAm-SH	298	0.0019	0.049
	308	0.0045	0.043
	318	0.0065	0.074
	328	0.0104	0.102
	338	0.0206	0.142

6.3.5 Thermodynamic estimations

The thermodynamic parameters involved in an adsorption process (i.e., ΔG°, ΔH°, and ΔS°) can provide additional information about the adsorption mechanism. However, the calculations of these parameters appear to be complicated because the physical meaning and numerical value of the equilibrium depends on the adsorption isotherm [Liu, 2009; Liu *et al.*, 2013]. Normally, for a Langmuir isotherm, the Gibbs free energy change (ΔG°) can be calculated as follows [Liu, 2009]:

$$\Delta G^\circ = -RT \ln K_a = -RT \ln \left[\frac{K_L}{\beta_e} \cdot (1 \; mol \cdot L^{-1}) \right] \tag{6.13}$$

where R is the gas constant, T is the absolute temperature, K_a is the adsorption equilibrium constant (dimensionless), K_L is the Langmuir equilibrium constant in unit of L·mol^{-1}, and β_e is the activity coefficient of the adsorbate in solution at the adsorption equilibrium. When the adsorbates are neutral or weakly charged ($\beta_e = 1$), equation (6.13) can be simplified to:

$$\Delta G° \approx -RT \ln[K_L \cdot (1\ mol \cdot L^{-1})] = -RT \ln K_L \tag{6.14}$$

In our study, the sorbate HgCl$_2$ is a covalent compound that exists mainly in molecular state, and only a very small amount may be dissociated into HgCl$^+$ and Cl$^-$ in aqueous solutions [Clever *et al.*, 1985]. In other words, HgCl$_2$ can be considered as a weakly charged adsorbate. Therefore, the $\Delta G°$ involved in Hg(II) adsorption on PVAm-SH can be reasonably calculated from the Langmuir equilibrium constant. The enthalpy change ($\Delta H°$) and the change in the standard entropy ($\Delta S°$) can also be determined from the van't Hoff equation [Argun *et al.*, 2007; Ma *et al.*, 2009]:

$$\ln K_L = \frac{\Delta S^0}{R} - \frac{\Delta H^0}{RT} \tag{6.15}$$

The plot result is shown in Figure 6.11 and the calculated thermodynamic parameters are listed in Table 6.4. The negative $\Delta G°$ values for Hg(II) adsorption on PVAm-SH indicates that the adsorption process is spontaneous, and the positive value of $\Delta H°$ indicates an endothermic adsorption process.
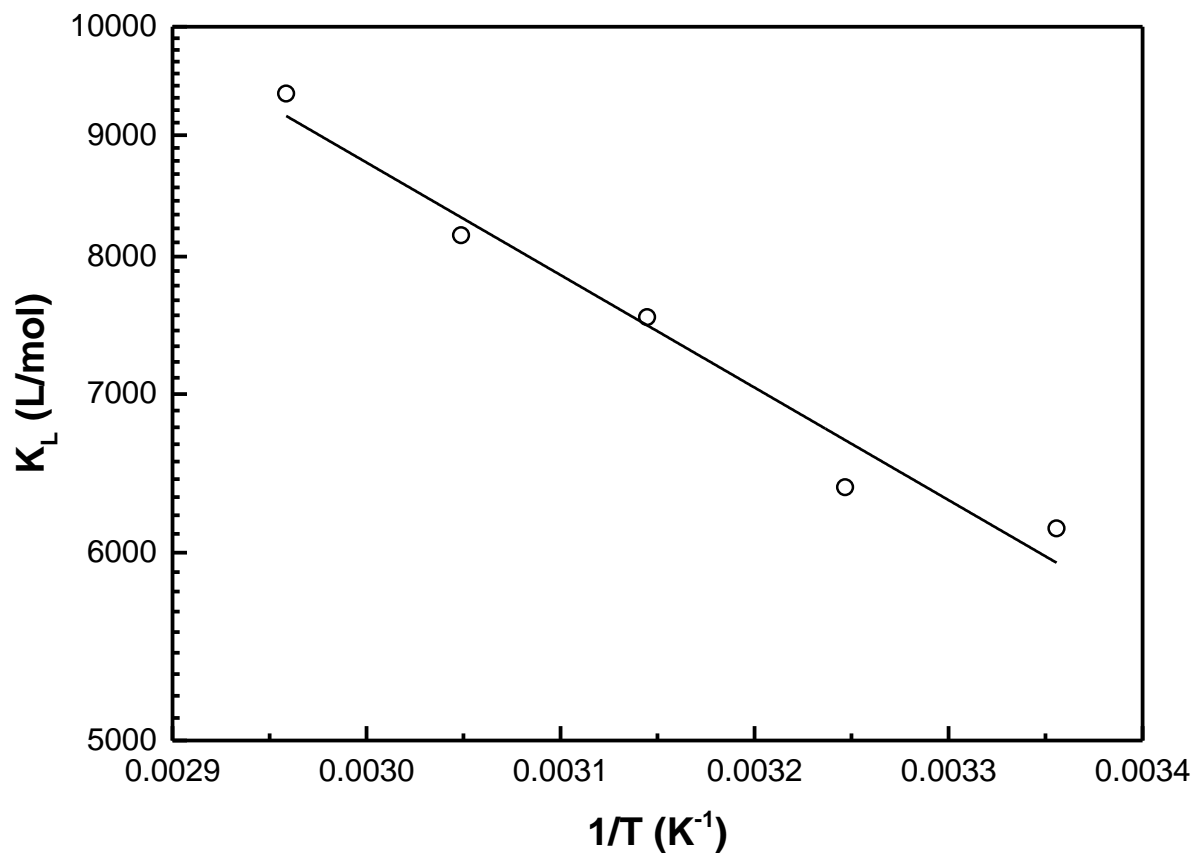
Figure 6.11 Plot of K_L in logarithmic scale v.s. $1/T$ for Hg(II) adsorption on PVAm-SH

Table 6.4 Thermodynamic parameters for Hg(II) adsorption on PVAm-SH based on K_L

Temperature (K)	$\Delta G\,°$(KJ mol^{-1})	$\Delta H\,°$(KJ mol^{-1})	$\Delta S\,°$(J mol^{-1} K^{-1})
298	-21.6		
308	-22.5		
318	-23.6	9.3	103.2
328	-24.6		
338	-25.7		

Activation energy for adsorption, which characterizes temperature dependence of adsorption rate can be calculated by using the Arrhenius equation [Al-Ghouti et al., 2005]:

$$\ln k = \ln A' - \frac{E_a}{RT} \tag{6.16}$$

where k is the adsorption rate constant, A' is the pre-exponential factor, and E_a is the activation energy of adsorption.

Figure 6.12 shows the Arrhenius plot for adsorption of Hg(II) on PVAm-SH. Both k_2^* (calculated by the modified pseudo-second-order model) and k_2 (calculated by the original pseudo-second-order model) were used for the plot. The activation energy E_a^* calculated by using k_2^* from the modified kinetic model was 46.97 kJ/mol, which is larger than 42 kJ/mol, suggesting that the adsorption of Hg(II) onto PVAm-SH is governed by chemical adsorption [Sharma and Das, 2013]. The process involves strong bonds between Hg(II) and amine or thiol groups corresponding with the analysis in adsorption isotherms and kinetics. It should be noted that the activation energy E_a calculated by using k_2 from the original kinetic model ($E_a = 24.51$ kJ/mol) is lower than 42 kJ/mol. This will lead to a wrong conclusion for the adsorption mechanism. It shows how important the accurate estimation of rate constant is, and also further proves that the modified pseudo-second-order kinetic model well describes the adsorption kinetics of Hg(II) sorption onto PVAm-SH.
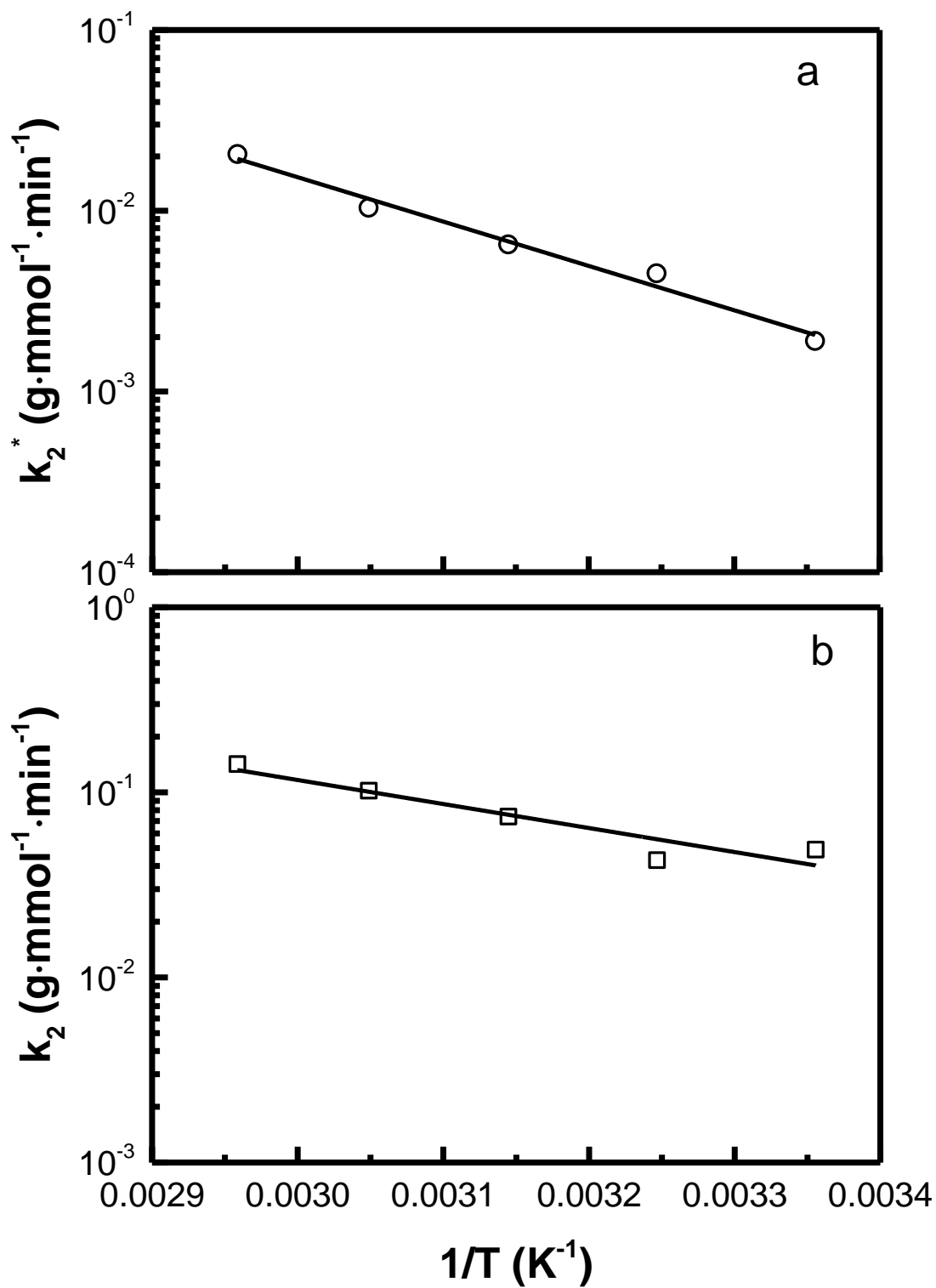
Figure 6.12 Semi-log plot of a) k_2^* (calculated by the modified pseudo-second-order kinetic model) and b) k_2 (calculated by the original pseudo-second-order kinetic model) v.s. $1/T$ for Hg(II) adsorption on PVAm-SH

6.3.6 Effects of pH and other water constituents on mercury sorption

The effects of solution pH and water constituents on mercury adsorption must be taken into consideration because they are important parameters in water effluents. Three common salts with different concentrations and a wide pH range were investigated in this study, and the results are shown in Figures 6.13 and 6.14.
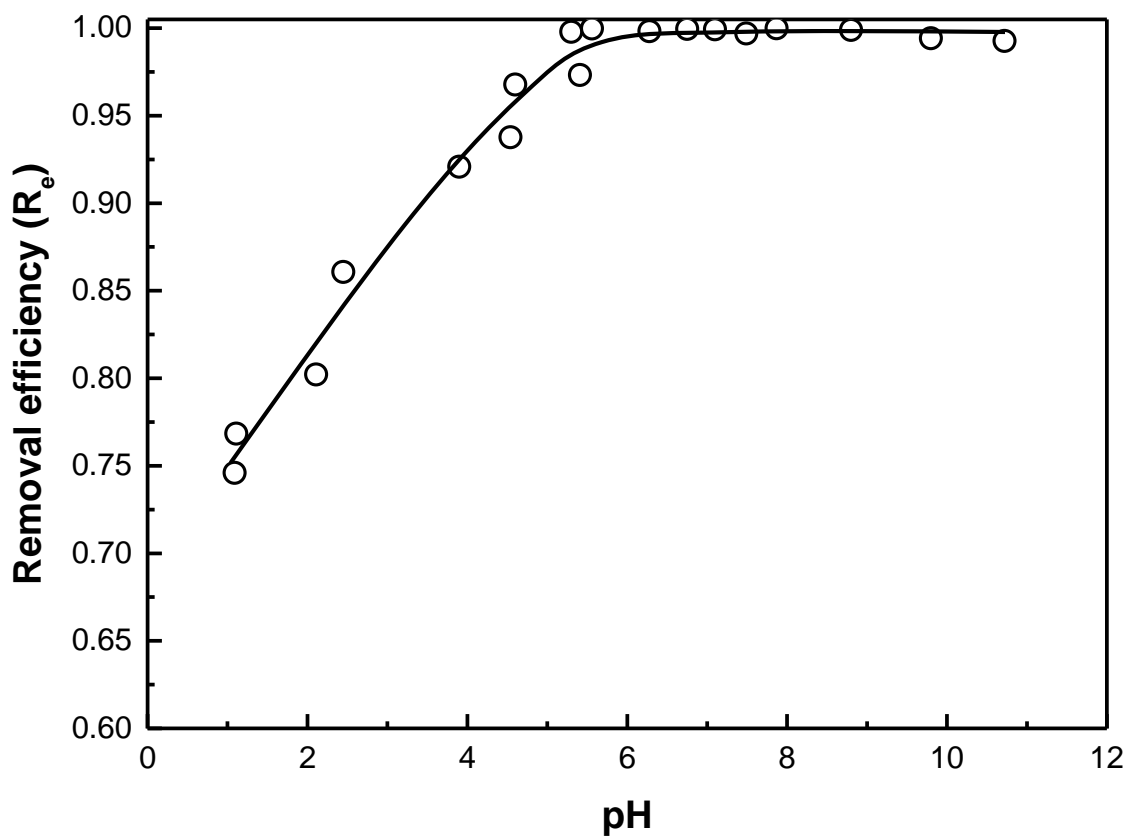
Figure 6.13 Effect of solution pH on mercury removal by PVAm-SH. Initial concentration of mercury: 83.7 ppm; PVAm-SH dosage: 1.67 g/L; pH adjusted by HCl and NaOH.

Figure 6.13 shows that acidic environment can inhibit mercury adsorption onto PVAm-SH. With an increase in the solution pH, the removal efficiency of mercury increases and then level-off after a pH of 5.5. At alkaline conditions, the protonated thiol groups on the polymer adsorbent may react with the excess amount of OH⁻, yielding a negatively charged surface.

The negative PVAm-S⁻ is more favorable for mercury binding to form stable complexes. This is consistent with the study by Li *et al.* [UNEP], who found that mercury adsorption by thiol-functionalized activated coke also increased with the solution pH. It should be pointed out that even at a strong acidic pH (i.e., pH = 1), the sorbent is still quite effective to adsorb mercury, with a removal efficiency of 75%. This reveals the high affinity of mercury towards thiol groups in PVAm-SH, which is desirable for mercury removal, but it may also impose difficulty for the desorption of mercury from PVAm-SH for sorbent regeneration.
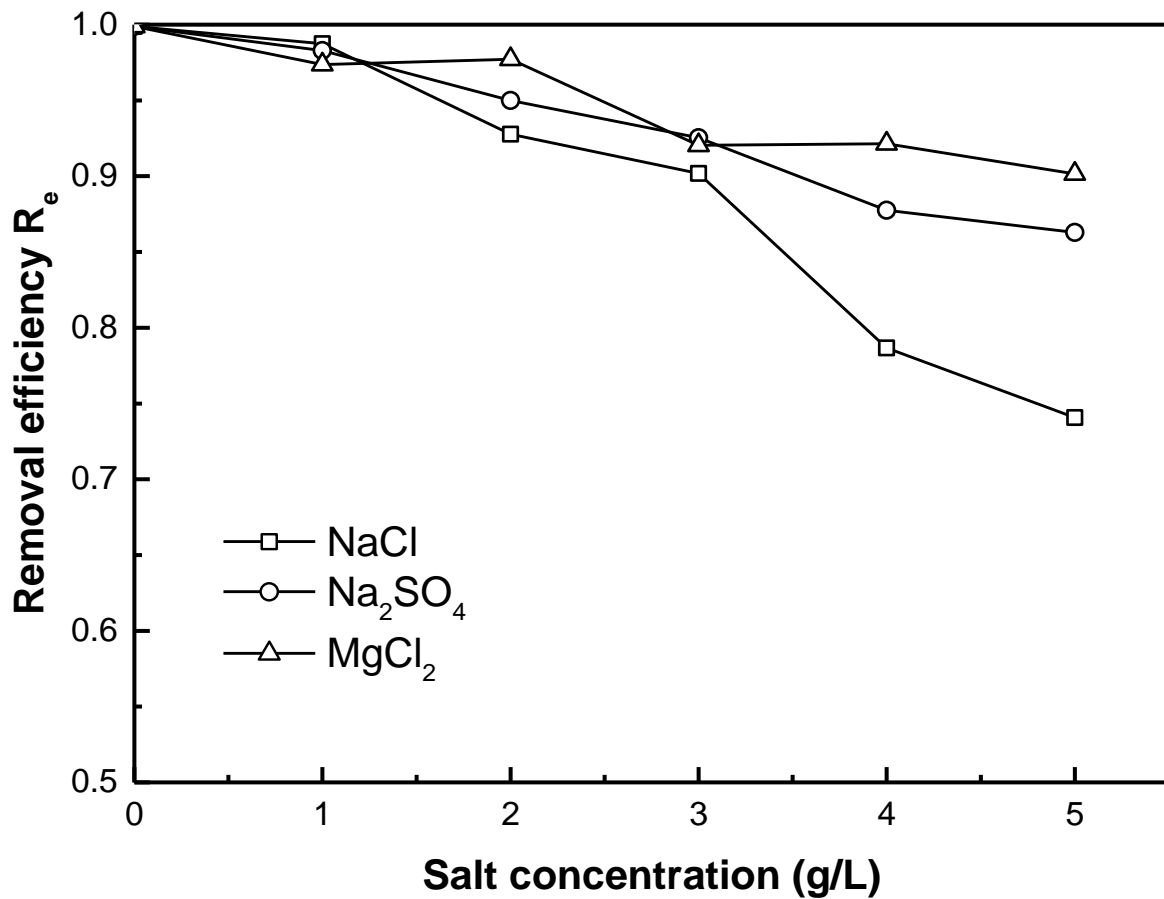
Figure 6.14 Mercury removal by PVAm-SH when other salts are present in water. Initial concentration of mercury: 20.5 ppm; PVAm-SH dosage: 0.5 g/L.

As shown in Figure 6.14, the presence of the salt in the aqueous solutions inhibited Hg(II) adsorption, and NaCl has the most pronounced effect on mercury sorption. However, the mercury removal efficiency decreased to 75% at a NaCl concentration as high as 5 g/L. This further indicates the strong interactions between Hg(II) and thiol groups. Thus, PVAm-SH can be used as an Hg(II) adsorbent for wastewater that contains other inorganic salts.

6.3.7 Desorption study

Because of the very strong affinity between thiol groups and Hg(II) in aqueous solutions, a strong aggressive extracting reagent may be needed for the Hg(II) desorption. Thiourea, which is another sulfur-containing compound, has been used to desorb Hg(II) from thiol functionalized adsorbents [Andaç *et al.*, 2007; Pillay *et al.*, 2013]. Thus, thiourea in a strong acid was used as the stripping agent to desorb mercury in this study.

Four adsorption-desorption cycles were conducted to investigate the reusability of PVAm-SH for Hg(II) removal. As shown in Figure 6.15, mercury desorption with thiourea worked well. Hg(II) desorbs readily from the Hg-loaded PVAm-SH when washed with 0.5% thiourea in 0.5 M HCl. The mercury removal efficiency remained above 95% after 4 cycles. Thiourea with sulfur and nitrogen center can compete with thiol groups and displace Hg(II) from the surface of PVAm-SH adsorbent. The PVAm-SH also retained its structural integrity throughout the test cycles, suggesting a potential long lifetime of this polymer adsorbent.
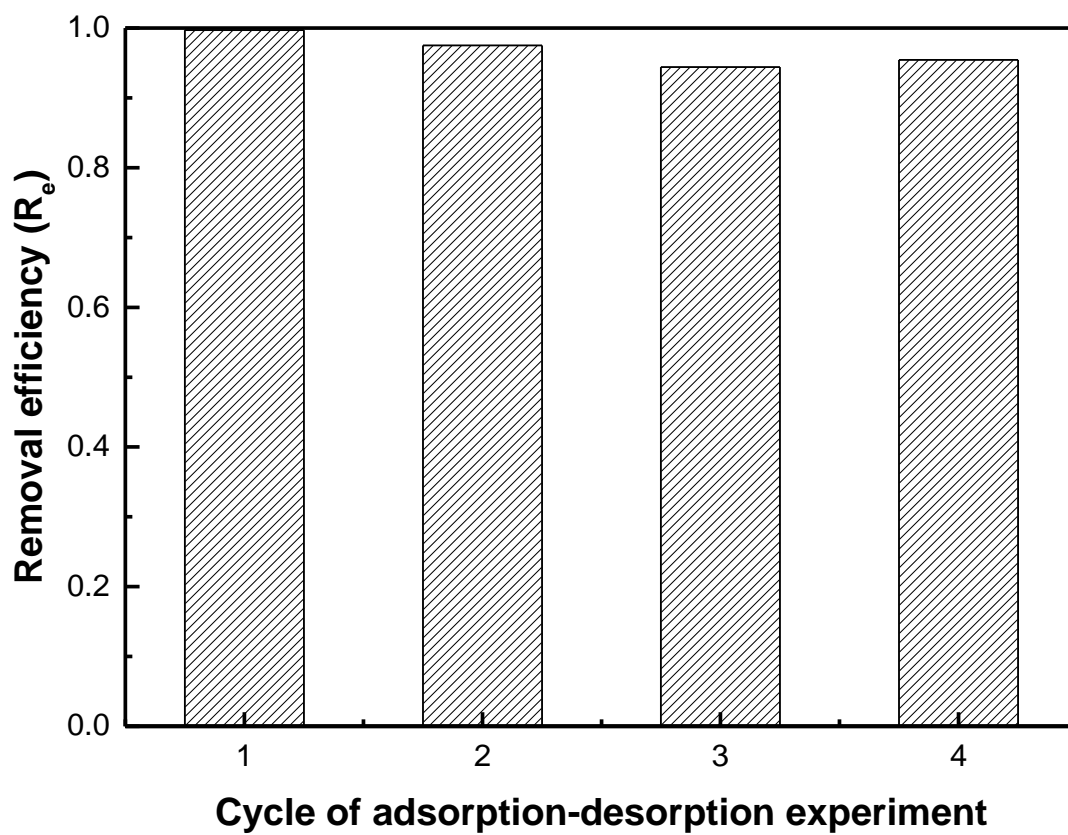
Figure 6.15 Hg(II) adsorption efficiency on PVAm-SH after several adsorption-desorption cycles. Initial Hg(II) concentration: 22.2 ppm, PVAm-SH dosage: 0.5 g/L.

6.4 Conclusions

Thiol functional groups were successfully grafted onto PVAm chains by taking advantage of the high reactivity of primary amine groups. The thiol-functionalization PVAm was confirmed by FTIR and UV analysis. The synthesized PVAm-SH showed a good adsorption capability for Hg(II) in aqueous solutions. Adsorption isotherms of Hg(II) onto PVAm-SH followed a Langmuir model, and the adsorption capacity increased from 0.797 mmol/g at 298 K to 4.56 mmol/g at 338 K. The sorption kinetics followed a modified pseudo-second-order model, and the adsorption process was shown to be endothermic. PVAm-SH was shown to work well for mercury removal from water, even over a broad range of solution pH and in the presence of other salts. Thiourea was found to be a good desorbing reagent for regeneration and reuse of the polymeric adsorbent. It can be concluded that PVAm-SH was a promising adsorbent for Hg(II) removal from wastewater.

Chapter 7

General Conclusions, Contributions and Recommendations

7.1 General conclusions

The application of water-soluble PVAm for heavy metal removal from wastewater by PEUF and adsorption were studied. The following general conclusions can be drawn from this research:

1. Using PVAm as a chelating agent in PEUF, the rejection of Pb(II), Cu(II), and Fe(III) reached 99%, 97%, and 99% respectively at a relatively low concentration of PVAm (0.1wt%). Increasing PVAm dosage in the feed would enhance the metal rejection, but the flux would decrease. The transmembrane pressure and temperature had little effect on the metal rejection in the range tested, but the permeation flux was influenced significantly. The metal rejection in PEUF was highly related to the coordination properties between the metals and PVAm.

2. Sulfate anions with a sufficiently high concentration in the solution would induce the precipitation of PVAm-metal complexes presumably by ionic cross-linking of PVAm. The concentrations of both PVAm and sulfate anions affected the formation of precipitates. The precipitation resulted in two phases in the PVAm-heavy metal aqueous system in a similar fashion as in flocculation. The water-soluble PVAm appeared to be suitable for use in the two different separation processes for heavy metal removal.

178

3. Removal of Hg(II) from aqueous solution using PVAm-enhanced ultrafiltration was investigated. A Hg(II) rejection as high as 99% was achieved, which was otherwise impossible with a conventional UF membrane process in the absence of PVAm. Due to the macromolecular nature of the PVAm "solutes" in the feed solution, a typical flux vs pressure relationship was observed, which appeared to follow the concentration polarization and gel layer formation model. Periodic cleaning of the membrane surface with dilute hydrochloric acid was effective to recover the membrane permeability, but the flux that declines over time due to membrane fouling remained an issue to be resolved for practical applications. Mercury removal with the PEUF was also tested with a simulated chlor-alkali wastewater where other chemicals (i.e., sodium chloride and sulphate) were present as well, and the composition of the feed solution was shown to affect the performance for mercury removal.

4. Besides PVAm, PEI and PAA were also studied for use in PEUF for removal of Hg(II) from aqueous solutions. PVAm showed the best performance in separating Hg(II) from water. A set of equations representing permeate flux as a function of feed polymer concentration was obtained experimentally. Membrane fouling in PEUF with PVAm and PEI in cross-flow mode at a relatively low polymer concentration was negligible, whereas there was a considerable membrane fouling when PAA was used in the PEUF. Batch operation of PEUF process was modelled using a set of equations for heavy metal separation by the PEUF technique, and the model predictions were validated with experimental data.

5. Chemical modification of PVAm was carried out via grafting with thiol groups, making use of the high reactivity of primary amines in PVAm. The thiol-grafted PVAm (i.e.,

PVAm-SH) was insoluble in water and showed favorable sorption properties for Hg(II) in aqueous solutions. Adsorption isotherms of Hg(II) onto PVAm-SH followed a Langmuir model, and the sorption kinetics could be described by the pseudo-second-order model. Hg(II) adsorption onto PVAm-SH was shown to be a spontaneous and endothermic process. The PVAm-SH adsorbent worked well for Hg(II) sorption over a broad range of solution pH and in the presence of other salts in water due to strong specific affinity of thiol groups towards Hg(II). Thiourea was found to be a good desorbing reagent for regeneration and reuse of PVAm-SH in Hg(II) removal.

7.2 Contributions to original research

1. The feasibility of using PVAm as a chelating agent in PEUF for heavy metal removal from wastewater was studied in this thesis. The interactions between PVAm and heavy metals determined the metal removal efficiency of the PEUF process. In addition, to our knowledge, precipitation of PVAm-metal complexes caused by divalent sulfate anions was observed for the first time, and its potential use as a flocculant for metal removal along with PEUF was identified.

2. The recovery of Hg(II) from aqueous solutions by PEUF was investigated. The PVAm showed superior performance in removing Hg(II) from wastewater by PEUF, making it a promising alternative to solve the mercury pollution problem. A set of mathematical equations modelling the batch operation of PUEF was developed, and the applicability of the model was validated with experimental data. The mechanism of membrane fouling caused by the water-soluble polymer itself in PEUF process as well as its influence on the batch modelling was analyzed in this thesis.

3. A new PVAm derivative bearing thiol groups was successfully synthesized by the amide formation reaction. This PVAm derivative showed good adsorption capability towards Hg(II) in aqueous solutions, and its potential use as an adsorbent for Hg(II) removal from wastewater was demonstrated through sorption equilibrium and kinetics studies.

7.3 Recommendations for future work

1. PVAm showed good performance for removal of heavy metals from wastewater by PEUF process. In addition to the heavy metals, organic contaminants in wastewater are a further concern nowadays. Organic compound removal by PEUF using PEI and PAA as binding agents has been investigated [Dasgupta *et al*., 2014]. Such organic contaminants as dyes, phenols, and organic acids exhibited strong interactions with many water-soluble polymers, though the mechanism is still not very clear. Thus, it is expected that the PVAm used in this thesis work is also suitable for separating organic contaminants from wastewater by PEUF process.

2. Molecular weight and molecular weight distribution of the soluble polymers may also affect the performance of PEUF process. The feed solution with a water-soluble polymer of large molecular weight may have high viscosity, and thus make the permeation flux decrease. It is thus suggested that the PVAm with lower molecular weight but still larger than the MWCO of the UF membrane could be used in the future in order to improve the water production.

3. It has been shown that the design of membrane module and fluid management within that module affect the performance of PVAm-enhanced ultrafiltration for heavy metal removal. Although the theory of conventional UF for each configuration is well established, an

optimum design for specific applications of PEUF is yet to be investigated in light of the polymers and polymer-metal complexes involved in the process. Therefore, it is highly necessary to investigate the performance of different UF membrane configurations for PEUF process. There are basically four configurations for UF membranes in industrial applications: plate-and-frame, spiral wound, tubular, and hollow fiber modules. To select a proper membrane module, various aspects of the process including membrane fouling and cleaning, replacement and maintenance must be considered to make the process commercially viable and competitive.

4. The use of water-soluble polymer in the PEUF process is an important consideration. It is helpful to regenerate the used polymer to minimize production of secondary waste from the PEUF process. According to the previous research, one of the feasible methods for polymer regeneration is adding proper chemical reagents to strip the bonded metals from the polymer in the concentrated solution and to remove the unbounded metals by a subsequent UF process, thereby regenerating the polymer for reuse. The amine-based PVAm-metal complexes can be broken down by acids or strong chelating agents (e.g., ethylenediaminetetraacetic acid and nitrilotriacetic acid), and this is a possible approach for PVAm regeneration.

5. In addition to the polymer regeneration, the reuse of the captured heavy metals from wastewater as a new resource is another subject of study with regards to the overall process economics and environmental friendliness. Many of the heavy metals in wastewater are highly valuable. Up to date, one of the best metal recovery techniques in terms of economics and operability is the electrochemical process. For instance, copper has been successfully recovered from PEI-Cu(II) complexes by electrodeposition using a batch

rotating-electrode electrochemical cell. It is thus recommended to investigate the recovery of heavy metals from the concentrated PVAm metal complexes in the PEUF process for heavy metal removal from wastewater.

6. The synthesized thiol-grafted PVAm is insoluble in water and is thus not suitable for PEUF process, it shows excellent adsorption capacity towards Hg(II). The strong affinity between thiol groups and Hg(II) makes PVAm-SH an efficient adsorbent for Hg(II), especially at low mercury concentrations commonly encountered in wastewater. This suggests that the permeate solution from the PEUF process can be further treated by the PVAm-SH adsorbent. It will be of interest to study the combination of these two separation processes (i.e., PEUF and adsorption), thereby improving the overall process performance.

References

Aimar, P., C. Taddei, J.P. Lafaille and V. Sanchez, Mass transfer limitations during ultrafiltration of cheese whey with inorganic membranes, *J. Membrane Sci.* 38 (1988) 203-221.

Al-Ghouti, M., M.A.M. Khraisheh, M.N.M. Ahmad and S. Allen, Thermodynamic behaviour and the effect of temperature on the removal of dyes from aqueous solution using modified diatomite: A kinetic study, *J. Colloid Interf. Sci.* 287(1) (2005) 6-13.

Algarra, M., M.I. Vázquez, B. Alonso, C.M. Casado, J. Casado and J. Benavente, Characterization of an engineered cellulose based membrane by thiol dendrimer for heavy metals removal, *Chem. Eng. J.* 253 (2014) 472-477.

Almutairi F.M., Williams P.M. and L.R.W., Effect of membrane surface charge on filtration of heavy metal ions in the presence and absence of polyethylenimine, *Desalin. Water Treat.* 42(1-3) (2012) 131-137.

Andaç, M., S. Mirel, S. Şenel, R. Say, A. Ersöz and A. Denizli, Ion-imprinted beads for molecular recognition based mercury removal from human serum, *Int. J. Biol. Macromol.* 40(2) (2007) 159-166.

Argun, M.E., S. Dursun, C. Ozdemir and M. Karatas, Heavy metal adsorption by modified oak sawdust: thermodynamics and kinetics, *J. Hazard. Mater.* 141(1) (2007) 77-85.

Aroua, M.K., F.M. Zuki and N.M. Sulaiman, Removal of chromium ions from aqueous solutions by polymer-enhanced ultrafiltration, *J. Hazard. Mater.* 147(3) (2007) 752-758.

Ba, C., J. Langer and J. Economy, Chemical modification of P84 copolyimide membranes by polyethylenimine for nanofiltration, *J. Membrane Sci.* 327(1-2) (2009) 49-58.

Barakat, M.A. and E. Schmidt, Polymer-enhanced ultrafiltration process for heavy metals removal from industrial wastewater, *Desalination* 256(1-3) (2010) 90-93.

Barat, J.L. and J.F. Joanny, Theory of polyelectrolyte solutions, I. Prigogine and S. Rice (Eds.), *Advances in Chemical Physics: Polymer Systems*, John Wiley, New York, 94**,** (1996) 1-66.

Barron-Zambrano, J., S. Laborie, P. Viers, M. Rakib and G. Durand, Mercury removal and recovery from aqueous solutions by coupled complexation–ultrafiltration and electrolysis, *J. Membrane Sci.* 229(1-2) (2004) 179-186.

Batley, G.E. and T.M. Florence, A novel scheme for the classification of heavy metal species in natural waters, *Anal. Lett.* 9(4) (1976) 379-388.

Bayer, E., K. Geckeler and K. Weingartner, Preparation and derivatization of linear polyvinylamine for selective complex formation in homogeneous phase, *Makromol. Chem.* 181 (1980) 585-593.

Bayer, E., B.Y. Spivakov and K. Geckeler, Poly(ethyleneimine) as complexing agent for separation of metal ions using membrane filtration, *Polym. Bull.* 13 (1985) 307-311.

Beolchini, F., F. Pagnanelli, I.D. Michelis and F. Veglio, Micellar enhanced ultrafiltation for arsenic (V) removal: effect of main operating conditions and dynamic modelling, *Environ. Sci. Technol.* 40 (2006) 2746-2752.

Bessboussea, H., J.F. Verchèrea and L. Lebruna, Characterisation of metal-complexing membranes prepared by the semi-interpenetrating polymer networks technique. Application to the removal of heavy metal ions from aqueous solutions, *Chem. Eng. J.* 187 (2012) 16-28.

Bitter, J.G.A., *Transport Mechanisms in Membrane Separation Processes*, Plenum Press, New York, (1991).

Bodnar, M., I. Hajdu, E. Rőthi, N. Harmati, Z. Csikos, J.F. Hartmann, C. Balogh, B. Kelemen, J. Tamas and J. Borbely, Biopolymer-based nanosystem for ferric ion Removal from Water, *Sep. and Purif. Technol.* 112 (2013) 26-33.

Bolto, B.A., Soluble polymers in water purification, *Prog. Polym. Sci.* 20 (1995) 987-1041.

Borbély, G. and E. Nagy, Removal of zinc and nickel ions by complexation–membrane filtration process from industrial wastewater, *Desalination* 240(1-3) (2009) 218-226.

Bouchard, R.C., P.J. Carreau, T. Matsuura and S. Sourirajan, Modeling of ultrafiltration predictions of concentration polarization effects, *J. Membrane Sci.* 97 (1994) 215-229.

Brant, J.A. and A.E. Childress, Assessing short-range membrane–colloid interactions using surface energetics, *J. Membrane Sci.* 203(1–2) (2002) 257-273.

Bryjak, M. and I. Gancarz, Plasma treatment of polyethylene ultrafiltration membrane, *Angew. Makromolek. Chem.* 219 (1994) 117-124.

Cai, J.H. and C.Q. Jia, Mercury Removal from Aqueous Solution Using Coke-Derived Sulfur-Impregnated Activated Carbons, *Ind. Eng. Chem. Res.* 49(6) (2010) 2716-2721.

Camarillo, R., Á. Pérez, P. Cañizares and A. de Lucas, Removal of heavy metal ions by polymer enhanced ultrafiltration: Batch process modeling and thermodynamics of complexation reactions, *Desalination* 286 (2012) 193-199.

Cañizares, P., A.d. Lucas, Á. Pérez and R. Camarillo, Effect of polymer nature and hydrodynamic conditions on a process of polymer enhanced ultrafiltration, *J. Membrane Sci.* 253(1-2) (2005) 149-163.

Canizares, P., A. Perez, R. Camarillo and J.J. Linares, A semi-continuous laboratory-scale polymer enhanced ultrafiltration process for the recovery of cadmium and lead from aqueous effluents, *J. Membrane Sci.* 240(1-2) (2004) 197-209.

Cañizares, P., A. Pérez, R. Camarillo and R. Mazarro, Simultaneous recovery of cadmium and lead from aqueous effluents by a semi-continuous laboratory-scale polymer enhanced ultrafiltration process, *J. Membrane S.* 320(1-2) (2008) 520-527.

Canstein, H.V., Y. Li, K.N. Timmis, W.-D. Deckwer and I. Wagner-Dobler, Removal of mercury from chloralkali electrolysis wastewater by a mercury-resistant pseudomonas putida strain, *Appl. Environ. Microb.* 65(12) (1999) 5297-5284.

Celik, E., L. Liu and H. Choi, Protein fouling behavior of carbon nanotube/polyethersulfone composite membranes during water filtration, *Water Res.* 45(16) (2011) 5287-5294.

Chaturvedi, B.K., A.K. Ghosh, V. Ramachandhran, M.K. Trivedi, M.S. Hanra and B.M. Misra, Preparation, characterization and performance of polyethersulfone ultrafiltration membranes, *Desalination* 133 (2001) 31-40.

Chaufer, B. and A. Deratani, Removal of metal ions by complexation-ultrafiltration using water-soluble macromolecules: perspective of application to wastewater treatment *Nucl. Chem. Waste. Man.* 8 (1988) 175-187.

Chiron, N., R. Guilet and E. Deydier, Adsorption of Cu(II) and Pb(II) onto a grafted silica: isotherms and kinetic models, *Water Res.* 37(13) (2003) 3079-3086.

Clever, H.L., S.A. Johnson and M.E. Derrick, The solubility of mercury and some sparingly soluble mercury salts in water and aqueous electrolyte solutions, *J. Phys. Chem. Ref. Data* 14(3) (1985) 631-680.

Cojocaru, C., G. Zakrzewska-Trznadel and A. Miskiewicz, Removal of cobalt ions from aqueous solutions by polymer assisted ultrafiltration using experimental design approach: part 2: Optimization of hydrodynamic conditions for a crossflow ultrafiltration module with rotating part, *J. Hazard. Mater.* 169(1-3) (2009) 610-620.

Connolly, S., S.N. Rao and D. Fitzmaurice, Characterization of protein aggregared gold nanocrystals, *J. Phys. Chem. B* 104 (2000) 4765-4776.

Dabrowski, A., Z. Hubicki, P. Podkoscielny and E. Robens, Selective removal of the heavy metal ions from waters and industrial wastewaters by ion-exchange method, *Chemosphere* 56(2) (2004) 91-106.

Das, S.K., A.R. Das and A.K. Guha, A study on the adsorption mechanism of mercury on Aspergillus versicolor biomass, *Environ. Sci. Technol.* 41 (2007) 8281-8287.

Dasgupta, J., M. Singh, J. Sikder, V. Padarthi, S. Chakraborty and S. Curcio, Response surface-optimized removal of Reactive Red 120 dye from its aqueous solution using polyethyleneimine enhanced ultrafiltration, *Ecotox. Environ. Safe.* 121 (2014) 271-278

Daufin, G., F. Rene and P. Aimar, *Les séparations par membrane dans les procédés de l'industrie alimentaire*, Technique & Documentation, Paris, (1998).

De, S. and S. Mondal, *Micellar Enhanced Ultrafiltration: Fundamentals & Applications*, CRC Press, (2013).

Denisov, G.A., Theory of concentration polarization in cross-flow ultrafiltration gel-layer model and osmotic-pressure model, *J. Membrane Sci.* 91(1-2) (1994) 173-187.

Di Natale, F., A. Erto, A. Lancia and D. Musmarra, Mercury adsorption on granular activated carbon in aqueous solutions containing nitrates and chlorides, *J. Hazard. Mater.* 192(3) (2011) 1842-1850.

Dilek, Ç., H.Ö. Özbelge, N. Biçak and L. Yılmaz, Removal of boron from aqueous solutions by continuous polymer-enhanced ultrafiltration with polyvinyl alcohol, *Separ. Sci. Technol.* 37(6) (2002) 1257-1271.

Doğanay, C.O., H.Ö. Özbelge, N. Bıçak, N. Aydoğan and L. Yılmaz, Use of specifically tailored chelating polymers for boron removal from aqueous solutions by polymer enhanced ultrafiltration, *Separ. Sci. Technol.* 46(4) (2011) 581-591.

Driscoll, C.T., R.P. Mason, H.M. Chan, D.J. Jacob and N. Pirrone, Mercury as a global pollutant: sources, pathways, and effects, *Environ. Sci. Technol.* 47(10) (2013) 4967-4983.

El-Abbassi, A., M. Khayet and A. Hafidi, Micellar enhanced ultrafiltration process for the treatment of olive mill wastewater, *Water Res.* 45(15) (2011) 4522-4530.

Evans, D.R.H., J.K. Romero and M. Westoby, Concentration of proteins and removal of solutes, R. R. Burgess and M. P. Deutscher, *Methods in Enzymology*, Acdemic Press, 463, (2009) 97-120.

Fane, A.G., C.Y. Tang and R. Wang, Membrane technology for water: microfiltation, ultrafiltration, nanofiltration, and reverse osmosis, K. Hanaki and T. Vereijken (Eds.), *Treatise on Water Science*, Elsevier, Singapore, 4**,** (2011) 301-335.

Feng, X. and R.Y.M. Huang, Separation of isopropanol from water by pervaporation using silicone-based membranes, *J. Membrane Sci.* 74 (1992) 171-181.

Fillipi, B.R., L.W. Brant, J.F. Scamehorn and S.D. Christian, Use of micellar-enhanced ultrafiltration at low surfactant concentrations and with anionic–nonionic surfactant mixtures, *J. Colloid Interf. Sci.* 213 (1999) 68-80.

Fu, F. and Q. Wang, Removal of heavy metal ions from wastewaters: a review, *J. Environ. Manage.* 92(3) (2011) 407-418.

Gallo, D., E.J. Acosta, J.F. Scamehorn and D.A. Sabatini, Pilot-scale study of polyelectrolyte enhanced UF for arsenic removal, *J. Am. Water Works Ass.* 98(1) (2006) 106.

Gao, G., Y. Wei and Y. Qiu, Treatment of wastewater containing nickel ions by polymer enhanced ultrafiltration with copolymer of acrylilc acid-maleic acid, *J. Cent. South Univ. T.* 43(1) (2012) 54-58.

Geckeler, K., G. Lange, H. Eberhardt and E. Bayer, Preparation and application of water-soluble polymer-metal complexes, *Pure Appl. Chem.* 52 (1980) 1883-1905.

Geckeler, K.E., E. Bayer, B.Y. Spivakov, V.M. Shkinev and G.A. Vorob'eva, Liquid-phase polymer-based retention: a new method for separation and preconcentration of elements *Anal. Chim. Acta.* 189 (1986) 285-292.

Geckeler, K.E., B.L. Rivas and R. Zhou, Poly[1-(2-hydroxyethyl) aziridine] as polychelatogen for liquid-phase polymer-based retenntion, *Angew. Makromolek. Chem.* 193 (1991) 195-203.

Geckeler, K.E. and K. Volchek, Removal of hazardous substances from water using ultrafiltration in conjunction with soluble polymers, *Eviron. Sci. Technol.* 30(3) (1996) 725-734.

Geckeler, K.E., R. Zhou and B.L. Rivas, Metal complexation of poly[1-(2-hydroxyethyl)aziridine-co-2-methyl-2-oxazoline] in aqueous solution, *Angew. Makromolek. Chem.* 197 (1992) 107-115.

Geng, X. and D.M. Zebolsky, The Stoichiometric Displacement Model and Langmuir and Freundlich Adsorption, *J. Chem. Educ.* 79(3) (2002) 385.

Ghosh, R., Ultrafiltration-based protein bioseparation, A.K. Pabby, S.S.H. Rizvi and A.M. Sastre (Eds.), *Handbook of Membrane Separations*, CRC Press, (2009) 497-512.

Gilron, J. and D. Hasson, Calcium sulphate fouling of reverse osmosis membranes: flux decline mechanism, *Chem. Eng. Sci.* 42(10) (1987) 2351-2360.

Gispert, J.R., *Coordination Chemistry*, WILEY-VCH, (2008).

Golovanov, V.I., V.M. Shkinev, B.Y. Spivakov, K.E. Geckeler and E. Bayer, Mathematical description of metal retention with water-soluble polymers during membrane filtration, *Separ. Sci. Technol.* 28(10) (1993) 1887-1898.

Goosen, M.F.A., S.S. Sablani and R. Roque-Malherbe, Membrane fouling: recent strategies and methodologies for its minimization, A. K. Pabby, S. S. H. Rizvi and A. M. Sastre (Eds.), *Handbook of Membrane Separations*, CRC Press, (2009) 325-341.

Hadi, P., M.-H. To, C.-W. Hui, C.S.K. Lin and G. McKay, Aqueous mercury adsorption by activated carbons, *Water Res.* 73(0) (2015) 37-55.

Hajdu, I., M. Bodnár, Z. Csikós, S. Wei, L. Daróczi, B. Kovács, Z. Győri, J. Tamás and J. Borbély, Combined nano-membrane technology for removal of lead ions, *J. Membrane Sci.* 409-410 (2012) 44-53.

Hanemaaijer, J.H., T. Robbertsen, T. Boomgaard and J.W. Cunnink, Fouling of ultrafiltration membranes.The role of protein adsorption and salt precipitation, *J. Membrane Sci.* 40 (1989) 199-217.

Hashino, M., K. Hirami, T. Ishigami, Y. Ohmukai, T. Maruyama, N. Kubota and H. Matsuyama, Effect of kinds of membrane materials on membrane fouling with BSA, *J. Membrane Sci.* 384(1-2) (2011) 157-165.

Ho, W.S. and K.K. Sirkar, *Membrane Handbook*, Van Nostrand Reinhold, (1992).

Ho, Y.S., Review of second-order models for adsorption systems, *J. Hazard. Mater.* 136(3) (2006) 681-689.

Ho, Y.S. and G. McKay, A comparison of chemisorption kinetic models applied to pollutant removal on various sorbents, *Process Saf. Environ.* 76(4) (1998) 332-340.

Ho, Y.S. and G. McKay, The kinetics of sorption of divalent metal ions onto sphagnum moss peat, *Water Res.* 34(3) (2000) 735-742.

Hong, J. and R. Pelton, The surface tension of aqueous polyvinylamine and copolymers with N-vinylformamide, *Colloid Polym. Sci.* 280 (2002) 203–205.

Hu, S.Y., Y. Zhang, D. Lawless and X. Feng, Composite membranes comprising of polyvinylamine-poly(vinyl alcohol) incorporated with carbon nanotubes for dehydration of ethylene glycol by pervaporation, *J. Membrane Sci.* 417-418 (2012) 34-44.

Hutchison, P.R. and T.W. Healy, *Surface and Colloid Chemistry in Natrual Waters and Water Treatment*, Plenum Press, (1990).

Islamoglu Kadioglu, S., L. Yilmaz and H. Onder Ozbelge, Estimation of binding constants of Cd(II), Ni(II) and Zn(II) with polyethyleneimine (PEI) by polymer enhanced ultrafiltration (PEUF) technique, *Separ. Sci. Technol.* 44(11) (2009) 2559-2581.

Jana, S., A. Saikia, M.K. Purkait and K. Mohanty, Chitosan based ceramic ultrafiltration membrane: Preparation, characterization and application to remove Hg(II) and As(III) using polymer enhanced ultrafiltration, *Chem. Eng. J.* 170(1) (2011) 209-219.

Jawor, A. and E.M.V. Hoek, Removing cadmium ions from water via nanoparticle-enhanced ultrafiltration, *Environ. Sci. Technol.* 44 (2010) 2570-2576.

Jellinek, H.H.G. and M.D. Luh, A novel method of metal ion removal and recovery from water by complex formation with polyelectrolytes, *J. Polym. Sci. A1* 7(8) (1969) 2445-2449.

Jellinek, H.H.G. and S.P. Sangal, Complexation of metal ions with natural polyelectrolytes (removal and recovery of metal ions from polluted waters), *Water Res.* 6(3) (1972) 305-314.

Jia, J., A. Wu and S. Luan, Spectrometry recognition of polyethyleneimine towards heavy metal ions, *Colloid Surface A* 449 (2014) 1-7.

Jiang, G., J. Shi and X. Feng, Mercury pollution in China, *Environ. Sci. Technol.* 40(12) (2006) 3672-3678.

Jones, G.D., J. Zomlefer and K. Hawkins, Attempted preparation of polyvinylamine, *J. Org. Chem.* 9 (1944) 500.

Jönsson, C. and A.-S. Jönsson, Influence of the membrane material on the adsorptive fouling of ultrafiltration membranes, *J. Membrane Sci.* 108(1–2) (1995) 79-87.

Juang, R.S. and M.N. Chen, Measurement of binding constants of poly(ethylenimine) with metal Ions and metal chelates in aqueous media by ultrafiltration, *Ind. Eng. CHem. Res.* 35 (1996) 1935-1943.

Juang, R.S. and C.H. Chiou, Ultrafiltration rejection of dissolved ions using various weakly basic water-soluble polymers, *J. Membrane Sci.* 177 (2000) 207-214.

Juang, R.S. and J.F. Liang, Equilibrium studies for the interaction of aqueous metal ions and polyacrylic acid by a batch ultrafiltration method, *J. Membrane Sci.* 82(1-2) (1993) 163-174.

Juang, R.S., Y. Xu and C. Chen, Separation and removal of metal ions from dilute solutions using micellar-enhanced ultrafiltration, *J. Membrane Sci.* 218(1-2) (2003) 257-267.

Khosa, M.A., S.S. Shah and X. Feng, Metal sericin complexation and ultrafiltration of heavy metals from aqueous solution, *Chem. Eng. J.* 244 (2014) 446-456.

Kim, H.J., K. Baek, B.K. Kim and J.W. Yang, Humic substance-enhanced ultrafiltration for removal of cobalt, *J. Hazard. Mater.* 122(1-2) (2005) 31-36.

Kobayashi, S., K.D. Suh and Y. Shirokura, Chelating ability of poly(vinylamine): effects of polyamine structure on chelation, *Macromolecules* 22(5) (1989) 2363-2366.

Koltuniewicz, A. and A. Noworyta, Dynamic properties of ultrafiltration systems in light of the surface renewal theory, *Ind. Eng. Chem. Res.* 33 (1994) 1771-1779.

Korus, I., Galvanic wastewater treatment by means of anionic polymer enhanced ultrafiltration, *Ecol. Chem. Eng. S* 19(1) (2012) 19-27.

Kuncoro, E.P., J. Roussy and E. Guibal, Mercury recovery by polymer‐enhanced ultrafiltration: comparison of chitosan and poly(ethylenimine) used as macroligand, *Separ. Sci. Technol.* 40(1-3) (2005) 659-684.

Kutowy, O. and S. Sourirajan, Cellulose acetate ultrafiltration membranes, *J. Appl. Polym. Sci.* 19 (1975) 1449-1460.

Labanda, J., M.S. Khaidar and J. Llorens, Feasibility study on the recovery of chromium (III) by polymer enhanced ultrafiltration, *Desalination* 249(2) (2009) 577-581.

Labanda, J., M.S. Khaidar, J. Sabaté and J. Llorens, Study of Cr(III) desorption process from a water-soluble polymer by ultrafiltration, *Desalination* 281 (2011) 165-171.

Lagergren, S., Zur theorie der sogenannten adsorption geluster stoffe, *K.Sven. Vetenskapsakad.Handl.* 24 (1898) 1-39.

Langmuir, I., The Constitution and fundamental properties of solids and liquids. part I. solids., *J. Am. Chem. Soc.* 38(11) (1916) 2221-2295.

Lee, C.-R., H.-S. Kim, I.-H. Jang, J.-H. Im and N.-G. Park, Pseudo first-order adsorption kinetics of N719 dye on TiO_2 surface, *ACS Appl. Mater. Interfaces* 3(6) (2011) 1953-1957.

Li, C.W., C.H. Cheng, K.H. Choo and W.S. Yen, Polyelectrolyte enhanced ultrafiltration (PEUF) for the removal of Cd(II): effects of organic ligands and solution pH, *Chemosphere* 72(4) (2008) 630-635.

Li, P., X.B. Feng, G.L. Qiu, L.H. Shang and Z.G. Li, Mercury pollution in Asia: A review of the contaminated sites, *J. Hazard. Mater.* 168(2–3) (2009) 591-601.

Liao, L.F., C.F. Lien, D.L. Shieh, M.T. Chen and J.L. Lin, FTIR study of adsorption and photoassisted oxygen isotopic exchange of carbon monoxide, carbon dioxide, carbonate, and formate on TiO_2, *J. Phys. Chem. B.* 106 (2002) 11240-11245.

Liu, B., X. Lv, X. Meng, G. Yu and D. Wang, Removal of Pb(II) from aqueous solution using dithiocarbamate modified chitosan beads with Pb(II) as imprinted ions, *Chem. Eng. J.* 220 (2013) 412-419.

Liu, F., N.A. Hashim, Y. Liu, M.R.M. Abed and K. Li, Progress in the production and modification of PVDF membranes, *J. Membrane Sci.* 375(1-2) (2011) 1-27.

Liu, F., B. Qin, L. He and R. Song, Novel starch/chitosan blending membrane: Antibacterial, permeable and mechanical properties, *Carbohyd. Polym.* 78(1) (2009) 146-150.

Liu, W., P. Yin, X.G. Liu, X.Q. Dong, J. Zhang and Q. Xu, Thermodynamics, kinetics, and isotherms studies for gold(III) adsorption using silica functionalized by diethylenetriaminemethylenephosphonic acid, *Chem. Eng. Res. Des.* 91(12) (2013) 2748-2758.

Liu, X., H. Cheng, T. Zhao and C. Zhang, Facile routes of manufacturing silicon quantum dots on a silicon wafer and their surface activation by esters of N-hydroxysuccinimide, *J. Colloid Interf. Sci.* 426(0) (2014) 117-123.

Liu, Y., Is the free energy change of adsorption correctly calculated, *J. Chem. Eng. Data* 54 (2009) 1981-1985.

Llanos, J., Á. Pérez and P. Cañizares, Water-soluble polymer ultrafiltration process at pilot scale: Study of hydrodynamics and factors limiting flux, *J. Membrane Sci.* 341(1-2) (2009) 37-45.

Lo, S.I., P.C. Chen, C.C. Huang and H.T. Chang, Gold nanoparticle-aluminum oxide adsorbent for efficient removal of mercury species from natural waters, *Environ. Sci. Technol.* 46(5) (2012) 2724-2730.

Ma, F., R. Qu, C. Sun, C. Wang, C. Ji, Y. Zhang and P. Yin, Adsorption behaviors of Hg(II) on chitosan functionalized by amino-terminated hyperbranched polyamidoamine polymers, *J. Hazard. Mater.* 172(2-3) (2009) 792-801.

Macedo, A., E. Duarte and M. Pinho, The role of concentration polarization in ultrafiltration of ovine cheese whey, *J. Membrane Sci.* 381(1-2) (2011) 34-40.

Manohar, D.M., K.A. Krishnan and T.S. Anirudhan, Removal of mercury(II) from aqueous solutions and chlor-alkali industry wastewater using 2-mercaptobenzimidazole-clay, *Water Res.* 36 (2002) 1609-1619.

Martell, A.E. and R.D. Hancock, *Metal Complexes in Aqueous Solutions*, Plenum Press, (1996).

Matsuyama, H., M. Yuasa, Y. Kitamura, M. Teramoto and D.R. Lloyd, Structure control of anisotropic and asymmetric polypropylene membrane prepared by thermally induced phase separation, *J. Membrane Sci.* 179 (2000) 91-100.

McDonogh, R.M., H. Bauser, N. Stroh and U. Grauschopf, Experimental in Situ Measurement of Concentration Polarisation During Ultra- and Micro-filtration of Bovine Serum Albumin and Dextran Blue Solutions, *J. Membrane Sci.* 104 (1995) 51-63.

Molinari, R., P. Argurio, T. Poerio and G. Gullone, Selective separation of copper(II) and nickel(II) from aqueous systems by polymer assisted ultrafiltration, *Desalination* 200(1-3) (2006) 728-730.

Molinari, R., T. Poerio and P. Argurio, Chemical and operational aspects in running the polymer assisted ultrafiltration for separation of copper(II)–citrate complexes from aqueous media, *J. Membrane Sci.* 295(1-2) (2007) 139-147.

Monier, M. and D.A. Abdel-Latif, Modification and characterization of PET fibers for fast removal of Hg(II), Cu(II) and Co(II) metal ions from aqueous solutions, *J. Hazard. Mater.* (2013).

Mulder, M., *Basic Principles of Membrane Technology*, Kluwer Academic, (1991).

Muslehiddinoglu, J., Y. Uludag, H.O. Ozbelge and L. Yilmaz, Effect of operating parameters on selective separation of heavy metals from binary mixtures via polymer enhanced ultrafiltration, *J. Membrane Sci.* 140 (1998) 251-266.

Nabetani, H., M. Nakajima, A. Watanabe, S.I. Nakao and S. Kimura, Effects of osmotic pressure and adsorption on ultrafiltration of ovalbumin, *AIChE J.* 36(6) (1990) 907-915.

Navarro, R.R., S. Wada and K. Tatsumi, Heavy metal precipitation by polycation-polyanion complex of PEI and its phosphonomethylated derivative, *J. Hazard. Mater.* 123(1-3) (2005) 203-209.

Nguyen, Q.T., P. Aptel and J. Neel, Application of ultrafiltration to the concentration and separation of solutes of low molecular weight, *J. Membrane Sci.* 6 (1980) 71-82.

Ozay, O., S. Ekici, Y. Baran, N. Aktas and N. Sahiner, Removal of toxic metal ions with magnetic hydrogels, *Water Res.* 43(17) (2009) 4403-4411.

Palencia, M., B. Rivas and E. Pereira, Polymer-enhanced ultrafiltration: counterion distribution and its relation with the divalent metal-ion retention properties by sulfonic acid polyelectrolytes, *Polym. Bull.* 67(7) (2011) 1123-1138.

Palencia, M., B.L. Rivas and E. Pereira, Metal ion recovery by polymer-enhanced ultrafiltration using poly(vinyl sulfonic acid): Fouling description and membrane–metal ion interaction, *J. Membrane Sci.* 345(1-2) (2009a) 191-200.

Palencia, M., B.L. Rivas, E. Pereira, A. Hernández and P. Prádanos, Study of polymer–metal ion–membrane interactions in liquid-phase polymer-based retention (LPR) by continuous diafiltration, *J. Membrane Sci.* 336(1-2) (2009b) 128-139.

Pastor, M.R., E. Samper-Vidal, V.P. Galvhn and R.D.P., Analysis of the variation in the permeate flux and of the efficiency of the recovery of mercury by polyelectrolyte enhanced ultrafiltration (PEUF), *Desalination* 151 (2002) 247-251.

Pelton, R., Polyvinylamine: A Tool for Engineering Interfaces, *Langmuir* 30(51) (2014) 15373-15382.

Pillay, K., E.M. Cukrowska and N.J. Coville, Improved uptake of mercury by sulphur-containing carbon nanotubes, *Microchem. J.* 108(0) (2013) 124-130.

Pinschmidt, R.K., Polyvinylamine at last, *J. Polym. Sci. A1* 48 (2010) 2257-2283.

Pivokonsky, M., J. Safarikova, P. Bubakova and L. Pivokonska, Coagulation of peptides and proteins produced by Microcystis aeruginosa: Interaction mechanisms and the effect of Fe-peptide/protein complexes formation, *Water Res.* 46(17) (2012) 5583-5590.

Polyakov, Y.S. and A.L. Zydney, Ultrafiltration membrane performance: Effects of pore blockage/constriction, *J. Membrane Sci.* 434(0) (2013) 106-120.

Pookrod, P., K.J. Haller and J.F. Scamehorn, Removal of Arsenic Anions from Water Using Polyelectrolyte‐Enhanced Ultrafiltration, *Separ. Sci. Technol.* 39(4) (2004) 811-831.

Porter, M.C., Concentration polarization with membrane ultrafiltration, *Ind. Eng. Chem. Prod. Rd.* 11(3) (1972) 234-248.

Porter, M.C., Ultrafiltration, M.C. Porter (Eds.), *Handbook of Industrial Membrane Technology*, Noyes Publications, (1990) 137-255.

Pretsch, E., P. Buhlmann and M. Badertscher, *Structure Determination of Organic Compounds*, Springer, (2009).

Qiao, Z., Z. Wang, C. Zhang, S. Yuan, Y. Zhu, J. Wang and S. Wang, PVAm-PIP/PS Composite Membrane with High Performance for CO_2/N_2 Separation, *AIChE J.* 59(1) (2013) 215-228.

Qiu, G.M., L.P. Zhu, B.K. Zhu, Y.Y. Xu and G.L. Qiu, Grafting of styrene/maleic anhydride copolymer onto PVDF membrane by supercritical carbon dioxide: Preparation, characterization and biocompatibility, *J. Supercrit. Fluid* 45(3) (2008) 374-383.

Qiu, Y.-R. and L.-J. Mao, Removal of heavy metal ions from aqueous solution by ultrafiltration assisted with copolymer of maleic acid and acrylic acid, *Desalination* 329 (2013) 78-85.

Radeva, T., *Physical Chemistry of Polyelectrolytes*, Marcel Dekker, (2001).

Rajesh, S., P. Maheswari, S. Senthilkumar, A. Jayalakshmi and D. Mohan, Preparation and characterisation of poly (amide-imide) incorporated cellulose acetate membranes for polymer enhanced ultrafiltration of metal ions, *Chem. Eng. J.* 171(1) (2011) 33-44.

Reis, A.T., S.M. Rodrigues, C. Araujo, J.P. Coelho, E. Pereira and A.C. Duarte, Mercury contamination in the vicinity of a chlor-alkali plant and potential risks to local population, *Sci. Total Environ.* 407(8) (2009) 2689-2700.

Reynolds, D.D. and W.O. Kenyon, The preparation of polyvinylamine, polpinylamine salts, and related nitrogenous resin, *J. Am. Chem. Soc.* 69 (1947) 911-915.

Rivas, B.L., E. Martínez, E. Pereira and K.E. Geckeler, Synthesis, characterization and polychelatogenic properties of poly[(2-acrylamido-2-methyl-1-propane sulfonic acid)-co-(methacrylic acid)], *Polym. Int.* 50 (2001) 456-462.

Rivas, B.L. and M. Palencia, Removal-concentration of pollutant metal-ions by water-soluble polymers in conjunction with double emulsion systems: A new hybrid method of membrane-based separation, *Sep. Purif. Technol.* 81(3) (2011) 435-443.

Rivas, B.L. and E.D. Pereira, Selective retention properties to silver and mercury ions of poly (4-vinylpyridine) methyl iodide studied by the liquid-phase polymer-based retention technique, *J. Appl. Polym. Sci.* 80(13) (2001) 2578-2582.

Rivas, B.L., E.D. Pereira, P. Gallegos and K.E. Geckeler, Water-soluble acidic polyelectrolytes with metal-removing ability, *Polym. Advan. Technol.* 13 (2002) 1000-1005.

Rivas, B.L., E.D. Pereira and M.V. Ignacio, Water-soluble polymer-metal ion interactions, *Prog. Polym. Sci.* 28 (2003) 173-208.

Rivas, B.L., E.D. Pereira, E. Martínez and I. Moreno-Villoslada, Metal ion interaction with poly(2-acrylamide-2-methyl-1-propanesulfonic acid-co-methacrylic acid), *Bol. Soc. Chil. Quim.* 45 (2000) 199-205.

Rivas, B.L. and M.I. Villoslada, Chelation properties of polymer complexes of poly(acrylic acid) with poly(acrylamide), and poly(acrylic acid) with poly(N,N-dimethylacrylamide), *Macromol. Chem. Phys.* 199 (1998) 1153-1160.

Saad, D.M., E.M. Cukrowska and H. Tutu, Selective removal of mercury from aqueous solutions using thiolated cross-linked polyethylenimine, *Appl. Water Sci.* 3(2) (2013) 527-534.

Saber-Samandari, S. and M. Gazi, Removal of mercury (II) from aqueous solution using chitosan-graft-polyacrylamide semi-IPN hydrogels, *Separ. Sci. Technol.* (2013).

Say, R., E. Birlik, Z. Erdemgil, A. Denizli and A. Ersöz, Removal of mercury species with dithiocarbamate-anchored polymer/organosmectite composites, *J. Hazard. Mater.* 150(3) (2008) 560-564.

Shao, J., S. Qin, J. Davidson, W. Li, Y. He and H.S. Zhou, Recovery of nickel from aqueous solutions by complexation-ultrafiltration process with sodium polyacrylate and polyethylenimine, *J. Hazard. Mater.* 244-245 (2013) 472-477.

Sharma, P. and M.R. Das, Removal of a Cationic Dye from Aqueous Solution Using Graphene Oxide Nanosheets: Investigation of Adsorption Parameters, *J. Chem. Eng. Data* 58(1) (2013) 151-158.

Singh, S., B.N. Rai and L.C. Rai, Ni (II) and Cr (VI) sorption kinetics by Microcystis in single and multimetallic system, *Process Biochem.* 36(12) (2001) 1205-1213.

Snceyink, V.L. and D. Jenkins, *Water Chemistry*, John Wiley & Sons, (1980).

Spivakove, B.Y., K. Geckeler and E. Bayer, Liquid-phase polymer-based retention the separation of metals by ultrafiltration on polychelatogens, *Nature* 315(23) (1985) 313-315.

Strathmann, H., Selective removal of heavy metal ions from aqueous solutions by diafiltration of macromolecular complexes, *Separ. Sci. Technol.* 15(4) (1980) 1135-1152.

Swanson, C.L., R.E. Wing, W.M. Doane and C.R. Russell, Mercury removal from waste water with starch xanthate-cationic polymer complex, *Environ. Sci. Technol.* 7(7) (1973) 614-619.

Tanford, C., *Physical Chemistry of Macromolecules*, JOHN WILEY & SONS, (1961).

Taty-Costodes, V.C., H. Fauduet, C. Porte and A. Delacroix, Removal of Cd(II) and Pb(II) ions, from aqueous solutions, by adsorption onto sawdust of Pinus sylvestris, *J. Hazard. Mater.* 105(1–3) (2003) 121-142.

Teyssie, P., C. Decoene and M.T. Teyssie, Structure and properties of polymeric chelates, *Makromol. Chem.* 84 (1965) 51-63.

Tu, Y.J., C.F. You and C.K. Chang, Kinetics and thermodynamics of adsorption for Cd on green manufactured nano-particles, *J. Hazard. Mater.* 235-236 (2012) 116-122.

Tuncay, M., S.D. Christian, E.E. Tucker, R.W. Taylor and J.F. Scamehorn, Ligand-modified polyelectrolyte-enhanced ultrafiltration with electrostatic attachment of ligands. 1. removal of Cu and Pb with expulsion of Ca, *Langmuir* 10 (1994) 4688-4692.

Tweddle, T.A., O. Kutowy, W.L. Thayer and S. Souriraja, Polysulfone ultrafiltration membranes, *Ind. Eng. Chem. Prod. Res. Dev.* 22(2) (1983) 320-326.

Uludag, Y., H.O. Ozbelge and L. Yilmaz, Removal of mercury from aqueous solutions via polymer-enhanced ultrafiltration, *J. Membrane Sci.* 129 (1997) 93-97.

Urgun-Demirtas, M., P.L. Benda, P.S. Gillenwater, M.C. Negri, H. Xiong and S.W. Snyder, Achieving very low mercury levels in refinery wastewater by membrane filtration, *J. Hazard. Mater.* 215-216 (2012) 98-107.

Uzal, N., A. Jaworska, A. Miskiewicz, T.G. Zakrzewska and C. Cojocaru, Optimization of Co^{2+} ions removal from water solutions via polymer enhanced ultrafiltration with application of PVA and sulfonated PVA as complexing agents, *J. Colloid Interf. Sci.* 362(2) (2011) 615-624.

van Oss, C. J., Acid—base interfacial interactions in aqueous media, *Colloid Surface A* 78(0) (1993) 1-49.

van Oss, C. J., Development and applications of the interfacial tension between water and organic or biological surfaces, *Colloid Surface B* 54(1) (2007) 2-9.

Vela, M.C.V., S.A. Blanco, J.L. Garcia, E.B. Rodriguez, Analysis of membrane pore blocking models applied to the ultrafiltration of PEG, *Sep. Purif. Technol.* 62 (2008) 489-498.

Vieira, R.S. and M.M. Beppu, Mercury ion recovery using natural and crosslinked chitosan membranes, *Adsorption* 11 (2005) 731-736.

Wang, G., Q. Chang, X. Han and M. Zhang, Removal of Cr(VI) from aqueous solution by flocculant with the capacity of reduction and chelation, *J. Hazard. Mater.* 248-249 (2013) 115-121.

Wang, J., B. Deng, H. Chen, X. Wang and J. Zheng, Removal of aqueous Hg(II) by polyaniline: sorption characteristics and mechanisms, *Environ. Sci. Technol.* 43 (2009) 5223-5228.

Wang, Q., D. Kim, D.D. Dionysiou, G.A. Sorial and D. Timberlake, Sources and remediation for mercury contamination in aquatic systems—a literature review, *Environ. Pollut.* 131(2) (2004) 323-336.

Wang, W.-H., J.-L. Dong, G.L. Baker and M.L. Bruening, Bifunctional polymer brushes for low-bias enrichment of mono- and multi-phosphorylated peptides prior to mass spectrometry analysis, *Analyst* 136(18) (2011) 3595-3598.

Wijmans, J.G., S. Nakao and C.A. Smolders, Flux limitation in ultrafiltration: Osmotic pressure model and gel layer model, *J. Membrane Sci.* 20 (1984) 115-124.

Wu, D., Y. Huang, S. Yu, D. Lawless and X. Feng, Thin film composite nanofiltration membranes assembled layer-by-layer via interfacial polymerization from polyethylenimine and trimesoyl chloride, *J. Membrane Sci.* 472 (2014) 141-153.

Yan, L., Y.S. Li and C.B. Xiang, Preparation of poly(vinylidene fluoride) (PVDF) ultrafiltration membrane modified by nano-sized alumina (Al_2O_3) and its antifouling research, *Polymer* 46(18) (2005) 7701-7706.

Yang, S.F., H.L. Duan, J.J. Lin, J.Y. Zhu and Z.B. Gong, A New Method for the Measurement of Complexation Stability Constant and Average Coordination Number of Metallic Element with Polymer, *Chinese J. Inorg. Chem.* 30(4) (2014) 853-859.

Zaidi, S.K. and A. Kumar, Experimental studies in the dead-end ultrafiltration of dextran: analysis of concentration polarization, *Sep. Purif. Technol.* 36(2) (2004) 115-130.

Zeng, J., H. Ye and Z. Hu, Application of the hybrid complexation-ultrafiltration process for metal ion removal from aqueous solutions, *J. Hazard. Mater.* 161(2-3) (2009) 1491-1498.

Zeng, J.X., Q.N. Guo, Z.Z. Ou-Yang, H. Zhou and H.J. Chen, Chromium(VI) removal from aqueous solutions by polyelectrolyte-enhanced ultrafiltration with polyquaternium, *Asia-Pac. J. Chem. Eng.* 9(2) (2014) 248-255.

Zerze, H., H.O. Ozbelge, N. Bicak, N. Aydogan and L. Yilmaz, Novel boron specific copolymers with quaternary amine segments for efficient boron removal via PEUF, *Desalination* 310 (2013) 169-179.

Appendix I

Sample Calculations

I.1 Ultrafiltration performance

Calculation of permeation flux

The permeation of flux in the PEUF process was calculated as follow:

Membrane module: Dead-end

Feed: PVAm-CuSO$_4$-H$_2$O

Effective membrane area (A): 36 cm^2

Transmembrane pressure: 200 kPa

Operating temperature: room temperature (25 ℃)

Mass of permeate collected (m): 7.306 g

Filtrated weight: 39.377 g

Time interval (t): 4.17 min

PVAm concentration in feed: 1 wt%

Cu(II) concentration in feed (C_f): 25.43 ppm

Cu(II) concentration in permeate (C_p): 0.15 ppm

Permeation flux:

$$J = \frac{m}{A \times t} = \frac{7.306 \text{ g}}{36 \text{ cm}^2 \times 4.17 \text{ min}} = 29.2 \text{ kg/(h·m}^2)$$

Calculation of metal rejection

$$R_m = \frac{C_f - C_p}{C_f} \times 100\% = \frac{25.43 \text{ ppm - 0.15 ppm}}{25.43 \text{ ppm}} \times 100\% = 99.41\%$$

I.2 Adsorption performance

Calculation of adsorption capacity

The adsorption capacity of PVAm-SH towards Hg(II) was calculated from the following data:

Adsorbent: PVAm-SH

Adsorbate: $HgCl_{2(aq.)}$

Operating temperature: 25 °C

Total volume of aqueous solution (V): 0.02 L

Solution pH: neutral

Hg(II) concentration before adsorption (C_0): 1471.4 ppm

Hg(II) concentration after adsorption (C_t): 700.1 ppm

Quantity of adsorbent (m_s): 0.102 g

Molar mass of Hg: 200.59 g/mol

Adsorption capacity (Q):

$$Q = \frac{(C_0 - C_t) \times V}{m_s} = \frac{(1471.4 \text{ ppm - } 700.1 \text{ ppm}) \times 0.02 \text{ L}}{0.102 \text{ g}} = 151.2 \text{ mg/g} = 0.754 \text{ mmol/L}$$

Calculation of adsorption isotherms and kinetics

The data of adsorption isotherms and kinetics in this study was well fitted by Langmuir and pseudo-second order models, respectively. The Langmuir constant and pseudo-second order kinetic constant can be obtained by the plotting based on the following equations:

$$\frac{C_e}{Q_e} = \frac{C_e}{Q_m} + \frac{1}{Q_m K_L} \quad (C_e/Q_e \text{ vs. } C_e) \tag{I.1}$$

$$Slope_1 = 1/Q_m, \quad Intercept_1 = 1/(Q_m K_L) \tag{I.2}$$

$$\frac{t}{Q_t} = \frac{1}{k_2 Q_e^2} + \frac{t}{Q_e} \quad (t/Q_t \text{ vs. } t) \tag{I.3}$$

$$Slope_2 = 1/Q_e, \quad Intercept_2 = 1/(k_2 Q_e^2) \tag{I.4}$$

The Langmuir and pseudo-second order constants of adsorption of Hg(II) onto PVAm-SH at 25 ℃ were calculated from the following data:

Langmuir fitting		Pseudo-second order fitting	
C_e	C_e/Q_e	t	t/Q_t
(mmol/L)	(g/L)	(min)	min/(mmol/g)
0.0009	0.0513	10	366.2
0.0148	0.155	20	366.9
0.0544	0.140	30	336.8
0.0616	0.209	40	398.4
0.108	0.284	60	429.5
0.172	0.401	90	476.7
0.663	1.223	120	595.6
1.009	1.661	210	974.4
2.248	3.226	330	1390.2
3.490	4.629	525	2103.7
4.795	6.109		

Slope$_1$ = 1.263, Intercept$_1$ = 0.209, Q_m = 0.797 mmol/g, K_L = 6.144 L/mmol

Slope$_2$ = 3.6372, Intercept$_2$ = 233.56, Q_e = 0.287 mmol/g, k_2 = 0.0498 g/(mmol·min)

I.3 Calculation of interfacial free energy

To understand the self-fouling of water-soluble polymer in PEUF process, the interfacial free energy of adhesion between water-soluble polymer and PES membrane in water was calculated. At first, the free energy of interaction ΔG_{SL} when PES membrane immerses into three probe liquids can be obtained based on the following equation and data:

$$-\Delta G_{SL} = (1 + cos\theta)\gamma_L \tag{I.5}$$

Probe liquid	γ_L, (mJ/m^2)	Contact angel, θ	ΔG_{SL}, (mJ/m^2)
Water	72.8	$79°\pm5°$	-86.7
Ethylene glycol	47.9	$47°\pm4°$	-80.6
Diiodomethane	50.8	$37°\pm3°$	-91.4

With the free energy of interaction ΔG_{SL}, the solid surface tension parameters for PES membrane can then be calculated according to the extended Young-Dupré equation:

$$-\Delta G_{SL} = 2\left(\sqrt{\gamma_S^{LW} \cdot \gamma_L^{LW}} + \sqrt{\gamma_S^+ \cdot \gamma_L^-} + \sqrt{\gamma_S^- \cdot \gamma_L^+}\right) \tag{I.6}$$

Substituting the surface tension parameters of three probe liquids into equation I.6, one can obtain the following equation set:

$$Water: \qquad 86.7 = 2 \times \left(\sqrt{\gamma_S^{LW} \times 21.8} + \sqrt{\gamma_S^+ \times 25.5} + \sqrt{\gamma_S^- \times 25.5}\right)$$

$$Ethylene\ glycol: \qquad 80.6 = 2 \times \left(\sqrt{\gamma_S^{LW} \times 29.0} + \sqrt{\gamma_S^+ \times 47} + \sqrt{\gamma_S^- \times 1.9}\right)$$

$$Diiodomethane: \qquad 91.4 = 2 \times \left(\sqrt{\gamma_S^{LW} \times 50.8} + \sqrt{\gamma_S^+ \times 0} + \sqrt{\gamma_S^- \times 0}\right)$$

By solving the equations, the three surface tension parameters of PES membrane can be obtained.

PES membrane: $\qquad \gamma^{LW} = 41.1$ mJ/m^2, $\gamma^+ = 0.2$ mJ/m^2, $\gamma^- = 5.1$ mJ/m^2

Using the same calculation method, the surface tension parameters of mercury-polymer complexes can also be calculated. The result is shown as follow:

PAA-Hg complex: $\qquad \gamma^{LW} = 29.2$ mJ/m^2, $\gamma^+ = 1.2$ mJ/m^2, $\gamma^- = 2.7$ mJ/m^2

With the calculated surface tension parameters of two solid materials, the interfacial free energy of adhesion at contact when immersed in water "W" (ΔG_{SWM}) can be obtained by the following equation:
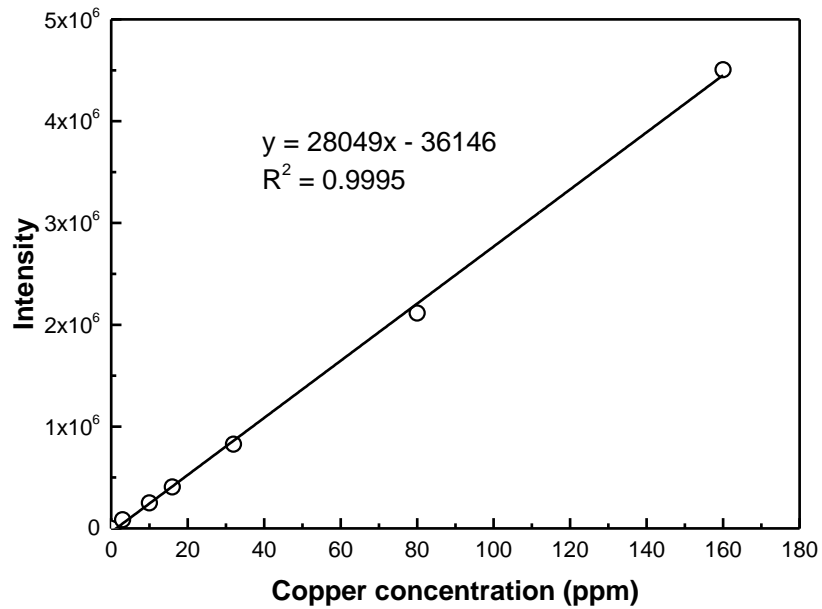
$$\Delta G_{SWM} = 2\left[\left(\sqrt{\gamma_W^{LW}} - \sqrt{\gamma_S^{LW}}\right) \cdot \left(\sqrt{\gamma_M^{LW}} - \sqrt{\gamma_W^{LW}}\right) + \sqrt{\gamma_W^+}\left(\sqrt{\gamma_S^-} + \sqrt{\gamma_M^-} - \sqrt{\gamma_W^-}\right) + \right.$$

$$\left. \sqrt{\gamma_W^-}\left(\sqrt{\gamma_S^+} + \sqrt{\gamma_M^+} - \sqrt{\gamma_W^+}\right) - \sqrt{\gamma_S^+\gamma_M^-} - \sqrt{\gamma_S^-\gamma_M^+}\right]$$

$$\Delta G_{SWM} = 2 \times \left[\left(\sqrt{21.8} - \sqrt{29.2}\right) \times \left(\sqrt{41.1} - \sqrt{21.8}\right) + \sqrt{25.5} \times \left(\sqrt{2.7} + \sqrt{5.1} - \sqrt{25.5}\right) + \right.$$

$$\left. \sqrt{25.5} \times \left(\sqrt{1.2} + \sqrt{0.2} - \sqrt{25.5}\right) - \sqrt{1.2 \times 5.1} - \sqrt{2.7 \times 0.2}\right] = 63.1 \text{ mJ/m}^2$$

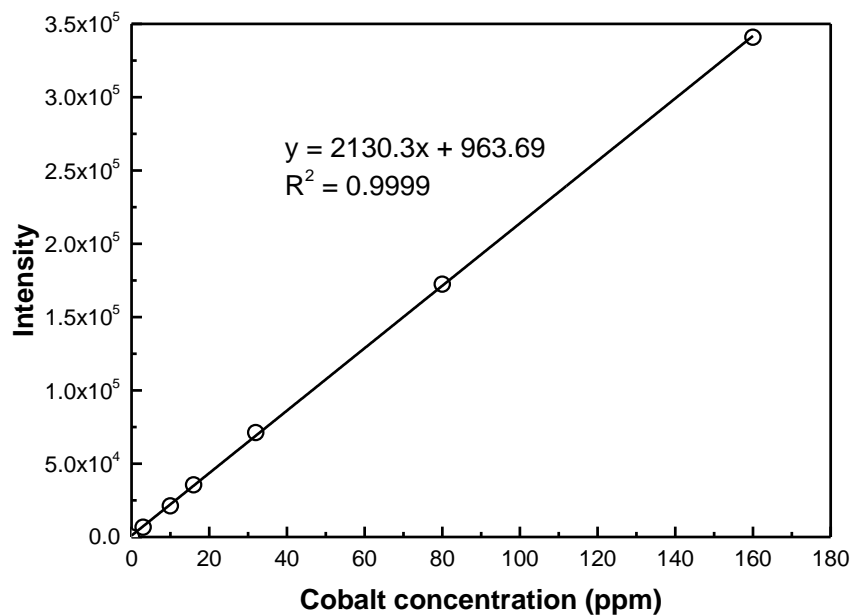# Appendix II

Calibrations of Heavy Metal Aqueous Solutions by ICP-OES

Calibration of copper standard aqueous solutions

$y = 28049x - 36146$
$R^2 = 0.9995$

Calibration of cobalt standard aqueous solutions

$y = 2130.3x + 963.69$
$R^2 = 0.9999$

Calibration of mercury standard aqueous solutions

$y = 1357.9x + 1735.1$
$R^2 = 0.9998$
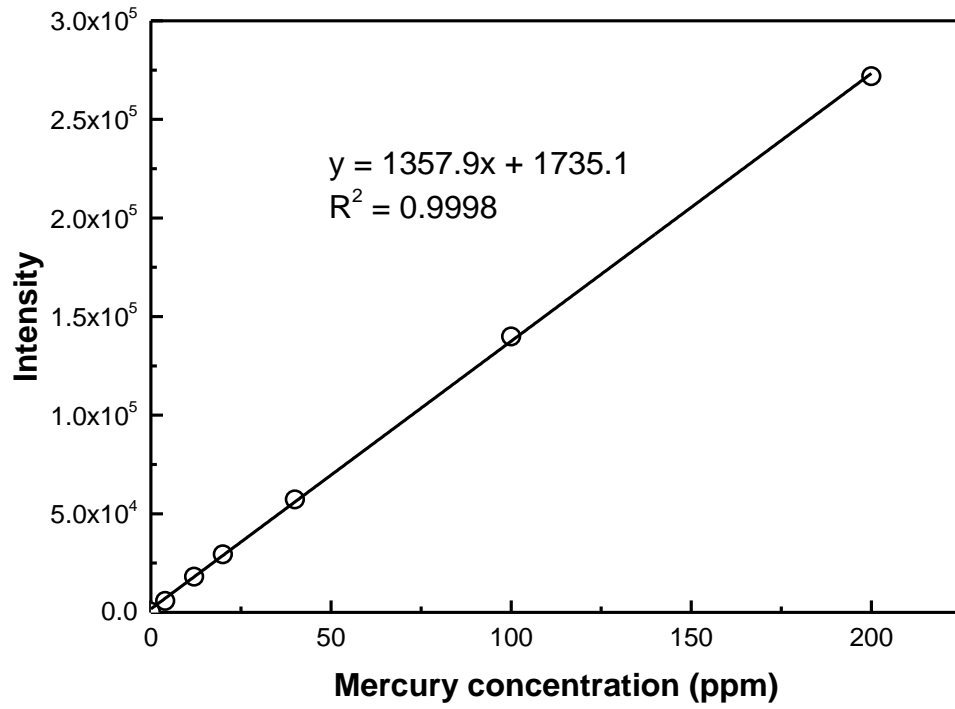
Appendix III

Confidence level

In order to estimate the confidence interval for the metal rejection in this experiment, I tested the copper rejections five times under the same conditions (initial concentration of Cu^{2+} and PVAm were 25ppm and 0.1wt%, respectively; operating pressure: 0.2MPa). The results are shown as follow:

Copper rejection: $\{67.1\%, 68.97\%, 69.52\%, 67.83\%, 71.12\%\}$

For illustration, I used t-distribution to find a 95% confidence interval for the copper rejection using PVAm as chelating agents in PEUF.

$$\bar{X} = \frac{1}{n}\sum_{i=1}^{n} X_i = 68.91\%$$

$$S^2 = \frac{\sum_{i=1}^{n}(X_i - \bar{X})^2}{n-1} = \frac{1}{n-1}\left\{\sum_{i=1}^{n} X_i^2 - \frac{1}{n}\left(\sum_{i=1}^{n} X_i\right)^2\right\} = 0.024256\%$$

$$1 - \alpha = 95\%$$

$$t_{\frac{\alpha}{2},n-1} = t_{0.025,4} = 2.776$$

$$\bar{X} \pm t_{\frac{\alpha}{2},n-1}\sqrt{\frac{S^2}{n}} = 68.91\% \pm 2.776 \times \sqrt{\frac{0.024256\%}{5}} = 68.91\% \pm 1.93\%$$

So we have a 95% confidence that the true copper rejection in this experiment will locate in the interval [66.98%, 70.84%].

The sources of error can include: measurement, analytical, sampling, ambient conditions, skills or alertness of personnel, and purity of reagents. In this experiment, the main source of

error comes from the batch to batch difference (different UF membrane batches). In addition, the concentration measurement by ICP is also a major source of error.

The following table shows the confidence bounds of adsorption kinetics parameters in Chapter 6. The confidence level for the parameters is 95%:

T (K)	$Q_{e, exp}$ (mmol/g)	Pseudo-first-order			Pseudo-second-order		
		k_1 (min)$^{-1}$	$Q_{e, cal}$ (mmol/g)	R^2	k_2 (g/mmol·min)	$Q_{e, cal}$ (mmol/g)	R^2
298	0.264	0.0045 ± 0.0014	0.182 ± 0.061	0.884	0.049 ± 0.014	0.287 ± 0.022	0.996
308	0.370	0.0082 ± 0.0014	0.263 ± 0.087	0.957	0.043 ± 0.016	0.414 ± 0.018	0.994
318	0.421	0.0062 ± 0.0024	0.201 ± 0.131	0.819	0.074 ± 0.030	0.444 ± 0.017	0.999
328	0.455	0.0054 ± 0.0033	0.162 ± 0.081	0.636	0.102 ± 0.051	0.467 ± 0.023	0.998
338	0.518	0.0049 ± 0.0023	0.162 ± 0.102	0.741	0.142 ± 0.048	0.514 ± 0.008	0.999

Appendix IV

Matlab Code for Calculation of k_2 in Modified Pseudo-second-order Model

```
function err = odefit(exp_t, exp_Q, K2, const, Q_0)


Qm = const(1);

Kl = const(2);

C0 = const(3);

M = const(4);

V = const(5);

odefun = @(t, Q) K2 * (Qm*Kl*(C0-Q*M/V)/(1+Kl*(C0-Q*M/V)) - Q)^2;

options = odeset('RelTol',1e-6);

[t, Q] = ode113(odefun, exp_t, Q_0, options);

err = sum((Q - exp_Q).^2);       % compute error between experimental Q and fitted Q

end


%% Estimating Coefficients of ODEs to Fit Given Experimental Data

clear all

clc

clf
```

```matlab
filename = 'kinetic_data.xlsx';

data = xlsread(filename);

dataGroup = 1; % dataGroup could be either 1,2 or 3, corresponding to three experimental
results

K2_0 = 0.001; % guess of initial value of K2

Q_0 = 0.001; % guess of initial value of Q


exp_t = data(1:11, dataGroup*3-2);

exp_Q = data(1:11, dataGroup*3-1);

const = data(13:17, dataGroup*3-2);

Qm = const(1);

Kl = const(2);

C0 = const(3);

M = const(4);

V = const(5);


options1 = optimset('TolX',1e-8);

K2_estimate = fminsearch(@(K2)odefit(exp_t, exp_Q, K2, const, Q_0), K2_0, options1);


%% Data comparison

K2 = K2_estimate;

odefun = @(t, Q) K2 * (Qm*Kl*(C0-Q*M/V)/(1+Kl*(C0-Q*M/V)) - Q)^2;
```

```matlab
options2 = odeset('RelTol',1e-9);

[t, Q] = ode113(odefun, exp_t, Q_0, options2);

figure(1)

plot(t, Q, 'r-*', t, exp_Q, 'b+-')

xlabel('t (h)');

ylabel('Q (mmol/g)');

legend('Estimated results', 'Experimental results', 'Location','northwest')
```